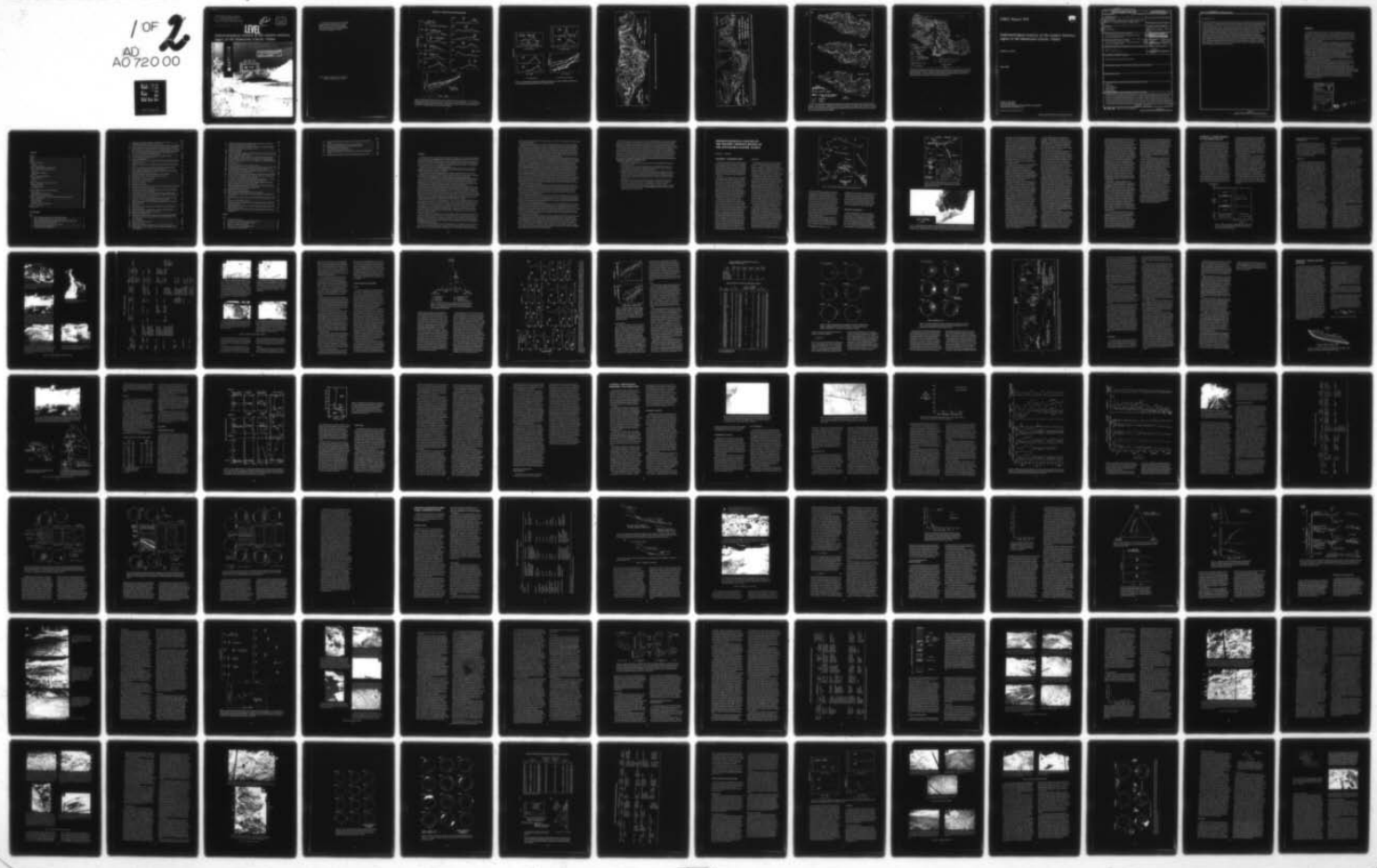
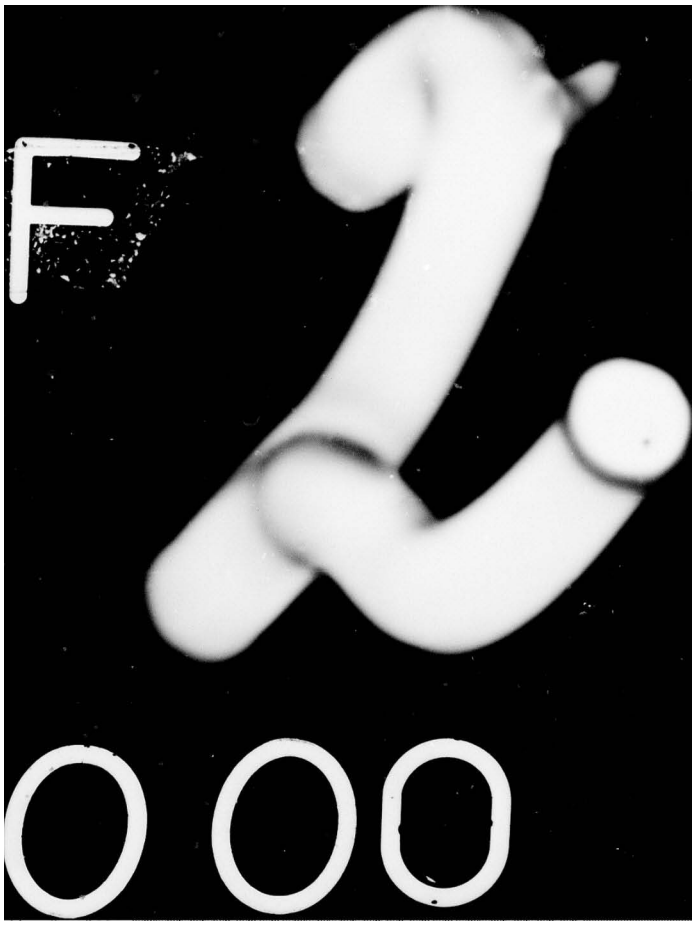
AD-A072 000 COLD REGIONS RESEARCH AND ENGINEERING LAB HANOVER NH F/G 8/12
SEMDIMENTOLOGICAL ANALYSIS OF THE WESTERN TERMINUS REGION OF TH--ETC(U)
MAY 79 D E LAWSON

UNCLASSIFIED CRREL-79-9 NL

1 OF 2
AD
A072000



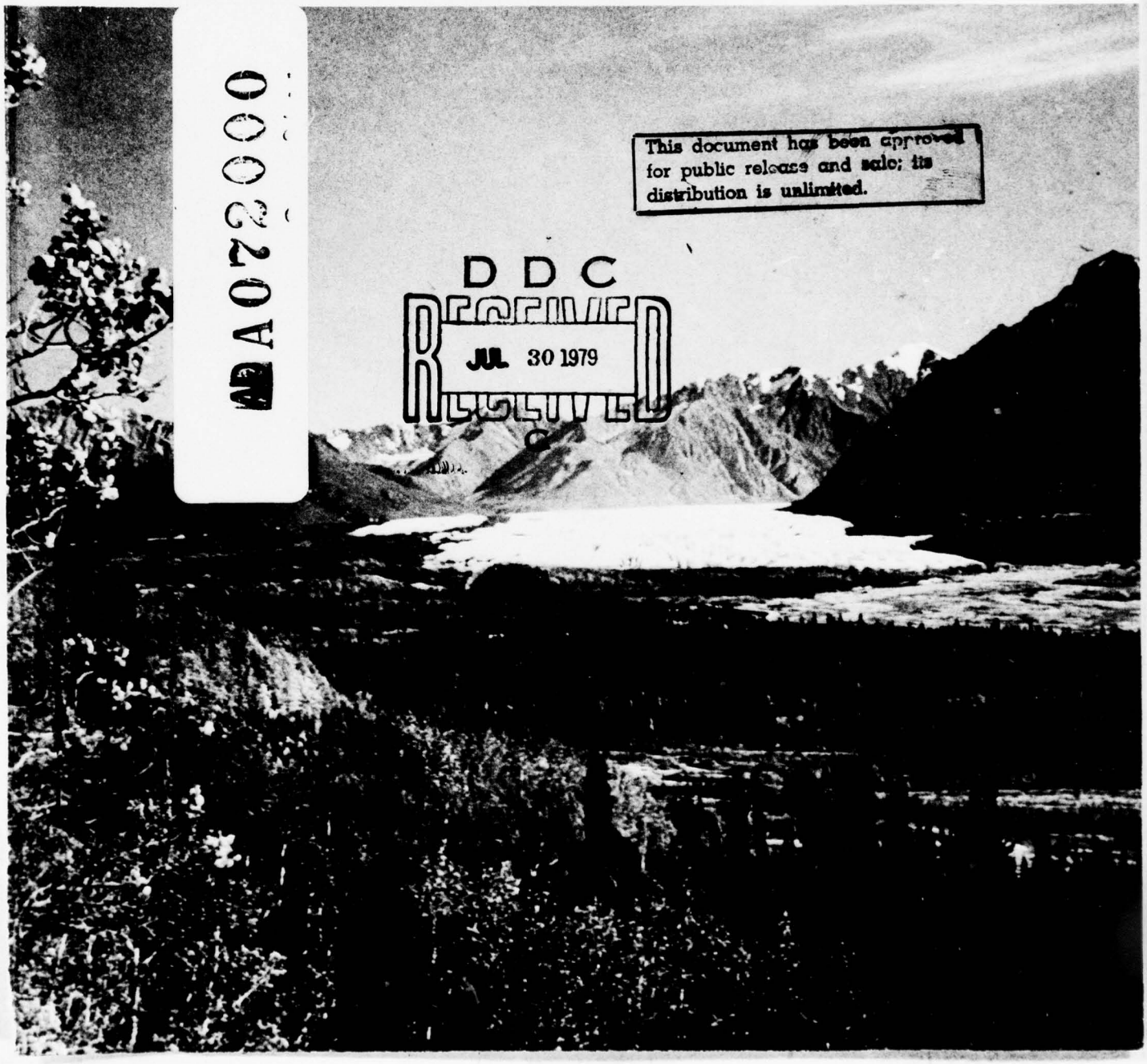

F
1.
000

CRREL

REPORT 79-9

LEVEL

Sedimentological analysis of the western terminus region of the Matanuska Glacier, Alaska



AD A072000

This document has been approved for public release and sale; its distribution is unlimited.

DDC
RECEIVED
JUL 30 1979

For conversion of SI metric units to U.S./British customary units of measurement consult ASTM Standard E380, Metric Practice Guide, *published by the American Society for Testing and Materials, 1916 Race St., Philadelphia, Pa. 19103.*

Cover: Matanuska Glacier as seen from the Glenn Highway. (Photograph by D. Lawson.)

ADDENDUM. CORRECTIONS OF PRINTING ERRORS.

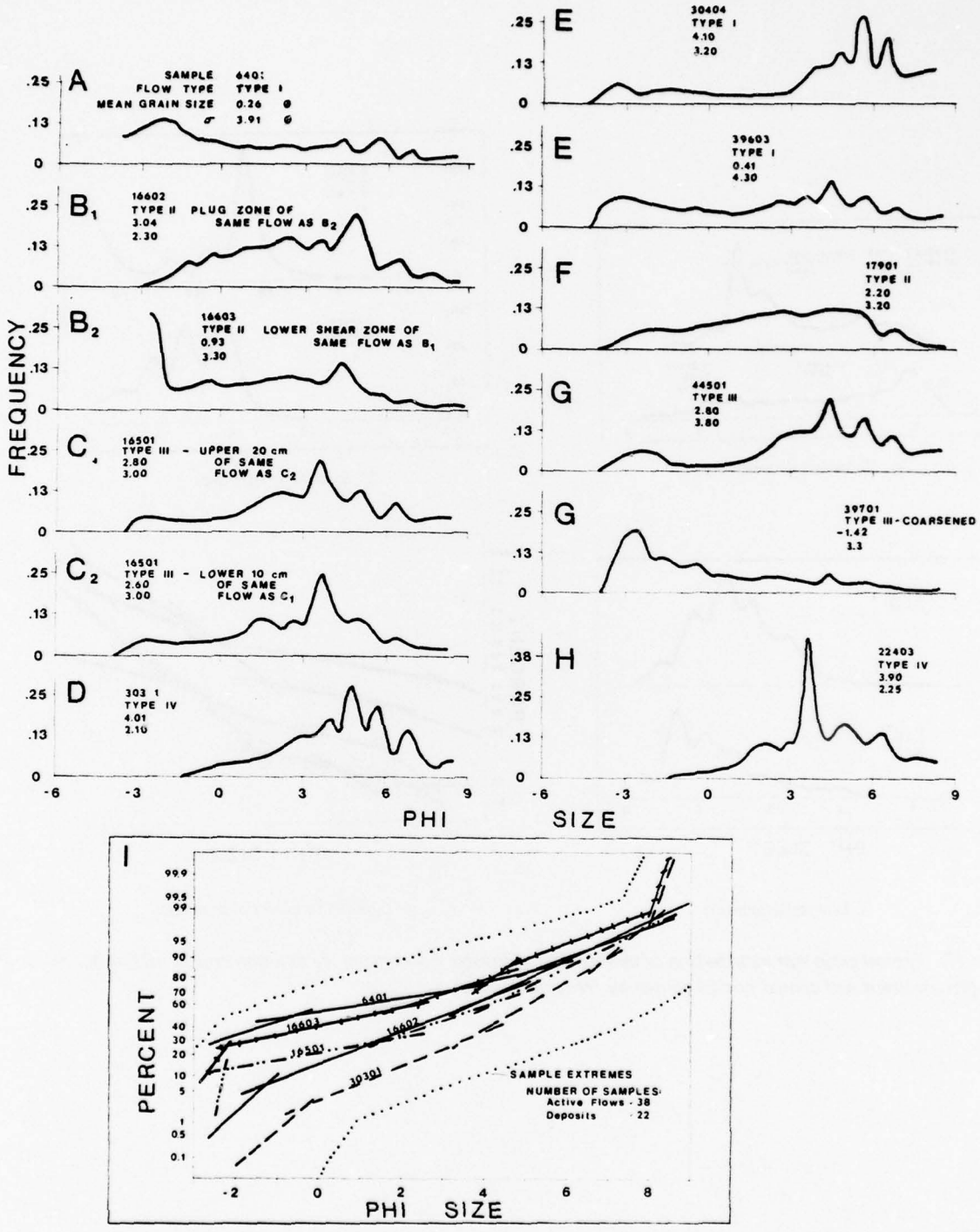
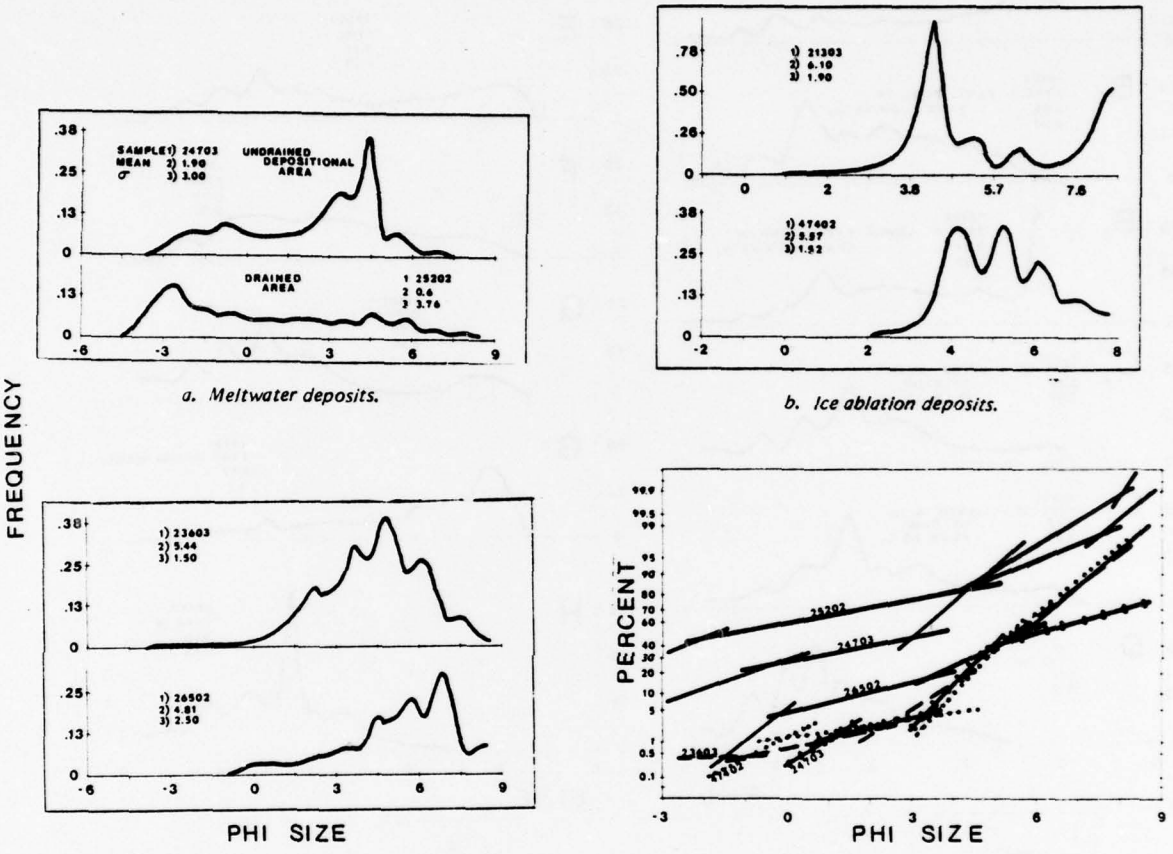


Figure 35. Representative textural variations in active sediment flows and their deposits. A, B, C and D show typical frequency curves of grain size distribution in active type I-IV flows as indicated; E, F, G and H show grain size distributions of deposits from each flow type. Cumulative curves of active flow materials and of deposits are shown in I; extremes of grain size distribution are indicated.



a. Meltwater deposits.

b. Ice ablation deposits.

c. Lacustrine deposits.

d. Cumulative curves of samples.

Figure 47. Typical grain size distribution of deposits of meltwater flow origin, ice ablation and lacustrine activity (intermittent and annual ponds) shown by frequency curves.

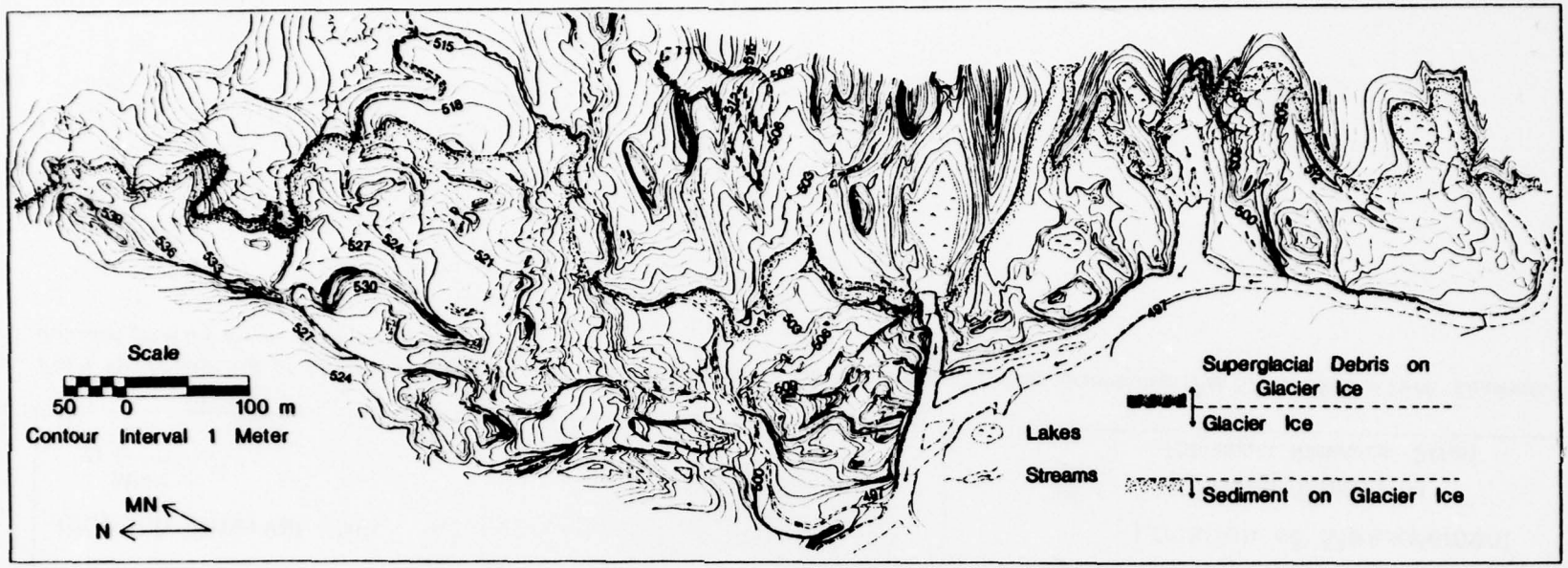


Figure 57. Topographic map of study area of terminus region, Matanuska Glacier, Alaska, 1974.

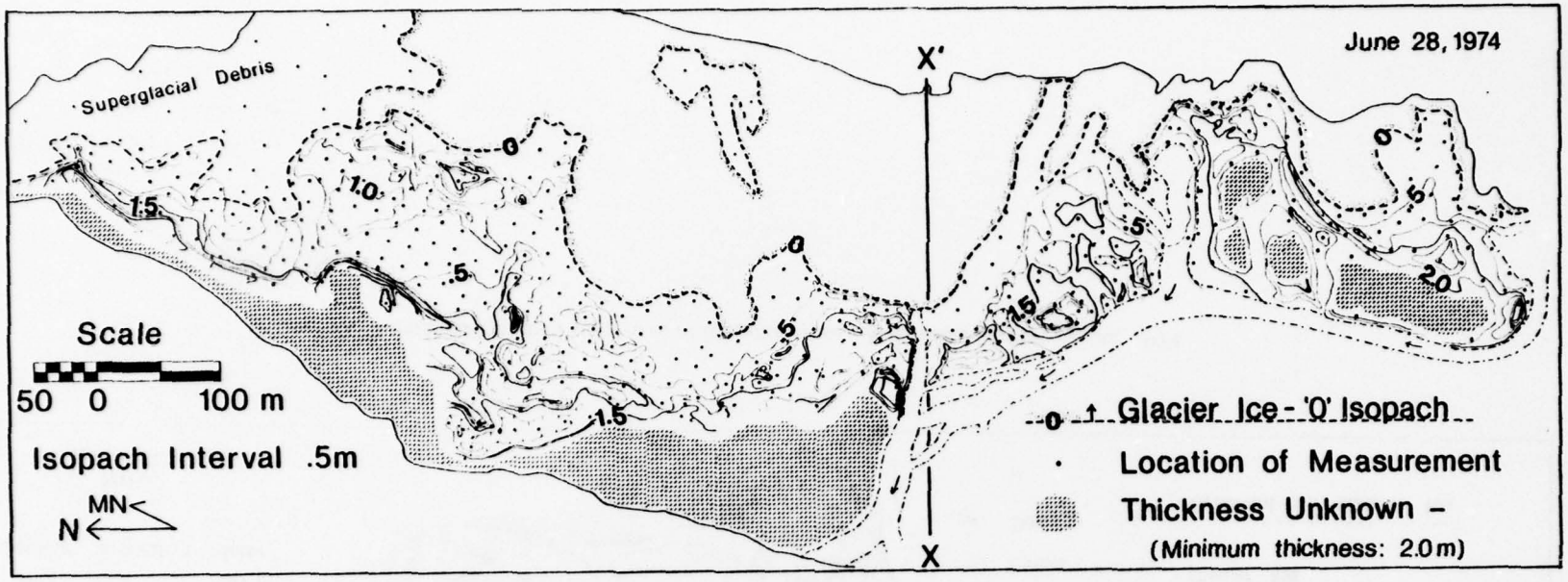


Figure 59. Isopach map of thickness of sediment covering the stagnant basal ice of terminus in area of topographic map (Fig. 57) on 28 June 1974. Thickness decreases generally toward active ice margin.

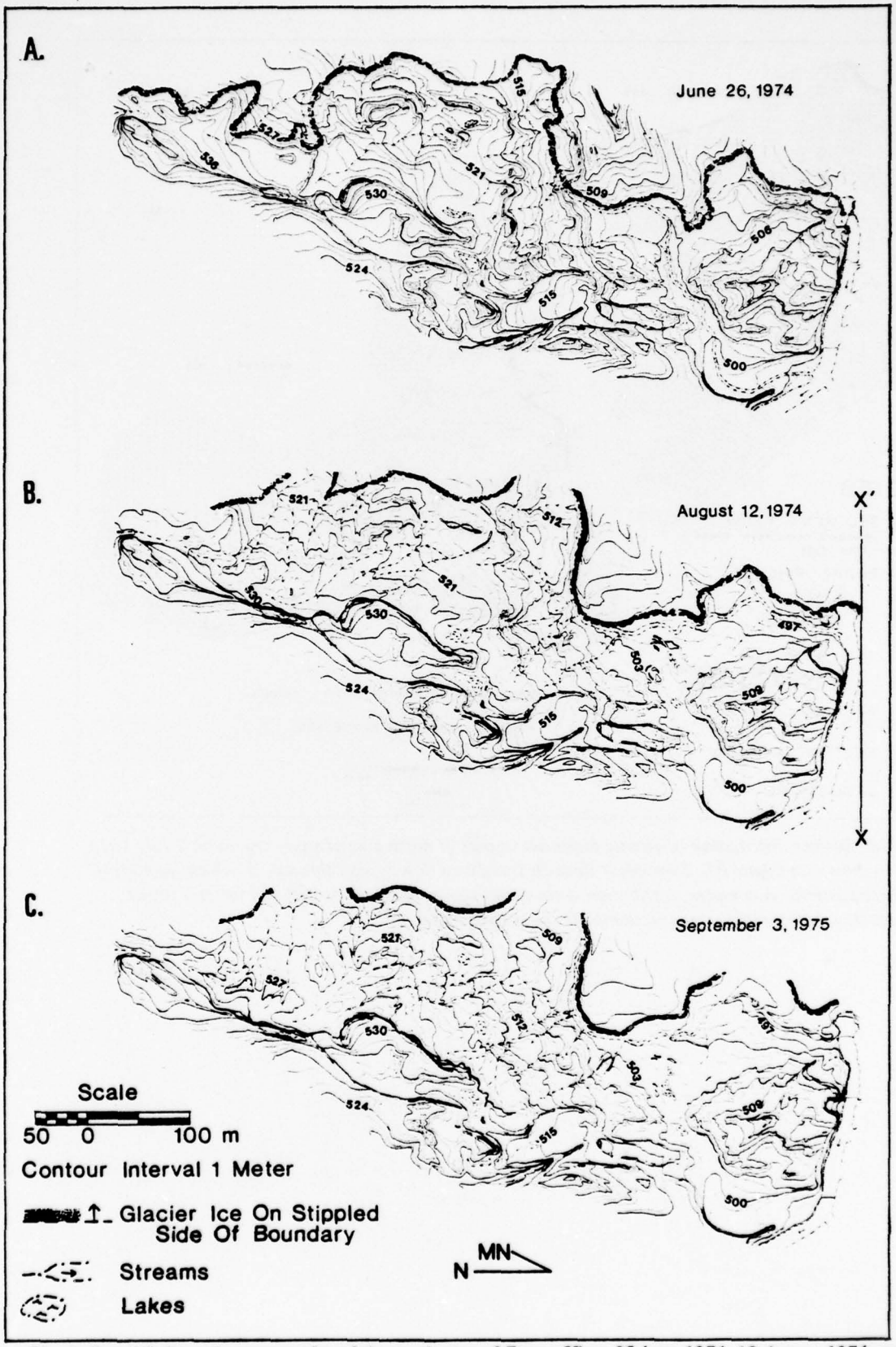


Figure 61. A, B and C show the topography of the north area of Figure 57 on 26 June 1974, 12 August 1974 and 3 September 1975, respectively. During this time period, most sediments of the mapped region underwent reworking at least 2 to 3 times, while the area of resedimentation expanded and the surface elevation decreased. Rates of change are more rapid than time between mappings.

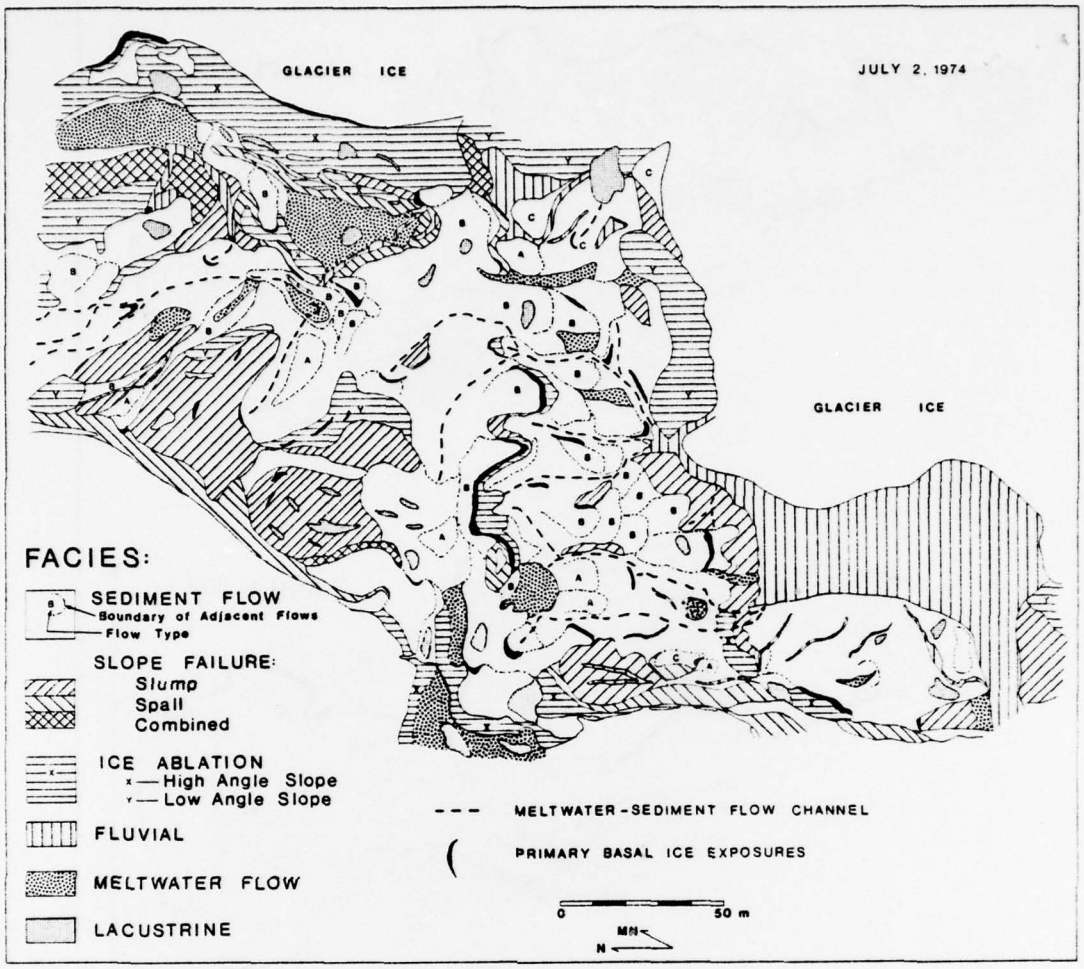


Figure 68. Surface distribution of genetic facies over a part of north area of study region on 2 July 1974. Location shown on Figure 67. Symbols A through D indicate flow types I through IV which were identified where possible. A complex distribution without definitive relationships between facies is shown. Sediment flow facies, mainly type II, dominate the surface materials.

CRREL Report 79-9



Sedimentological analysis of the western terminus region of the Matanuska Glacier, Alaska

Daniel E. Lawson

May 1979

UNITED STATES ARMY
CORPS OF ENGINEERS
COLD REGIONS RESEARCH AND ENGINEERING LABORATORY
HANOVER, NEW HAMPSHIRE, U.S.A.

Approved for public release; distribution unlimited.

SECURITY CLASSIFICATION OF THIS PAGE (When Data Entered)

Unclassified

SECURITY CLASSIFICATION OF THIS PAGE (When Data Entered)

REPORT DOCUMENTATION PAGE

READ INSTRUCTIONS BEFORE COMPLETING FORM

1. REPORT NUMBER: CRREL Report 79-9
2. GOVT ACCESSION NO.:
3. RECIPIENT'S CATALOG NUMBER:
4. TITLE (and Subtitle): SEDIMENTOLOGICAL ANALYSIS OF THE WESTERN TERMINUS REGION OF THE MATANUSKA GLACIER, ALASKA
5. TYPE OF REPORT & PERIOD COVERED:
6. PERFORMING ORG. REPORT NUMBER:
7. AUTHOR(s): Daniel E. Lawson
8. CONTRACT OR GRANT NUMBER(s): CRREL-79-9
9. PERFORMING ORGANIZATION NAME AND ADDRESS: U.S. Army Cold Regions Research and Engineering Laboratory, Hanover, New Hampshire 03755
10. PROGRAM ELEMENT, PROJECT, TASK AREA & WORK UNIT NUMBERS: 4A161102AT24
11. CONTROLLING OFFICE NAME AND ADDRESS: U.S. Army Cold Regions Research and Engineering Laboratory, Hanover, New Hampshire 03755
12. REPORT DATE: May 1979
13. NUMBER OF PAGES: 122
14. MONITORING AGENCY NAME & ADDRESS (if different from Controlling Office): 132 p.
15. SECURITY CLASS. (of this report): Unclassified
15a. DECLASSIFICATION/DOWNGRADING SCHEDULE:

16. DISTRIBUTION STATEMENT (of this Report)

Approved for public release; distribution unlimited.

17. DISTRIBUTION STATEMENT (of the abstract entered in Block 20, if different from Report)

18. SUPPLEMENTARY NOTES

19. KEY WORDS (Continue on reverse side if necessary and identify by block number)

Glaciers
Glacial deposits
Glaciai morphology
Sedimentology
Sediment transport

20. ABSTRACT (Continue on reverse side if necessary and identify by block number)

Sedimentation at the terminus of the Matanuska Glacier has been found to be primarily subaerial in a 100- to 300-m wide, ice-cored zone paralleling the edge of the active ice. Certain physical and chemical characteristics of the ice and debris of the superglacial, englacial and basal zones of the glacier indicate the debris of the basal zone, the primary source of sediment, is entrained during freeze-on of meltwater, probably surficially derived, to the glacier sole. Till formation results from the melting of buried ice of the basal zone. Melt-out till inherits the texture and particle orientations of basal ice debris; other properties are not as well preserved. Most deposits result from resedimentation of till and debris by sediment gravity flows, meltwater sheet and rill flow, slump, spall, and ice ablation. Depositional

037 100

DD FORM 1 JAN 73 1473 EDITION OF 1 NOV 65 IS OBSOLETE

Unclassified

SECURITY CLASSIFICATION OF THIS PAGE (When Data Entered)

20. Abstract (cont'd)

processes are interrelated in the process of backwasting of ice-cored slopes. Sediment flows are the primary process of resedimentation. Their physical characteristics, multiple mechanisms of flow and deposition, and characteristics of their deposits vary with the water content of the flow mass. Deposits of each process are distinguished from one another by detailed analysis of their internal organization, geometry and dimensions, and the presence of other internal and related external features. Genetic facies are defined by these characteristics. The interrelationship of processes develops a composite depositional sequence defined in terms of genetic facies associations: an upper, resedimented facies association, a middle, till facies association, and a lower, subglacial-resedimented facies association. The lateral and vertical distribution of genetic facies within the associations is mainly non-repetitive. This distribution reflects the variability in sediment and meltwater availability, local and regional slope, location of the active ice margin, and extent and thickness of the sediment cover and buried basal ice. The sequence may vary due to extensive reworking, override of the ice-cored terminus, or changes in the factors listed above. This study implies that previously interpreted tills may be of resedimented origin, multi-till sequences may originate from a single ice advance-retreat cycle, and an exhaustive study of an assemblage of properties of glacigenic materials is required for regional correlation.

PREFACE

This report was prepared by Dr. Daniel E. Lawson, Research Physical Scientist, of the Earth Sciences Branch, Research Division, U.S. Army Cold Regions Research and Engineering Laboratory. It is based mainly upon his research during 1973 to 1975 for the doctoral degree from the University of Illinois and also on more recent investigations in 1977 while at CRREL. The report was technically reviewed by P.V. Sellmann, Dr. W.F. St. Lawrence, and Dr. S.C. Colbeck of CRREL.

Field research was supported financially by Geological Society of America Penrose Grants in 1974 and 1975, an Arctic Institute of North America Small Grant Award in 1975, Sigma Xi Grants-in-Aid of Research in 1974 and 1975, Dissertation Research Grants from Graduate College, University of Illinois, in 1974 and 1975, and Shell Oil Foundation Grants through the Department of Geology, University of Illinois at Urbana-Champaign. The U.S. Geological Survey provided financial support and furnished field equipment and laboratory facilities in Alaska. The Department of Geology, University of Illinois, provided computer and laboratory facilities and field equipment.

The 1977 research was funded by DA Project 4A161102AT24, *Research in Snow, Ice and Frozen Ground*, Scientific Area 01, *Properties of Cold Regions Materials*, Work Unit 02, *Cold Regions Environmental Factors.*

The author wishes to thank Dr. George deVries Klein, thesis advisor, who initially encouraged the study and provided guidance and assistance during all stages of the research; Dr. A. Thomas Ovenshine of the U.S. Geological Survey who was instrumental in initiating the study, critically evaluating the project, and furnishing field, laboratory and financial assistance; Professor W. Hilton Johnson who discussed all aspects of the study and offered valuable suggestions on the research; and Sue Lawson for her support and encouragement throughout the study. Jean B. Kulla performed all oxygen isotope analyses in the Isotope Lab, Department of Geology, University of Illinois at Urbana-Champaign. Susan R. Bartsch-Winkler analyzed grain size distributions on the hydrophotometer at the U.S. Geological Survey, Menlo Park, California. D.W. Baker furnished a computer program for contouring equal-area nets.

Accession For
NTIS GRA&I ☒
DDC TAB ☐
Unannounced ☐
Justification
By
Distribution/
Availability Codes
Dist | Avail and/or special
A

79 07 30 095

CONTENTS

Abstract	Page
Abstract	i
Preface	iii
Summary	
Chapter 1. Introduction	1
Field site	1
Historical background	2
Chapter 2. Characteristics of the debris and ice	6
Characteristics of the facies and subfacies	7
Basal zone	7
Characteristics of the debris	11
Discussion	19
Chapter 3. Oxygen isotope analysis	21
Sampling and analysis	21
Results	23
Discussion	23
Chapter 4. Depositional processes-till formation	28
Methods of analysis	28
Environmental setting	29
Till formation	29
Chapter 5. Depositional processes-resedimentation	40
Sediment flows	40
Other resedimentation processes	71
Resedimentation process relationships	80
Chapter 6. Process distribution, sediment dispersal and depositional patterns	83
Physical characteristics	83
Sediment dispersal	89
Sedimentary facies	90
Patterns of terminus sedimentation	98
Chapter 7. Conclusions	102
Literature cited	109

ILLUSTRATIONS

Figure		
1.	Map of Alaska showing location of the Matanuska Glacier	2
2.	Map of the Matanuska Glacier with area of study indicated	3
3.	Aerial composite photograph of primary study area in western margin of the Matanuska Glacier taken in August 1969.	3
4.	Idealized stratigraphic relationships of the ice facies	6
5.	Ice zones and facies in Matanuska Glacier	8
6.	Examples of stratified ice subfacies	10

		Page
7.	Comparison of grain size components in samples from each ice facies	12
8.	Typical grain size frequency curves for debris samples	13
9.	Typical cumulative curves plotted on arithimetic probability paper for debris samples	14
10.	Typical Schmidt equal-area net distributions of pebble orientations in the basal ice	16
11.	Schmidt equal-area nets of Figure 10 contoured according to Kamb at a 2 σ interval	17
12.	Map of study area showing sample mean axes in relation to local direction of glacier flow as determined from aerial photographs taken in 1949, 1969 and 1974	18
13.	Flow lines in a valley glacier as deduced by Reid	21
14.	Partial exposure of the ice sequence in the Matanuska glacier terminus	22
15.	Location of Matanuska Glacier study area	22
16.	Logs of sample transects 1-3	24
17.	Comparison of δO^{18} values of ice samples of the diffused, dispersed and stratified facies from transect 4	25
18.	Slump-flow exposed section of the stagnant, debris-laden basal ice at the terminus edge	29
19.	Frozen, overridden interstratified fluvial and sediment flow deposits located between upper and middle sections of basal ice in Figure 18	30
20.	Rates of sediment accumulation due to melting of upper surface of buried basal ice during the 1974 and 1975 field seasons	31
21.	Weather and sediment temperature of terminus for 1974 and 1975	32
22.	Photograph of melt-out till, 0.5 m thick, over basal ice source	34
23.	Characteristics of a surface melt-out till	36
24.	Characteristics of a surface melt-out till	37
25.	Characteristics of basal melt-out till	38
26.	Sediment flow initiation	42
27.	Sediment flow source areas	43
28.	Comparison of mean grain size with water content of central part of active sediment flows sampled from across the terminus	45
29.	Comparison of largest clast in suspended transport with water content sampled from central part of active sediment flows	46
30.	Ternary diagram of grain size of composite samples of active sediment flows	47
31.	Representative frequency curves of texture of active sediment flows of different water contents derived from same source area	47
32.	Comparison of surface shear strength, porosity and bulk wet density with water content for samples of flowing and adjacent nonflowing sediments	48
33.	Idealized cross sections, transverse and parallel to direction of flow, of the four sediment flow types	49
34.	Type I flows	50
35.	Representative textural variations in active sediment flows and their deposits	52
36.	Type II and III flows	53
37.	Idealized characteristics of sediment flow system and modes of deposition	56
38.	Idealized characteristics of sediment flow deposits	59
39.	Surface forms of sediment flows	60
40.	Comparison of mean grain size of composite samples of sediment flow deposits and the bulk water content of the source flow from samples upchannel of the area of deposition	61
41.	Type I flow deposits	62
42.	Type II and type IV flow deposits	64
43.	Sediment flow contacts	66
44.	Scatter diagrams of pebble orientations in recent sediment flow deposits	67
45.	Schmidt equal-area nets of samples in Figure 43 contoured according to Kamb at a 2 σ interval	68

Page

46. Comparison of statistical data of pebble orientations in basal ice, melt-out till, sediment flow deposits and ice slope colluvium 69
47. Typical grain size distribution of deposits of meltwater flow origin, ice ablation and lacustrine activity shown by frequency curves 72
48. Meltwater flow deposits 73
49. Ice ablation sediments 73
50. Scatter, contour and rose diagrams of pebble orientations in sediments deposited by ablation of high-angle, basal ice slopes 75
51. Schematic diagram of slump of sediment on buried basal ice of low-angle slope 76
52. Schematic diagram of spall of sediment on buried basal ice of high-angle slope 77
53. Extension fractures developed in surface cover adjacent to a slope undergoing spall. 77
54. Miscellaneous features 78
55. Ice-cored slopes 79
56. Results of monitored slope retreat at stake V in 1974 81
57. Topographic map of study area of terminus region, Matanuska Glacier, Alaska, 1974. 82
58. Aerial photograph showing upper two-thirds of north area of Figure 57 83
59. Isopach map of thickness of sediment covering the stagnant basal ice of terminus in area of topographic map on 28 June 1974 84
60. Texture of the surface sediments in the study area of the terminus on 5 July 1974.. 86
61. A, B and C show the topography of the north area of Figure 57 on 26 June 1974, 12 August 1974 and 3 September 1975, respectively 87
62. A, B and C are isopach maps of sediment thickness of north area of Figure 57 on 28 June 1974, 15 August 1974 and 7 September 1974, respectively 88
63. Sediment dispersal pattern observed for active sediment flows and some recent deposits of sediment flows on 5 and 6 August 1974 89
64. Sediment dispersal pattern observed for meltwater flows and streams from active and abandoned rills and channels in early August 1974 90
65. Pebble orientations in melt-out tills 91
66. Pebble fabric in sediment flow deposits 92
67. Map of surface distribution of genetic facies in late June 1974 94
68. Surface distribution of genetic facies over a part of north area of study region on 2 July 1974 96
69. Surface distribution of genetic facies in area of Figure 68 approximately one month later 97
70. Variations in vertical facies distribution 98
71. Idealized cross section and map view of process distribution at glacier margin with regional upglacier slope 99
72. Idealized cross section and map view of process distribution at glacier margin with regional downglacier slope 100
73. Idealized development of sedimentary sequence from Matanuska Glacier terminus sedimentation 101

TABLES

Table

I. Attributes of the ice facies 9
II. Roundness of 100 pebbles as classified by Powers' scale 15
III. Results of the analysis of pebble fabric in basal ice 15
IV. Results of the oxygen isotope analysis 23
V. Characteristics of melt-out and lodgement tills 35
VI. Attributes of active sediment flows 41

		Page
VII.	Characteristics of sediment flow deposits, terminus region, Matanuska Glacier, Alaska	58
VIII.	Results of the pebble fabric analyses of sediment flow deposits	69
IX.	Characteristics of some deposits of resedimentation processes	70
X.	Backwasting rates of ice-cored slopes	81
XI.	Genetic facies classification of sediments	93
XII.	Summary of depositional processes, conditions of occurrence, and influencing factors	103
XIII.	Characteristics of the deposits, terminus region, Matanuska Glacier, Alaska	106

SUMMARY

The Matanuska Glacier is a large valley glacier in south-central Alaska. It flows north approximately 40 km from icefields in the Chugach Mountains to the head of the Matanuska River valley where it terminates about 138 km northeast of Anchorage. At the terminus, it is about 5 km wide and consists of stagnant and active ice that may be covered by debris. Its position has been relatively constant, lying within about 4 km of its present position for the last 8000 years. During Wisconsinan time, however, it extended into the upper portion of the Cook Inlet, south of Anchorage.

Adjacent to the terminus ice, sediments deposited by the glacier are ice-cored (i.e. overlie and bury stagnant ice of the glacier). They form well-defined linear or arcuate ridges, or randomly distributed mounds and depressions. Relief may exceed 40 m.

The terminus environment of this glacier represents conditions considered similar to those of continental glaciers that covered much of North America during the Pleistocene. Hence, studies of this glacier should further our knowledge of glaciers of the past and apply to analyses of their deposits.

This study analyzed sedimentation in the western terminus region of the Matanuska Glacier. The objectives of the study were to identify and analyze the processes of sediment entrainment, transport and deposition, and to characterize the debris, ice, deposits and terminus environment of the glacier. The sedimentology of active glaciers has previously received little study and consequently knowledge of sedimentation by glaciers is largely inferred from the studies of Pleistocene glacial deposits.

Sedimentation at the margin of the Matanuska Glacier is a complex interaction between ice, water and sediment under boundary conditions imposed by the terminus environment. The primary source of sediment in the terminus area is the debris transported in a thin (3 to 23-m-thick) basal zone of the glacier, in particular, within the lower stratified facies of this zone. The stratified facies ranges from 3 to 15 m thick and contains a mean of 25% debris by volume, while the upper facies of the basal zone (the dispersed facies) is thinner (0.2 to 8.0 m thick) and contains about 4% debris by volume. Above the basal zone is a thick (est. 300-m) englacial zone containing negligible amounts of sediment (mean of 0.002% by volume) except in randomly scattered debris bands. A thin (0-0.2 m) superglacial zone caps the glacier.

Most sediment in the glacier is entrained subglacially. The δO^{18} values of englacial and basal zone ice, the physical characteristics of the ice and debris of each ice facies, and the radiocarbon dates of wood from the stratified facies define the origin of the ice and debris. These data show that the stratified facies ice forms subglacially by freeze-on to the glacier sole of meltwater that may be surface-derived, and that ice of the englacial zone and the dispersed facies originates from snow in the accumulation area. Freeze-on simultaneously entrains the debris of the stratified facies. Subglacial, localized pressure-melting and freeze-on of particles of sediment appear to entrain the debris of the dispersed facies. Debris of the englacial zone is surficially derived.

Debris of the basal zone is released at the terminus by ablation of active ice exposed at the margin and by melting of sediment-covered ice that occurs in a 100-to 300-m-wide zone paralleling the active ice. The sediment on this ice exceeds 8 m in some places. This sediment cover is continually reworked by several processes that are often related to the melting and lateral retreat (backwasting) of ice-cored slopes (slopes with stagnant ice exposed in them). In fact, the bulk of these sediments were reworked and resedimented several times during 1974 and 1975.

The results of this study indicate the need to distinguish deposits derived directly from the glacier from those that are reworked and resedimented. Therefore, till is defined as sediment released directly from glacial ice that has not undergone subsequent disaggregation and resedimentation. Only about 5% of the

deposits at the terminus result from till-forming processes. This definition is required so that older deposits can be identified genetically.

Sediment flow, the downslope flow of sediments under the action of gravity, is the primary depositional process in the terminus region. It reworks and resediments debris and other deposits and induces new properties that are inherited in their deposits. The properties of active sediment flows and their deposits are primarily controlled by their water content. Sediment flows range from those of low water content, in which the gross sediment strength is the primary grain support mechanism, to those of high water content that appear fully liquefied. Sediment flows and their deposits occurring in the glacial environment have been incorrectly referred to as "flowtill." Because sediment flow is a process of resedimentation, the use of this term is inappropriate and should be discontinued.

Sediment flows are generally derived from sediment and meltwater released during ablation and lateral retreat of slopes with massive ice in their centers. Disaggregated and remolded sediment may accumulate at the base of the ice-cored slope, or it may mix sufficiently with meltwater so that flow originates directly off the slope. A rotational landslide failure of the downslope end of an accumulating sediment pile initiates a second remolding and then flow. Dense, low water content flows are apparently initiated by failure along discrete planes at the base of the sediment pile. The body of these flows possesses strength with shear limited to a thin basal zone. They are lobate, non-channelized, relatively thick (to 2 m), and they flow at a slow rate. Physical properties of the sediment appear similar throughout the body of the flow. As the water content of the flow mass increases, the zone of shear increases in thickness and a rafted, nondeforming plug forms in the central part of the flow. At even greater water contents, the entire flow is in shear. The density, maximum thickness, overall dimensions, shear strength and mean grain size generally decrease, while the degree of channelization, erosion and maximum flow rate increase. Other processes of grain support and transport that may include traction and saltation of coarse bedload materials, grain interactions, local liquefaction and fluidization, and transient turbid mixing increase in importance with increased water content. At the largest water contents, these mechanisms are reduced in effectiveness as flows become liquefied.

Sediment flow deposition results from a decrease in slope angle, thickness of the flow mass or water content. The morphology and other properties of lower water content flows are mostly retained in their deposits, but the deposits of flows containing more water retain fewer properties. Meltwater flowing in the channel after sediment flow may destroy sediment flow properties. The deposits of sediment flows are generally distinguishable from one another by their internal organization, surface features, bulk texture, geometry, and pebble fabric.

The in-situ melting of buried basal zone ice forms a type of till called "melt-out till." Rates of till deposition at the upper surface of such ice ranged from 2.0 to 24.5 cm/yr in 1974 and 1975, whereas rates at the base of this ice were at least an order of magnitude slower. This rate is influenced by the topography, thickness and other properties of the sediment cover, short- and long-term changes in weather, the debris content of the ice and the geothermal heat flow.

The properties of till formed by melting of buried basal ice are inherited primarily from the ice source because of the confined conditions under which deposition occurs. The mixing of debris during melt-out is generally sufficient to modify debris stratification and properties of individual ice strata, but the bulk texture and major variations in debris properties are often preserved. Pebbles in the basal zone are oriented with their long axes parallel to ice flow, and this orientation is preserved in the till. Melt-out increases the scatter of orientations about the mean axis of the pebble orientations and decreases the angle of dip of the mean axis to near horizontal.

Processes intimately associated with sediment flow include meltwater sheet and rill flow, slope spall and slump, ice ablation, and other minor processes. Slope failure by spalling occurs in the sediment cover overlying high-angled slopes of ice as the result of differential melting of this ice. Slumping is initiated by melting of buried ice with low-angled slopes and rotational slip of the sediment at the ice/sediment interface. Meltwater sheet and rill flows are similar to fluvial and lacustrine processes and result in an effective sorting of sediments. The ablation of exposed basal zone ice forms deposits similar in texture to the debris source when released from a high angle slope, but low angle slopes are conducive to sediment and meltwater flow removal of the finer grained material.

The sediments derived from the depositional processes are distinguishable from one another by detailed analysis of an assemblage of characteristics; the primary properties are the internal structure (including pebble fabric, deposit geometry and dimensions), and the surface, contact and deformational features. Genetic facies are defined on the basis of these characteristics. The interrelationship of processes develops a composite depositional sequence which can be defined in terms of three genetic facies associations: 1) an upper, resedimented facies association, 2) a middle, till facies association and 3) a lower subglacial resedimented facies association. The lateral and vertical distributions of genetic facies within these facies associations are nonrepetitive and without a distinct pattern. This distribution reflects the variability in sediment and meltwater availability, local and regional slope, location of the active ice margin, and extent and thickness of the sediment cover and buried basal ice. This idealized sequence varies in some places because of reworking of the deposits, or advance of the glacier and override of older deposits, causing stacking and repetition of the facies associations.

The major conclusions of this study are:

1. Most sediment transported by the Matanuska Glacier is entrained subglacially during freeze-on of water to its base.
2. Till-like deposits are not necessarily derived directly from the glacier but may result from several different, complexly related resedimentation processes. These latter processes are most important to sedimentation in the Matanuska Glacier.
3. Deposits of past glaciers that were previously interpreted as till may originate from resedimentation processes. Hence, stratigraphic sequences interpreted as composed of several tills that were deposited during different glacial advances may consist of till and resedimented materials that were deposited during a single ice advance. Historical records may therefore be incorrect.
4. Depositional processes of this glacier impart properties to the sediments that permit the identification of their origins. However, a single property is insufficient to distinguish their origins, and actually the analysis of an assemblage of properties is required.
5. In order to interpret the origins of older glacigenic deposits, an exhaustive study of numerous properties of each material is required. This study implies that genetic correlation of older glacial deposits is extremely difficult.

SEDIMENTOLOGICAL ANALYSIS OF THE WESTERN TERMINUS REGION OF THE MATANUSKA GLACIER, ALASKA

Daniel E. Lawson

CHAPTER 1. INTRODUCTION

The analysis of sedimentation by Holocene glaciers has been neglected in the interpretation of Pleistocene and ancient glacial deposits. Most of our knowledge of the processes of sedimentation by glaciers has been empirically deduced from investigations of Pleistocene glacial deposits. Sedimentation by active glaciers has rarely been studied; no quantitative sedimentological analysis of an active glacier has been conducted prior to this study.

Sedimentation in a selected part of the terminus of the Matanuska Glacier (see cover photo) was investigated in 1974, 1975 and 1977 to provide a quantitative approach to the analysis of glacial deposits. The primary goals of this study were to identify and monitor the processes of sedimentation in a selected portion of the terminus and to describe in detail the deposits formed by each process. Emphasis was placed on the formation of till and related sediments. The characteristics and origin of the debris and ice of the glacier and the physical sedimentology of the study area were analyzed to define the sedimentary environment of the western terminus region.

The problem was approached at two levels. A macroscale analysis defined the basic characteristics of the terminus environment and monitored changes in these characteristics over a period of three years. These characteristics included the topography, sediment thickness, sediment properties (such as grain size and fabric), facies distribution and sediment dispersal patterns. A mesoscale analysis examined individual processes and the deposits resulting from each process, and monitored changes in their characteristics over short periods of time (hours and days). Characteristics of individual processes (such as rate, texture, water content) and of the resulting deposits (such as texture, structure, bedform) and the relationship of processes to one another were examined. Characteristics of the debris and ice of the glacier (such as debris distribution, texture and fabric, ice crystal size and oxygen isotope content) were also analyzed.

FIELD SITE

The Matanuska Glacier (61°47′N; 147°45′)(Fig. 1) was chosen for this study because of the following factors: 1. Large size and hence relatively simple boundary conditions, 2. Occurrence in the terminus region of a large suite of sedimentary processes, 3. Lack of superglacial debris over a substantial area of the terminus, 4. Continued activity, 5. Accessibility. The characteristics of the glacier appear to represent those which approximate former continental ice sheets.

The Matanuska Glacier flows north from the icefields of the central Chugach Mountains into the upper Matanuska River Valley where it terminates approximately 138 km northeast of Anchorage (Fig. 1). The glacier drains 647 km^2 of the highest part of the Chugach Mountains (Williams and Ferrians 1961). Two major ice streams from the icefields join to form the main body of the glacier approximately 34 km from the terminus (Fig. 2). The glacier increases from 2.2-km width at the ice stream confluence to about 5.0-km width at the terminus. Most of the terminal lobe consists of apparently stagnant, debris-covered ice, the outermost regions of which are forested. The western part of the terminus, however, consists of active ice with a surface predominantly free of debris (Fig. 3). The primary area of study was located in this region.

The position of the glacier terminus has been relatively constant in the recent past. Williams and Ferrians (1961) conclude that the ice front has been located within 4 km of its present location over the last 8000 years. During Wisconsinan time, however, the glacier filled the present Matanuska River Valley and extended west-southwest into the Anchorage area where the ice in upper Cook Inlet reached elevations of 900-1200 m (Karlstrom 1965). In Late Wisconsinan time, the glacier retreated by some process not fully understood to a position southeast of its present location. Down-cutting by the Matanuska River accompanied this retreat. Readvance of the ice to within 4-8 km of the present glacier terminus took

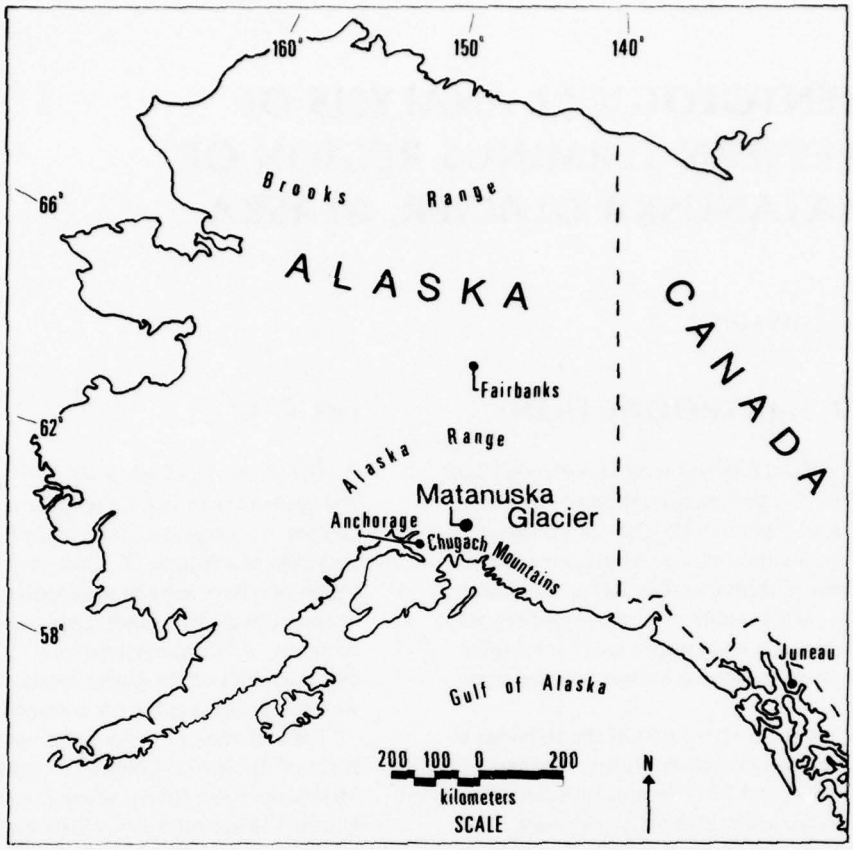


Figure 1. Map of Alaska showing location of the Matanuska Glacier.

place prior to 8000 years ago; glacier retreat and a second period of downcutting followed. Within the last 4000 years, the glacier readvanced into the deepened valley, forming end moraines located at approximately 1.6 and 0.4 km and a group of small moraines at less than 0.4 km from the most recent location of the terminus. The glacier deposited the youngest moraines directly adjacent to the present active terminus prior to 1898. Since 1898, the position of the ice front has been relatively stable, but the ice mass has thinned considerably (Williams and Ferrians 1961). Residents of the area have observed minor advances of parts of the western area of the terminus, the most recent beginning in the winter of 1966 and ending in 1970.*

Reconnaissance field mapping provides the only information on the bedrock geology of the area. These studies show that the icefields and upper two-thirds of the glacier lie on metasediments (predominantly sandstone, phyllitic graywacke, shale, minor conglomerates, and limestone) of Cretaceous age. Near the lower reaches of the glacier, metasediments also predominate, but Jurassic-Early Cretaceous granitic intrusives (primarily granodiorite and quartz diorite), Tertiary volcanics (mainly basaltic lava flows) and granitic intrusives, and Cretaceous sedimentary rocks (sandstone, conglomeratic mudstone, and siltstone) also occur (Dutro and Payne 1957, Grantz 1964).

HISTORICAL BACKGROUND

Studies of sedimentation in the Holocene glacial environments are limited; the majority are descriptive and qualitative. Early investigations documented the locations of glaciers, identified glacier movements within the historically recent past, and described the surfaces of active glaciers and the associated sediments (e.g. Garwood and Gregory 1898, Grant and Higgins 1913, Tarr and Martin 1914). Specific features on the surfaces of glaciers or the landforms which were found

* J. Kimball, personal communication, 1974).

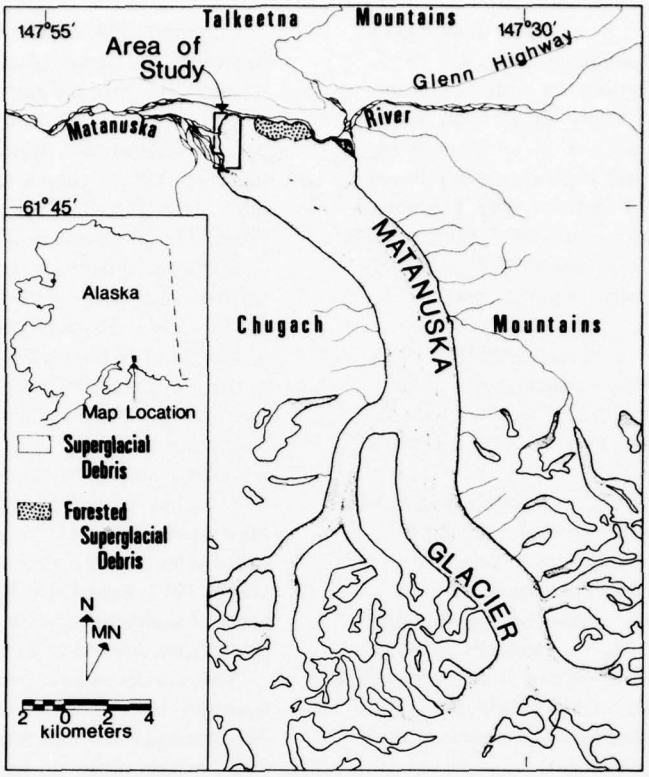


Figure 2. Map of the Matanuska Glacier with area of study indicated. Map drawn from USGS topographic maps (Anchorage Quadrangle C-2, D-2, D-3).

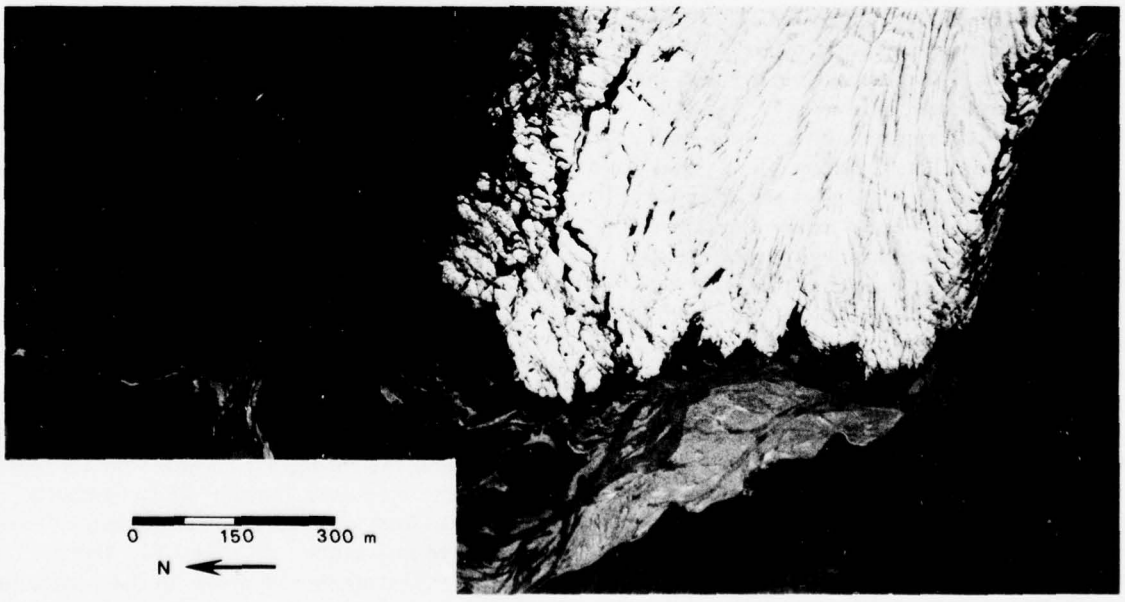


Figure 3. Aerial composite photograph of primary study area in western margin of the Matanuska Glacier taken in August 1969. Nonvegetated zone of sediment directly adjacent to active ice is underlain by glacial ice and the primary area of sedimentation. This zone increased in width to about 200 to 300 m by 1974 due to ice recession.

at the edge of active ice fronts were also described (e.g. Russel 1893, Tarr 1908, Lamplugh 1911, Ray 1935).

More recently, investigations concentrated on the proglacial environment or, rarely, the terminus region of glaciers. Proglacial fluvial processes and the form, texture and structure of their deposits are well documented (Hjulström 1952, Krigström 1962, Fahnestock 1963, Slatt and Hoskin 1968, Rust 1972, Church 1972, Boothroyd and Ashley 1975, Østrem 1975). Glaciofluvial processes and deposits are similar; specific studies of eskers, kames, and other ice-cored sediments now exposed in the proglacial zone have also been made (e.g. Lewis 1949, Jewtuchowicz 1965, Price 1966, 1969, Howarth 1971). Loomis et al. (1970) defined characteristics and physical parameters of superglacial streams.

Glaciolacustrine sedimentation is poorly documented. Gustavson (1975) and Gustavson et al. (1975) provide the most detailed investigations to date of processes of sedimentation in a proglacial lake. Ovenshine (1970) examined iceberg rafting of glacial sediments in Glacier Bay, Alaska. Howarth and Price (1969) described proglacial lakes near Breidamerkojökull, Iceland, and Stone (1963), Reid and Callender (1965), and Moravek (1973) discussed various aspects of the superglacial lacustrine environment.

Studies of sedimentation in the terminus region of modern glaciers, especially analyses of the depositional processes, are of primary importance to this research. Two conditions of the ice of the terminus are recognized: stagnant (no glacier flow) and active. Stagnant conditions of modern glaciers are typically associated with a thick cover of superglacial debris of medial and lateral moraines. This cover varies in thickness and texture. Consequently, differential melting of the buried ice results in numerous inversions of the topography (Sharp 1949). Østrem (1959) found that a sediment cover of 1 cm or less on glacier ice accelerates the melting rate, whereas sediment thicknesses greater than 1 cm inhibit melting at a rate inversely proportional to the sediment thickness. Loomis et al. (1970) determined that a 0.5-m minimum thickness of heterogeneous superglacial debris is required to prevent measurable melting; however, McKenzie (1969) calculated rates of melting due to conductive heat flow of 0.24 m per year under 4 m of coarse-grained debris in an ice-cored kame terrace. Features such as crevasses, moulins, and meltwater streams, as well as the slope and aspect of the surface and the texture of the sediment cover, impose controls on the ablation rates (Loomis et al. 1970). McKenzie (1969) recognized that slumping and sliding of debris, debris flow, and meltwater erosion reduce the thickness of the sediment cover and locally increase the ablation rate.

Clayton (1964) described the topography and hydrology of stagnant glacier ice in terms of karst topography. Tarr and Martin (1914) and Jewtuchowicz (1968), among others, discussed the general characteristics of stagnant ice. Minor features of stagnant ice, such as dirt cones (Lewis 1940, Swithenbank 1950), table rocks (Russel 1893), and drainage related features (Ray 1935), have also been described.

Superglacial debris is typically coarse, angular, and poorly sorted (Garwood and Gregory 1898, Tarr and Martin 1914). Sharp (1949) concluded that reworking of this debris in the superglacial environment reduces its size and angularity and improves sorting, but coarsens the mean grain size of the deposit through meltwater removal of the fine-grained fraction. Numerous observations indicate the source of superglacial debris to be mainly erosion of valley walls and nunataks and mass movement (rockfalls, avalanches) of material off valley sides onto the glacier surface (e.g. Tarr and Martin 1914, Reid 1968, Reheis 1975). A superglacial cover of sediment consisting of englacial debris may result from ablation of ice of the terminus (Sharp 1949).

Several authors have investigated entrainment, transport, and deposition of sediment by active glaciers. Goldthwait (1951) examined end moraine formation at the margin of Barnes Ice Cap, Canada, and concluded that debris is brought to the surface along shear planes. At the margin, ablation releases the debris, which slides down the marginal slope and accumulates as a ridge at the base of the ice slope. Differential melting increases the relative height of the ridge thus formed. Bishop (1957) concluded that a similar shear process resulted in the formation of moraines in northwest Greenland. Weertman (1961) argued that the shear hypothesis was mechanically unsound, but offered no field evidence. Hooke (1973) concluded that the shear moraines of Bishop (1957) develop from normal processes of glacial flow coupled with ice movement over snow and superimposed ice that had accumulated at the glacier margin. Boulton (1967) observed that complex hummocky moraines at the margins of several Spitsbergen glaciers resulted from ablation of thick englacial debris bands, which he concluded were derived by subglacial freezing to the glacier sole (Boulton 1970a).

The formation of till and related deposits has been examined only recently in any detail. Hartshorn (1958) recognized that mixing of meltwater with superglacial sediments produces a "flowtill" which transports materials from ice-cored, topographic highs to lower ice-cored and ice-free areas. Typically, "flowtills" show a fine-grained matrix with numerous clasts distributed throughout; sediment grain size, water content, and topographic position apparently influence their behavior (Boulton 1968). Long axes of pebbles in

"flowtills" tend to be parallel with the direction of flow and imbricated upslope (Boulton 1971). "Flowtills" occur in association with fluvial and lacustrine sediments as well as other "flowtills," and vertical sequences of till-outwash-till that are not indicative of glacier movements may develop by this process (Boulton 1968).

Boulton (1970b) recognized two other types of till: melt-out till, which forms as the result of melting of ice buried beneath a stable overburden, and lodgement till, which forms subglacially as the result of stagnation and overriding of debris-rich basal ice followed by melting in-situ, pressure-melting of basal ice against bedrock obstructions, or increased frictional drag between particles that are in traction in the glacier sole and subglacial materials (Lavrushin 1970a, Boulton 1975). Melt-out till formation was not observed by Boulton, but supposed deposits of melt-out origin showed englacial fabric preservation. With the exception of a reduced angle of dip, the clast orientations in the plane of deposition are similar to those of the ice source (Boulton 1971). Pebbles in fluted melt-out till observed at Spencer Glacier, Alaska (Lawson 1976), are aligned parallel to glacier flow at deposition; however, post-depositional changes increase the scatter in pebble orientations.

The character of subglacial lodgement tills is affected by the process of deposition and by deformation caused by subsequent glacial flow. Pebble fabrics of lodgement till formed by pressure melting show some variations from their ice source. In some places, fabrics are related to the underlying bedrock configuration rather than the direction of ice flow (Boulton 1971). Lavrushin (1970a, 1970b) concluded that the characteristics of "ground moraine" (lodgement till) reflect the "internal dynamics of glacier movement" and recognized "dynamic" facies whose properties are determined by the mode of ice flow at deposition. Mickelson (1973) used lodgement till fabrics and historical data on deglaciation to determine that the rate of deposition of lodgement till beneath Burroughs Glacier, Alaska, was 0.5 to 2.5 cm/yr. Boulton and Dent (1974) measured rates of 1 to 2 cm/yr beneath an Icelandic glacier.

Textural variations in glacial sediments are well-known, but little studied. Slatt (1971) recognized in samples taken from ice-cored material adjacent to 10 Alaskan valley glaciers two sediment types: subangular amodal and subrounded to rounded modal. Slatt concluded that the first was the product of glacial erosion, frost action or both, and the second was the result of reworked proglacial deposits which had been reincorporated into the glacier during an advance. Buller and McManus (1973) recognized three distinct grain-size distributions in samples from Pleistocene and modern glacial deposits and, assuming that physically weathered rock was their source, concluded that subsequent modification results from the addition of fresh material during flow, comminution with transport, and grain subtraction during deposition. Reheis (1975) concluded that the degree of roundness, presence of striations and amount of polish distinguish englacial material entrained in an alpine glacier by subglacial erosion from material deposited on the glacier by rock falls and avalanches.

Boulton (1972a) formulated a qualitative model of deposition by continental glaciers, based on his observations in Spitsbergen, that considers both till and ice contact sedimentation. Although the model indicates the complexity of sedimentation by glaciers, it fails to provide detailed description and analysis of the depositional processes and suitable criteria for recognition of deposits resulting from each of the processes. Further, neither seasonal effects (Hewitt 1967) nor post-depositional changes are considered. Boulton and Dent (1974) concluded that rapid changes, most within 10-20 years after deposition, occurred in the texture and structure of a currently forming lodgement till in Iceland. Post-depositional changes in the texture and density of the till result from subglacial shearing and crushing and from erosion by wind and water. Rapid changes of similar effect were observed at the surface of ice-cored melt-out till (Lawson 1976). Boulton et al. (1974) concluded that the structure and fabric as well as the texture of lodgement till may be altered by glacial flow after deposition.

Shaw (1977) recently described a general model for deposition by arid polar glaciers, in contrast to Boulton's model based upon humid polar glaciers. Tills in this environment differ from those described by Boulton (1972a) in that they retain properties of debris originating during transport.

CHAPTER 2. CHARACTERISTICS OF THE DEBRIS AND ICE

Selected characteristics of the Matanuska Glacier, Alaska, were analyzed to determine the origin of the ice and debris and the relationship of debris and ice properties with those of deposits derived from these materials. Characteristics of the debris are the products of the source material and of its entrainment and transport by the glacier. The debris of a glacier may be introduced at the surface, generally from valley walls and nunataks, or derived subglacially from the bed of the glacier. Whereas the processes of addition of material at the surface are accessible to study and relatively well-known, processes of subglacial entrainment are difficult to observe and poorly understood. Theories of subglacial debris incorporation (e.g. Weertman 1961, Boulton 1972b, 1975) remain largely unproven. Analyses of ice and debris characteristics provide an indirect means of defining the processes operative at the glacier sole.

In this report, *debris* refers exclusively to sediment in transport by glacial ice. It is found in three zones with varying boundaries which are described as *superglacial, englacial,* and *basal. Basal* refers to the lower, relatively thin and often debris-laden portion of the glacier including the sole, where the character of the ice and debris reflects their interaction with subglacial materials during flow. The basal zone ranges from 3 to 15 m thick in the Matanuska Glacier. *Englacial* designates the major part or body of the glacier that is not affected by surface and subglacial processes. The thickness of this zone in the lower part of the accumulation area of this glacier is estimated at 300 m for an assumed basal shear stress of 1 bar. *Superglacial* refers to the thin surface layer of the glacier; here, surface processes such as freeze-thaw influence the characteristics of the debris and ice.

Field observations in 1973 of the characteristics of the ice and the relative concentration and mode of distribution of debris in it were used to define ice facies and subfacies in the basal and englacial zones of the glacier. Properties of the superglacial zone varied little in the area of study and therefore no facies were defined in this zone. The four ice facies are the upper *dispersed* and the lower *stratified* facies of the basal zone and the *diffused* and *banded* facies of the englacial zone (Fig. 4). In the stratified facies, three ice subfacies were also defined: the *discontinuous, suspended* and *solid* subfacies. During 1974, 1975 and 1977, field and laboratory analyses of the debris content, oxygen isotope content, crystal size and other properties of the ice, and the texture, fabric, degree of roundness and mode of distribution of the debris were conducted.

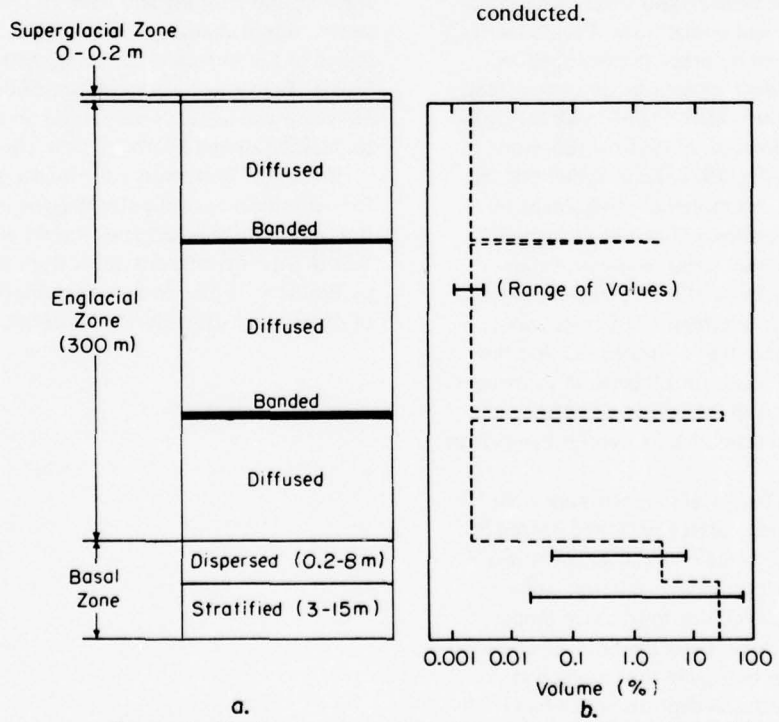


Figure 4. Idealized stratigraphic relationships of the ice facies (a). The mean and range of debris content by volume percent for samples from each facies are shown (b).

CHARACTERISTICS OF THE FACIES AND SUBFACIES

Samples obtained throughout the study area revealed major differences in ice and debris properties, which vary between and within each zone of the glacier. The characteristics of the ice and the quantity and distribution of debris define ice facies and subfacies. The stratigraphic relationships of the facies are shown schematically in Figure 4. Table I summarizes the attributes of each facies.

Englacial zone

Characteristics of the diffused facies, which composes most of the englacial zone, are relatively uniform throughout the glacier. This facies consists primarily of white, coarse-bubbly ice and blue, coarse-clear ice (Kamb 1959) (Fig. 5). The white ice grains are coarse (2 to 20 or more mm in diameter) and contain numerous spheroidal bubbles that are often elongated in the up- and downglacier directions. Less often, fine-grained ice inclusions occur. The blue ice is also coarse (20 to 100 mm in diameter) but predominantly free of bubbles. Generally, fine-grained debris is distributed uniformly in this ice; occasionally, zones of ice containing more abundant debris form a sedimentary layering. Also, sand to granule size aggregates of clay-size particles are sometimes present. For 20 samples, the debris content was consistently around 0.002% by volume (Fig. 5). Concentrations of about 0.05 to 0.1% were measured in ice displaying sedimentary layering. Superglacial debris incorporated into this facies also results in locally abundant debris concentrations. Angular pebbles, cobbles and boulders are scattered widely throughout this facies. Detailed observations of the structural features of this ice were not made; however, a weak foliation was observed in some areas.

The banded facies (debris bands) is distributed randomly throughout the englacial zone (Fig. 5). Near the margin, the debris bands usually dip steeply upglacier; some have near vertical orientations. Upice from the terminus, they generally dip less steeply and most lie subparallel to sedimentary layering and debris stratification. Near the ice margin, they often show no relationship to these features. Debris concentrations of up to 25% by volume were measured in the banded facies, although more abundant concentrations estimated at 50 to 75% were observed in the field. The thickness of individual bands ranges from about 0.02 to 0.5 m. Debris bands are distinguished from sedimentary layering by their higher, but internally variable debris content, random distribution, tendency to lens-out in a lateral direction, and generally coarser texture.

Basal zone

Facies

A distinct, relatively planar contact, resulting from a rapid change in the debris content of the ice, separates the dispersed facies of the basal zone from the englacial zone (Fig. 5). The debris content of the dispersed facies ranges from 0.04 to 8.4% by volume; the mean of 16 samples is 3.8% (Fig. 4). Cla[illegible]hrough pebble-size debris is distributed uniformly (rarely in small clusters) in ice of the dispersed facies (Fig. 5). The ice structure is not well-defined and the ice rarely contains bubbles. Ice grains tend to be smaller than those in the englacial zone (10 to 40 mm diameter), but significantly larger than those in the stratified facies. The color of weathered ice is white whereas at depth it is black to very dark blue to clear. The thickness of the dispersed facies ranges from 0.2 to 8.0 m across the terminus, but over short distances it remains relatively constant.

An irregular but well-defined boundary separates the stratified and dispersed facies of the basal zone. The abrupt decrease in grain size of the ice, rapid increase in debris content and onset of debris stratification mark its location (Fig. 5). Although the dispersed-stratified facies contact is sharp, stones and occasionally granule- to cobble-size aggregates of sediment may cross it. These aggregates consist of clay- to pebble-size particles that often contain interstitial ice. Ice is very fine-grained, generally less than 2 mm in diameter (exceptionally 10 mm), and appears as lake ice. Due to the debris content, the ice is black in an exposure but once removed from the glacier, it is clear. Most ice is bubble-free. When bubbles occur, they are generally elongated in the direction of ice flow, often contain or are adjacent to particles and aggregates of sediment, and tend to be concentrated along planes that parallel the debris stratification.

Stratification results from the alternation of layers or zones of ice containing abundant debris with those containing much less debris. Although these strata are referred to as layers or zones, they may actually be found upon close inspection to be lenses, pods, or discontinuous layers that are unconformably or conformably interstratified (Fig. 5). Debris content of individual strata ranges from 0.02 to 74% by volume with a mean for 45 samples of 25%. Stratification lies subparallel to the overall zonation of the glacier. In the terminus, strata usually dip 5° to 85° upglacier. In a few places, strata are overturned and in one part of the terminus, where the glacier bed slopes away from the ice front, they dip downglacier. Layer



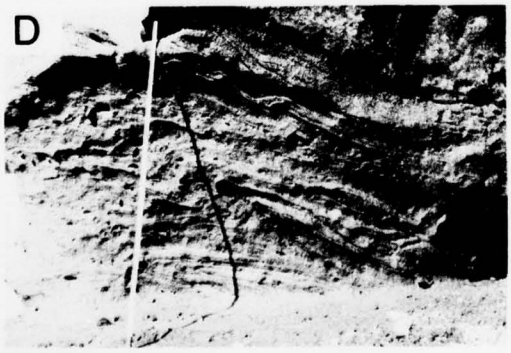
a. Englacial zone with superglacial lake near ice margin. White ice is the diffused ice facies; black layers are banded ice facies. Vertical distance from lake surface to top of upper spire is about 50 m.



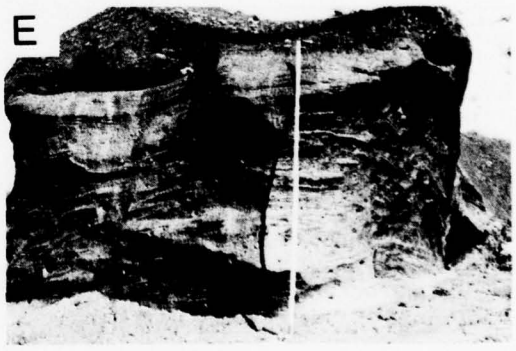
b. Closeup of debris band (steeply dipping to right) in diffused ice facies.



c. Partial exposure of the ice facies sequence at the margin of the Matanuska Glacier. End of 2-m-long stick rests on dispersed facies of the basal zone, just above the contact between the dispersed and stratified facies. White ice at top of photo is diffused facies. Uniform distribution of debris in the dispersed facies contrasts with debris stratification in the stratified facies.



d. Upper part of the stratified facies of the basal zone. Ice flow from right to left. The well-defined stratification, random dispersal of gravel clasts, thrust faulting and folding of strata, and large debris content are shown. Sharp, unconformable contact with dispersed facies is evident in top right of photo. Scale is 3 m long.



e. Stratified facies (full length of 3-m scale) and upper, dispersed facies. Ice flows towards camera location. Figure 5d shows ice face trending into photo at right.

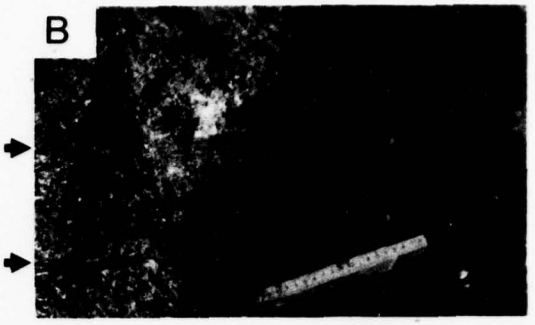
Figure 5. Ice zones and facies in Matanuska Glacier.

Table I. Attributes of the ice facies.

Zone / Ice facies / Subfacies	Thickness (m)	Features	Ice: Grain diameter (cm)	Ice: Color	Ice: Debris content (vol %)	Debris: Internal distribution and features	Debris: Texture (Max. - 5φ) (Mean, σ - φ)	Debris: Pebble roundness	Fabric
Superglacial	0-0.2	Ice surface cover					Gravel to sandy gravel M: −3-1 σ: 1.5-3.3	Very angular to angular	
Englacial									
Diffused	Estimated at 300	Ice massive to foliated; minor sedimentary layering	2-10	White to blue	0.002 (rarely 0.1)	Uniform, occasional increase in debris to form layering	Silt to sand M: 2-4 σ: 0.9-1.4	Angular	
Banded	0.02-0.5	Random distribution in diffused facies; gentle to steep up-glacier dip; lateral extent variable	Variable	White	<50-75	Apparently random; massive	Silt to gravel M: −1-6 σ: 1.5-3	Very angular to angular	
Basal									
Dispersed	0.2-8	Uniform in appearance; upper contact distinct and planar; horizontal to up-glacier dip	1-4	White at surface; black to clear at depth	0.04-8.4	Uniform, massive	Sandy gravel to gravelly sand M: −1-1 σ: 1.5-3	Subangular to angular with minor sub-rounded to round	
Stratified	3-15	Stratification, often showing internal deformation; down-glacier to steep up-glacier dip; irregular, sharp upper contact; subfacies interlayered	<0.4 (exceptionally 1)	Black at surface; clear at depth	0.02-74	Layers, lenses, zones compose strata; thin and thicken rapidly; lateral extent limited	Silt to sand to gravel	Rounded to subrounded	Strong single mode; mean axis (V_1) parallels local ice flow; S_1>0.8
discontinous	0.05-2				Variable (0.02-36); dependent on sampling technique	Lenses, layers, platelets, aggregates aligned subparallel to stratification; debris streaming	Silt to sandy silt M: 3.5-6.5 σ: 1.3-1.9		
suspended	0.001-1.2				0.02-60	Suspended particles and aggregates without orientation	Silt to silty sand M: 4.3-6 σ: 1.3-2.5		
solid	0.01-1.7				>60	Well-defined layers; may show sedimentary structures	Silt to gravel M: −2.5-5 σ: 1-2.6		



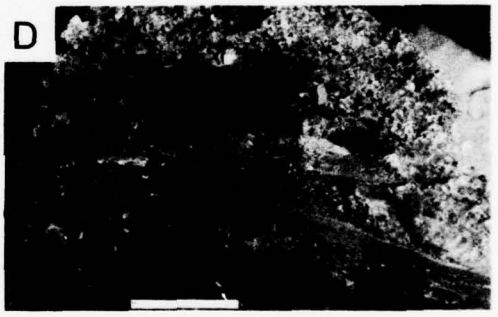
a. Complex relationships among stratified ice subfacies. Scale (15 cm long) marks content of upper, thick, low debris content suspended subfacies layer (only base shown) and a lower zone of alternating thin solid and suspended subfacies layers. Individual stones and aggregates cross this boundary. Brackets mark a 20-cm-thick suspended subfacies layer. Lower third of photo consists of alternating high debris content suspended and solid (smooth, dull gray) subfacies layers and lenses. Lack of gravel-size particles is shown.



b. Stratified basal ice consisting of lower solid ice subfacies of normally graded pebbles, a central zone of alternating layers of silt-laden discontinuous and solid subfacies, and an upper zone of suspended subfacies containing sand and pebble grains. Arrows mark approximate location of contacts. Scale in centimeters.



c. Piece of stratified basal ice consisting of discontinuous subfacies of silt plates which are aligned subparallel to one another, the solid subfacies layer in the sample, and debris stratification of the basal zone. Scale in centimeters.



d. Debris-laden zone overlain and underlain by low debris content suspended and discontinuous subfacies layers. Central zone consists of thin, sandy silt solid layers separated by sandy to pebbly, high-debris-content suspended layers. Layers in this zone are often abruptly terminated, as shown by the solid layers at the left. Bar is 10 cm long.

Figure 6. Examples of stratified ice subfacies.

thickness ranges from 0.001 to 2.0 m with most layers less than 0.3 m thick. Layers show limited lateral extent (maximum 50 m) and thin and thicken rapidly. Total thickness of the stratified facies ranges from 3 to 15 m.

Stratification permits the development of structures. Structural features include thrust faults and folds developed transverse and parallel to the direction of ice flow (Fig. 5). The effects of deformation on active ice are, however, localized. For example, thrust faults offset the debris stratification and facies contacts generally one meter or less and have little effect on the stratigraphic sequence of the glacier.

Subfacies

Subfacies represent differences in the mode of debris concentration of individual strata. Figure 6 shows examples of each subfacies and some of their

diverse modes of occurrence. Ice of the *suspended* subfacies contains suspended particles and aggregates of fine-grained sediment without a preferential orientation. Granules and pebbles are sometimes present and they may transect layer contacts. Debris content ranges from 0.02 to 55% by volume in layers that range in thickness from less than 0.001 to 1.2 m. This subfacies includes the relatively pure ice that occurs throughout the stratified facies.

Ice is an interstitial component in the *solid* subfacies. Individual strata are well-defined layers in contrast to "strata" of the discontinuous and suspended subfacies which tend to have gradational and poorly-defined boundaries. Debris content exceeds 50% by volume. Layers range in thickness from 0.01 to 1.7 m with 0.1- to 0.15-m-thick layers most prevalent. Suspended layers with low debris contents (less than 1%) and without bubbles often lie beneath solid layers. Pebbles and aggregates of sediment protrude from the base of these solid layers into this clean ice.

Sediments that are internally massive and those with prominent sedimentary structures were observed in the solid subfacies. Undisturbed sedimentary structures include parallel laminations, graded bedding, and small scale cross bedding, apparently of fluvial origin, and laminated silts, apparently of lacustrine or meltwater sheet flow origin. Some of these structures are unconformably terminated at their base.

In contrast to the distinct layers or other forms in which the solid and suspended subfacies occur, the *discontinuous* subfacies is a zone of ice containing irregular aggregates of mostly fine-grained sediment. Some bubbles may be contained in the ice associated with the debris. The lenses, discontinuous layers, and platelets lie subparallel to the stratification of the basal zone, while irregular aggregates and individual stones lie along and mainly project below planes that parallel the stratification. In plan view, debris and bubble cavities are generally aligned in the apparent direction of ice flow, but they appear randomly dispersed on this plane.

Individual "strata" of the discontinuous subfacies may thin and thicken rapidly and are often slightly deformed. The thickness of these zones ranges from 0.05 to 2.0 m. Lateral extent may vary from a few centimeters to tens of meters. Thickness of the entrained sediment ranges from less than 0.5 mm for platelets to 200 mm for aggregates. Although individual lenses and layers rarely exceed 0.5 m in length, they often overlap to form a mostly continuous zone of ice with a high debris content.

Subfacies are complexly distributed in the stratified facies without quantifiable, systematic relationships between them. Each was observed in contact with the other. The solid subfacies was not, however, observed in contact with the dispersed facies, whereas the more prevalent suspended and discontinuous subfacies occur throughout this facies. In general debris-poor ice of the suspended subfacies occurs as a "matrix" throughout the entire facies. In one part of the terminus, suspended layers about 5 mm thick containing about 35 to 50% debris by volume alternate with suspended layers of similar thickness containing less than 1 to 5% debris, suggesting repetition of some process of entrainment.

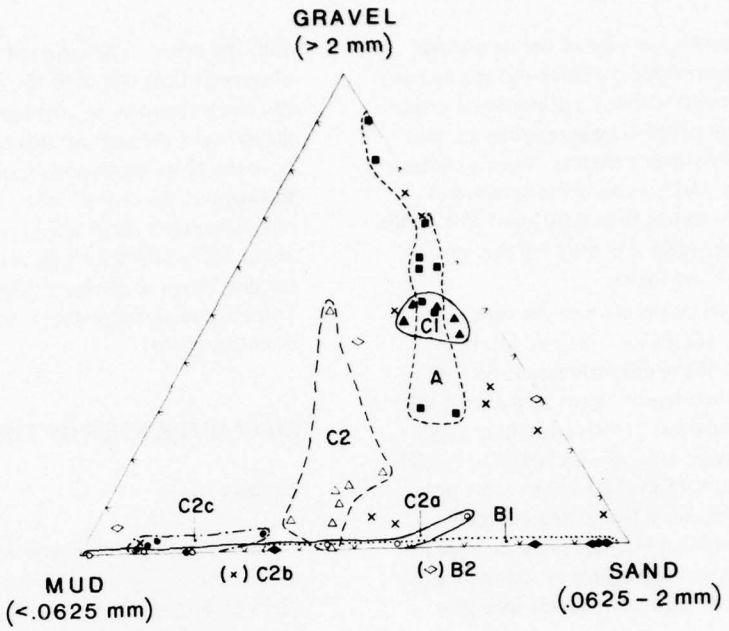
CHARACTERISTICS OF THE DEBRIS

Texture

The texture of the debris was analyzed by sieving at -5 ϕ and at ½-ϕ intervals for the grain size range of -2.75 to 4.25 ϕ. The silt- and clay-size particle content was determined by hydrophotometer using the procedure of Jordan et al. (1971). Moment measures were determined by computer analysis of sieve weights. Frequency curves were derived by computer by fitting a spline curve to the cumulative size distribution of each sample and differentiating that curve to yield the continuous size-frequency distribution. Burger (1976) discussed a similar procedure.

Each ice facies is texturally distinct. A comparison of the proportion of standard grain-size components shows a grouping by facies and in two of the three subfacies (Fig. 7). The solid subfacies does not follow this pattern and represents texturally each of the other facies and subfacies. Fine-grained sediment is transported almost exclusively in the stratified facies of the basal zone. Silt, the ubiquitous "glacial flour," is primarily transported in the discontinuous and suspended subfacies. Clay-size particles constitute less than 3% of most samples. Coarse-grained sediment is concentrated in the superglacial zone and dispersed facies. The textural similarity of the dispersed facies and superglacial zone was inadvertently introduced by restricting the sample size to particles less than 32 mm in diameter. Superglacial debris consists of 40 to 80%, by *area*, particles greater than 32 mm in diameter, whereas grains larger than 32 mm in diameter were rarely observed in the dispersed facies.

Grain-size frequency curves (Fig. 8) demonstrate the polymodal nature of debris and also reveal the textural groupings shown in Figure 7. These groupings result because facies contain a limited range of particle sizes and differ in their primary modal size fraction. For example, the grain size of the suspended facies is restricted to particles less than 0.0625 mm in diameter;



A – Superglacial zone
B1 – Diffused facies
B2 – Banded facies
C1 – Dispersed facies
C2a – Discontinuous subfacies
C2b – Solid subfacies
C2c – Suspended subfacies
C2 – Stratified facies composite

Figure 7. Comparison of grain size components in samples from each ice facies; note that only the solid subfacies debris lacks a preferred size distribution. Textural diversity and poor to very poor sorting characterize the assemblage of debris samples.

the dispersed facies ranges from 16 to 0.0625 mm; and the superglacial debris is greater than 1 mm in size. Cumulative curves of the samples shown in Figure 8 are presented in Figure 9. The textural similarities and differences are less apparent in these curves. The envelope for the cumulative curves of all samples analyzed in this study reveals a much wider grain size distribution in debris samples than in till samples at active glacier margins (Boulton 1976). These data suggest that mixing of the debris occurs during and following its release from the glacier. Thus, sediments are not transported in the Matanuska glacier as a heterogeneous dispersal that contains particles of all sizes present in the ice, as the "classic" till implies, but in texturally distinct units. The restricted grain size distribution of a given facies reflects either an initially size-segregated source, the effects of entrainment or both. The extreme variations in the grain size distribution of the solid subfacies indicate the source of its sediment, rather than the process of entrainment, determined the texture of this subfacies. Whatever its process of entrainment, it did not significantly affect the texture of the source material.

These differences in the texture of the facies and subfacies also indicate that the textural similarity of any one till must result from the process of deposition and not from transport as concluded by Goldthwait (1971). If the debris sequence of this glacier were deposited by simple removal of the ice "matrix," a recognizable sedimentary sequence would result. Because all particle sizes are present in the basal zone, mixing of adjacent layers during release of the debris from the glacier would produce a texturally diverse, poorly sorted deposit. The size distribution of composite samples of adjacent layers in the stratified basal ice (Fig. 7) confirms that mixing of these size-segregated populations produces a uniform size distribution. Thus, the analysis of texture suggests that whereas the processes of entrainment result in textural subpopulations in the glacier, the processes of deposition most often result in mixing and elimination of these subpopulations. Analyses of the depositional processes and deposits in the terminus region of the Matanuska Glacier in this study indicate that most of the debris does undergo significant homogenization prior to final deposition. Only melt-out tills show varying degrees of preservation of ice and debris properties.

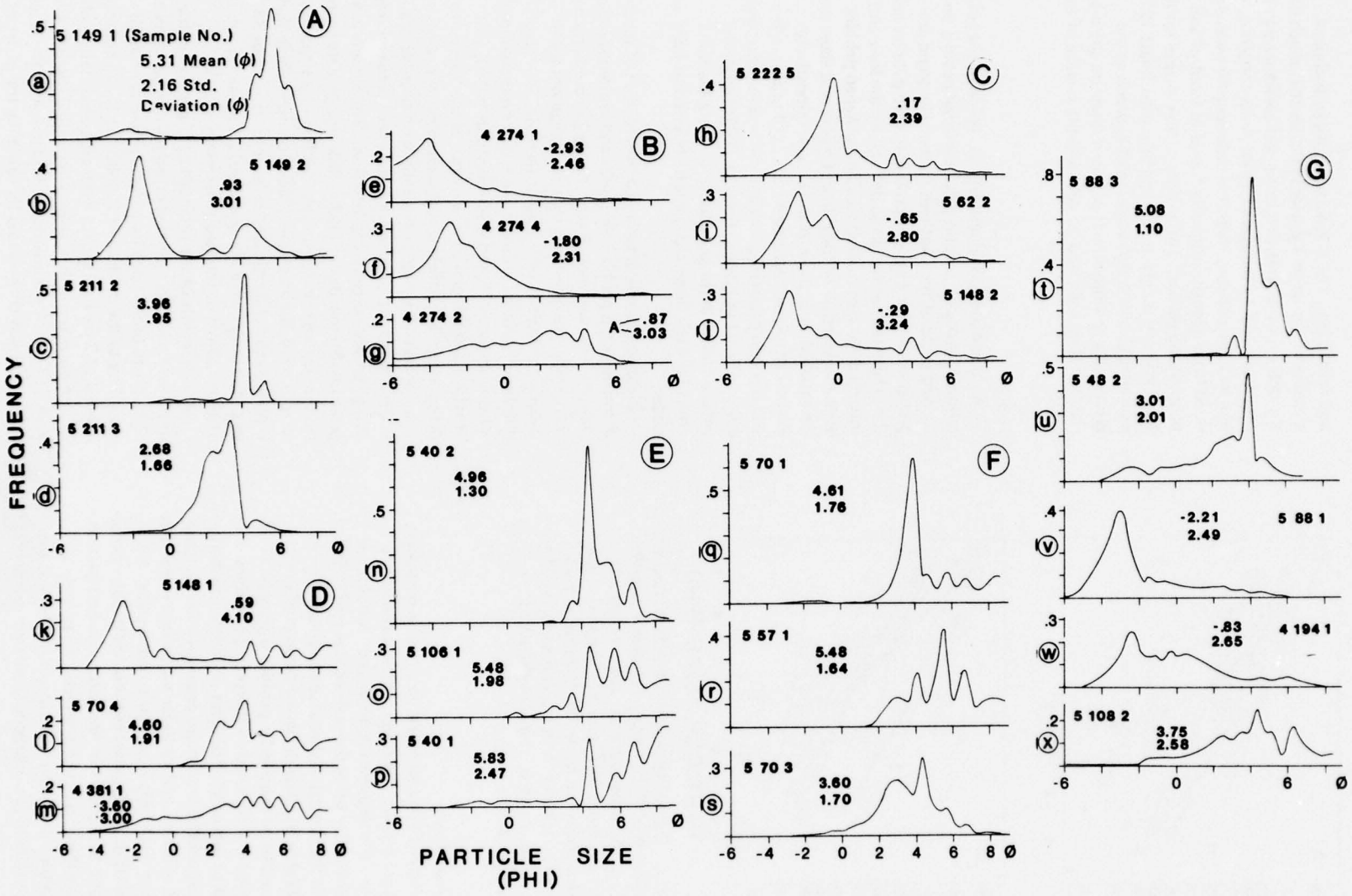


Figure 8. Typical grain size frequency curves for debris samples of: A) the banded facies (a, b) and the diffused facies (c, d), B) superglacial debris, C) the dispersed facies, D) composites of the stratified facies, E) the suspended subfacies, F) the discontinuous subfacies, and G) the solid subfacies. In set D, k is a composite of solid and suspended subfacies, l of suspended and discontinuous subfacies, and m of all these subfacies. Cumulative curves for each sample are shown in Figure 9.

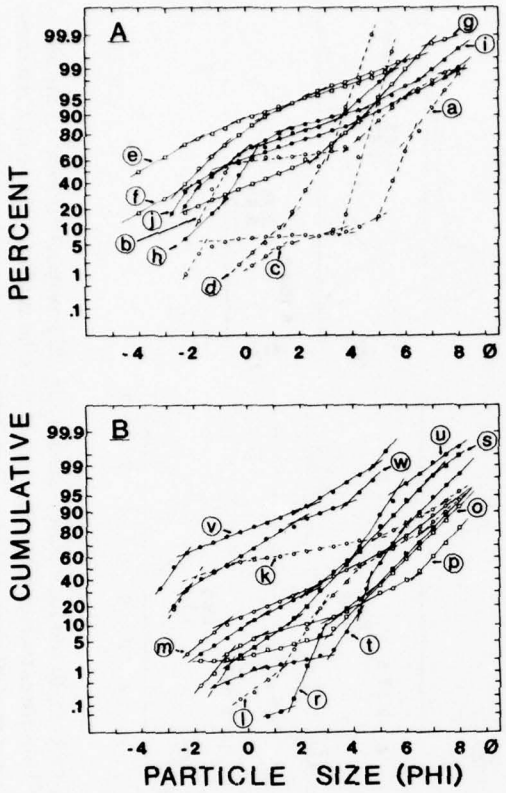


Figure 9. Typical cumulative curves plotted on arithmetic probability paper for debris samples. Small circled letters refer to same letters and samples as shown in Figure 8. Samples of the stratified facies are shown in B; other sets are shown in A. Curves for samples n and x are similar to curves t and o, respectively, and were omitted for clarity.

Particle roundness

The degree of roundness of particles, in particular those of pebble size and larger, varies distinctly in each zone. The degree of roundness of pebbles was estimated visually using the scale of Powers (1953). Pebbles in the superglacial zone are angular to very angular (Table II). The dispersed facies contains mostly angular to subangular pebbles with only a small fraction of rounded to subrounded pebbles. Rounded to subrounded pebbles dominate the stratified facies; pebbles with more angularity were seldom observed. Granule and sand-size particles are generally subangular; coarse silt is angular to subangular. Englacial particles are angular, but too few pebbles occur in this zone to permit a comparative visual estimation.

Because the degree of roundness of a particle is related to the abrasion it experiences, pebbles of the stratified facies have undergone significant transport and reworking. The normal passivity of sediment transport in or upon a glacier indicates that much of the debris of the stratified facies was abraded by processes external to the glacier, prior to its entrainment. Much of the debris is therefore sediment that was derived from deposits originally found in front of and beneath the glacier. The angular pebble shapes result from primary sediment forming processes (Slatt 1971), including abrasion and crushing of bedrock at the glacier sole and the effects of freeze-thaw on the materials in valley walls and on debris at the surface of the glacier.

Fabric

A three-dimensional analysis was made of the orientation of disk-, blade- and prolate-shaped pebbles entrained in ice of the stratified facies. The trend and plunge of the long axes of prolate-shaped pebbles and the orientation of the plane defined by the long and intermediate axes of blade- and disk-shaped pebbles were measured. The long, intermediate and short axes are referred to as the *a*, *b* and *c* axes, respectively. Particle shapes are defined by the axial ratios: $a/b \geq 2$ and $b \cong c$ in prolates; $a \cong b$ and $a/c \geq 2$ in disks; and $a/b/c \geq 3/2/1$ in blades. Boulton (1974) analyzed pebble fabrics in till and glacial ice using the same limits for each shape class, but he referred to disks as plates.

Field conditions determined the location of measurement of the pebble fabric sites and limited standardization of the number of sets of data gathered at a particular site. Two or more sets of 25 readings were usually taken in an exposure of the basal zone ice. The number of pebbles sampled was based on the sampling scheme analyses of Andrews and Smith (1970) that provided a maximum of 5° variance at the 95% confidence level. The fabric was measured in an area of 1 m^2 or less on ice facies typically with near-vertical slopes. Horizontal and vertical distances between sets at a given site ranged from 2 to 6 m. Sample sets were generally composites of blade-, disk- and prolate-shaped pebbles because, in most cases, pebbles of a single type were too few for an analysis based on one pebble shape. Prolate particles dominated most sets. A total of 38 sets of readings were measured at 17 sites along approximately 1200 m of the glacier terminus.

Measurements of the orientation of pebbles in the stratified facies were plotted on equal-area nets (lower hemisphere projection) by computer and contoured according to the method of Kamb (1959) at a contour interval of 2 $\check{\sigma}$. Fabric data were evaluated statistically by computer using the eigenvalue method discussed by Mark (1973). A symmetric 3x3 matrix *A* of the orientation data was constructed by summing the matrices

Table II. Roundness of 100 pebbles (4 to 64 mm) as classified by Powers' scale.

Debris type	Very angular (%)	Angular (%)	Subangular (%)	Subrounded (%)	Rounded (%)	Well rounded (%)
Superglacial	43	42	15			
Superglacial	55	37	8			
Basal - Dispersed	3	52	39	5	1	
Basal - Dispersed	5	33	48	11	3	
Basal - Stratified		4	19	34	32	11
Basal - Stratified		2	17	42	33	6

Table III. Results of the analysis of pebble fabric in basal ice.

Sample set	Sample number	V_1 Azimuth (°)	V_1 Plunge (°)	S_1	Local direction of glacier flow (°)	Divergence of V_1 from glacier flow (°)	V_3 Azimuth (°)	V_3 Plunge (°)	S_3
A	521401	119	16	0.773	122	3	26	9	0.068
B	521301	123	38	0.823	117	6	296	51	0.063
	521302	107	27	0.898		10	203	11	0.034
C	521501	125	37	0.951	115	11	268	46	0.017
D	521502	101	27	0.821	100	1	324	55	0.065
E	521601	98	35	0.900	100	2	316	49	0.039
F	438402	95	24	0.896	80	15	315	60	0.032
G	516101	110	28	0.857	85	25	358	36	0.067
H	521701	69	41	0.904	78	9	307	31	0.029
	521701P*	74	39	0.876		4	308	35	0.049
	521701B†	102	44	0.743		34	350	21	0.099
I	59601	64	6	0.781	70	6	316	73	0.032
	59701	83	19	0.800		13	335	41	0.085
	59901	70	34	0.808		0	244	56	0.074
	510101	84	42	0.848		14	273	48	0.027
	59602P	70	6	0.798		0	163	21	0.085
	59603B	72	21	0.800		2	287	65	0.043
J	443801	73	29	0.964	71	2	230	59	0.009
K	510701	92	67	0.892	76	16	232	19	0.033
	510702B	88	70	0.951		12	211	11	0.019
L	436401	117	48	0.923	76	41	282	41	0.025
	436402	108	12	0.862		32	358	57	0.065
M	510401	130	66	0.963	74	56	13	11	0.010
	510402	137	70	0.988		63	30	6	0.002
N	521801	102	22	0.780	94	8	5	14	0.077
	521802	92	30	0.868		2	288	59	0.060
O	512101	99	51	0.928	102	3	195	5	0.025
	512102P	95	53	0.930		7	198	10	0.016
	512102B	91	48	0.949		11	223	31	0.014
P	437901	96	15	0.924	107	11	211	57	0.031
	437902	97	19	0.913		10	330	61	0.041
	437903	105	19	0.930		2	4	30	0.026
	437904P	102	20	0.893		5	283	70	0.047
	438302	94	16	0.896		13	273	74	0.010
	438303B	108	22	0.906		1	286	68	0.016
	438304	96	14	0.921		11	284	75	0.034
Q	438401	89	31	0.868	85	4	263	59	0.019
	438402	95	17	0.865		10	298	72	0.017
	Mean	95	34	0.856		12 (σ = 1.3)	355	15	0.047

* P - prolate-shaped pebbles only.

† B - blade-shaped pebbles only.

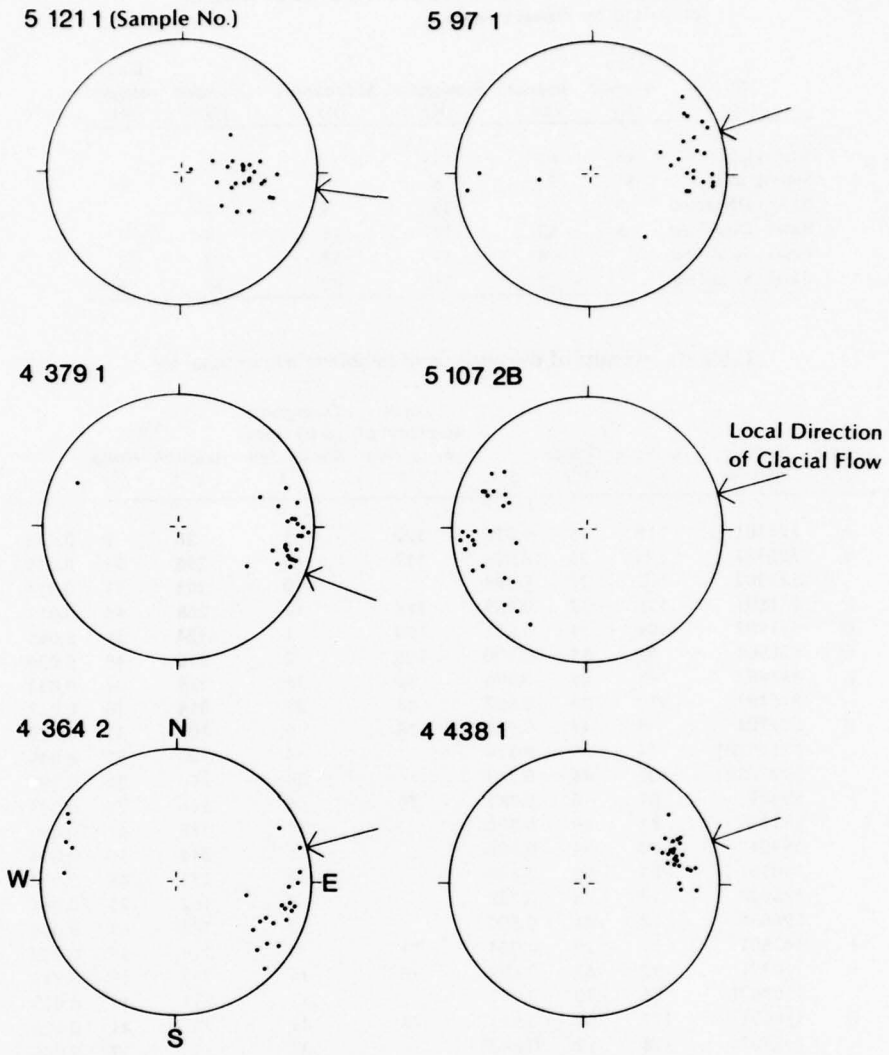


Figure 10. Typical Schmidt equal-area net distributions of pebble orientations in the basal ice. All represented data sets except 51072B are of composite pebble shapes; 51072B is of blades only. At each site 25 measurements were made.

formed as the product of each measured axis and its transpose in Cartesian coordinates:

$$A = \sum_{i=1}^{N} X_i X_i^T \qquad (1)$$

where X_i is a unit vector paralleling the ith observation axis, X_i^T is the transpose of X_i, and N is the number of readings. The eigenvalues ($\lambda_1 \geq \lambda_2 \geq \lambda_3$) and eigenvectors ($V_1$, V_2, and V_3) of the matrix A were determined. The largest eigenvector V_1 indicates the direction of maximum clustering and represents the mean axis while the smallest eigenvector V_3 indicates the direction of minimum clustering and lies orthogonal to the best plane through the data. V_2 lies normal to V_1 and V_3. Significance values, $S_1 \geq S_2 \geq S_3$, indicate the degree of clustering of the axes about the eigenvectors V_1, V_2, and V_3. They are computed by dividing the eigenvalues by the total number of readings, N. S_1 measures the strength of clustering about the mean axis whereas S_3 is inversely proportional to the strength of the preferred plane of the fabric. V_1, V_3, S_1 and S_3 are used in this study to characterize the data.

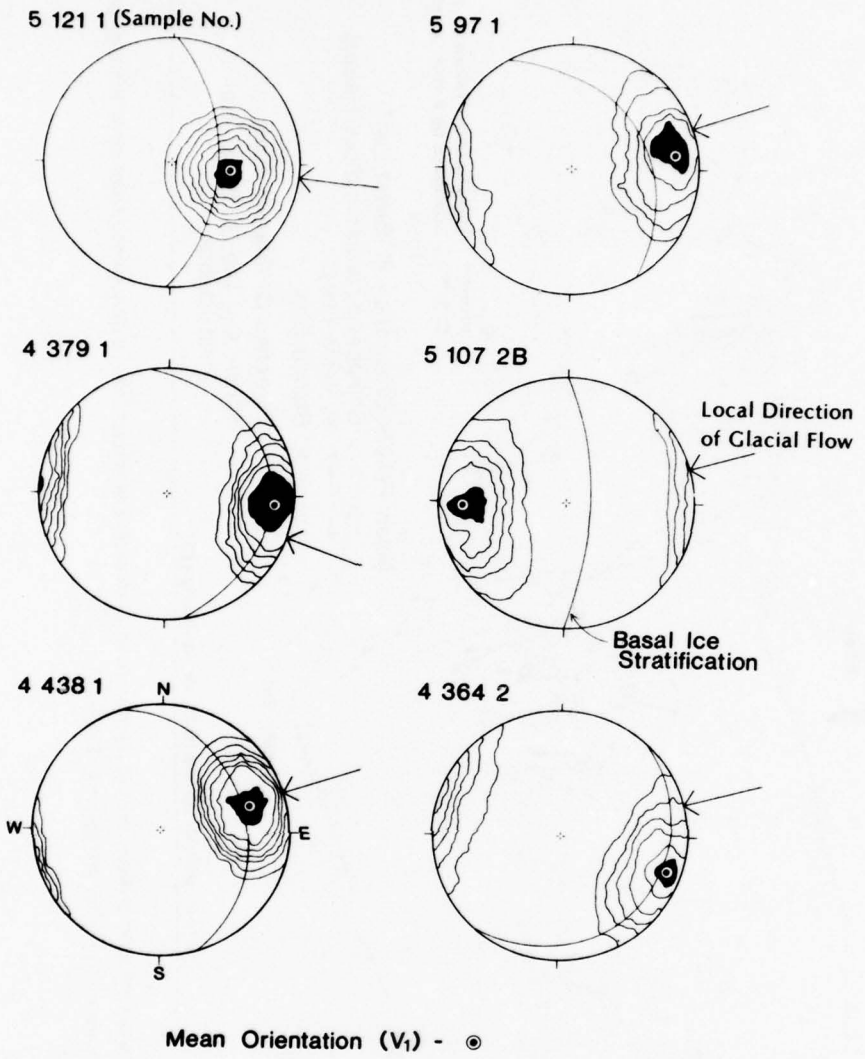


Figure 11. Schmidt equal-area nets of Figure 10 contoured according to Kamb (1959) at a 2 σ interval. Mean orientation represents local direction of glacier flow. Dip of pebbles is not preferentially oriented with respect to flow.

The scatter plots and contoured stereograms typical of the data gathered from the stratified facies (Table III) are shown in Figures 10 and 11. The direction of ice flow determined from aerial photographs taken in 1949, 1969, and 1974, and the orientation of the stratification are shown for comparison. These measurements are not "corrected" for the strike and dip of the enclosing stratification, as suggested by Andrews and Smith (1970) for tills and as is commonly done in sedimentological studies (Potter and Pettijohn 1963). In the Matanuska Glacier, the orientation of this stratum does not necessarily correspond to that of either the surface along which debris is released or the surface upon which it is deposited, and this stratification is generally not preserved in till (Chapter 4 and Boulton 1970b). Therefore, the orientation of the stratification is not useful as a plane of reference in deposits or ice.

Most samples plot as a strong, single mode, with a mean axis orientation representative of the local direction of flow of the glacier. The mean axis (V_1) of individual compositive samples varies by a maximum of 56° from the local direction of ice flow; the mean divergence is 12° (Table III). The significance values (S_1, S_3) indicate a tight clustering of the pebble axes about

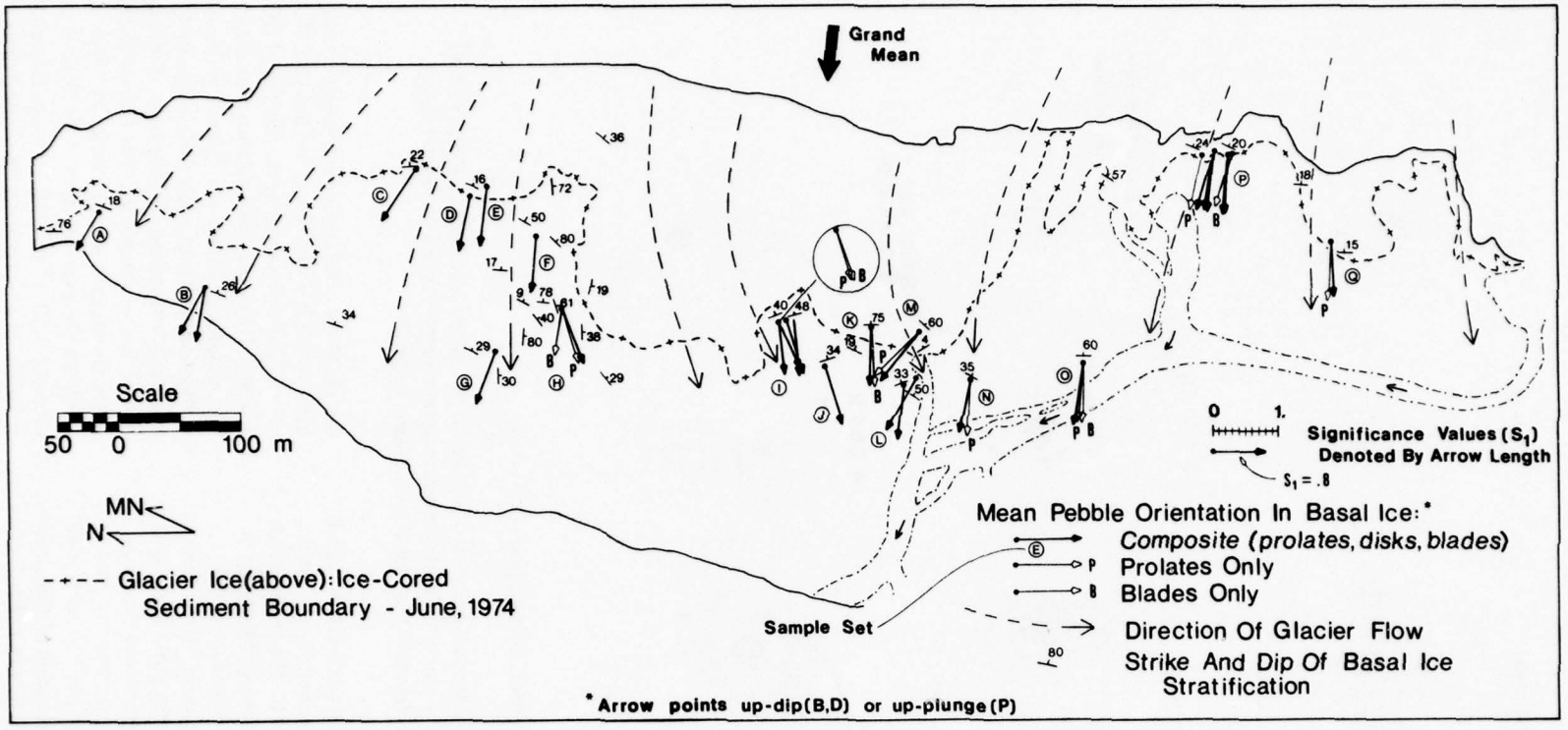


Figure 12. Map of study area (location on Fig. 4) showing sample mean axes in relation to local direction of glacier flow as determined from aerial photographs taken in 1949, 1969 and 1974. Statistical data for each sample set are given in Table III.

the mean axis. There is generally good agreement between data sets consisting of all pebble types, blades only, and prolates only. Between-site variability of all data sets is large (73°), but it is consistent with differences in the local direction of ice flow (52°). At a given site, lateral variations apparently exceed vertical variations. At the few sites where multiple data sets could be measured, the lateral variability was a maximum of 20° (Set I) over a distance of 10 m. Differences of 1 to 6° were measured over a vertical distance of about 3 m in each case. The few studies made previously of pebble orientations in ice (Richter 1936, Boulton 1971) found similar well-oriented pebbles. Boulton (1971) measured transverse orientations in zones of compressive flow and parallel orientations in zones of extending flow; this difference was not observed here.

The strong parallelism of the fabric mean axes to the local direction of ice flow is shown in Figure 12. Only in a zone of converging flow lines do they vary significantly; the mean axis of data set M lies nearly transverse to the direction of ice flow. The grand mean axis computed from all measurements represents the general direction of glacial flow. Thus, if the debris examined here were little altered during deposition, the orientation of the mean axis of fabric measurements of this deposit would represent the local direction of ice flow.

The direction of plunge of the long axes of prolates and of the dip of the orientation plane of blades and disks is upglacier in the terminus region; however, this direction is not necessarily related to the direction of ice flow. The *a*-axes and the *ab*-planes of pebbles lie mostly subparallel to the debris stratification of the basal zone ice (Fig. 11, Table III). When examined with reference to that plane, they are not preferentially oriented with respect to ice flow. Exposures of the basal zone in the lateral margins of the glacier, upice from the terminus, indicate the stratification and thus the pebbles lie oriented subparallel to the slope of the bed of the glacier. Therefore, the dip or plunge of the pebbles is merely a reflection of compressive flow in the terminus region and only under these conditions are they indicative of the direction of glacial flow.

DISCUSSION

The distinct differences in the physical characteristics of the ice and debris, and their consistent variation in a vertical stratigraphic column of the glacier indicate multiple origins for both. The properties of the englacial and superglacial debris are consistent with those established for this debris by previous studies; hence, their origins are assumed to be similar. In both cases, debris is derived principally from surface sources.

The angularity, coarse texture, and extreme size distribution characteristic of the superglacial debris and its occurrence as a surface covering indicate that it is material weathered from valley walls and nunataks which were mass transported onto the glacier surface (Tarr and Martin 1914, Ray 1935, Reid 1968, Reheis 1975).

Englacial debris and ice originate predominantly in the accumulation area of the glacier. Texture and sorting of the diffused facies debris as well as its uniform and "layered" distribution are compatible with an eolian origin (Grove 1960, Holdsworth 1974). Debris bands of a texture, angularity, and sorting similar to superglacial debris and which lie conformably with sedimentary layering are mass transported onto the snow in the accumulation area. Snow diagenesis and glacier flow incorporate this material and result in its occurrence and orientation in the englacial ice of the terminus (Grove 1960). Debris bands which contain sediment with properties different from superglacial debris and with orientations not compatible with ice layering are of uncertain origin but may result from thrusting (Goldthwait 1951, Boulton 1970a).

In contrast, the characteristics of the basal zone suggest a subglacial origin for most of the debris and ice. Most researchers of active glaciers have concluded the debris of the basal zone to be subglacially-derived, but have not agreed upon the mechanism of entrainment (e.g. Goldthwait 1951, Kamb and LaChapelle 1964, Boulton 1970, Holdsworth 1974).

The ice facies of the basal zone of the Matanuska Glacier appear to be of two distinct origins. The upper dispersed facies is apparently a transitional or boundary zone, with properties indicative of both subglacial and surficial origins. The similarity in coarseness and color of this ice to the englacial ice, the angularity and relative coarseness of the debris, and the characteristics of the upper contact with the englacial zone, which is marked mainly by a change in the debris content of the ice, are evidence of an accumulation area source for the ice and debris. The presence of rounded pebbles mixed with angular ones, the overall coarse texture but lack of particles greater than 32 mm in diameter, the uniform distribution of the debris, and the planarity of the upper contact support subglacial debris entrainment as the debris source. The apparent ambiguity in the evidence for surficial or subglacial debris sources results because several processes of entrainment may produce similar debris and ice properties. Thus, the characteristics of the ice and debris of the dispersed facies suggest that it is the product of both subglacial and surfical processes.

Properties of the ice and debris indicate a subglacial origin for the stratified facies. These properties include clear fine-grained ice, diverse texture of the debris, predominantly rounded pebbles, debris stratification, properties of individual strata (such as debris streaming in the discontinuous subfacies and the occurrence of sedimentary structures in the solid subfacies), and sharp, but irregular contact with the dispersed facies.

Each characteristic has previously been interpreted as subglacial in origin. They are not, however, indicative of a single process of ice formation and sediment entrainment. For example, the debris stratification, debris streaming, and fine-grained ice may result from regelation-slip (Kamb and LaChapelle 1964, Peterson 1970). The thickness and debris content of the stratified facies are apparently not compatible with this mechanism. This glacier contains a quantity of sediment comparable to the subpolar glaciers described by Boulton (1970a) in basal ice of a thickness incompatible with that originating by regelation (Nye 1970).

The unaltered sedimentary structures in solid subfacies layers were attributed by Weertman (1961) and Boulton (1970a) to be the product of subglacial freezing. Boulton (1970a) also suggested that the flow of externally-derived waters into low pressure zones of freezing, where glacial flow results from regelation-slip, would increase the thickness and debris content of ice formed by this mechanism.

A comparison of the vertical and lateral distribution of the sediment in the discontinuous subfacies to the distribution of sediments observed adhering to the soles of active glaciers indicates the freezing of waters around these sediments would produce many of the distributions observed in individual ice strata of the Matanuska Glacier basal zone (Peterson 1970, Vivian and Bocquet 1973, Boulton 1974). Tractional entrainment with local regelation and pure regelation-slip have also been cited as possible means of suspending individual particles in basal ice (Boulton 1975, Kamb and LaChapelle 1964).

In order to determine more precisely the origin of the debris and ice of the basal zone of the Matanuska Glacier and to provide evidence for theories of debris entrainment, the oxygen isotope content of ice of the lower part of the englacial zone and the basal zone in the terminus region was determined. This analysis assumes that the O^{18}/O^{16} ratios of glacier ice are distributed systematically in ice formed in the accumulation area of the glacier. Perturbations in this distribution result from either an alteration in the O^{18} content of the ice by some process of fractionation or isotope exchange during glacial flow, or an origin different from snow diagenesis in the accumulation area of the glacier. The basis for the analysis is discussed in more detail in the next chapter.

CHAPTER 3. OXYGEN ISOTOPE ANALYSIS

A number of studies have established trends in δO^{18} values in glaciers that primarily reflect the temperature dependence of the isotopic composition of precipitation. This dependence results in a reasonably systematic variation of the δO^{18} value with latitude, altitude, storm, and season (e.g. Epstein and Sharp 1959, Dansgaard 1964, Deutsch et al. 1966, Macpherson and Krouse 1967). In a glacier where the diagenesis of snow in its accumulation area involves recrystallization in the presence of percolating meltwater and meteoric water, the effects of altitude dominate, whereas the effects of storm and season are obliterated (Sharp et al. 1960, Deutsch et al. 1966, Ambach et al. 1972). Epstein and Sharp (1959) and Sharp et al. (1960), among others, determined that the δO^{18} values of firn decrease consistently with increasing altitude. These variations in δO^{18} values of firn are preserved in the isotopic ratios of glacial ice along the longitudinal profile of the glacier. Unless modified, δO^{18} values are lowest near the terminus and increase with distance from the terminus to the equilibrium line (Epstein and Sharp 1959, Sharp et al. 1960). This trend in δO^{18} values agrees with the model proposed by Reid (1896) for longitudinal ice flow in a valley glacier. According to Reid, ice from the upper part of the accumulation area moves downward close to the base of the glacier and emerges in the lower terminus, whereas ice formed at progressively lower elevations in the accumulation area emerges at progressively higher elevations in the ablation area (Fig. 13). Studies of ice flow (e.g. McCall 1960) have also substantiated Reid's model.

SAMPLING AND ANALYSIS

Samples of basal and englacial ice from the Matanuska Glacier were obtained in 1975 from the dispersed, stratified and diffused facies (Fig. 14) along three transects that parallel the local direction of glacier flow (Fig. 15). In addition, ice was sampled in detail in 1977 adjacent to the boundaries of these facies at a fourth location (transect 4). Because Sharp et al. (1960) concluded that only the coarse-bubbly ice in the diffused facies was isotopically unaltered, only this type of ice in this facies was sampled. Samples of meltwater were also taken just down-glacier from the location of several of the ice samples.

Samples were taken after first removing the upper 30 cm of partially ablated ice. Dry pieces of the underlying "fresh" ice were packed into polyethylene bottles which were then sealed with paraffin to prevent evaporation.

Glacial meltwater was equilibrated with CO_2 according to the method of Epstein and Mayeda (1953). The CO_2-H_2O fractionation factor utilized was 1.0412 (O'Neil et al. 1975). Analysis of CO_2 was made in a conventional 15-cm, 60° double collecting mass spectrometer. Isotope values are expressed as a relative per mil deviation (δ) from Standard Mean Ocean Water (Craig 1961) using the corrections described by Craig (1957), where

$$\delta(^0/_{00}) = \frac{(O^{18}/O^{16}_{sample} - O^{18}/O^{16}_{std})}{O^{18}/O^{16}_{std}} \times 10^3. \qquad (2)$$

Precision of the measurements is about $0.2^0/_{00}$.

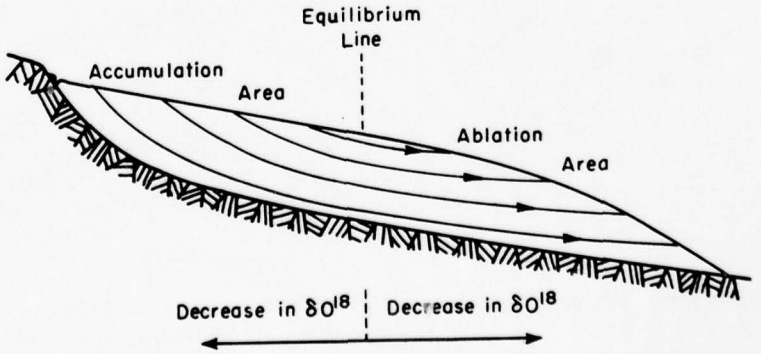
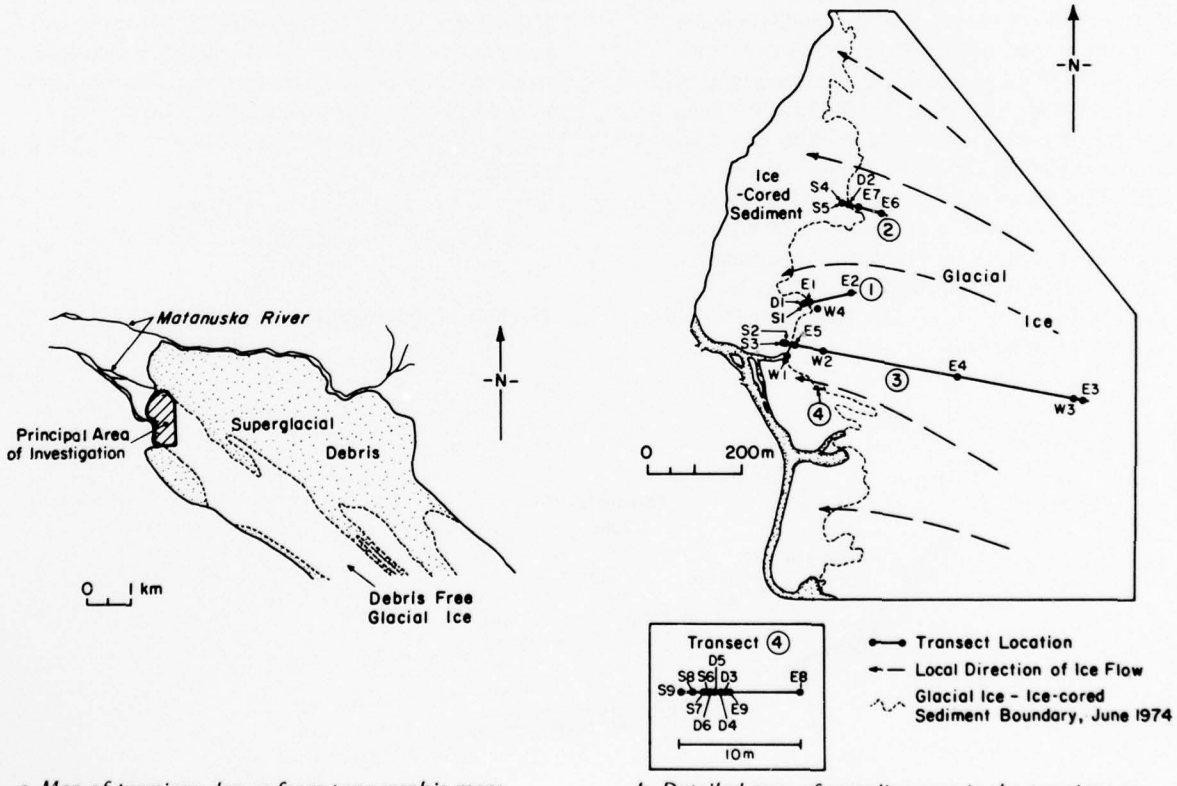


Figure 13. Flow lines in a valley glacier as deduced by Reid (1896). Arrows indicate expected surface trend in δO^{18} values of the ice.



Figure 14. Partial exposure of the ice sequence in the Matanuska Glacier terminus. End of 2-m-long stick rests in the dispersed facies of the basal zone, just above the contact between the dispersed facies and the stratified facies of the basal zone. White ice at top of photo is diffused facies of the englacial zone.



a. Map of terminus drawn from topographic maps (Anchorage Quadrangles D-2, D-3).

b. Detailed map of sampling area in the terminus region of the Matanuska Glacier showing sample locations and their relationship to direction of glacier flow. Area mapped by plane table and alidade in 1974.

Figure 15. Location of Matanuska Glacier study area.

Radiocarbon dates of two pieces of wood chopped from the stratified facies (sample numbers ISGS-295, ISGS-312) were determined by the Illinois State Geological Survey using standard liquid scintillation techniques.

RESULTS

The δO^{18} values, texture of the debris, debris content of the ice, and grain size of the ice of each sample from transects 1 to 3 are summarized in Figure 16. Each sample possessed characteristics typical of the facies from which it was taken. The pronounced change in the physical characteristics of the ice and debris at the contact of the dispersed and stratified facies coincides exactly with an abrupt change in the O^{18} content of the ice (Fig. 16, 17).

The δO^{18} values decrease by more than $4^0/_{00}$ from the uppermost sample of the diffused facies of the englacial zone through the dispersed facies of the basal zone (Fig. 16). Delta values in the diffused facies range from $-21.7^0/_{00}$ at approximately 80 m above datum (basal-englacial zone contact) to about $-25.0^0/_{00}$ near datum (Table IV). δO^{18} values of ice samples from the dispersed facies range from -22.7 to $-25.7^0/_{00}$ and are as negative as those of ice of the diffused facies overlying each sample (Fig. 16, 17).

In contrast, δO^{18} values of ice in the stratified facies range from -19.7 to $-24.2^0/_{00}$ (Table IV). In all four transects, this ice contains significantly more O^{18} than ice of the dispersed and lower diffused facies overlying each sample. This abrupt increase in the δO^{18} values at the dispersed-stratified facies contact is clearly shown in Figure 17. The maximum difference between the δO^{18} values of the stratified and dispersed facies is about $6^0/_{00}$.

Table IV. Results of the oxygen isotope analysis.

Sample	Datum height (m)	δO^{18} ($^0/_{00}$)	Sample	Datum height (m)	δO^{18} ($^0/_{00}$)
E-1*	+ 1.0	-26.0	S-1	- 3.0	-23.3
E-2	+10.0	-24.7	S-2	- 4.0	-19.7
E-3	+80.0	-21.7	S-3	- 9.0	-20.1
E-4	+40.0	-23.0	S-4	- 7.2	-21.6
E-5	+ 1.6	-25.7	S-5	- 1.8	-24.2
E-6	+ 8.0	-26.3	S-6	- 0.6	-20.9
E-7	+ 3.0	-26.6	S-7	- 0.65	-21.0
E-8	+ 1.8	-23.7	S-8	- 0.90	-20.9
E-9	+ 0.1	-24.6	S-9	- 1.15	-20.3
D-1	- 0.6	-25.7	W-1	- 1.0	-25.1
D-2	- 0.4	-25.5	W-2	+ 7.0	-26.1
D-3	- 0.1	-24.7	W-3	+78.0	-22.6
D-4	- 0.35	-24.7	W-4	+ 1.4	-26.4
D-5	- 0.45	-23.8			
D-6	- 0.50	-22.7			

*E – diffused facies, englacial zone
D – dispersed facies, basal zone
S – stratified facies, basal zone
W – meltwater

The δO^{18} values of four samples of water derived from melting of the ice surface near the terminus were measured. Meltwater adjacent to the upper sample of diffused facies ice (W-3) has a δO^{18} value of $-22.6^0/_{00}$, whereas this ice sample (E-3) has a value of $-21.7^0/_{00}$ (Table I). Meltwater samples from the lower part of the glacier near the contact of the dispersed and diffused facies were more negative (-25.1, -26.1 and $-26.4^0/_{00}$).

Wood located 0.5 m below the contact between the dispersed and the stratified facies in transect 3 gave a radiocarbon age of 515 ±75 B.P. (Fig. 16). The age of wood removed from 0.1 m below the same contact in transect 2 is 350 ±75 B.P. These dates apparently represent maximum ages for the stratified basal ice at the sample location.

DISCUSSION

Diffused and dispersed facies

The decrease in the δO^{18} values of ice of the diffused facies with decreasing depth above the datum is compatible with the isotopic trends found by others in temperate glaciers. Assuming that the vertical trend of decreasing δO^{18} values reflects the increasing elevation of the source area, these data indicate that the lower englacial ice originated in the accumulation area of the glacier. Physical characteristics of the diffused facies, including the angularity and coarse texture of the debris, and the grain size, abundance of air bubbles and insignificant debris content of the ice, support this conclusion (e.g. Kamb 1959, Grove 1960, Slatt 1971). Debris in the diffused facies is therefore entrained surficially in the accumulation area.

The isotopic composition of ice of the dispersed facies is as negative as the overlying ice of the diffused facies, suggesting a mutual source for ice of both facies. Physical characteristics of the dispersed facies suggest that it is the product of surficial and subglacial processes. The similarity in coarseness and color to the overlying diffused facies ice, the angularity of the debris, and the demarcation of the upper contact with the englacial zone primarily by a change in the debris content are characteristics that may be derived from

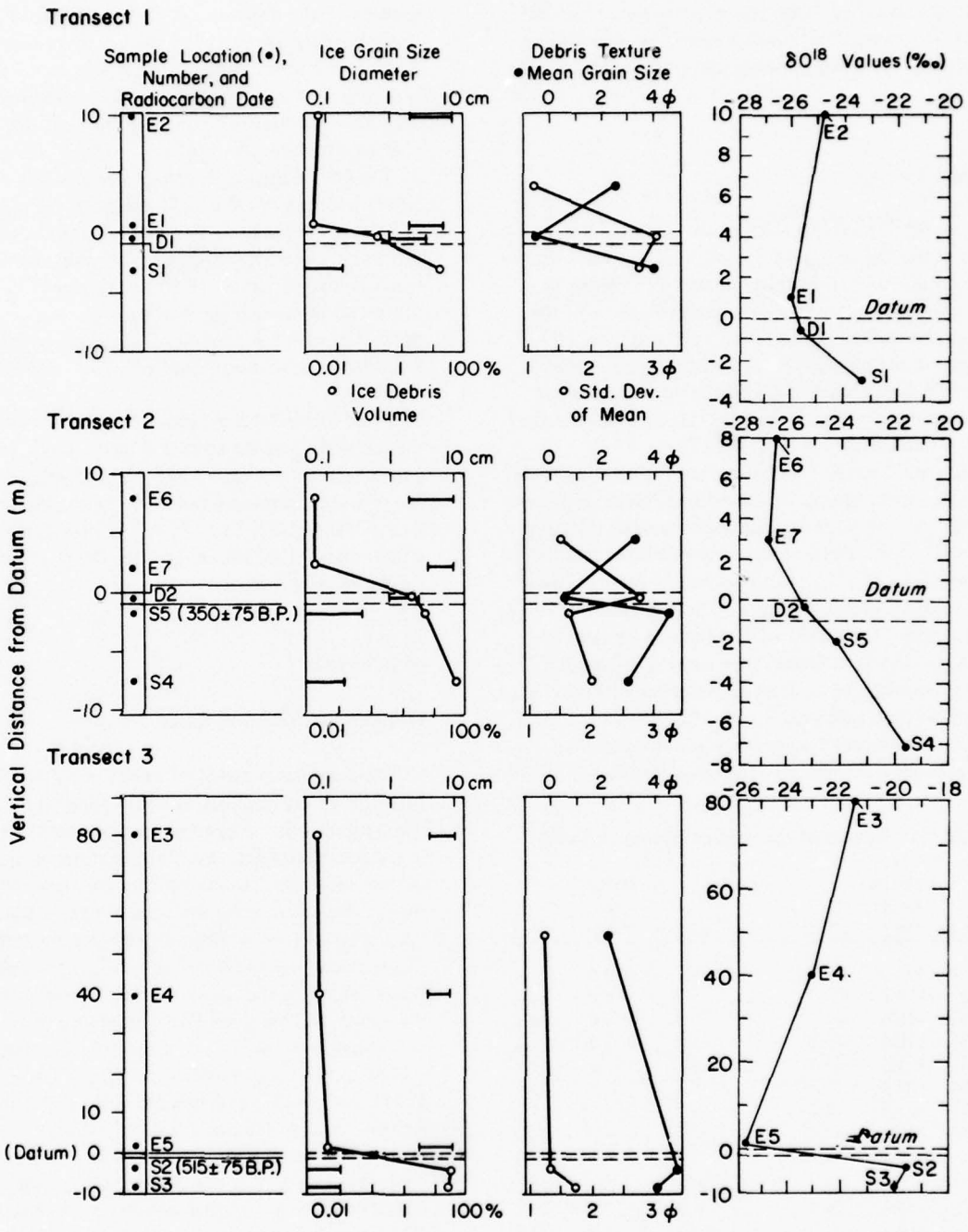


Figure 16. Logs of sample transects 1-3. Grain size and debris content of the ice, texture of the debris and δO^{18} values of the ice of each sample of the diffused (E), dispersed (D) and stratified (S) facies are shown. In each transect, ice of the stratified facies contains more O^{18} than the overlying ice of the dispersed and diffused facies. Radiocarbon dates are from wood in the stratified facies.

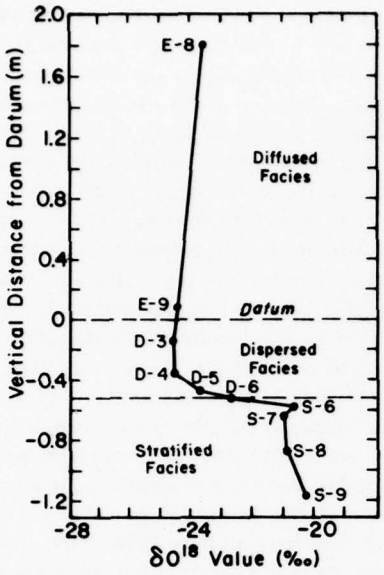


Figure 17. Comparison of δO^{18} values of ice samples of the diffused, dispersed and stratified facies from transect 4. Abrupt increase in δO^{18} values of ice of stratified facies at contact of dispersed and stratified facies is shown. Ice grain size, debris content of the ice, and texture of the debris of each sample are similar to those of samples shown in Figure 16.

an accumulation area source (Grove 1960, Slatt 1971). Likewise, the rounded pebbles mixed with the mostly angular debris, the coarse texture but absence of particles greater than about 32 mm in diameter, the uniform dispersion of the debris in the ice, and the planarity of the upper facies contact also suggest mainly subglacial debris entrainment, rather than the surficial addition of sediment in the accumulation area during ice formation (Holdsworth 1974, Slatt 1971).

Because the δO^{18} values of this ice are similar to those of the overlying diffused facies ice, the mechanism of debris entrainment could not have altered the isotopic composition established during ice formation. This fact, as well as the physical characteristics of this facies, suggest that the debris is entrained by localized pressure melting and freeze-on, without water loss, of individual particles from the glacier bed. The well-defined planar contact with the diffused facies, relatively uniform distribution of particles, and lack of particles in excess of 32-mm diameter suggest that this material undergoes a limited upward dispersion following freeze-on. This vertical dispersion may result from the interactions of particles within and beneath the glacier (Boulton 1975) or from vertical strains induced by ice flow (Holdsworth 1974). Further study is required to determine the process of entrainment of diffused facies debris.

Stratified facies

The radiocarbon dates of two pieces of wood from the stratified faces and the abrupt increases in the O^{18} content of this ice indicate that the origin of the ice of this facies is different from that of ice of the overlying diffused and dispersed facies. Estimates of the rate of flow at the surface of the glacier from aerial photographs taken in 1949, 1969, and 1974 suggest that the ice of the englacial zone is at least three times as old as the 350- to 515-year maximum radiocarbon age of the stratified facies. It is probably many times older than this age. If this estimate of the flow rate is assumed correct, the stratified ice must have formed subglacially outside the accumulation area.

The oxygen isotope analyses suggest two possible subglacial mechanisms as the origins for the stratified facies ice. The first mechanism involves the creation of new ice at the glacier sole by freeze-on of water that is isotopically enriched relative to the overlying ice of the diffused and dispersed facies. Weertman (1961) and Boulton (1972b) theorized that zones of freezing will develop at the base of a glacier where the temperature gradient in the ice is just large enough to conduct away the heat of sliding and geothermal heat. Meltwaters flowing in or on subglacial materials from the interior region of the glacier will freeze to the moving glacier sole here. The second mechanism

requires an O^{18} enrichment of the overlying dispersed facies ice as the result of fractionation during regelation of water derived from pressure melting of this ice during glacial sliding. This regelation mechanism of basal sliding (Weertman 1957, 1964; Kamb and LaChapelle 1964) occurs where ice at the base of the glacier is at the pressure melting point.

The physical characteristics of this facies support the first hypothesis. The rounded and subrounded pebbles are indicative of sediments that were reworked before their incorporation into the ice and probably represent sediments that were overrun by the advancing glacier. Intact sedimentary structures require the incorporation of blocks of sediment from below the ice/sediment interface without disruption of particle orientation and distribution. Boulton (1967, 1970a) concluded that Weertman's (1961) "freezing in" hypothesis accounted for the addition of such blocks of sediment. Similarly, the subparallel, planar alignment of granule- to cobble-sized clots of debris (mainly consisting of silt mixed with sand- to pebble-size grains) and individual grains suggests that these materials are subglacial debris which were surrounded by and then frozen with subglacial water onto the sole of the glacier. The small grain size and the paucity of air in the stratified ice supports subglacial freezing of water at a rate low enough to allow rejection of dissolved air under confining conditions that limit crystal growth. Gow et al. (1978) observed this condition in ice of the basal zone of the Antarctic ice sheet and concluded that this ice originated by slow freezing-in of basal meltwater. Also, the extreme variability in the debris texture, the large debris content of this facies, the abundant strata of variable dimensions and debris content, the disposition of individual particles of debris, and the thickness of this facies are characteristics attributed by Boulton (1967, 1970a) to ice and debris added to the glacier by freeze-on of basal meltwater.

The second hypothesis for isotopic enrichment is not considered to be the primary mechanism by which the stratified facies originates because the thickness and undisturbed sedimentary structures in the debris require a net addition of ice at the glacier sole. Regelation of water derived from pressure melting against bed obstructions does not produce a net gain of ice, but merely cycling and redistribution of it on the glacial sole. Ice generated by regelation-slip is limited to an order of thickness of about 0.1 m (Nye 1970, Boulton 1975), whereas the stratified facies ranges from 3 to 15 m thick. Similarly, only partial refreezing of this water is permitted if fractionation is to occur. Therefore, a net loss of ice would result unless water from another source were added. Further, characteristics acquired by sediments prior to incorporation in the glacier would be destroyed by pressure melting against succeeding obstructions.

The first hypothesis – that the stratified facies originated subglacially by the freeze-on of water to the glacier sole – requires a source of water which is isotopically-enriched relative to the ice of the lower diffused and dispersed facies and a means of transport to areas at the glacier sole in which thermal conditions permit net freezing. The sources of water in the glacier system are meltwater, meteoric water, and externally-derived groundwater. Theoretical calculations (Weertman 1972) and field measurements (Ambach et al. 1973) of the basal meltwater contribution indicate it to be a relatively insignificant source. The englacial contribution to the total amount of water at the bed of the Matanuska Glacier is unknown, but calculations of the amount of water generated by plastic flow of ice suggest that it is also small in comparison to surface meltwater contributions (Nye and Frank 1973). Theoretical analyses (Nye 1976) imply, however, that in some cases this contribution may be larger. Shreve (1972) estimated that the total quantity of meltwater of englacial and basal origin is only about 10 mm of water per year per unit area of bed in a temperate glacier, and thus surface meltwater is normally orders of magnitude greater in volume than meltwater and meteoric water. The quantity of groundwater in the Matanuska Glacier is also unknown, but apparently small. It appears to be a minor constituent because water flow from the ice margin, which apparently has a subglacial source, varies rapidly with daily and seasonal changes in the weather. Cold, cloudy days reduce outflow significantly in a matter of hours. Similarly, flow ceases by mid-winter. Melting of the surface and near-surface ice upglacier of the terminus is therefore assumed to be the predominant source of water in the subglacial region of the Matanuska Glacier.

The δO^{18} values of surface-derived meltwater are expected to be less negative than the values measured in ice sampled in the terminus. The data obtained in this study and the trend observed in several other glaciers of decreasing δO^{18} values along the longitudinal profile of the glacier with distance both above and below the equilibrium line mean that the ice and snow sources of surface meltwater contain more O^{18} than the ice of the dispersed and lower diffused facies in the terminus. Published changes of δO^{18} with altitude measured at other glaciers suggest that a variation of from 3 to 14‰ in the δO^{18} value of surface accumulation might occur along the approximate 1500 m of relief in the accumulation area of the Matanuska Glacier. The O^{18}/O^{16} ratios of meltwater samples examined in this study suggest that meltwaters are

isotopically similar to their ice source and thus surface meltwater derived from ice located up-glacier of the terminus is assumed to contain significantly more O^{18} than the sampled ice of the terminus.

The O^{18}/O^{16} ratio of meltwater in the subglacial region is determined by the amount of dilution that occurs as the result of mixing of surface meltwater with water containing less O^{18} from melting of the basal and englacial ice, and by the amount of fractionation and isotopic exchange that takes place during flow of this water through the glacier and during its refreezing to form the stratified ice. Because the volume of surface meltwater far exceeds that of other sources, mixing probably has little overall effect on the O^{18}/O^{16} ratio of subglacial water. Most surface meltwaters flow to the subglacial region through large drainage features such as moulins and fractures (Shreve 1972), and thus the contribution of waters reaching the base of the glacier through intergranular passages, where isotopic exchange and possibly fractionation may occur, is considered small. Hence, the O^{18}/O^{16} ratio of surface meltwater flowing through large drainage features will dominate the O^{18}/O^{16} ratio of all waters reaching the subglacial region.

It is not known if fractionation and isotopic exchange occur in the process of water flow through the subglacial region. This water flows in a direction generally toward the ice margin either over impermeable materials in thin discontinuous sheets separated by one or more channels (tunnels) or in permeable subglacial materials (Weertman 1972). Fractionation may be important because partial freezing of water under equilibrium conditions forms ice that is 3 per mil richer in O^{18} than the water source (O'Neil 1968). The O^{18} content of the unfrozen water is, however, reduced, and therefore all unfrozen water must be removed from the subglacial region to produce stratified ice that is consistently enriched in O^{18} relative to the overlying dispersed and diffused facies ice. To produce the large difference in the δO^{18} values of the facies in the Matansuka Glacier, isotopic enrichment must occur several times. In order to obtain a net increase in the thickness of the ice and to require the entire difference in δO^{18} values of these facies to result from fractionation of dispersed or diffused facies ice, it would appear that unusual conditions, not documented to date, are needed. It seems more plausible that limited fractionation may be occurring that accounts for a small increase in the O^{18} content of the stratified ice.

Variations in ice formation and debris entrainment

The location and extent of areas of net freezing and also the rates of ice formation and sediment entrainment appear to vary with time beneath the Matanuska Glacier. These variations are suggested by the differences in the thickness of the stratified and dispersed facies, the lack of continuity and variation in the thickness and extent of individual debris-rich and debris-poor ice strata, and the disparity in the radiocarbon ages of wood taken from the stratified ice at about the same depth below the stratified and dispersed facies contact. The differences in these properties occur over short distances (m) across the terminus. Further, the large volumes of meltwater observed flowing from fountains at the margin of the glacier in the summer season suggest that the total extent of areas of net freeze-on is not large and that these areas may be discontinuous. Because thermal conditions at the base of a glacier are determined by the temperature gradient in the ice, the amount of heat produced by sliding of the glacier over its bed, and the geothermal heat flux (Weertman 1961), these conditions and thus the location and extent of the areas of freeze-on may be altered by changes in the rate of ice flow, ice thickness, air temperature, and bed topography (Boulton 1972b). At the glacier sole, only small temperature effects in the range of 0.01°C are needed in glaciers near the pressure-melting point to develop an irregular distribution of freezing zones and shifts in their location (Robin 1976). The data obtained in this study, the abundant surface and subsurface flow of meltwater in the glacier, and the climate of this region suggest that the Matansuka Glacier is thermally complex, and characterized by ice at and near the pressure-melting point. Thus, it appears that the distribution of freeze-on areas at the base of the glacier is complex and that the extent of freezing may result in the entrainment of intact blocks of stratified sediments that contain sedimentary structures (Weertman 1961).

CHAPTER 4. DEPOSITIONAL PROCESSES—TILL FORMATION

A detailed sedimentological investigation of the Matanuska Glacier was made to determine and, where possible, to quantitatively evaluate the mode of formation of till and related sediments, and to determine the characteristics of the deposits formed by each process. Relatively well understood glaciofluvial processes (e.g. Rust 1972, Church 1972, Boothroyd and Ashley 1975) and large scale glaciolacustrine processes (Gustavson 1975, Theakstone 1976) were not examined.

Examination of the properties of processes active in Holocene glacial environments and linking those properties to the characteristics of their deposits permits not only their identification in older glaciogenic materials but also an understanding of the origin of these characteristics and hence the genesis of the deposit. Continued research on sedimentation processes of glaciers in different climates and under varying physical conditions may eventually permit the determination of these parameters from the sediments. Thus, it is important that future studies of Pleistocene and ancient glacial deposits attempt to identify the origin of their components through a detailed sedimentological analysis.

For this reason, a relatively conservative genetic definition of till is used in this study. *Till is defined as sediment, deposited directly from glacier ice, which has not undergone subsequent disaggregation and resedimentation.* Types of till are distinguished by their mode of formation. The use of this definition limits the term till to deposits that are directly related to the debris of the glacier and its process of release from the ice.

This definition is modified from Boulton (1972a, p. 379). Boulton considers flow of sediment simply a post-depositional deformation and therefore the resulting deposit a till. This deposit is referred to as "flowtill" (Hartshorn 1958). This process is excluded from the definition of till because the flow of sediment-water mixtures under the influence of gravity in the superglacial environment has been found by this investigation to be, as in other environments, *a process of resedimentation. Sediments referred to as "flowtill"* are in fact resedimented materials that can be distinguished from true tills, principally by characteristics inherited from their method of transport and deposition. Therefore, deposits from sediment gravity flow and other resedimentation processes are not tills.

This study shows that till, as used in a traditional sense (see e.g. Flint 1971), is formed by a complex series of processes with products that are generally distinguishable from one another by detailed analysis of an assemblage of characteristics. These characteristics are primarily derived from the depositional processes and, except for melt-out till, secondarily from the characteristics of the debris source. Textural subpopulations and other features in the ice and debris of the basal zone are generally lost during release from the ice and deposition. The interrelationship of surface and subsurface processes and the similarity of some of the deposits permits sedimentary sequences that were interpreted previously as "multi-till" in origin to develop during a single depositional cycle.

METHODS OF ANALYSIS

A three-dimensional analysis of pebble fabric in till and other deposits was performed as described previously. For this analysis, the location of a given data set was determined by the characteristics and dimensions of the deposit. Stable deposits formed by certain processes were often limited in occurrence and thus few measurements could be taken in these materials.

Surface rates of sediment erosion and deposition were measured using sedimentation stakes (Clifton 1969). The rate of sediment accumulation resulting from melting of buried ice was determined by trenching to the ice interface, inserting several wooden dowels at that interface in the sediments of the trench wall, and filling the hole with the excavated materials in the order in which they were removed. The thickness of the sediment layer found beneath the dowels after re-trenching the hole at the end of the field season was assumed to be of melt-out origin. Flow rates of sediment gravity flows were determined by placing blocks of variable density on flow surfaces and timing their movement over a measured distance with a stopwatch. Meltwater flow rates were measured with a portable, vane-type current meter.

Temperatures in the sediments were measured using a YSI Model 42SC tele-thermometer and buried thermistors. Precision of the metering system is ±0.5°C. Thermistors were checked for accuracy in an ice-water bath and found to be within 0.2°C. Each thermistor was inserted at the base and mid-depth of holes augered or trenched to a maximum depth of 2 m in the surficial sediment cover. Holes were refilled with sediments in the order of their removal. Thermistors indicated temperature equilibration in 24 to 48 hours.

A weather station was established on the ice-cored sediment cover. Air temperature and relative humidity were recorded on a hygrothermograph, solar radiation

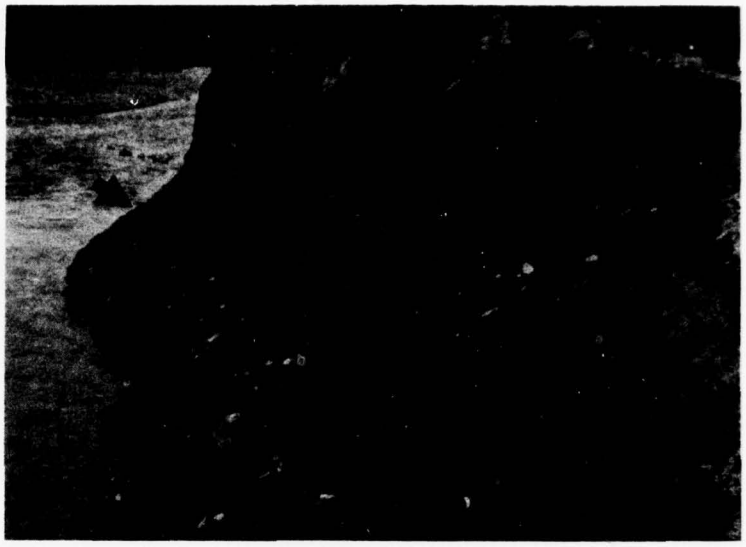


Figure 18. Slump-flow exposed section of the stagnant, debris-laden basal ice at the terminus edge. Ice comprises three basal zone sections, each deposited following override of lower, sediment-covered stagnant basal ice. Arrows mark location of overridden sediments. Scale to right of man is 2 m long.

intensity was monitored on a mechanical pyranograph, and precipitation measured twice daily in a standard U.S. Weather Bureau 8-in. rain and snow gauge.

ENVIRONMENTAL SETTING

Sedimentation by the Matanuska Glacier occurs predominantly in an ice-cored zone of about 300-m width which parallels the edge of the terminal lobe. The source of nearly all sediment in the ice-cored zone is the debris-laden basal zone of the glacier. The total thickness of the basal zone ranges from about 4 to 23 m; however, the burial, stagnation, and overriding of older basal zone ice by the glacier increased its thickness and the area underlain by it to form the marginal ice-cored zone (Fig. 18).

Release of sediment from this ice has resulted in a sediment cover that exceeds 8 m in thickness in some places. This cover consists mainly of resedimented materials deposited by sediment gravity flows and other surface processes. The thickness of this cover, and hence the distribution of sediment, varies considerably during the melt season and from year to year because of its continuous reworking by these same processes. Most reworking is initiated by melting of the buried and partially buried ice.

TILL FORMATION

In the terminus region of the Matanuska Glacier, debris is released by ablation of exposed surfaces of the ice and by melting of the upper and lower surfaces of buried ice. Other methods of release were observed only upglacier in subglacial caverns; these include the lodgement of particles in transport in ice of the basal zone, apparently by pressure-melting against bed obstacles, and the melt-out deposition of sediment from the ice roofs of caverns located on the lee side of bed obstructions. According to Boulton (1975), lodgement will occur only where the basal ice is at or near the pressure-melting point. Although the active sole of the glacier was not observed in the terminus region, the isotope analysis suggests that these conditions occur upglacier from the terminus. If lodgement occurs in the terminus, it is located at depth, probably along active planes of shear associated with the override of stagnant ice. Sediments located beneath overriding basal ice, however, usually show characteristics indicative of deposition by surface processes (Fig. 19). Lodgement is therefore thought to be of minor importance in the terminus region.

Thus, lodgement till [used in the sense of Chamberlain (1894) and more recently Boulton (1972a)] probably forms upglacier of the terminus and therefore may

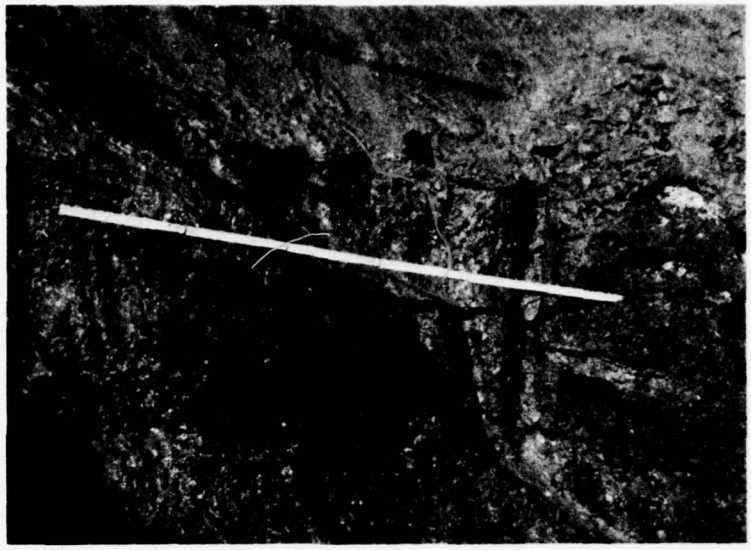


Figure 19. Frozen, overridden interstratified fluvial and sediment flow deposits located between upper and middle sections of basal ice in Figure 18. Arrow marks base of upper layer of basal ice. Effects of override could not be discerned. Scale is 1 m long.

be preserved as a basal unit in the depositional sequence of the glacier. Lodgement till will be preserved if it is not entrained by subglacial freezing prior to or during glacier recession or reworked by processes of sedimentation at the terminus. Lodgement tills formed upglacier of the terminus may vary significantly in character from till formed in the terminus region because their method of deposition, the conditions of glacial flow during deposition, and their source of debris may differ. Hence, two or more till units with marked differences in their characteristics may be deposited in a single stratigraphic sequence from the same glacier.

Genesis of melt-out till

At the present time, the primary mechanism of till formation is the melting of buried, stagnant basal ice. Melting of the upper and lower surfaces of buried ice releases the entrained sediment under confining conditions that inhibit its deformation and reworking. Thus, deposition in the simplest case involves removal of the ice component from the debris and ice of the basal zone of the glacier. Other processes of till formation were not identified in the terminus region.

The rates of sediment production due to melting of the upper surface of buried ice vary across the terminus. Rates of accumulation ranged from 2.5 to 24.5 cm from June 1974 through August 1974, and from 2.0 to 20.5 cm from July 1975 through September 1975. Figure 20 shows a poorly defined trend of decreasing rates of sediment production with increasing sediment thickness. The rates of accumulation were an average of 2.1 cm higher in 1974 than 1975, probably in part a response to the warmer weather of 1974. The mean daily temperature (over the same period of observation) was 2.5°C higher in 1974 than in 1975 (Fig. 21). The scatter in values results apparently from the influence of factors that are not considered by this relationship, such as debris content of the melting ice, and conditions affecting the temperature of the sediment, such as the texture, composition and porosity of the sediment, slope angle and aspect, and weather (temperature, precipitation, solar radiation, wind) (Sharp 1949, Scott 1964, McKenzie 1969, Loomis et al. 1970). The areal and vertical variability in sediment content of the basal zone ice (0.02 to 74% by volume) is significant and may account for much of the scatter in Figure 20.

The individual effects of the many variables mentioned above on the rate of ice melt and sediment production could not be determined. They were to be examined by monitoring the change in temperature of the sediment with change in each variable. Unfortunately, most of the sites established to monitor these changes were destroyed by reworking of the sediment cover by sediment flows and other subaerial processes. The few

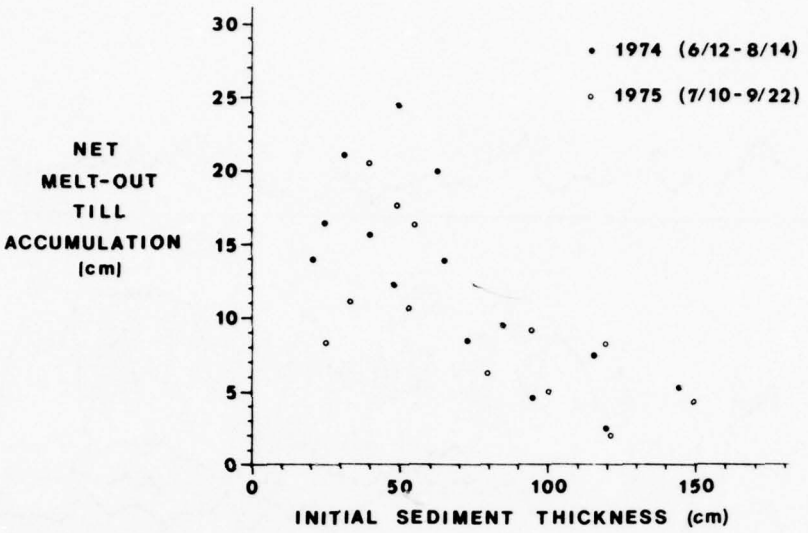


Figure 20. Rates of sediment accumulation due to melting of upper surface of buried basal ice during the 1974 and 1975 field seasons.

remaining sites provided insufficient data for correlation of these factors with sediment production.

There are, however, two important short-term influences on the temperature of the sediment cover which increase melting rates over that due to the annual sinusoidal heat fluctuation. Temperatures at the ice interface at depths up to 2 m (maximum depth monitored) reflected daily variations in the mean air temperature in 3 to 4 days at all sites, apparently irrespective of other properties. For example, a 3°C rise in the daily mean temperature on 2 July 1974 increased temperatures at the buried ice surface by 1.25° to 2.5° by 5 July. Thus, large increases in the daily mean temperature can cause increased melting for short periods of time.

The most important factor for rapid short-term changes in temperature and thus the rate of ice melt was precipitation. When there is sufficient precipitation, the sediments become thoroughly saturated and in the process, surface heat is conducted to the ice/sediment interface. Precipitation of this magnitude is most effective when preceded by a period of warm sunny weather with relatively high temperatures. Several periods most indicative of this effect in 1974 were 11 to 16 June which was followed by 3 cm of rain in 36 hours, 9 to 11 July with 3.8 cm of rain in 36 hours, and in 1975, 7 to 11 July with 3.3 cm of rain in 48 hours (Fig. 21). The average rise in temperature near the ice/sediment interface was 3.3°C, 2.8°C and 4°C, respectively, with temperatures returning to previous values about 24 to 36 hours after cessation of rainfall. The rise in temperature varies with depth and the initial temperature at that depth. Moderate rainfalls (1.0 to 2.5 cm) cause saturation of the sediment in poorly drained areas and only these areas show increased temperatures at the ice surface. Lower quantities of precipitation showed little effect on subsurface temperatures. McKenzie (1969) observed a similar effect on the temperature of gravelly sand in an ice-cored kame terrace. Sediments here are basically sandy silts.

Groundwater flow at the ice/sediment interface results in abnormally high temperatures and locally increased melting rates. Excavation indicated that the large and sustained temperature rise (+9°C) in the lower thermistor at site N in 1974 corresponds to the downslope flow of meltwater at the ice surface. Collapse of the surface and the formation of a stream along the thermally-eroded channel resulted from its continued flow. Transport of fine-grained sediments by groundwater flow was suggested by the coarse textured sediments observed at the interface adjacent to the channel at the time of collapse.

Rates of sedimentation by basal melting of buried ice could not be measured. It is likely that they are much smaller than rates observed for top-surface melting, because the basal temperature is determined mainly by the geothermal heat flux and the temperature gradient in the ice (Boulton 1970b). If it is assumed that the regional value for the geothermal heat flux is 6.70×10^{-6} J/cm^2 s (Lee and Davidson 1963) and that the debris content of the ice is 25% by volume, 0.68

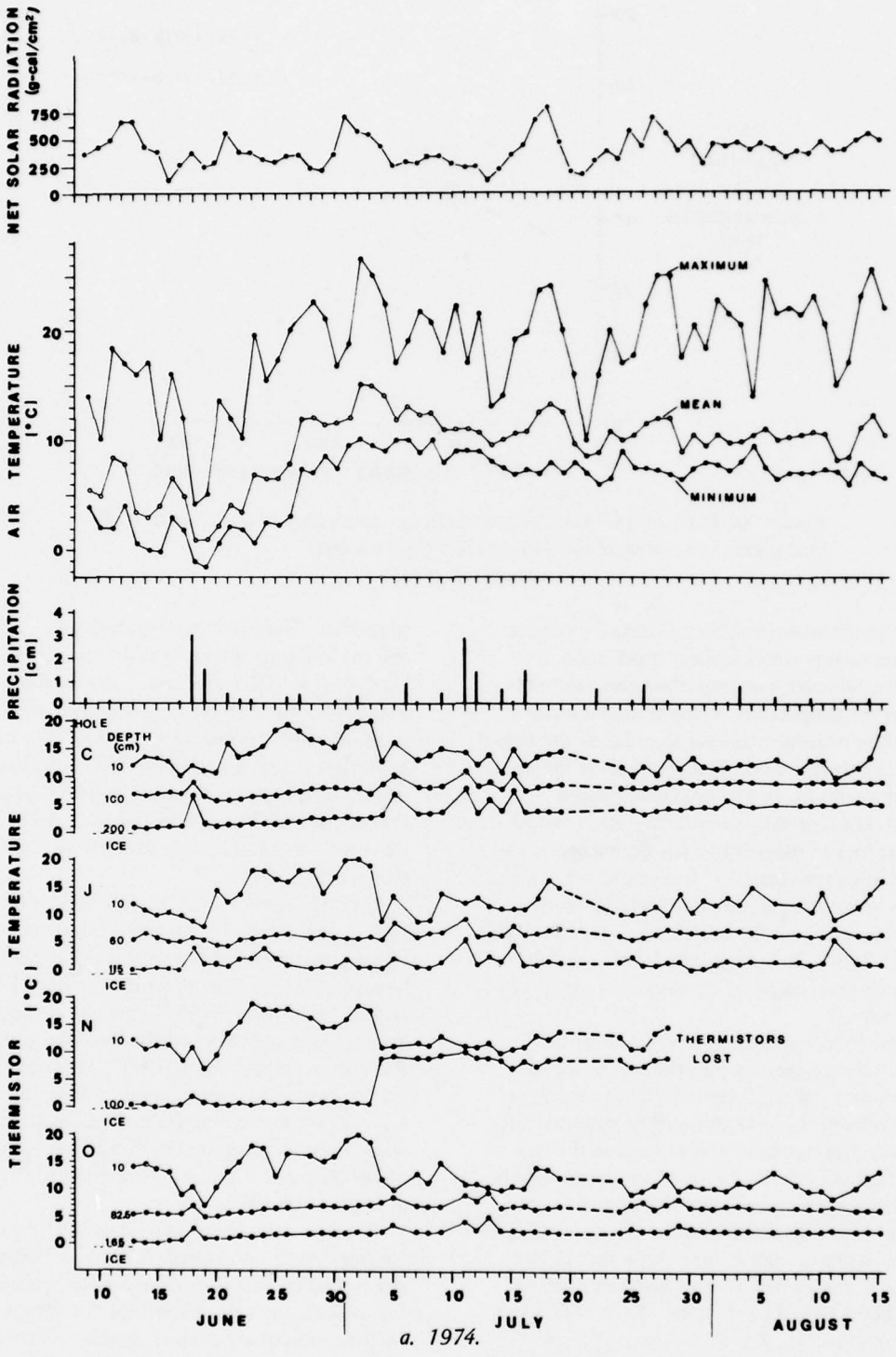
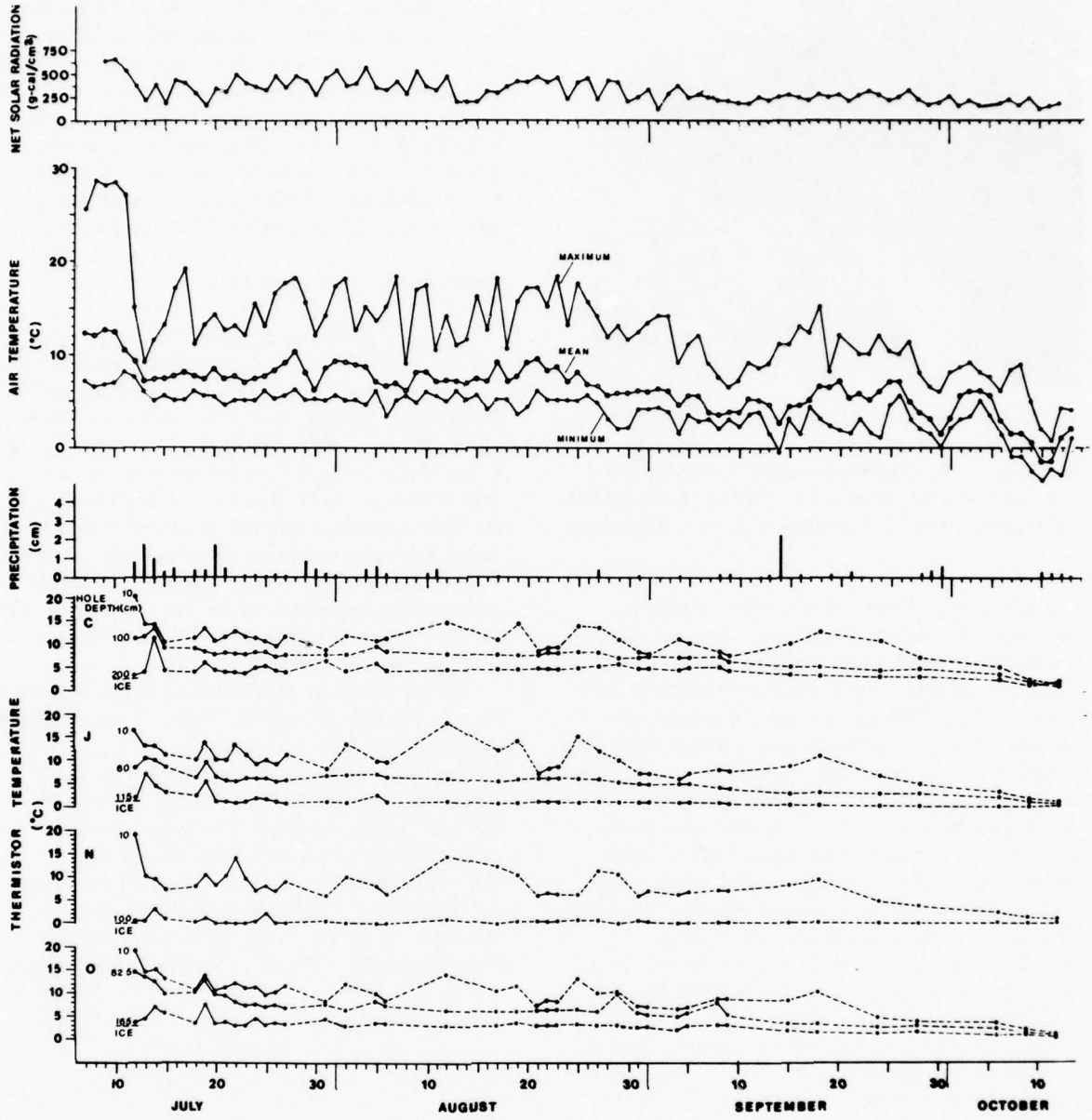


Figure 21. Weather and sediment temperature of terminus for 1974 (a) and 1975 (b). Daily mean and range of air temperature, precipitation, total solar radiation and temperature at surface, mid-point and base of sediment column on stagnant basal ice are shown.



b. 1975.

Figure 21 (cont'd).

cm/year of ice would melt from the base of the buried ice and a yearly till deposit of about 0.2 cm thick would form. Conduction of heat by groundwater flow from the glacier's interior or from a local ground-water system would increase these rates.

Sediment release and till formation results from in-situ melting of basal ice under confined conditions. The horizon of melting moves gradually upward or downward into the buried ice mass and only limited mixing of the debris takes place during deposition. Sediment released in this process essentially collapses, causing a readjustment of grain contacts and particle packing that is coincident with localized migration of fine-grained sediment into the pore spaces between

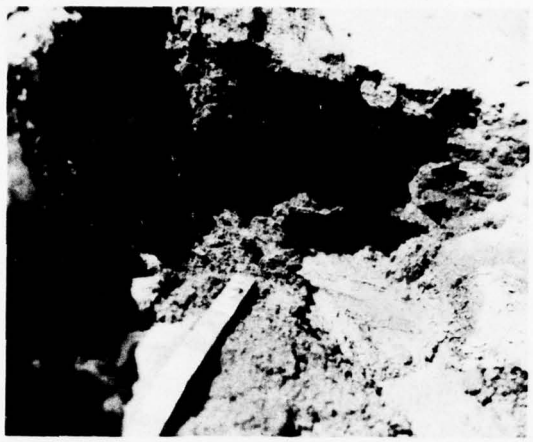


Figure 22. Photograph of melt-out till, 0.5 m thick, over basal ice source. Two thin, light-colored silt layers (arrows) and well-oriented pebble fabric with near-horizontal dip preserved in otherwise homogeneous till of pebbly, sandy silt are shown. Scale is 30 cm long.

larger particles. The extent of mixing is mainly a function of the volume of sediment contained in the source and its distribution, and to a lesser extent the texture of the debris and drainage conditions (Boulton 1970b, 1971). Thus, zones of ice with a high debris content, such as the solid subfacies, are more likely to be preserved than those with little debris, such as the discontinuous subfacies. The total debris content over a given thickness of ice is also important, since a single solid layer surrounded by low debris content ice of the discontinuous and suspended subfacies may undergo deformation and mixing due to the abundance of ice and thus open pore space upon melting. In most cases, preservation of debris zones (layers, lenses, aggregates) is limited to those that have well-defined boundaries in the ice, and that consist of well-sorted sediment or sediment of a grain size different from that of the surrounding debris, so that they are apparent in an otherwise homogeneous deposit (Fig. 22). A faint stratification may be preserved where till is derived from zones of ice with a high debris content. Discontinuous and low-debris-content suspended layers with poorly defined boundaries and similarity in texture undergo sufficient mixing to blur layer or zonal boundaries and are not preserved. Preserved features of the basal ice were only observed in deposits of the terminus region that were a maximum of 1 m thick; hence, the effect of melting an entire buried ice block is unknown. Because of the variable debris content, the variable extent, thickness and orientation of debris-laden strata in a given section of basal ice, and the presence of multiple overthrusted sections of basal ice, the features that are preserved may be deformed and large segments of the sequence may be reoriented during melt-out. Limited observations of melt-out tills (20) suggest that the combination of debris-ice properties and the limited laminar mixing which occurs during melt-out often eliminates most structural features, strata boundaries, and other properties of the ice source but preserves the bulk texture and fabric of that source. Specific examples are presented in the next section.

Characteristics of melt-out till

Sediments produced by the in-situ melting of the basal zone are true tills. These tills have been termed melt-out tills by Boulton (1970b) and this terminology is used here. Because the deposits form in-situ their properties are inherited principally from the basal ice source and secondarily from depositional and post-depositional processes. Thus, under ideal conditions, debris characteristics would be preserved in the sediment. Such ideal conditions are apparently met only rarely, because none of the stratigraphic sections observed retained all aspects of the debris character. The general characteristics of melt-out till and, for comparison, lodgement till are listed in Table V.

The characteristics of tills formed by bottom and top melting of ice of the stratified facies are represented by Figures 23-25. Figure 23 illustrates the formation of a melt-out till by top surface melting. The ice source consists of well-defined strata that dip upglacier about 60° and contain from 30 to 55% debris by volume. Individual strata are mostly of the solid and suspended (high debris content) subfacies. Debris in most layers is coarse-grained. The slope of the melting surface of the ice is 5° upglacier. The sediment cover consists of resedimented materials deposited by a dense sediment gravity flow with a low water content and the still-forming melt-out till. As at two other localities, a transitional zone of variable thickness of partially melted basal ice occurs between ice containing coarse-grained sediment and a sediment cover exceeding a thickness of 1 m. A sharp contact between sediment and ice was observed beneath sediment less than 1 m thick.

The texture of the till, as indicated in Figure 23, is much coarser than the debris source. This difference appears to have resulted from the downslope migration of the fine-grained particles in the water released during melting. The stratification and textural variations in individual layers are not preserved in the till. It is also loose, with an open framework and a high void ratio. In contrast, the overlying sediment flow deposit is denser than the till.

Table V. Characteristics of melt-out and lodgement tills.

Process	*Deposit*	*Texture* *Type*	*1) Mean (ϕ)* *2) σ(ϕ)*	*Internal organization* *General*	*Structure*	*Pebble fabric*	*Surface forms*	*Contacts- basal surface features*	*Pene- contemporaneous deformation*	*Geometry- maximum dimensions*	***Miscellaneous*** *properties*
Buried ice melt	Melt-out till	Gravel-sand-silt; silty sand; sandy silt.	1) 1 to 6 2) 1.8 to 3.5	Clasts randomly dispersed in matrix.	Massive; may preserve individual or sets of ice strata.	Strong; unimodal parallel to local ice flow; low angle of dip; S_1>0.75	Similar to ice surface; may be deformed.	Upper sharp, may be transitional; sub-ice probably sharp.	Possible; observable if structured sediments present.	Sheet to discontinuous sheet; km^2 to m^2 in area, m thick.	Internal contacts of strata are diffuse; loose.
Lodgement at glacier sole	Lodgement* till	Gravel-sand-silt; silty sand		Clasts randomly dispersed to culstered in matrix.	Massive; shear foliation, other "tectonic" features.	Strong; unimodal(?) pattern; orientation influenced by ice flow and substrate; low angle of dip.	Similar to base of ice.	Image of substrate.	Possible subglacial.	Discontinuous pockets or sheets of variable thickness and extent.	Usually dense, compact.

*From Boulton (1970b, 1971); Lavrushin (1970a, 1970b); Mickelson (1973); Boulton and Dent (1974).

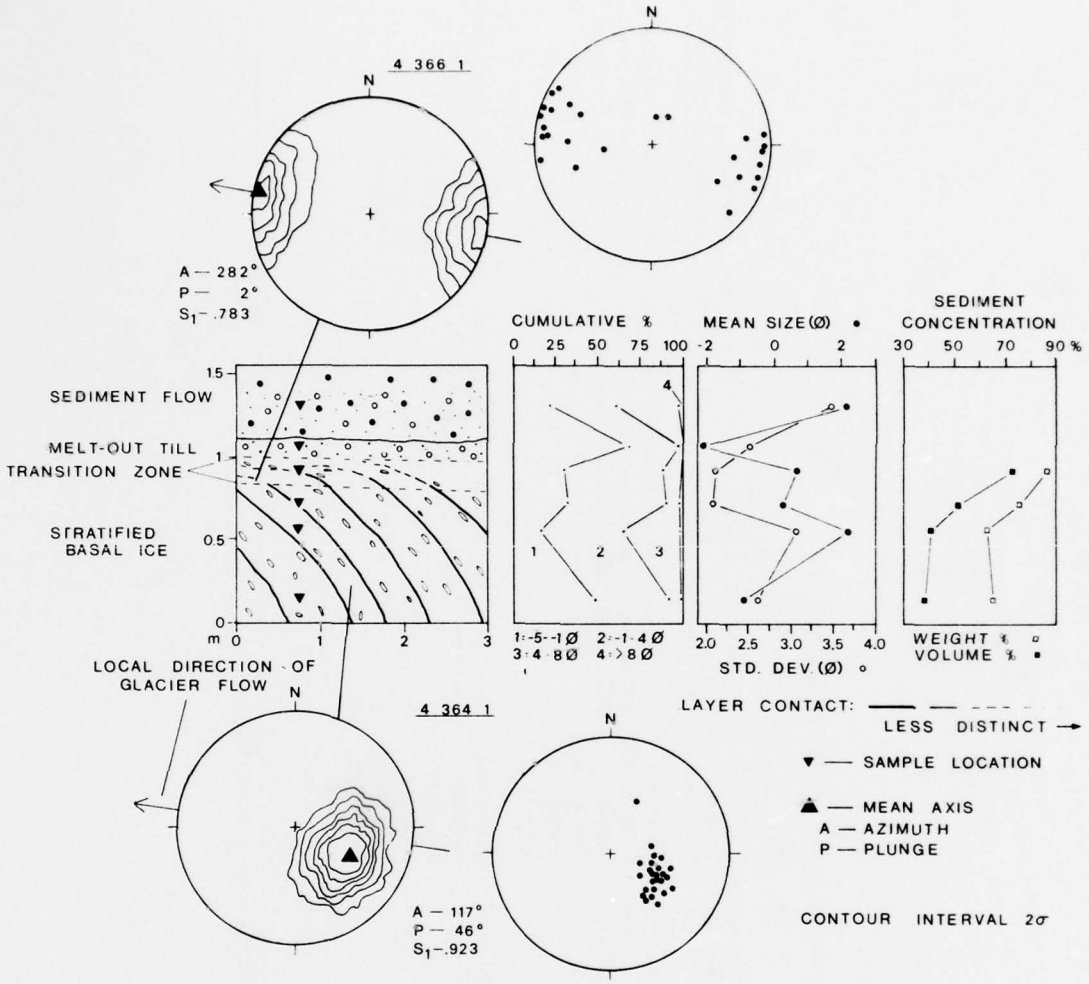


Figure 23. Characteristics of a surface melt-out till. Grain size components, mean and standard deviation of debris and sediment grain size, sediment concentration of basal ice source and pebble fabric on equal-area nets of ice and till are shown. Till is coarsened relative to debris source. Bulk texture and pebble orientations are preserved. A transitional, partially melted zone separates ice and till.

Although the texture and structure of the debris are lost during melt-out, the orientation of pebbles in the basal ice is preserved with only minor modification. The long axis orientations of prolate pebbles and the direction of dip of the *ab*-plane of blades and disks were measured in an ice stratum and in the deposit resulting from that same stratum (Fig. 23). A unimodal pattern indicative of a significant distribution and a relatively small degree of dispersion is derived from the pebble fabrics of both the ice and sediment. Melting increases the scatter about the mean axis, decreasing S_1 from 0.923 to 0.783, and decreases the angle of dip of the mean axis to a near-horizontal orientation. Thus, the amount of dispersion from the local direction of ice flow is increased but the general parallelism to that direction is preserved. The change in orientation results both from the loss of the supporting ice matrix and from the interaction of adjacent particles brought into contact during melting, mixing, and compaction. As will be evident later in the discussion, the significance values (S_1) for melt-out tills remain larger than those for fabrics developed in sediments deposited by other processes at the terminus.

Figure 24 shows the characteristics of a second till formed by surface melt-out. The stratification in the basal zone dips upglacier about 25°, and the slope of the ice surface is approximately horizontal. Debris contents of the ice range from about 1 to 45% by

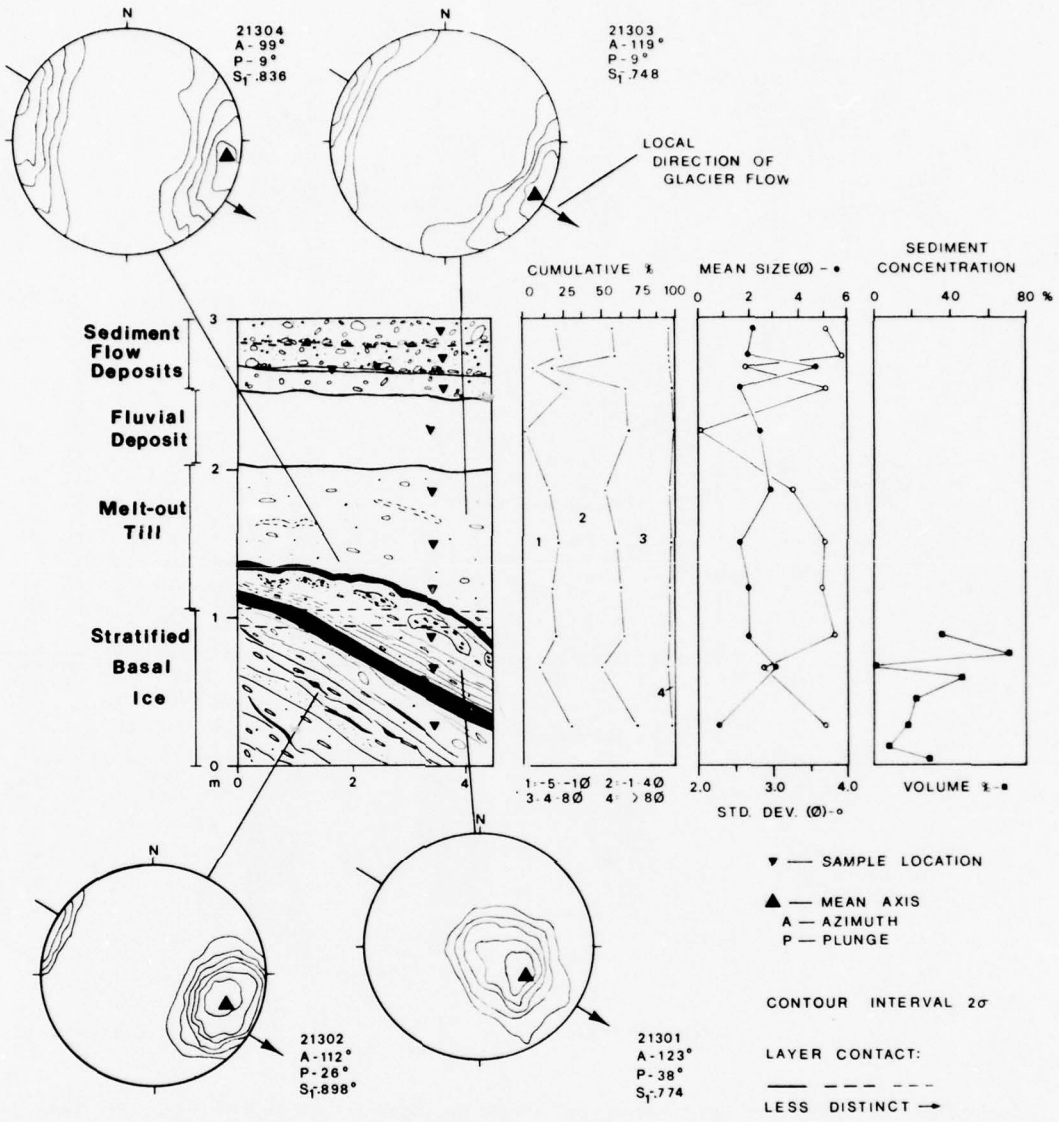


Figure 24. Characteristics of a surface melt-out till. Properties shown are as stated for Figure 23. Individual strata, lenses of debris and thin zone of debris stratification are preserved in otherwise massive melt-out till. Pebble orientations of ice are preserved in till with increased scatter and descreased angle of dip.

volume, except in two solid layer strata which contain 74% debris by volume. Individual strata are mainly of the suspended and discontinuous subfacies. The surface cover consists of an upper zone of three sediment flows (each of about 15 cm thick) over sandy fluvial materials (50 cm thick). The melt-out till itself is approximately 1 m thick. Samples were taken from three levels in the till and three points in the underlying ice. In this case, the bulk texture is preserved in most of the till. However, the two solid strata of the basal ice composed of clayey silts are also preserved in the till. Their dip has been reduced from 25° to near horizontal and they are now slightly folded. Also, the small lenses of coarse sand that occur beneath the upper clayey silt layer are derived from the lenses or discontinuous layers of well-sorted coarse material of the discontinuous subfacies that occur beneath it in the ice. A subhorizontal, poorly-defined stratification, apparently inherited from the layers of the suspended subfacies concentrated at this level in the ice, was observed below the lenses of coarse sand.

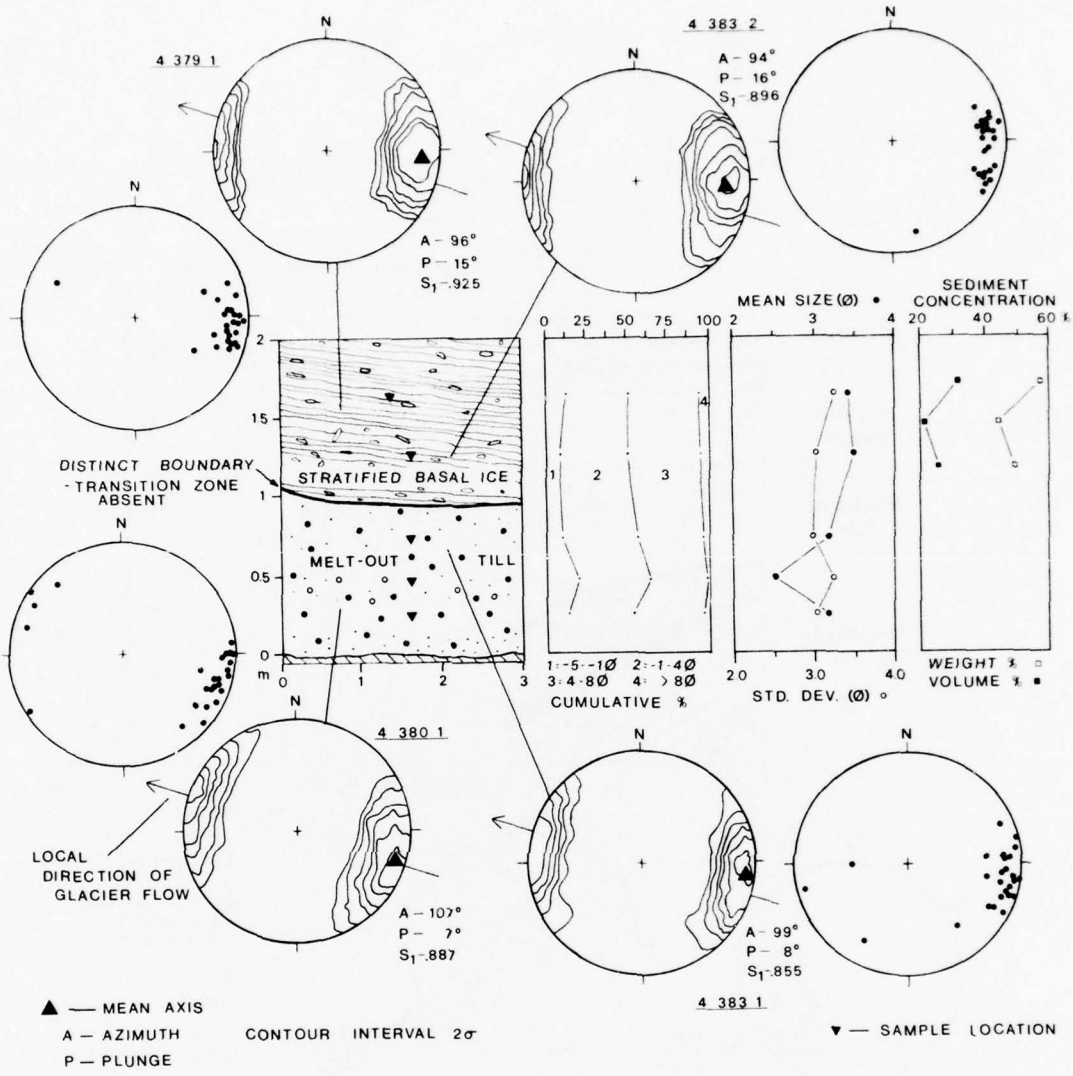


Figure 25. Characteristics of basal melt-out till. Properties shown are as stated for Figure 23. Exposed massive melt-out till is overlain by about 20 m of ice. Bulk texture and pebble fabric of till are virtually identical to ice source. Ice/sediment interface is sharp without cavities.

The orientation of pebbles in both the ice and till is approximately parallel to the local direction of flow of the glacier (Fig. 24). The mean orientation of pebbles in the ice differed from this direction by ±10°; the mean orientation in the till differed by ±20°. The scatter of pebble orientations about the mean is larger in the till than in the ice. The dip of pebbles in the till is also lower than in the ice, but unrelated to the direction of ice flow. The pebble fabric in the overlying sediment flow deposits does not correlate with the local direction of ice flow. It also differs from that of the till due to a larger degree of scatter in individual measurements and hence less significant modal pattern.

Figure 25 represents the effects of basal melt-out on debris characteristics. This stratigraphic sequence was exposed by stream erosion near the present ice margin. It is overlain by an estimated 20 m of ice and sediment. The melt-out origin for this sediment is indicated by the unconformable contact between strata in the ice and the sediment pile, the local crossing of that contact by pebbles (embedded in ice and sediment), and the similarity in texture of the debris, the underlying sediment, and the sediment deposited due to the associated increase in temperature subsequent to exposure. A 2-cm-thick layer was deposited about 0.3 m behind the face.

The bulk texture of the till (pebbly sandy silt) is virtually identical to that of the ice source. The basal zone ice is composed of alternating high and low debris content layers of the suspended subfacies. Individual layers vary in sediment content; a range of about 0.5 to 55% by volume was measured. The bulk sediment concentration ranged from 20 to 30% by volume. Here, as in the only other exposure of basal melt-out till that was observed (about 8 cm thick), the ice contact is sharp without cavities and characteristics of the texture of the debris are preserved in the till. The overburden pressure of the ice apparently compacts and consolidates the sediment as it is released and only limited mixing of the debris in the ice strata occurs. The slow rate of melt-out may enhance preservation of the characteristics of the debris. The density and compactness of the till is indicated by an inability to penetrate it more than 1 or 2 cm with a blow of a pick. This condition contrasts with surface melt-out tills which are generally loose and readily disaggregate. If undrained conditions exist, excess pore water pressures may develop that limit consolidation and may induce internal deformation under a differential overburden (Boulton 1971). The amount of pore water pressure at the top and bottom of the melting ice is determined by the rate of meltwater production and the rate of meltwater expulsion (Boulton and Paul 1976). Although neither of the basal melt-out tills examined in this study was derived from ice composed of the solid subfacies, the observed absence of change in the texture of the till implies that solid subfacies layers will be preserved. Thus, a complex till may form which contains discontinuous layers and lenses, some with structures and textures indicative of other sedimentological processes.

As in other melt-out tills, the orientation of pebbles is inherited from the ice source with little change. Individual pebbles and granules as well as aggregates are aligned parallel to the ice strata. The mean axis varies by a maximum of 11° between ice and till measurements. The degree of scatter in the pebble orientations, as shown by S_1, increased by a small amount in the till (a maximum difference of 0.07), while the dip of the mean axis decreased by about half. The absence of cavities between the base of the ice and the till suggest that the shape of the melting surface and the overburden pressure exerted by the ice probably affect the orientation of pebbles in the till during melt-out.

CHAPTER 5. DEPOSITIONAL PROCESSES—RESEDIMENTATION

Sedimentation in the terminus region is dominated by processes of resedimentation; it is estimated that only 5% of the sediments forming are true tills. The predominant process is sediment gravity flow, hereafter called sediment flow.

SEDIMENT FLOWS

Sediment flow refers to the downslope flow of sediment or sediment-water mixtures under the force of gravity, and the types of sediment flow in the subaqueous environment have been defined on the basis of the predominant mechanism of grain support (Middleton and Hampton 1973, 1976). Theory suggests the importance of four mechanisms: fluid turbulence, upward intergranular flow of fluid correspondent with grain settlement, dispersive pressures generated by direct grain-to-grain interaction of cohesionless particles, and support of larger grains by the strength of a fine-grained matrix. Corresponding flow types are referred to as turbidity currents, fluidized sediment flows, grain flows, and debris flows. Semiquantitative analysis by Lowe (1976a, 1976b) indicated that pure grain flows and pure fluidized flows are probably unimportant geologically. Lowe suggested liquefaction rather than fluidization as a significant transport mechanism. Liquefaction, the transformation of a granular material from a solid state into a liquefied state, is the consequence of increased pore-water pressures (Youd 1973). Laboratory, theoretical and field studies of sediment flows have led many authors to suggest that single mechanism flow models are highly idealized, that two or more mechanisms may be important in natural sediment flows and, further, that flow types may be gradational from one to another (Middleton and Hampton 1973, Hampton 1975, Low 1975, Carter 1975).

Observations of active subaerial sediment flows in the terminus region of the Matanuska Glacier indicate that theoretical, single mechanism flow models do not represent these flows. There, sediment flows are characterized by multiple mechanisms of grain support and transport. Properties of these flows also suggest that they are transitional to one another and are members of a predominantly water content-controlled continuum. Sediment flows range from those in which sediment strength is the primary grain support mechanism to those that appear to be fully liquefied. Grain interactions, local fluidization, traction, and other grain support and transport mechanisms are also important. Because these mechanisms vary, the general term **"sediment flow" will be used throughout** this discussion.

As stated above, active (moving) sediment flows are gradational in terms of physical properties and mechanisms of grain support and transport; however, for purposes of discussion four types of sediment flows that are distinguishable because of differences in these properties and mechanisms are described. The properties of active sediment flows are listed in Table VI at the outset and grouped within these four general types.

Sediment flows and their deposits which occur in the glacial environment have been incorrectly referred to in the literature as "flowtill" (Hartshorn 1958, Boulton 1968). Sediment flows result generally in the disaggregation of sediment in transport and in its resedimentation. Sediment flow deposits acquire properties from their mode of transport and deposition which distinguish them from true tills. Their source includes deposits of the terminus region, such as tills and resedimented materials, as well as debris of the glacier. The distinction between a true till and resedimented material of sediment flow or other origin must be maintained in order to interpret the depositional sequence of a glacier in terms of the processes of sedimentation and the environmental conditions under which they were deposited. Therefore, "flowtill" is an incorrect reference to sediment gravity flows and deposits of sediment flow origin and its use should be discontinued.

Flow initiation

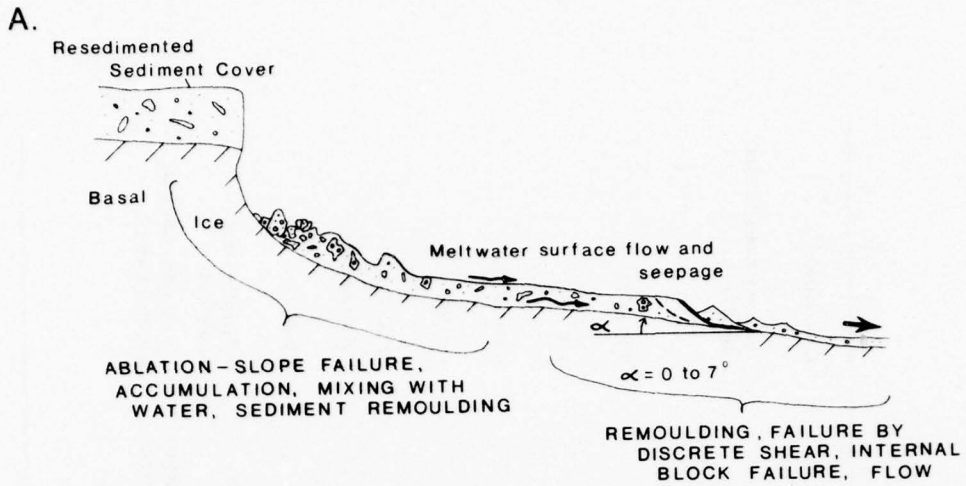
Most sediment flows are derived from water and sediment released by ablation of active basal ice exposed at the glacier margin and of stagnant basal ice exposed in ice-cored slopes (Fig. 26). Sediment flows are also initiated by saturation of sediment due to the melting of ice buried beneath a relatively thin sediment cover, saturation of surface materials by a large quantity of rain, and melting and concentration of water released by thawing due to solar heating of frozen sediment during winter. In each of these cases, flows are initiated in sediment on low angled slopes (1-7°) that are underlain by ice of the basal zone. Saturation of the sediment is required to reduce its shear strength to failure. Flows initiated under these conditions are generally smaller in size and flow shorter distances (2 to 10 m) than those of ablational sources. Their characteristics, however, are similar to those derived from ablation.

The sources of sediment, which include the sediment cover of mainly melt-out till and resedimented

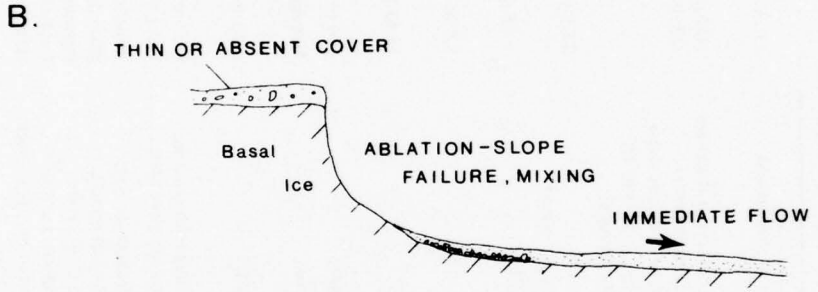
Table VI. Attributes of active sediment flows.

Attribute	*Flow type* I	II	III	IV
Morphology	Lobate with marginal ridges; non-channelized.	Lobate to channelized.	Channelized.	Channelized.
Channel-wise profile	Body constant in thickness with planar surface; head stands above body; tail thins abruptly upslope.	Body constant in thickness with ridged to planar surface; head stands above body (less than Type I); tail thins upslope.	Mass thins from head to tail; irregular surface.	Thin continuous "stream"; planar surface.
Thickness (m)	0.01 to 2 (0.5 to 1 typical)	0.01 to 1.4 (0.1 to 0.7 typical)	0.03 to 0.6	0.02 to 0.1
Bulk water content (wt %)*	~ 8 to 14	~ 14 to 19	~ 18 to 25	725
Bulk wet density (g/cm^3)*	2.0 to 2.6	1.9 to 2.15	1.8 to 1.95	< 1.8
Surface flow rates (cm/s)	0.1 to 0.5	0.2 to 5	15 to 125	1 to 200
Typical length of flow (m)	10 to 300†	10 to 300†	100 to 400†	50 to 400†
Surface shear strength (kg/cm^2)	0.4 to 1.5	0.6 or less	Not measurable	Not measurable
Approx. bulk mean grain size (mm)*	2 to 0.3	0.4 to 0.1	0.15 to 0.06	≤ 0.06
Flow character (laminar)	Shear in thin basal zone with override at head.	Rafted plug with shear in lower and marginal zones.	Discontinuous plug to shear throughout.	Differential shear throughout.
Grain support and transport	Gross strength.	Gross strength in plug; traction, local liquefaction and fluidization, grain dispersive pressures and reduced matrix strength in shear zone.	Reduced strength, traction, grain dispersive pressures; possibly liquefaction-fluidization, transient turbidity.	Liquefaction; some traction; buoyancy (?).

*Sample from central part of flow.
†Maximum length of flow reflects boundary conditions of terminus region.



a. Most typical situation for sediment flow initiation. Types II and III are primarily the result of failure and flow of downslope edge of sediment accumulated at base of laterally retreating ice-cored slope. Type I flows result from failure in a thin zone at the base of a sediment pile with low water content.

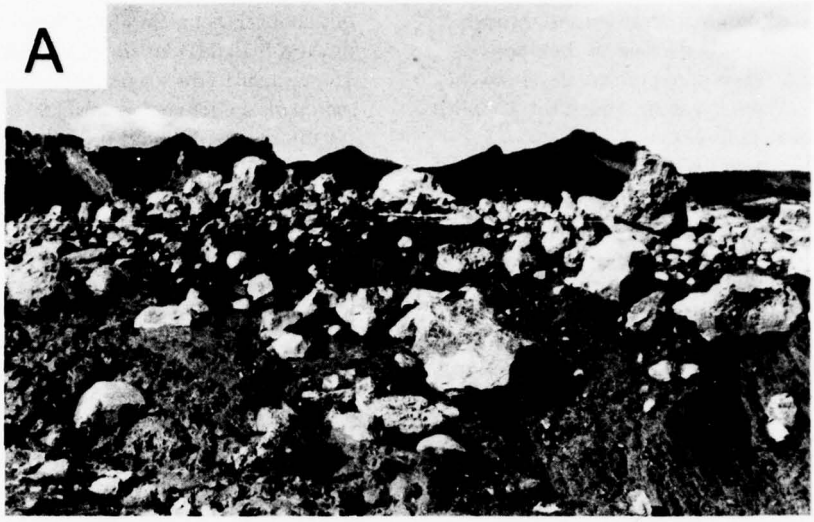


b. Type IV flows initiated directly from ablating ice-cored slope where relative availability of meltwater is high and sediment low.

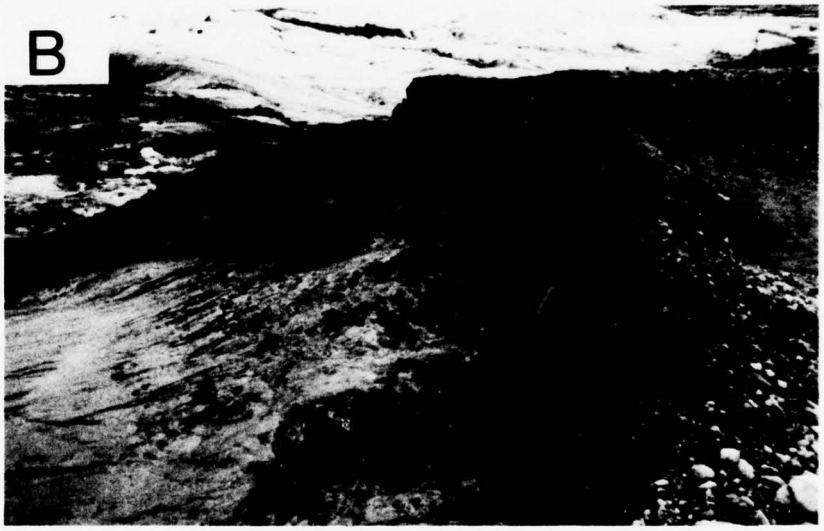
Figure 26. Sediment flow initiation.

materials as well as the debris of the basal ice, are texturally diverse. Thus, sediment flows may be texturally diverse as well. Flows are, however, initially selective and particles of a size exceeding that which can be transported are concentrated in the source area to form a coarse gravel lag on the ice surface that is exposed after flow initiation (Fig. 27). The formation of this gravel lag normally results where sediments accumulate under undrained conditions that permit the sediments to become oversaturated. The increase in water content due to the continued influx of meltwaters from the ablating slope and melting of the buried ice reduces the strength of the sediment and any grains that cannot now be supported settle to the ice interface.

The near-vertical slope of the moist to dry sediments covering the stagnant basal ice indicates stability and strength. These sediments collapse or slide after a loss of support due to ablation and lateral retreat of the exposed basal ice (Fig. 27). Materials released from the sediment cover and ice, slip, roll, and fall down the high-angled ice slope. Debris-laden meltwater flowing over the ablating ice in sheets and small rills mixes with the sediments during and after its transport to the base of the slope. Initially coherent blocks of sediment may slide along the irregular bed of ice. Collapse of these blocks into smaller blocks, aggregates, and individual particles, apparently as the result of vibrations and agitation due to sliding, and the mixing of this sediment with meltwater may follow. At the base of the slope, mixing continues and the sediment-water mixture is incorporated into the upslope end of the flow mass. Slope angles at the base of the ice-cored slope range from 0° to 7° and permit thorough saturation of the accumulating sediments. The net result of these processes is the remolding (loss of structure and reduction of strength) of the source materials (Terzaghi and Peck 1967).



a. Coarse gravel lag and intraformational blocks of unincorporated materials concentrated on stagnant basal ice in source area of recent sediment flow. Flow was incompetent to transport them. Scale is 1 m long.



b. Ice-cored slope showing typical vertical face of sediment cover of about 1 to 3 m thick. Covered ice closest to camera due to undermining and failure of sediment cover. Accumulating sediment is characterized by blocks of material that are incorporated by remolding downslope. Scale is 1 m long.

Figure 27. Sediment flow source areas.

Failure and flow of the accumulating sediment is usually not immediate. The sediments possess sufficient strength to resist the shear imposed by gravity. The applied shear stress due to gravity may, however, be increased by increasing the thickness and mass of the sediment pile with continued influx of sediment and water from the ablating ice, or, probably more importantly, the shear strength may be reduced by increasing the pore pressures (seepage, hydrostatic) in the sediments (Terzaghi and Peck 1967). Because the

sediment is saturated, fluids are transmitted through it and the influx of water at the base of the slope results in seepage and excess pore pressure development in the toe region. Where the shear strength and applied shear stress are equal, failure occurs.

Initiation of flow begins with the rotational slip of blocks of sediment along discrete shear planes (Fig. 26, 27). As blocks slide, other discrete planes develop upslope from the initial failure plane and in the block itself. The blocks rapidly disintegrate, mix with meltwaters flowing over their surface, and undergo complete remolding and flow. The blocks of sediment are probably in a metastable condition and fail as the result of strains imposed by the rotational slip failure. That process in turn triggers failure along an infinite number of other planes in the block (Morgenstern 1967). The rotational slip failure and block movement along the initial slip plane results in an effective oversteepening and loss of support for material further upslope, which then also fails and flows away (Andresen and Bjerrum 1967).

The cause of failure and thus the initiation of flow can be considered more quantitatively for a typical situation by making certain assumptions. Failure conditions can be considered by utilizing the modified Coulomb equation in terms of effective stress:

$$s = c + (p - \mu) \tan\phi \qquad (3)$$

where s is the shearing resistance or shear strength of the sediment, c apparent cohesion, p normal pressure (due to overburden), μ pore pressure, and ϕ the angle of internal friction (Terzaghi and Peck 1967). The sediment involved is granular, principally silt and sand, and the lack of clay size particles (less than 5%) and clay minerals (mostly well-crystallized mica and chlorite) indicates that it can be considered mostly cohesionless with a nominal value for c. Thus,

$$s = (p - \mu) \tan\phi \qquad (4)$$

represents the shearing resistance per unit area for the sediment under saturated, undrained conditions. Because the accumulating sediment is saturated and lies on a slope of 1° to 7°, a hydraulic head develops in the toe region due to the transmittal of fluids through the sediment. This head determines the seepage pressure component of μ at any given point along the base of the deposit. For a typical sediment accumulation of 10 m in length sitting on an ice slope of angle 2° (conservative), a piezometric head of about 0.3 m develops at the toe. The value for μ is about 0.03 kg/cm^2. If a unit weight of 9 kg/m^2 is assumed for the sediment, p is about 0.04 kg/cm^2 for a thickness of 0.3 m and just less than 0.03 kg/cm^2 for a thickness of 0.15 m. These calculations suggest that under these conditions, sediments are inherently unstable in the toe region for thicknesses of about 0.15 m or less. This discussion shows clearly that the properties of the sediments, low angled slopes of impermeable ice and constant availability of water are particularly conducive to sediment failure and the initiation of sediment flows.

Sediment flows that contain more water than those initiated by the procedure described above (type IV) and those that contain less (type I) are usually not associated with a rotational block failure. Type IV flows are often formed where there is a large quantity of water available in relation to the amount of sediment available. In this case, sufficient mixing and remolding of the sediment and water occurs so that flow takes place directly from the base of the slope (Fig. 26). Mixing with meltwater during flow increases the water content beyond saturation. Because insufficient sediment is available to form a "stable" mass at the base of the slope, an open channel extends to it and the flow is umimpeded by accumulating sediment. Type IV flows may also arise from sediment flows with lower water content by mixing of such flows with additional water during transport from the source area, and from sediment-water mixtures that accumulate under undrained conditions in ice-floored basins. If the influx of meltwater is sufficient to cause liquefaction of sediments accumulated in such basins, grain settlement, pore fluid expulsion, and sedimentation will occur.

When the quantity of meltwater available is small and the source material lies on horizontal to low angled slopes, the development of type I flows is favored. These dense, low water content flows appear to fail by shearing within a discrete zone at their base. The body of the flow possesses strength (shear strength at the surface during flow of 0.4 to 1.5 kg/cm^2) but internal deformation is observed in the head region. Bubble cavities indicate the sediment is only partially saturated and much of the strength is probably an apparent cohesion due to capillary tension (Lambe and Whitman 1969). Apparently, flow only takes place after reaching some critical thickness at which the applied stress due to gravity exceeds the yield strength of the sediment or of the sediment/ice interface at the base of the flow. Sliding of the flow on underlying ice occurs sporadically in isolated areas, apparently where conditions are favorable to the development of excess pore pressures at the ice/sediment interface.

Thus, the mobilization of most sediment flows observed here involves basically the disaggregation of stable

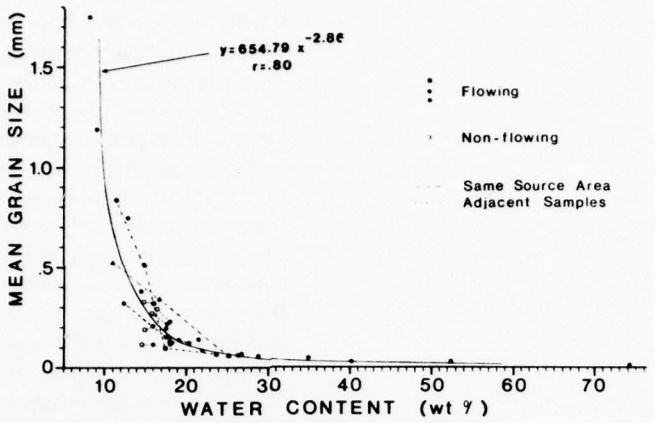


Figure 28. Comparison of mean grain size with water content of central part of active (flowing) sediment flows sampled from across the terminus. Dashed lines join samples of flows derived from the same source area; solid lines join samples of adjacent flowing and non-flowing materials in source area.

sediments, their mixing with meltwater, and their remolding into a metastable or unstable sediment pile. Further reduction of strength results from an increase in the water content of the sediment pile and the seepage of meltwater through it. Failure and then flow takes place when the applied stress due to gravity exceeds the shear strength of the sediment in a thin to thick zone above the ice/sediment interface.

Trends in flow parameters and general relationships

Observation and measurement of certain properties of active sediment flows indicate that their physical characteristics and mechanisms of grain support and transport vary systematically and that the various types of flows occurring in the terminus region are members of a continuum. Systematic changes in flow character, such as texture, shear strength, and mechanisms of transport, can be related directly to measured changes in water content and thus the bulk wet density of the flow. Previous studies indicated the importance of water to mobilization of various types of sediment flows (e. g. Blackwelder 1928, Sharp and Nobles 1953, Curry 1966) and, more recently, Rodine (1974) defined the potential for debris flow in terms of water content. The same changes in sediment flow characteristics were observed with the movement of a flow downslope on a bed of increasing slope angle. The net effect of slope angle and water content could not, however, be separated because the water content also increased during flow. The relationship between water content and texture and three other physical properties are presented below and their implications with respect to sediment flow behavior discussed.

Figure 28 shows the basic relationship between texture and water content; this comparison suggests that a mechanism that results in selective size sorting of particles operates in sediment flows. The mean grain size was computed for composite samples (finer than 16 mm size) of the central part of flows of different character and the angle of slope of the bed ranged from 1° to 7° in the upper region of the flow system where all samples were taken. A fairly strong correlation exists between the two variables: the mean grain size decreases rapidly with slight increases in water content for quantities between 8 and 17% by weight, whereas changes in water content above about 17% result in only minor changes in mean grain size. Deviations from this trend as indicated by the water contents of flows derived from the same source area probably represent initial differences in the texture of the sediment source, local changes in slope angle or other factors influencing flow competence. The water content of adjacent non-flowing and flowing sediment in the source area may differ by as little as about 1% (Fig. 28).

Less correlation exists between the water content of a flow and the size of the largest clast in transport in the central part of that flow (Fig. 29). Hampton (1975) used this correlation to define the competence (largest grain size supported by a clay-fluid matrix) of experimentally produced debris flows. The competence, used here to denote simply the largest clast supported in the sediment flow, probably differs from that found

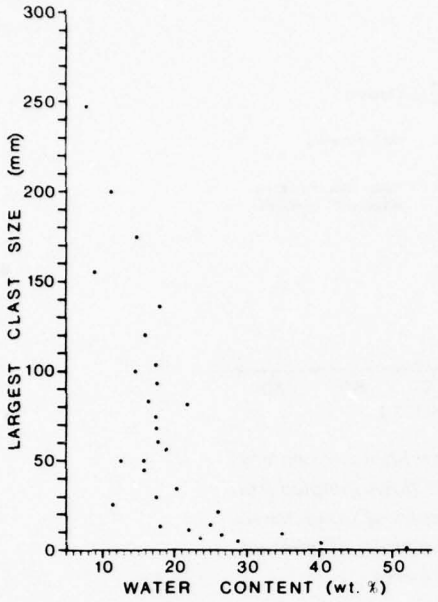


Figure 29. Comparison of largest clast in suspended transport with water content sampled from central part of active sediment flows. A poorly-defined trend and correlation are apparent.

by Hampton because of three factors. First, fine-grained flows of low water content may contain only small clasts, even though they have the capacity to support larger ones, because these particles were not present in the source materials. Sediment flows of this type are often characteristic of those derived from ablating active basal ice where gravel-size particles are scattered widely through the ice source. Secondly, inadvertent sampling of bedload debris that is much coarser than sediment actually suspended in the flow produces excessively large competence values, whereas point sampling in active flows may easily miss the largest particle and thus underestimate the competence of the flow. Inadvertent bedload sampling is particularly a problem in sediment flows with larger water contents; these flows are thin and tractional debris may extend through their surfaces. Similarly, samples containing particles in a transitory state, for example, those slowly settling out, would indicate values that are too large. Finally, Hampton (1975) used only matrix strength as a grain support mechanism. Sediment flows here are characterized by several support mechanisms operating simultaneously in a given flow. Therefore, a simple relationship between water content and the maximum size of clast supported by a sediment flow may not exist. The data obtained in this study indicate the mean grain size better represents the relative competence of active sediment flows.

Comparison of the grain size components of all grab samples from active sediment flows suggest the increase in mean grain size with decrease in water content results mainly from an increase in the quantity and size of the coarsest fraction. This trend shown in Figure 30 is general and exceptions occur. Representative frequency curves of composite samples of sediment flows derived from the same source area but that differ in bulk water content show a minor change in the matrix mode but a distinctive shift in the quantity and size of the coarse modal fractions with changes in the water content (Fig. 31). Similar differences are observed in samples from different parts of the same sediment flow when it is characterized by internal variations in water content. These frequency curves also illustrate the generally polymodal texture and poor to very poor sorting of sediment flows. Large pebbles, cobbles and boulders, which were not considered in this analysis, are transported in suspension and as bedload in many of the sediment flows.

The maximum thickness of sediment flows decreases generally with increasing water content (Table VI). The largest change in maximum thickness occurs at quantities of less than about 18% by weight of water, whereas the change for larger amounts of water is minor. No relationship was found for the minimum flow thickness, probably because no consideration was given to the effects of the flow surface area and bed slope (1° to 10°), although Johnson (1965) concluded that they were important.

Several soil properties in flowing and adjacent nonflowing deposits were also determined. These included, in addition to water content, the shear strength at the surface of the flow, bulk wet density, and porosity (Fig. 32). Increases in porosity and density from nonflowing to flowing materials occur with increases in water content of the sediment. Assuming the texture is identical, these data would indicate loss of strength due principally to a decrease in the frictional resistance to shear of the sediment (Lambe and Whitman 1969). The overall trend for active sediment flows is similar. Although the texture of each sample is not the same, the rapid decline of shear strength to a nominal value with increase in water content at relatively low quantities confirms this relationship and indicates increasing liquidity of mostly cohesionless sediment.

The trends in these factors and the observed relationship between water content and flow characteristics (described in a following section) suggest that water content is the most important parameter controlling the behavior of sediment flows. This relationship results

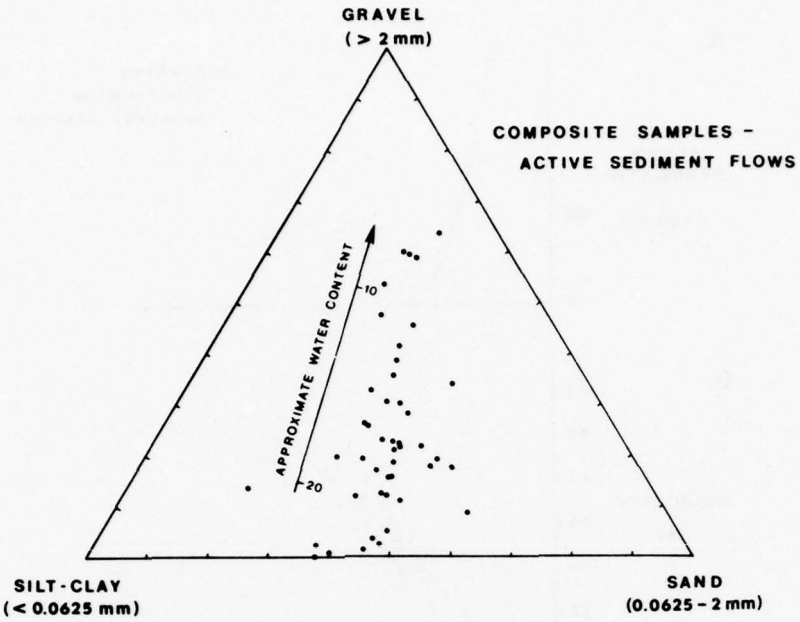


Figure 30. Ternary diagram of grain size (maximum size 32 mm) of composite samples of active sediment flows. Arrow indicates approximate trend in water content of the source flow.

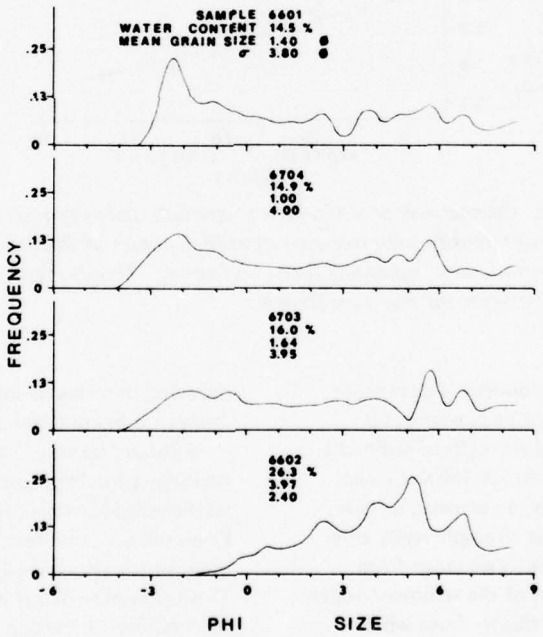


Figure 31. Representative frequency curves of texture of active sediment flows of different water contents derived from same source area. Increase in water content occurs from bottom to top. A similar variation in texture occurs internally in flows characterized by zones of different water content.

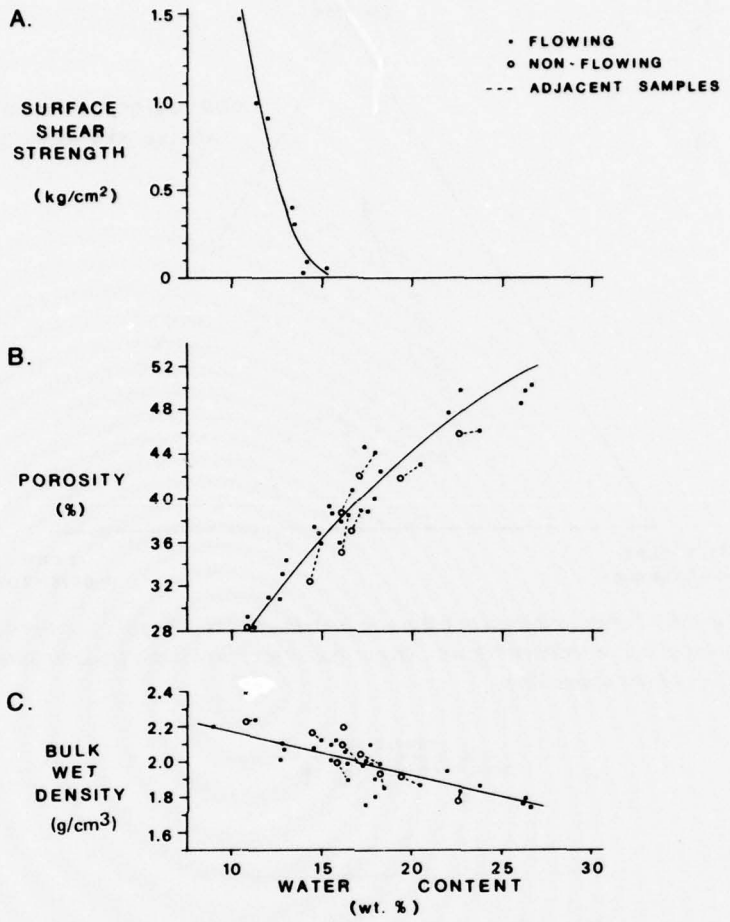


Figure 32. Comparison of surface shear strength, porosity (calculated) and bulk wet density with water content for samples of flowing and adjacent nonflowing sediments (prior to failure). Trends for samples from active sediment flows are shown.

because the in-situ strength of sediment is a function of its water content; the effect of increased water content is a decrease in the total strength of sediment under stress (e.g. Schofield and Wroth 1968, Lambe and Whitman 1969). The trends in porosity, density, water content, texture, and shear strength verify this relationship. Thus, the sediment flows range from those in which the total strength of the sediment-water mixture determines flow properties to those which are fully liquified.

The transitional nature of active sediment flows indicates the system is a continuum changing from plastic to liquid behavior. The proportions of the two phases, fluid (partially air) and solids, determines the shear strength exhibited by the sediment. This continuously deforming system must be evaluated and modeled in terms of soil dynamics, but such a rheological analysis is beyond the scope of this study.

It should be stated that Johnson (1965) modeled the rheology of debris flows with an empirically-derived relationship for stress and strain rate using the static Coulomb criterion for failure coupled with a term to account for viscous effects observed in debris flows. This Coulomb-viscous model has been shown to account successfully for certain features observed in laboratory and natural debris flows (Johnson 1970, Johnson and Hampton 1968, 1969, Johnson and Rahn 1970, Hampton 1970, 1972, 1975, Rodine 1974, Rodine and Johnson 1976). This model appears to account in part for the behavior observed in type I and II flows. Several important features of flows observed in this study are, however, not accounted for by this model. For

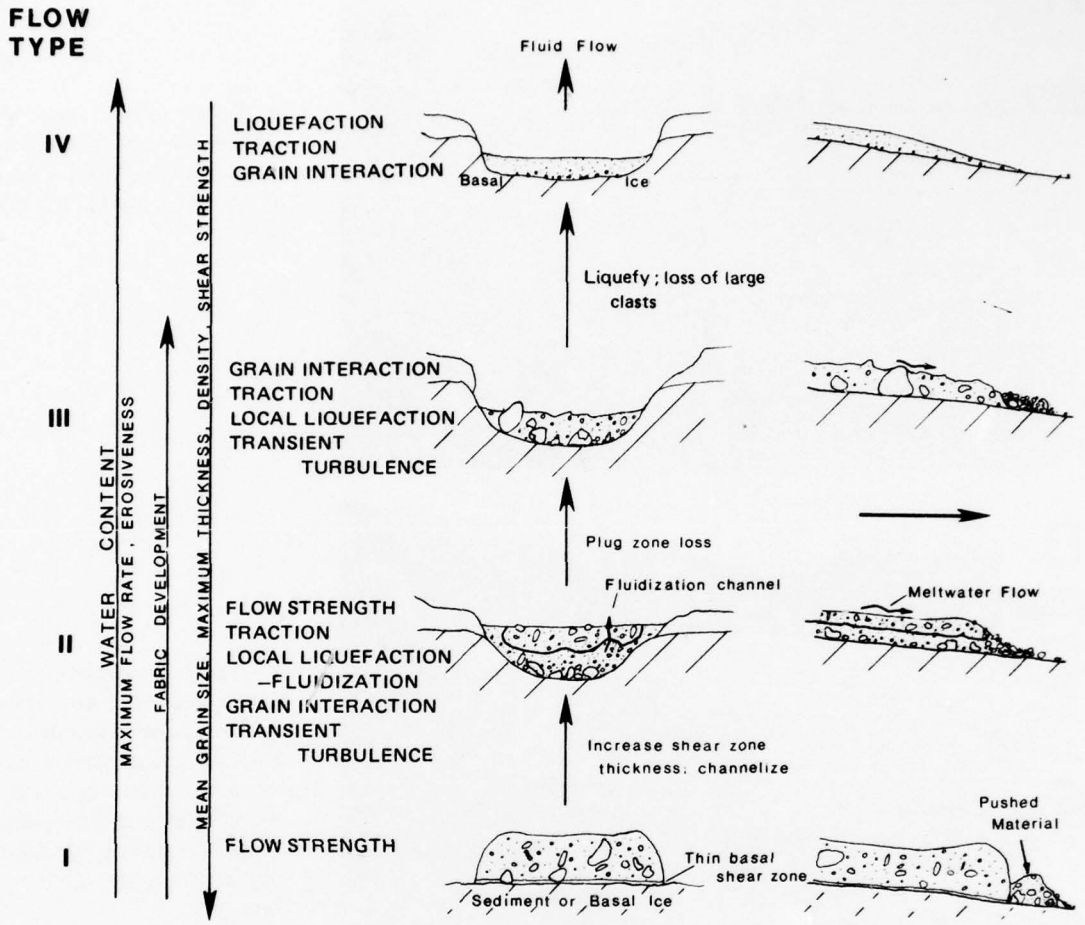


Figure 33. Idealized cross sections, transverse and parallel to direction of flow, of the four sediment flow types. Flow types are transitional to one another. Channels usually are ice-floored with walls of sediment and ice. Grain support and transport mechanisms are indicated. Trends in various parameters are shown; water content increases from bottom to top.

example, it predicts that a plug of some thickness will be present in all debris flows (Hampton 1975); hence, strength is never overcome throughout an entire flow. This empirical relationship also does not account for the occurrence and effects of multiple grain support and transport mechanisms that are observed here. In addition, because the Coulomb equation used by Johnson (1965) is representative of the conditions of failure under a static situation, it is not strictly indicative of conditions during flow.

Description of active sediment flows

Four types of active sediment flows that are distinguishable because of differences in their predominant deformation characteristics and mechanisms of grain support and transport are described below. It should be emphasized, however, that field observations and measurements indicate that active flows are transitional in terms of physical properties and mechanisms of grain support and transport and these flow types are used for purposes of discussion only. Figure 33 illustrates these four types of flows. Table VI lists their primary attributes.



a. Surface of type I flow. Smooth, wet surface with minor arcuate ridges are shown. Flow from lower left to upper right. Lobe is about 3 m wide.



b. Type I flow deposit; view toward source area. Flow was "channelized" by stable ridge of sediment on right. Small meltwater channel developed on surface at left; meltwater deposits on right adjacent ridge materials. Marginal ridge at head of flow is partially reworked. Staff is 3 m long.



c. Deformed fluvial sediment at frontal margin of type I flow lobe shown in panel B. Compression by shove of sediment flow formed ridges paralleling lobe margin. Scale is 1.5 m long.

Figure 34. Type I flows.

Type I flows

Sediment flows of low water content (about 8 to 14% by weight) and generally high bulk density are lobate-shaped during movement and after deposition (Fig. 34). They possess a well-defined blunt head which protrudes above the remainder of the flow but which is continuous with smaller marginal ridges. Marginal and frontal slopes are in excess of 45°, while the body of the flow shows a relatively planar, smooth surface. Higher water content flows of this type may have arcuate ridges paralleling the frontal margin on their surfaces. The thickness of all type I flows is relatively constant except in the head region and where the tail region thins towards the source area. The maximum thickness measured for active type I flows was 2 m; maximum areal dimensions were 15X45 m. Flow rates were generally of about 0.1 to 0.3 m/min on slopes of 1° to 10°, although rates of 0.1 m/day and less were also measured. The maximum observed distance of flow, which is in part controlled by sediment flow parameters and in part by the limited area in the terminus region within which resedimentation may occur, was about 300 m. Deposits from sequential flows coalesce to cover much larger areas.

Type I flows move in a sheet-like manner over sediments and ice in a general downslope direction irrespective of small variations in topography. The flow surface remains relatively planar during flow and masks or subdues the underlying topography after deposition. Channelization occurs only to the extent that larger topographic features, such as ice-cored ridges, restrict the location of flow.

The bodies of type I flows are texturally similar throughout (Fig. 35), except that the head regions are in some cases coarse by comparison to the body of the flow. This coarsening results from the incorporation of loose material encountered during flow and from an apparent "sifting" of coarse grains to the surface during rolling and collapse of snout sediments.

Apparently, flow occurs by shear in a thin discrete zone at the base of the lobe, with some internal deformation in the body of the lobe. Shear at the surface of the flow was imperceptible. Stones of various dimensions placed in it remained without settling and moved at equal rates. Poles inserted in the body of the flow remained upright unless they extended into the lowermost part of the flow, in which case they tipped downstream with movement of the sediment flow. At the head, the upper part of the lobe continually overrode the lowermost sheared sediments. Unconsolidated sediments encountered before the lobe may be shoved and rolled ahead, or overridden by the flow and apparently incorporated into it. Consolidated surfaces over which the flow moved, however, were unaltered. Internally, air filled voids indicate partial saturation and thus some strength due to an apparent cohesion. Surface shear strengths were low (Table V). Texture, water content, and sediment properties were invariant in the bodies of the flows, suggesting that they possess strength throughout. These observations suggest that the strength of the sediment mass maintains particles in suspension in the essentially nondeforming body of a flow and that shear in a thin basal zone results in movement of the entire mass. Rodine (1974) observed similar characteristics during mobilization of debris flows.

Flows encountering sediments of low strength at their frontal margin may deform them, often into well-defined folds, or cause failure of the material along high angle thrust faults (Fig. 34). Deformation of this type was observed in association with type II as well as type I flows. Typically, layers of sediment which are thin with respect to flow thickness are deformed and then incorporated into the flow margin, a method by which the arcuate surface ridges observed near the frontal margin of both type I and II flows may form. Thicker layers of such sediment and those low strength sediments surrounded by partially or fully consolidated sediments deform but cause cessation of flow and sometimes deformation of the flow's frontal margin. Saturated sediments encountered in this way exhibit rapid water expulsion through vertical and lateral channels and through fractures where surface materials are partially consolidated. In one case, the increase in overburden pressure due to movement of an active flow onto the consolidated crust of a recently deposited sediment flow caused lateral extrusion of the soft, unconsolidated sediment from beneath this crust. Ponded, sediment-laden pore fluids released during deformation and subsequent consolidation deposit fine-grained sediments in low areas of the flow surface.

Type II flows

As the water content increases further to about 14-19% by weight, the basal zone of shear increases in thickness to include the lateral margins so that a "plug" of unsheared, essentially rafted material (Johnson 1965) occurs in the central part of the flow. Type II flows are mostly channelized in stable and metastable sediments that lie on ice. Flow rates increase and range from 2 to 30 mm/s on slopes of 1° to 7°. In addition to support due the strength of the sediment, other mechanisms of grain support and transport become important. These sediment flows are similar to the plug-type debris flows modeled by Johnson (1965), Hampton (1970), and Rodine (1974). They differ, however, in that multiple mechanisms of grain support and transport, rather than the singular grain support

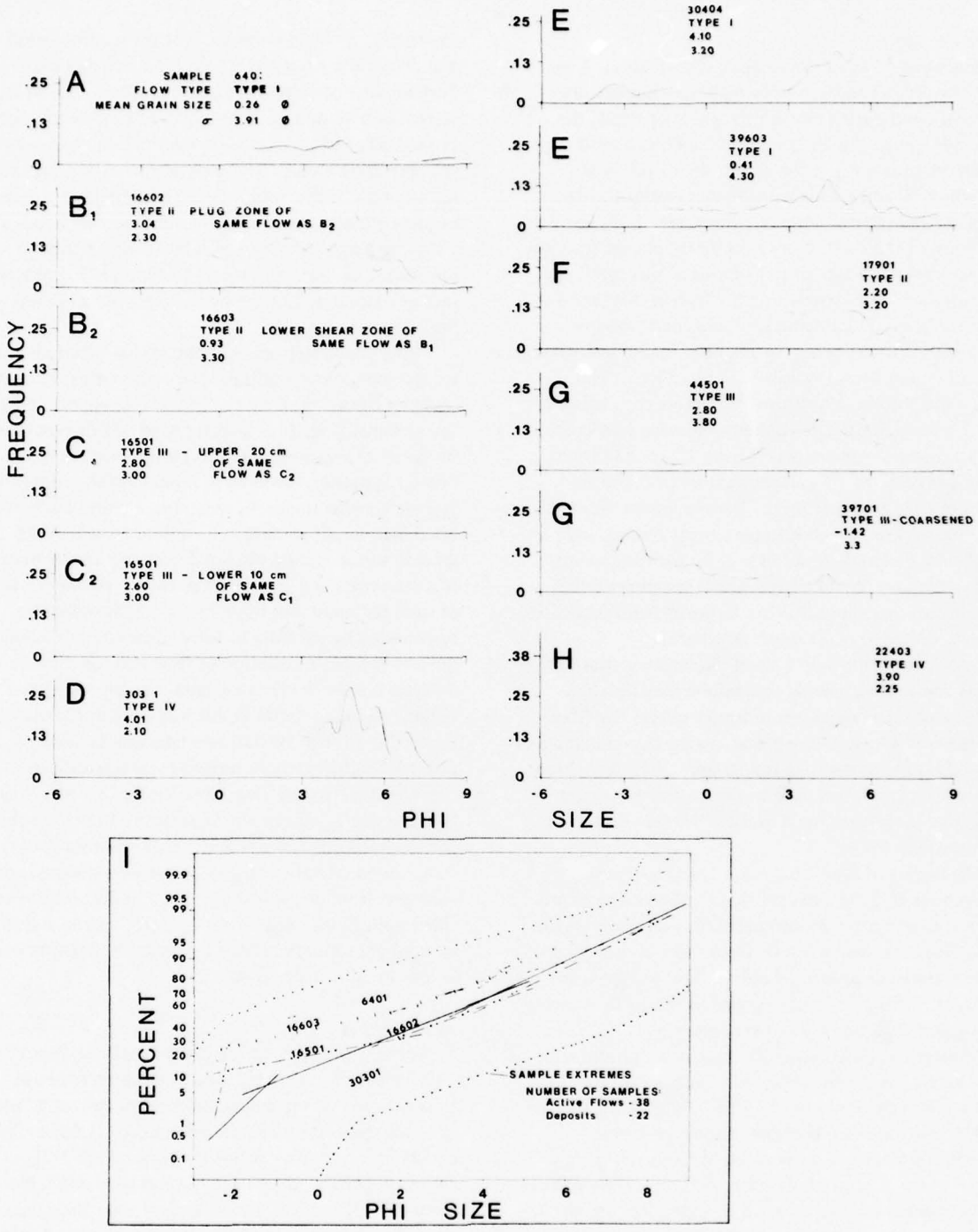
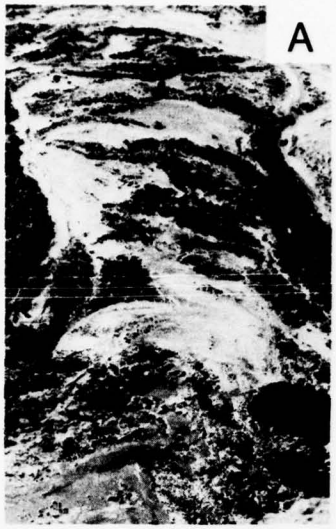


Figure 35. Representative textural variations in active sediment flows and their deposits. A, B, C and D show typical frequency curves of grain size distribution in active type I-IV flows as indicated; E, F, G and H show grain size distributions of deposits from each flow type. Cumulative curves of active flow materials and of deposits are shown in I; extremes of grain size distribution are indicated.



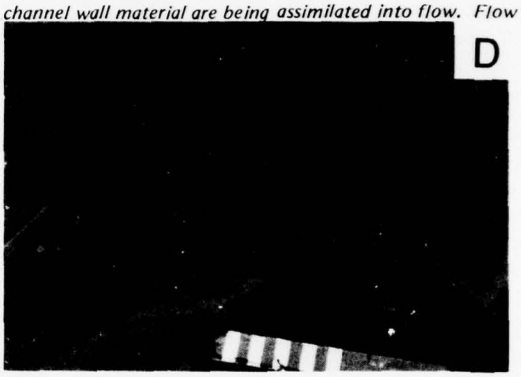
a. Type II lobe channelized by saturated, ice-floored sediments. Arcuate to linear ridges are of sediment sloughed from ice-cored slopes which is not fully assimilated into flow mass. Fine-grained sediments at bottom of photo were recently extruded onto lobe surface in the process of sloughing. Meltwater is pooled between several of the ridges. Direction of flow is from bottom to top of photo, and flow thickness is 1 m. At photo center, lobe is about 4 m wide.



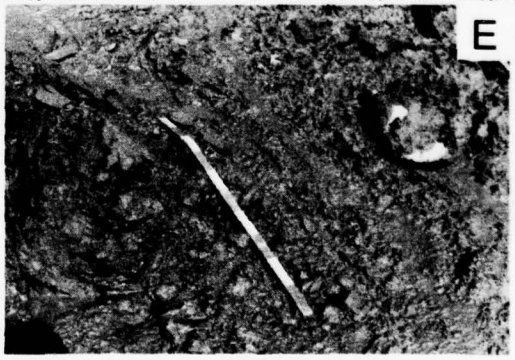
c. Surface view of thick (0.8 m) type II flow with well-developed braided rill pattern. Small pebble lags occur in some rills. Flow direction from bottom to top of photo. Scale on right is 1 m long.



b. Channelized type II flow. Direction of flow is from top center to bottom right of photo. Cobbles and boulders in tractional and suspended transport and thin sheet flow of meltwater on flow surface are shown. Cascading flow over steep drop in channel bed totally mixes plug and shear zones. Below this drop and adjacent to tributary, blocks of eroded channel wall material are being assimilated into flow. Flow



d. Photo of plug surface of type II flow showing clusters of pore fluid expulsion channels, which appear as dark dots with dark lineations to their left. Dark lineations are fluids from channels moving downslope while mixing with a thin sheet of meltwater on sediment flow surface. Scale is in centimeters.



e. Type III flow channelized in metastable sediments of source area. Flow adjacent to meter stick is about 0.3 m wide. Flow surface is irregular due to protrusion of gravels and particle interference during differential shear. Flow is 0.2 m thick. Clear meltwater is flowing on surface at margins.

Figure 36. Type II and III flows.

mechanism of matrix strength, exist simultaneously during flow.

With increased water content, the morphology of sediment flows alters from the type I form with self-supporting margins to that of channelized flows with lateral margins in shear (Fig. 36). The head region decreases in height relative to that of type I flows, but it still remains higher than the body of the flow. The entrainment of the coarse lag left by previous sediment flows in the channel bottom coarsens the front of the flow. Meltwater on the surface of type II sediment flows moves at rates greater than the flow itself and it cascades over the frontal zone, entraining fine-grained particles and coarsening this margin further.

Except at the lower range of water contents, the surface of the plug section of a type II flow is generally smooth and covered by sheet or rill flow of meltwater derived from the ablating ice source (Fig. 36). In the lower range of water contents, arcuate ridges may develop due to compressional deformation of plug sediments by influxing material released by backwasting of the ice-cored slope (Fig. 36). Ridges are in some cases composed of blocks of this material that did not disaggregate. Arcuate ridges are preserved during flow except when they become fully saturated and then fail or are eroded away by meltwater moving over the surface of the sediment flow.

The thickness and other dimensions of type II flows decline markedly with increasing water content; the maximum observed thickness was 1.4 m with most flows 0.2 to 0.7 m thick. Dimensions are primarily controlled by channelization. Channel widths range from 0.5 to 5 m with the larger widths being found where channel walls are composed of saturated sediments near failure and the channel bottom is ice. Smaller channels are fully entrenched in ice with only the uppermost parts of channel walls composed of sediment.

Flow may be continuous for short periods of time (minutes), or may be intermittent and occur in surges. Between flow events, channels contain tractional material left by previous sediment flows and a continuously flowing sediment-laden stream of meltwater. Surges, as well as continuous periods of low, simply reflect the availability of sediment and water and occur in areas where sediments must accumulate, mix with water, and build to some critical thickness before failure and flow takes place. This process must be repeated before a second flow is generated. On warm, sunny days, the availability of water and sediment reduces the time between flow events and sediment flows often appear to move in waves as described by Johnson (1970). This process is characteristic of type III flows also.

At any given point in time, the processes occurring in type II flows may vary. In the simplest conditions, the flow is characterized by a lateral and basal zone of shear,* and a nondeforming central plug. Clasts of various sizes and weights placed or dropped in the plug, if they do not immediately sink, are transported at the same rates and do not settle during continued flow. Similarly, channel wall erosion releases blocks of sediment which, if they fall into the plug regions, are transported intact. Those which fall into lateral zones or are larger than the sediment flow thickness are broken down and assimilated into the flow mass. Shear strengths measured in plugs low in water content were minimal in value but were either zero or at a nominal value not measurable with a Torvane (<0.01 kg/cm^2) at higher water contents (greater than about 16%). Further, perturbations initiated by flow over channel bed irregularities may extend into the plug and cause mixing of sediments, but when the flow passes the irregularity, the plug returns to its former state. Johnson (1965) and Hampton (1970) consider the plug to behave plastically but to be essentially non-deforming with respect to the basal zone of shear. Type II flows observed at the Matanuska Glacier suggest that laminar flow in the basal region is the primary mode of transport and that plastic deformation of the plug is minimal.

Other processes of grain support and transport may include traction and saltation of gravels in the basal zone of shear. Particles and aggregates of debris larger than the total thickness of the flow are also slid and rolled along by the force of the plug against them. The maximum size of particle moved by this process is determined by the driving force imparted by the plug, which is in turn controlled by its yield strength, its unit weight, and the surface area of the submerged part of the particle, as well as the resisting force imparted by friction between the bed and the base of the particle (Johnson 1965). Collision of grains in shear and traction in the basal shear zone may generate dispersive pressures (Bagnold 1954) that aid in grain support but reduce flow mobility (Hampton 1975).

Brief periods of turbid mixing result from flow over channel bed irregularities and sudden increases in the angle of slope of the bed. Particles in traction and shear in the basal zone as well as in the plug itself undergo a brief period of mixing. Meltwater moving over the sediment flow surface is added to both the plug and lower shear zone. A temporary or permanent loss of strength in the plug zone may result from an increase in the water content and from shear induced by this transient turbulence (Hampton 1975). Large grains suspended in the plug may settle out during this turbid mixing.

*Flow lines in the lateral zone of shear, as indicated by transported clasts and materials that differ in color, remain parallel, suggesting that laminar flow prevails in this region.

Localized liquefaction and fluidization apparently occur in type II flows characterized by shear zones with water contents that are larger than the plug zone. Small pore fluid expulsion tubes or fluidization channels (Lowe 1975) of about 1- to 2-mm diameter are sometimes visible in the plug during flow (Fig. 36). Water containing fine silt and clay flows through the channels to the surface where it mixes downslope with meltwater flowing on the sediment flow. Pore fluid expulsion channels occur mainly in clusters, rather than as individuals scattered randomly across the flow surface. The presence of these channels indicates the dissipation of excess pore pressures. The development of these pressures requires that, at least over small areas, an impermeable "cover" of sediments exists where fluids are concentrated. Plugs are relatively fine-grained and, over the period of time that movement occurs, they can be considered impermeable. The lateral extent of pore pressure development may be controlled by the impermeable ice of the channel bottom and walls or, on a smaller scale, by the base of the plug itself. In the latter case, hollows in the basal surface of the plug would form small impermeable "caps" that prohibit lateral dissipation of pore pressure. The net effect of liquefaction or fluidization may be a coarsening of the lower zone of shear, due to the removal or fine silt and clay, or the development of pockets or zones of materials from which the coarsest particles have settled out (Lowe 1975, 1976b).

The texture of type II flows (sampled while moving) varies internally to a greater degree than that of other flow types. Texture of the plug zone is dependent upon the source material. Generally, it is texturally heterogeneous with poor to very poor sorting and comparable to the texture of type I flows (Fig. 35). Blocks of sediment which fall into the plug zone from channel walls may be texturally diverse; however, because sediments of the walls are usually resedimented materials and often of sediment flow origin, there may be insufficient differences in texture to distinguish them from primary flow materials. Coarse, cohesionless sediment eroded by sediment flows loses its structure and falls as individual particles. Local concentrations of coarse particles in the shape of stringers or pods may result when the coarse sediment is in a matrix texturally similar to that of the surrounding material. A layer of silt or sandy silt may be deposited on the surface of some plugs by the sheet flow of meltwater.

The zone of shear is generally characterized by a lower layer of tractional gravels, occasionally graded, and an upper layer of variable texture. The upper layer is similar in texture to the plug zone whenever the water contents of the two zones are similar. When the zones differ in water content, the shear zone shows better sorting and an increased sand and coarse silt content (Fig. 35). Variations in grain size due to liquefaction and fluidization could not be observed in the samples.

Type III flows

As the water content increases further to about 18-25% by weight, the plug of nonshearing debris thins, becomes discontinuous, and eventually the entire flow is in shear. Most type III flows are characterized by differential rates of shear at their surface, and flows of this type are channelized. Flow rates range from 0.15 to 1.25 m/s. Thickness of these flows decreases generally from the head to the tail region, with a maximum observed thickness of 0.60 m. Flow surfaces are often irregular because of the protrusion of rolling and sliding tractional particles through it (Fig. 36).

Passage of a type III flow down a channel is marked by an increase in meltwater flow, passage of the head, and then gradual diminishment of the body until only sediment-laden meltwater, which is constantly present, is flowing in the channel. Large cobbles and boulders are shoved ahead by the flow and dam the channel at restrictions, allowing material to build to thicknesses in excess of 1 m. Breakage of the dam by overtopping or by the force of the amassing flow material results in its rapid release and turbulent mixing. With continued flow, thickness diminshes but remains thicker near the head of the sediment flow than prior to damming (type II flows may also be characterized by this damming process).

Type III flows, the most erosive of the four flow types, erode the outer banks of channels in sediments. Material released by this process is generally disaggregated and incorporated. Sloshing during flow around channel bends and following steep drops in the elevation of the channel bed forms generally thin, levee-like deposits.

As stated, type III flows show differential shear throughout—only at low water contents are transitory, discontinuous plug zones present. The shear strength of these plug zones was not measurable with a Torvane. Grain interactions are commonly observed at the surface and are probably important means of particle dispersion in the body of the flow (Bagnold 1954). A transient turbid mixing of the flow sediments with meltwater occurs during movement over channel bed irregularities. Tractional material includes large cobbles and boulders that may be larger than the thickness of the body of the flow. Flows composed of up to 50% by area gravel in traction were observed, but these flows were restricted to areas with steeply sloping channel bottoms. Type III flows are often coarsened during flow and deposition by loss of the matrix material when it is liquefied by seepage at the surface or eroded by meltwater flow.

Textural variations in type III flows are minimal in a given channel section (Fig. 35), apparently due to the

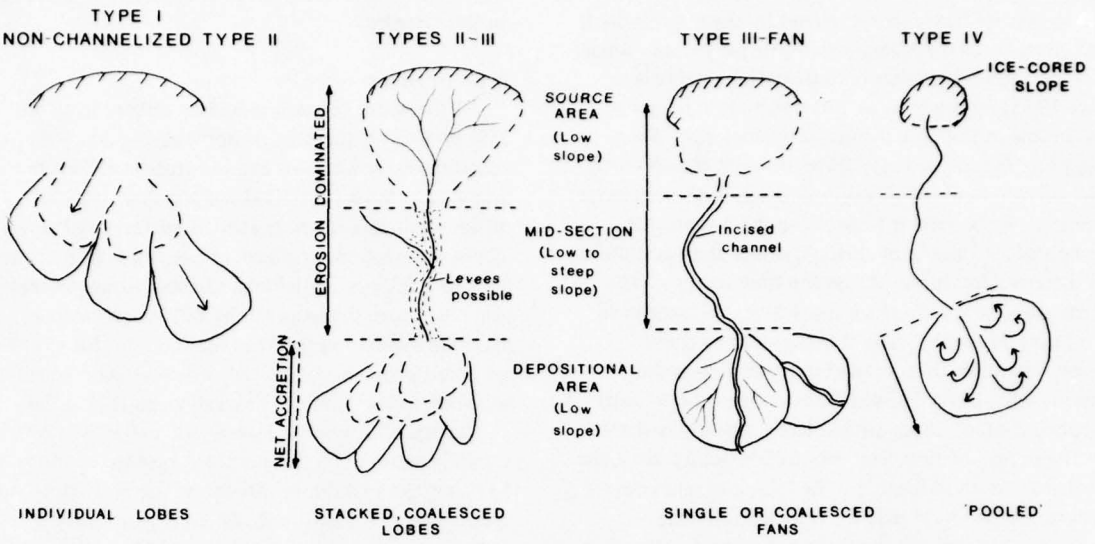


Figure 37. Idealized characteristics of sediment flow system and modes of deposition. In general, source and depositional areas are of low angled slope (1° to 70°), whereas the midsection may be steep and locally irregular in slope. Stacking and coalescing of deposits is common; different flow types may originate and be deposited from the same source area. Preservation of the system and sediments is limited to the depositional area; meltwater availability determines the extent of preservation.

thinness of the flow and the continual mixing of flow materials that occurs during shear. Tractional material is difficult to separate from material actually suspended in the flow. Texture varies, however, in a channel-wise direction. Tail regions are finer and contain less tractional gravels than the body of the flow and the head region is generally coarsened by gravels in the channel bed that are shoved and rolled ahead by the sediment flow.

Type IV flows

Type IV flows are characterized by large water contents (greater than 25% by weight), low density (1.4 to 1.8 g km^3), laminar flow with shear throughout, and fine grain size. There is no measurable shear strength in these flows, and coarse sand-size and granule-size particles placed on the flow sank immediately, indicating that strength is essentially absent. Hence, these flows are considered to be partially to fully liquefied. Rates of flow, which are rapidly affected by changes in the angle of slope of the channel bed, range from less than 0.01 to 2.0 m/s.

Type IV flows occupy channels generally less than 1.5 m wide and range in thickness from 20 to 100 m. They most often flow continuously over periods of hours from source areas characterized by sediment-poor ice and by an abundance of fine-grained sediment. A warm, sunny day is essential to maintain a water supply. Texture of the flow is a homogeneous sandy silt or coarse silty sand (Fig. 35). Although small pebbles and granules are carried in traction at the bed, no significant variations in texture were found in the body of type IV flows. The fine-grained texture is probably sufficiently impermeable to prohibit the reduction of excess pore pressures, causing liquefaction during flow, and therefore particles remain in suspension. Thus, deposition occurs in basins or on horizontal slopes under static conditions, where following the loss of tractional grains, particles in the flow settle out and displace pore fluids upward to the surface. Fabric and other features developed during flow are lost in the process. Grading may form due to differential rates of grain settlement.

Characteristics of the flow system and modes of deposition

The process of deposition varies with the characteristics of the flow system and the sediment flow at the time of deposition. Type I and other lobate non-channelized flows undergo deposition within a restricted area defined by the dimensions of the lobe. Channelized flows form deposits in the lower part of the flow system where channel confinement is lost.

The flow system for type II through type IV flows usually consists of three elements (Fig. 37). The upper, proximal source area is characterized by either a series

of tributary channels from ablating ice sources that join to form a single main channel out of the area, or a single channel leading from an unstable sediment pile that is being continuously fed with water and sediment from ablating ice-cored slopes. The latter source is more characteristic of sediment flows of lower water content, whereas the former is often associated with flows of higher water content.

In both cases, a single main channel, generally incised 0.5 to 2 m into sediment and ice, traverses the midsection of the flow system. The angle of slope in this region averages 5° to 25°, with slope angles locally of up to 90°. Mechanical and thermal erosion by sediment flow and meltwater are the primary processes occurring in the channel. Small levees a few centimeters thick may develop, but these are not preserved.

The lower, distal area of the flow system consists of a single active channel which may shift location because of blockage by sediment flow deposition but which always remains open due to erosion and channel formation by meltwater which continually flows between sediment flow events. A 1° to 5° slope is common here. In terms of sediment flow activity, the distal area is fully depositional or deformational and thus basal contacts of deposits are nonerosional.

Deposition occurs when the resistance to shear of the flow mass exceeds the applied shear stress (e.g. Hooke 1967). Observation suggests that deposition results from a change in bed slope, a decrease in thickness of the flow mass, a loss of interstitial fluids, or a combination of these. Channel-confined flows often spread laterally and thin with movement out of the restrictive channel walls prior to their deposition. Under these conditions, type II flows are sometimes characterized by deposition of the tractional sediment upchannel from the primary area of sedimentation. Although a change in slope angle is often difficult to document because of the low angles of slope common in the area of flow initiation and deposition (<10°) and errors inherent in measuring angles of slope of natural surfaces, the changes were sufficiently large in some instances to document a reduction in the slope angle at the depositional area. Water content at deposition is often larger than during the initiation of flow, suggesting lower slope angles are required for deposition. Loss of fluids to underlying sediment was observed for small, thin flows and for one type II flow which underwent sieve deposition (Hooke 1967) on fluvial gravels. Each of the three conditions observed here fulfill this requirement.

Morphology of the deposits depends upon the characteristics of the source flow and the abundance of water in the channel during and after deposition. Type I flows maintain their well-defined morphology during deposition because the shear strength of the surface materials of these flows resists reworking by secondary flow of water over their surfaces. Hence, when these types of flows are deposited in small streams, they resisted reworking and are preserved intact with only a coarsening of their surfaces by stream flow. The deposits of type I flows derived from the same source area show an accretionary stacking towards the source area due to slope angle reduction resulting from the deposition of previous flows (Fig. 37).

As the water content increases, the potential for preservation of the original morphology and other properties of the sediment flow decreases. Channelized type II flows are deposited in lobes which often vary in size and thickness from their source because of thinning prior to deposition. Deposition of multiple lobes is initially adjacent and then overlapping with a net accretion upchannel towards the source area (Fig. 37). As the distal area of sedimentation is filled, its effective gradient is decreased. After sediments have been deposited up to the lower limit of the mid-section of the channel system, deposition then returns to the most distal part of the area of sedimentation. Thus, a cyclical pattern of accretion may develop whenever sources of meltwater and sediment are sufficiently constant. The flow of meltwater in the channels between flow events often deposits fine-grained sediments on the lobe surface or erodes a channel in that surface.

Type III flows of relatively low water content may form deposits by cyclical accretion as type II flows; however, as the water content increases, fan-type deposition begins at the change in slope angle that occurs below the midsection of the channel system. Net accretion takes place in the down-channel direction. Fan sedimentation of type III flows of relatively low water content often occurs through the loss of the tractional particles at the head of the fan, the body of the flow in the central section of the fan, and the surface fluids and some upper matrix materials in the distal portion of the fan. At larger water contents, flow materials are deposited by size with the largest particles released at the head of the fan and systematically smaller sizes released towards the toe. Suspended fines are deposited downslope from the fan in topographic lows. In both cases, the more fluid tail of the sediment flow and the continued flow of meltwater coarsens the surface and may incise a channel into it. Successive periods of sedimentation are common.

Type IV flows most often move into streams where mixing dilutes and separates their constituents. Although not observed, they may be important sources of density undercurrents and turbidity currents in superglacial and proglacial lakes. Horizontal slopes or a basin is required for accumulation of type IV flows. On

Table VII. Characteristics of sediment flow deposits, terminus region, Matanuska Glacier, Alaska.

Sediment flow type	*Bulk texture* Type	*1) Mean (ϕ) 2) Std dev (ϕ)*	*Internal organization*			*Surface forms*	*Contacts and basal surface features*	*Pene-contemporaneous deformation*	*Geometry* and maximum observed dimensions (length×width, thickness, m)*
			General	*Structure*	*Pebble fabric*				
I	Gravel-sand-silt, sandy silt	1) -1 to 2 2) 3 to 4.5	Clasts dispersed in fine-grained matrix.	Massive.	Absent to very weak; vertical clasts. $S_1 \cong 0.49\text{-}0.55$	Generally planar; also arcuate ridges, secondary rills and desiccation cracks.	Nonerosional, conformable contacts; contacts sharp; load structures.	Possible subflow and marginal deformation during and after deposition.	Lobe: 50×20, 2.5
II	Gravel-sand-silt, sandy silt, silty sand	1) 2 to 3 2) 3 to 4	Plug zone; clasts dispersed in fine-grained matrix.	Massive; intraformational blocks.	Absent to very weak; vertical clasts.	Arcuate ridges; flow lineations, marginal folds, mud volcanoes, braided and distributary rills on surface.	Nonerosional, conformable contacts; contacts indistinct to sharp; load structures.	Possible subflow and marginal deformation during and after deposition.	Lobe; 30×20, 1.5; sheet of coalesced deposits.
			Shear zone; gravel zone at base, upper part may show decreased silt-clay and gravel content; overall, clasts in fine-grained matrix.	Massive; deposit may appear layered where shear and plug zones distinct in texture.	Absent to weak; bimodal or multimodal; vertical clasts. $S_1 \cong 0.50\text{-}0.65$				
III	Gravelly sand to sandy silt	1) -2.5 to 2.5 2) 3.5 to 2	Matrix to clast dominated; lack of fine-grained matrix possible; basal gravels.	Massive; intraformational blocks occasionally.	Moderate, multimodal to bimodal parallel and transverse to flow. $S_1 \cong 0.60\text{-}0.70$	Irregular to planar; singular rill development; mud volcanoes.	Nonerosional, conformable contacts; contacts indistinct to sharp.	Generally absent; possible subflow deformation on liquefied sediments.	Thin lobe; 20×10, 0.5; fan wedge; 30×65, 3.5; rarely, sheet of coalesced deposits.
IV	Sand, silty sand, sandy silt	1) ≥3.5 2) ≤2.5	Matrix except at base where granules possible.	Massive to graded (distribution, coarse-tail).	Absent.	Smooth, planar; mud volcanoes possible.	Contacts conformable; indistinct.	Absent.	Thin sheet; 20×30, 0.3; Fills surface lows of irregular size and shape.

*Length and width refer to dimensions parallel and transverse to direction of movement prior to deposition.

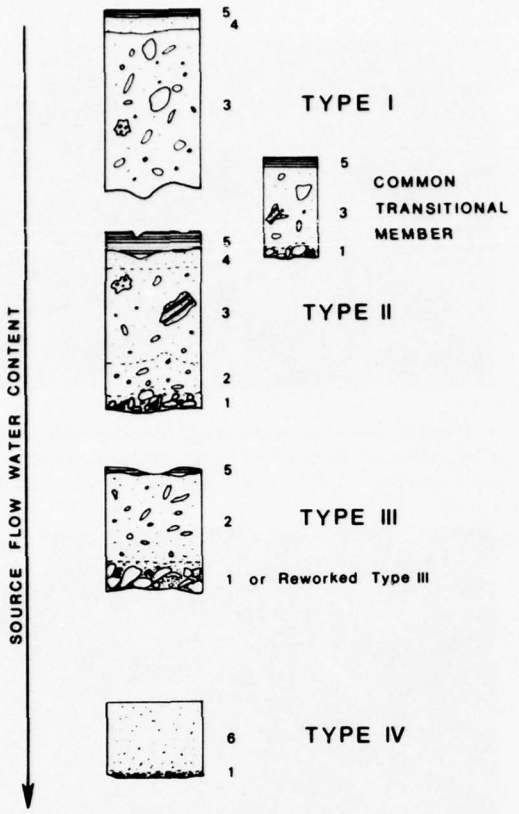


Figure 38. Idealized characteristics of sediment flow deposits. Six distinct zones are recognized; any may be missing due to erosion, nondeposition, or absence from source flow. The characteristics of the zones are 1) texturally heterogeneous with increased gravel content of tractional origin, massive to graded, weak to absent pebble fabric; 2) massive, texturally heterogeneous but absence of large grains due to settlement, possible decrease in silt and clay due to elutriation, weak pebble fabric; 3) massive, texturally distinct and sometimes structured sediments may occur, pebble fabric absent, vertical clasts common; 4) massive, fine-grained (sand to clay) similar to matrix of zone 2, lacks coarse clasts due to settlement during and after deposition; 5) stratified to diffusely laminated silts and sands of meltwater flow origin; and 6) massive to partially or fully graded, silty sand, fabric absent. Basal contacts vary from conformable to unconformable, sharp to transitional and deformed to planar. Type III flow sedimentation in fans results in selective deposition of each zone, or of individual particles by size.

horizontal slopes, flows spread laterally to form a thin sheet. Thicker sequences of 1 m or more may be formed by pooling a flow in a basin.

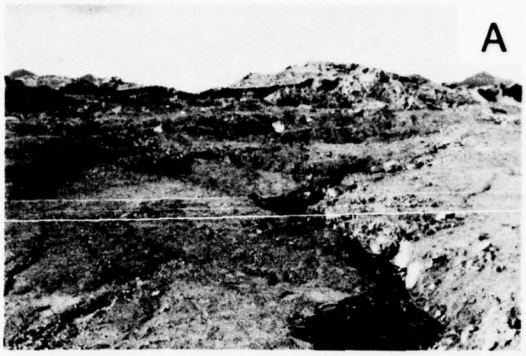
Rates of sedimentation are totally variable and dependent upon the rates of ice ablation and sediment production, which in turn are a function of the weather, sediment properties, and other conditions. Deposits of individual flows vary from a few millimeters to a few meters in thickness. Multiple deposits stacked upon one another may be tens of meters thick. The analysis of rates of lateral retreat of ice-cored slopes and the approximate volumes of sediment transported from the area by sediment flows during the period of observation indicate this process reworks the majority of the sediments in the study area. Dimensions of the deposits are similarly determined by a number of factors. Individual lobes may vary from an area of a few centimeters to hundreds of meters. The extent of coalesced deposits and the areal distribution of sediment flow deposits indicate they are the most important deposits of the terminus region of the Matanuska Glacier.

Characteristics of flow deposits

Deposits of each of the four flow types described earlier have distinguishing characteristics derived from their mechanisms of grain support and transport. These characteristics are summarized in Table VII and Figure 38. Because active sediment flows are transitional to one another, however, deposits that are completely transitional will form and characteristics of the source flow may be difficult to distinguish from the deposits. Further, the character of the deposit is determined by the last condition of flow. Because active flows change characteristics with changes in water content or density and bed slope angle, it is possible that the last mechanisms of flow will not be representative of conditions during their mobilization or during transport downslope. Transitional behavior would thus make it difficult to establish conditions prevailing at the time of sedimentation.

Surface forms

The features found on sediment flow surfaces are limited in type, but are often well-developed. Those which are exposed at the surface for a short period of time are often reworked. Most surfaces are irregular but relatively planar and partially covered by abandoned rills containing thin, discontinuous pebble lags (Fig. 39). Surface texture is generally coarsened to a silty sand with scattered, partially embedded pebbles and cobbles. The rapidity of reworking characteristic of



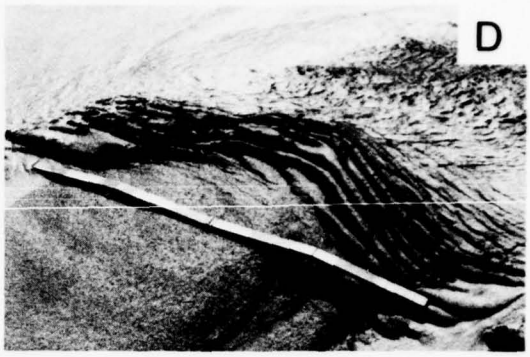
a. Surface of coalesced sediment flow deposits coarsened by meltwater flow and incised by channels of meltwater and fluvial origin. Channel in foreground is about 1 m wide.



b. Arcuate ridges, partially reworked, preserved at surface of type II flow deposit. Flow was from right to left. Scale at center of photo is 2 m long.



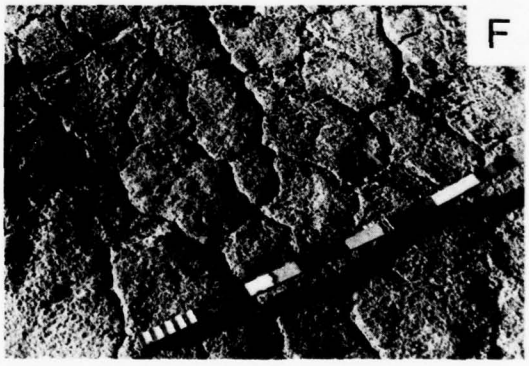
c. Flow lineations, apparently a result of flow obstruction by boulder. Flow from center right to lower left. Similar lineations may develop by reactivation of sediment flow deposit partially consolidated at surface. Scale is 1 m long.



d. Marginal concentric folding of surface of partially consolidated, fine-grained sediment flow deposit by compression at active flow margin. Flow from upper right to center. Scale is 1 m long.



e. Mud volcanoes developed on surface of recently deposited sediment flow due to pore fluid expulsion through fluidization channels at center of volcano. Scale in centimeters and decimeters.



f. Desiccation cracks in pitted surface of type II sediment flow deposit. Scale is 24 cm long.

Figure 39. Surface forms of sediment flows.

the terminus region suggests that unaltered flow surfaces are not likely to be preserved unless immediately covered by a second flow.

Features may be preserved in sediment flows of lower water content that are indicative of the direction of flow; these include arcuate ridges, flow lineations, and adjacent, marginally folded sediments (Fig. 39). Arcuate ridges develop mainly by compressional deformation of flow sediments in the source area due to a large, rapid influx of sediment off an ablating ice-cored slope and by incorporation of sediments deformed by pushing at the flow margin. Flow lineations apparently result from the break-up of a plug or a partially consolidated surface of a rejuvenated flow deposit. At the flow margin, folds develop by compression of higher strength surface sediments mostly underlain by sediments of high liquidity and low strength. Singular and distributary rill patterns are common on planar flow surfaces of plugs (Fig. 36).

Other features include mud volcanoes formed by pore fluid expulsion due to liquefaction of flow materials deposited on ice (Fig. 39). Surfaces wetted by seepage are conducive to raindrop print development and, upon drying, the development of desiccation cracks.

Internal organization

The general trend in texture observed with respect to changes in water content and density of active sediment flows is incompletely preserved in their deposits. Figure 40 compares the mean grain size of composite samples from the central part of sediment flow deposits

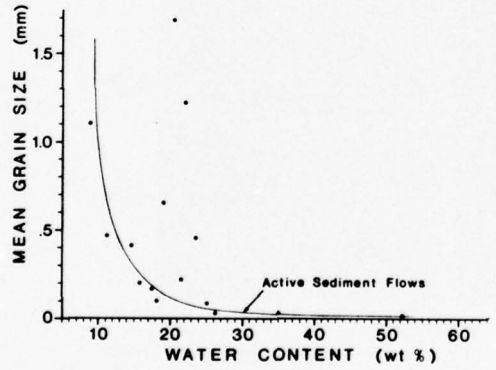


Figure 40. Comparison of mean grain size of composite samples of sediment flow deposits and the bulk water content of the source flow from samples upchannel of the area of deposition. The regression curve of Figure 28 is shown for comparison. Deposits of the lower central part of curve, which represent flows with discontinuous or absent plugs, are coarsened relative to their source.

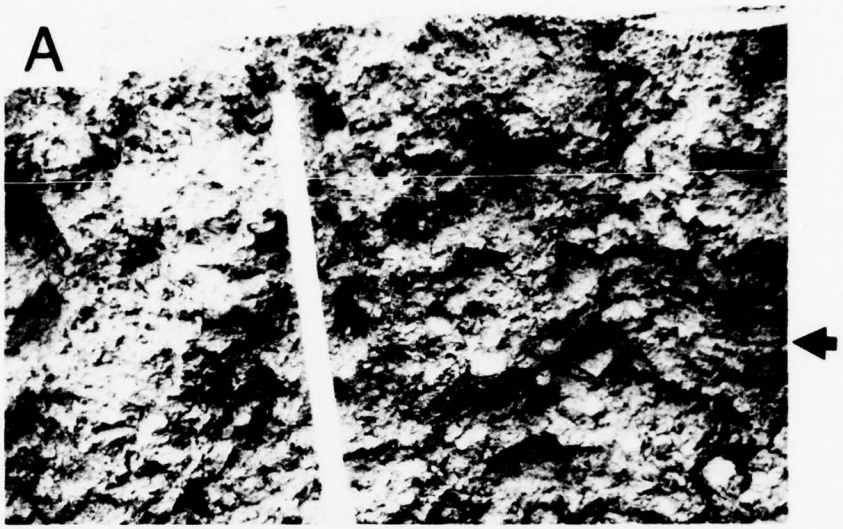
with the water content of the source flows prior to their deposition. Superimposed on that pattern is the curve of Figure 28 derived for active sediment flows. Although the number of samples is limited, the significance is apparent. Whereas the upper and lower tail regions of the curve are retained, much of the central part is not replicated and the mean grain sizes of the deposits are significantly coarser than their active flow counterparts. The coarse texture results from two processes: reworking by continued flow of meltwater over the surface of the deposit and, in fewer cases, selective deposition of the coarse fraction of the source flow with transport of the more fluid matrix from the area of deposition (as in fan sedimentation). Clay, silt, and sand may be preferentially removed by these processes.

Characteristics of deposits of each flow type

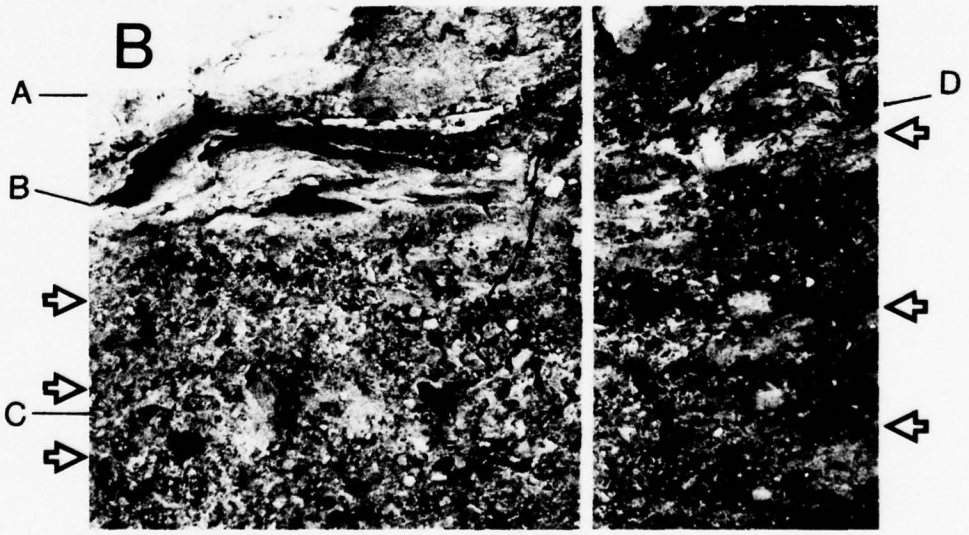
Differences in characteristics of the four flow types described above vary with the mechanisms of grain support and transport operative at the time preceding sedimentation, but are also influenced by flow history (for example, intermittent turbid mixing or localized liquefaction) and post-depositional processes. Figure 35 illustrates the range of textural variations found in sediment flow deposits.

Type I flows. Deposits of type I flows retain the properties of their source. They are characterized typically by diversity in grain sizes and thus very poor sorting ($\sigma \cong 3.5$-4.5), with clasts dispersed randomly in a fine-grained matrix (Fig. 41a). These flows are, however, texturally defined by their source. Blocks of source sediment which are not fully assimilated into the flow occur as pods or lenses of texturally distinct material (silt, coarse sand, and gravel) in an otherwise homogeneous mass. They are often not recognizable in recent deposits of active flows, but are common in older deposits of the terminus. Neither lateral nor vertical grain size variations were observed in the body of single flow deposits.

The head regions of type I flows are their most distinct element. Where there has been little incorporation of surface materials at the front of the lobe, the surface is "blocky" and somewhat disaggregated due to the development of extension fractures as the flow overrode itself. Sediment pushed and rolled ahead of the flow may be of any texture, but it often contains a number of gravel-size particles. Internally, it contains blocks of intraformational, sometimes deformed sediments in variable orientations. These materials include contorted, layered and massive silts of meltwater origin and older flow sediments broken apart by shoving of the lobe. The deposit of the flow is associated in some cases with compressional folding and flow of low strength sediments encountered at the frontal margin, and shear induced failure and flow in layered subflow materials (Fig. 41b).



a. Cross section of type I flow. Lack of structure and generally coarse texture (silty pebbly sand) are shown. Upper 10 to 15 cm showed a decrease in pebble content; surface was saturated after deposition, suggesting loss of strength and clast settlement. A laminated block of sandy silt not fully assimilated into flow indicated by arrow on right. Clasts with long axes in a near vertical orientation are common. Scale is 35 cm long and 1.5 cm wide. Flow is from right to left.



b. Sequence, composed of sediment and meltwater flow deposits, showing upper type I flow (A) and subflow-deformed, stratified meltwater flow silts and sands (B) which overlie a generally massive sequence of sediment flow deposits (C). Arrows indicate contacts of individual flow boundaries. Intraformational blocks are prominent in lower, type II flows. Load structures occur at contact of type I flow deposited on meltwater silts to right of scale (D). Upper part of unit C consists of interstratified, thin meltwater and sediment flow deposits. Scale is 1.5 cm wide and 90 cm long.

Figure 41. Type I flow deposits.

Load structures form at the base of sediment flows deposited on deformable sediments.

A thin (1 to 10 cm) and massive fine-grained layer, largely of silt, caps some deposits (Fig. 41). It seems to originate by two processes. Following cessation of flow, the surface of the sediment flow (which is approximately horizontal) becomes saturated by water from seepage during the initial stages of deposition and consolidation. At saturation, apparent cohesion is reduced and pore pressures may develop due to seepage to reduce the strength of the uppermost sediments. The loss of shear strength results in the settlement of coarse grains, and the remaining fine-grained zone is texturally similar to the matrix of the unaltered part of the flow deposit. Silt layers, usually distinctive from the flow matrix, are formed by deposition of sediment by meltwaters flowing onto the lobe surface.

Type II flows. The deposits of type II flows may vary considerably. These variations reflect the characteristics of the sediment during flow and their mode of deposition. The latter influence was observed in flows which thinned markedly in the area of deposition, apparently as the result of loss of the lower zone of shear. Sediments derived from flows deposited fully in this manner consist mainly of plug material (Fig. 42a); hence, they are similar to type I deposits. Coarse-grained particles in traction at the bed are usually deposited upslope in the channel.

Where deposition occurs with little loss of the shear zone, textural distinctions in the flow remain. Deposits consist generally of a structureless, heterogeneous upper zone and a lower zone, also texturally heterogeneous but with increased gravel content at its base (Fig. 42b). In thinner flows, large particles may extend into and through the plug. If the original flow has had similar water contents in the plug and shear zones, the distinction between these zones simply results from the occurrence of clasts transported initially as bedload. The matrix (clay to sand) is virtually identical. A poorly-defined coarse-tail grading develops with deposition, as matrix materials migrate into pore spaces between tractional clasts. The amount of clasts in traction varies, and in outcrop they may be widely dispersed. Tractional particles were observed to be graded in active flows and these produce a flow deposit with coarse-tail grading at its base.

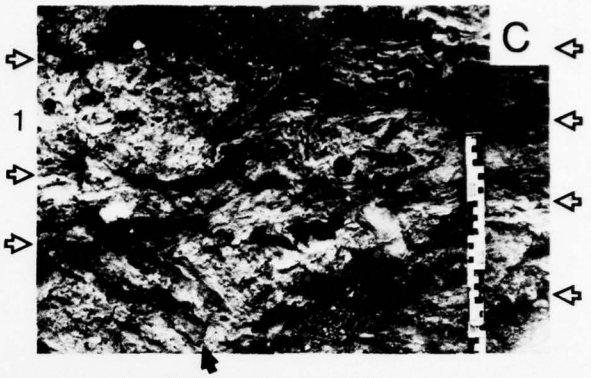
Type II flows with larger water contents in the zone of shear may vary texturally as the result of several processes. Partial and full liquefaction, accompanied perhaps by fluidization, may partly or completely alter the original texture. Fluidization results in pore fluid and clay-silt expulsion, perhaps local turbulent mixing, and formation of water expulsion structures (Lowe 1975). Liquefaction accompanied by shear inhibits the formation of sedimentary structures but may result in differential clast settlement during resedimentation and the development of a graded sequence (Lowe 1976b). Localized occurrence of either process may impart such characteristics to pockets in the flow mass. Such textural variations and structural features were observed in recent deposits. X-ray radiographs of box cores taken transverse and parallel to the original direction of flow revealed few textural or structural variations different from those observed in the sample. The lack of textural and structural features probably results from the initial similarity in texture of the sediments and from homogenization by shear and bedload processes. The net effects, coarsening by fluidization and fining due to liquefaction and shear, are retained if the processes operate for a sufficient length of time.

The plug zone may contain significant numbers of intact and partially disaggregated blocks of sediment (intraformational blocks), which fall or are sheared into this zone by lateral erosion and melting of the channel walls, or which are not disaggregated during slope collapse and flow initiation. Intraformational blocks are recognizable when texturally distinct or when possessing distinguishing features, such as stratification or former subaerial surfaces that are coated with calcium carbonate deposited earlier by evaporation during consolidation. Inclusions of sorted material, whether granular or fine-grained, appear as pods in an otherwise homogeneous mass and are particularly recognizable (Fig. 42c). Coarse-grained sands and gravels lose their structure during the process of entrainment and occur as coarse-grained pockets, partially or fully infilled with the matrix material of the flow. When disaggregated and "poured" onto the surface of the active flow, a streak or lens of coarse particles forms in the deposit. Fine-grained silts of meltwater origin remain intact due to their apparent cohesion and occur in the plug as lenses with variable orientations. The head regions of type II flows may contain blocks of sediment, but they are usually coarse-grained without structure.

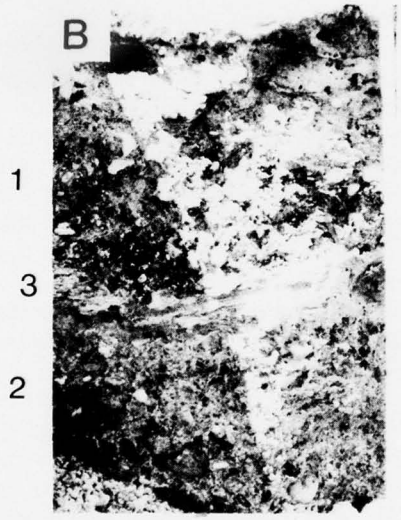
Surfaces of type II flows are normally covered by meltwater flowing in sheets and rills (Fig. 36). Reworking and the formation of channel systems result in lenses or a thin layer of granular materials near the surface. Deposition by sheet flow during and following sediment flow produces a thin, sandy silt layer, and stratification develops from multiple periods of sheet flow following deposition (Fig. 41). Ponded meltwater in low areas on the irregular surfaces of low water content type II flows deposits small lenses of massive, fine-grained sediment.



a. Three type II sediment flow deposits. Flow approximately right to left. Uppermost flow thinned prior to deposition with loss of tractional gravels; massive plug zone remains. Stratified meltwater sheet flow silts overlie second flow unit. Arrow indicates discontinuous stratified silt layer at base of second flow. Third flow deposit extends below it to bottom of photo; its gravel content increases towards base. Scale is 90 cm long.



c. Sequence of multiple type II sediment flows separated by meltwater flow and, occasionally, fluvial deposits. Marginal, open arrows indicate contacts of individual units. Deformation, including small load structures, or marginal and subflow stratified silts and sands (top center of photo) by type II flow is shown at left (1). Intraformational blocks of sediment, including aggregates of debris (solid arrow) and deformed silts occur throughout flow deposits. Scale in centimeters.



b. Cross section showing two type II flow deposits (1, 2) separated by partly deformed, stratified meltwater silts and sands (3). Upper flow deposit characterized by central massive zone and basal zone of tractional gravels. Upper zone contains fewer pebbles, is massive with pockets of silt of meltwater origin; decreased pebble content may indicate loss of fine-grained material from basal zone or post-depositional clast settlement from upper zone. Lower flow is massive with dispersed tractional gravels. Scale is 55 cm long and 1.5 cm wide.



d. Stratified sequence of type IV flow and meltwater sheet flow deposits. Distribution and coarse-tail graded, and massive type IV flow deposits are shown overlying stratified, meltwater sheet flow deposits. Scale is in centimeters.

Figure 42. Type II and type IV flow deposits.

With increased shear and loss of the plug zone, flow deposits become uniform in appearance and texturally similar throughout (Fig. 35). Deposits are coarsened in some cases by continued meltwater flow during deposition, dewatering (seepage and fluidization) during consolidation, and continued flow of the fluid matrix. Large particles (relative to flow thickness) extend from the base into and through the deposit. Lenses of sand and granules occur beneath and adjacent to larger particles in some flow deposits; occasionally, aggregates of mixed grain sizes occur in otherwise coarse sediments. Coarse zones may arise from

elutriation of fines by meltwater flow or fluidization. Aggregates may be intraformational blocks eroded from channel walls that possessed sufficient strength to prevent disaggregation.

Type III flows. Accumulation of type III flows in fan-shaped deposits is accompanied by a separation of flow components. In one case, fan deposits were formed by the initial deposition of tractional gravels at the head of the fan, followed by deposition of the body of the flow and of the fine-grained sediments washed from the toe. In a second case, a highly fluid flow moving from a steep channel onto a relatively planar surface deposited particles according to size, with coarsest clasts at the head of the fan and progressively finer clasts downslope. Particles were imbricated upslope. Fine-grained materials were deposited on the surface of both fans by continued flow of sediment-laden meltwater. Multiple flow deposition results in a stratified deposit of interlayered meltwater and sediment flow materials.

Type IV flows. With further increase in water content to type IV flows, deposits of fine to silty-sands and sandy silts with improved sorting ($\sigma \cong$ 1-2) (Fig. 35) are formed. Granules and sand carried in traction are preserved at the base of the deposit, while the remainder of the deposit is massive to graded (Figure 42). Distribution and coarse-tail grading is expected for sedimentation of poorly sorted liquefied flows (Lowe 1976b). Ponded type IV flows are characterized by distribution grading and, occasionally, an upper fine-grained structureless zone.

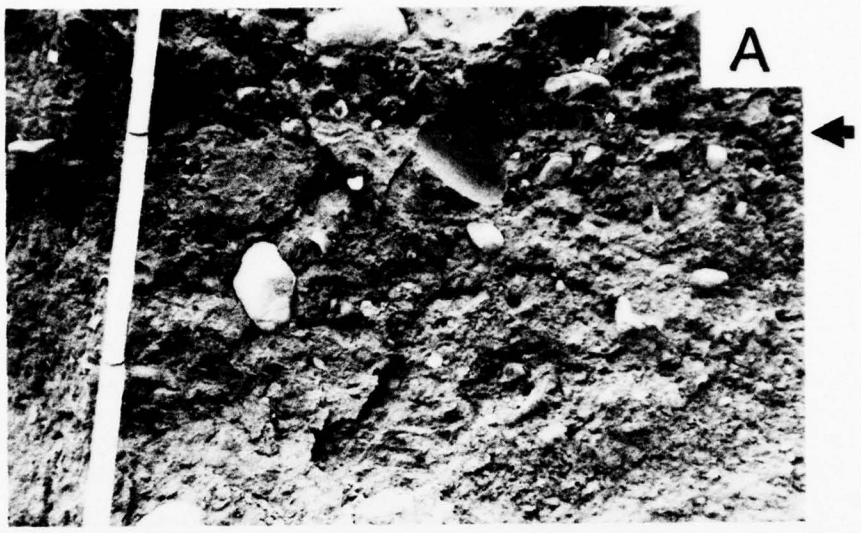
Other characteristics

Contacts between sediment flows and other deposits, including other recent flows, are nonerosional but vary in appearance. The basal contact for flows deposited on older consolidated sediments is usually sharp and conforming to the underlying surface. The compactness of the lower deposit in comparison to that of the upper, more recent flow deposit suggests that dessication, as is indicated by the caliche on some surfaces, causes overconsolidation of the lower material prior to deposition of the more recent flow. Partially embedded and loose gravel clasts are scattered across surfaces exposed a short period of time and mark the depositional interface. In cases where the texture of the flow sediments and the basal material are similar, the contact is less apparent. Where sediment flows are deposited on other freshly deposited flows not covered by meltwater flow deposits, contacts are hard to distinguish (Fig. 43). For example, in Figure 43a, a slight change in silt and sand content and a pebble cavity coated by silt and clay on only the lower two-thirds of its surface mark the location of a contact. Load structures identify basal contacts between flows and unstable bed material. In some cases, the distinction between multiple flows or a single thick flow may only be indicated by an increase in the content of pebbles of tractional origin or by thin, discontinuous lenses of sandy silt of meltwater origin (Fig. 43b). Multiple thin (0.5- to 2-cm) flows often develop a fissility along former flow surfaces, and scattered sand grains may be present on the surface of individual partings. These grains, as well as small lenses and plate-like fillings, are deposited by meltwater sheet and rill flow. Many flow deposits are overlain by stratified silts and sands deposited by the sediment-laden meltwater streams and sheet flows that separate flow events.

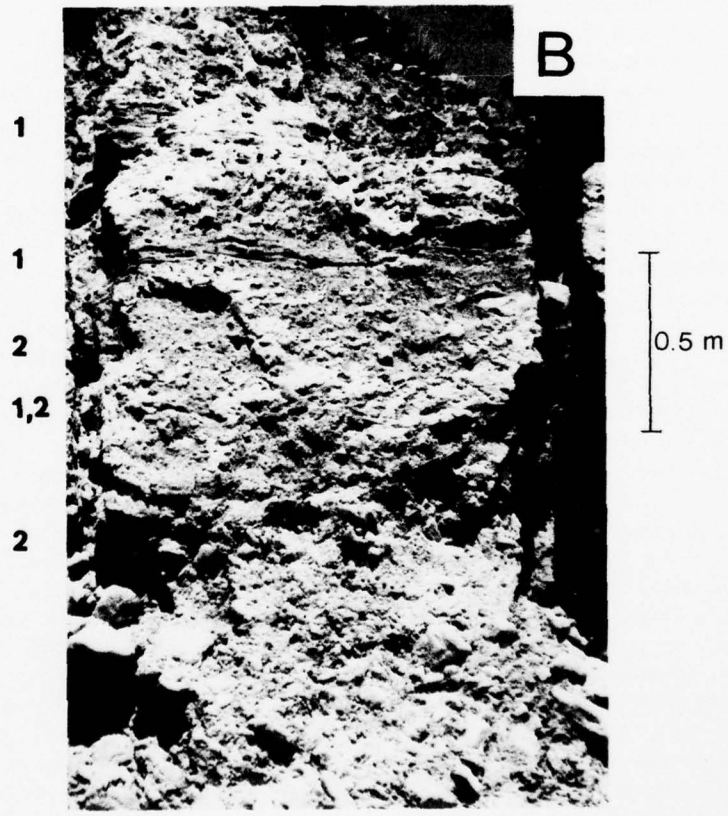
An additional property of sediment flow deposits that was investigated was the pebble fabric. Figure 44 shows scatter plots of pebble orientations in sediment flows on Schmidt equal-area nets. The measured orientations include the trend of the long-axis (*a*) of prolate particles and the direction of dip of the *ab*-planes of blade- and disk-shaped particles. Figure 45 shows the same samples on Schmidt equal-area nets contoured according to Kamb (1959). Equal-area nets are arranged in order of decreasing water content from left to right and top to bottom. The patterns for the flows examined are multimodal distributions, often with a distinct transverse element (MF 17). Type I flows and plug zones (MF 8, 19, 16) show no preferred orientation or weak orientations without a preferential direction of dip. As the water content increases, the scatter in orientations decreases and preferential orientations develop. Type III flows (MF 1, 6, 7) show a relatively strong alignment approximately parallel to the direction of sediment flow, but a nonpreferred, near-horizontal direction of dip. Trend and imbrication in the direction of flow are best developed in fan-deposited flows (MF 10).

The mean axes (V_1) and the degree of scatter of the measured axes about the mean (S_1) generally reflect the results indicated by the patterns of the contoured stereo nets (Table VIII). Mean axes are parallel to transverse to the direction of sediment flow. Values for S_1 range from 0.49 (statistically insignificant) to 0.70, increasing generally with increase in water content. The deviation of the mean axis trend in the upslope direction from the primary direction of flow ranges from 2° to 173° without an apparent relationship to the water content of the sediment flow (Table VIII).

The amount of deviation of V_1 from the source and the degree of dispersion (S_1) about the mean axis are



a. Subtle contact (arrow) between recent deposits of sediment flows marked by a downward increase in the coarse silt and fine sand content and scattered pebbles (here a cavity at photo center) partially embedded in the lower flow. Scale in centimeters.



Sediment flow deposits in older sediments of terminus region showing contacts idenced by discontinuous layers and lenses of meltwater-deposited silts and fine d (1) or increased gravel content at base of sediment flow deposit (2).

Figure 43. Sediment flow contacts.

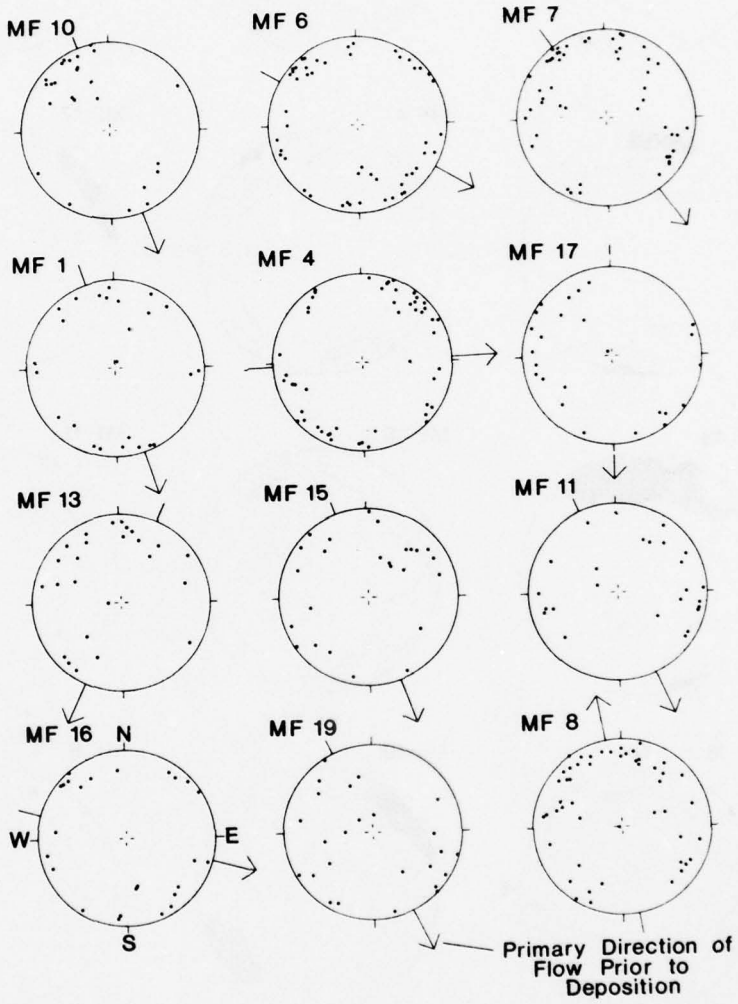


Figure 44. Scatter diagrams (three-dimensional, Schmidt equal-area nets) of pebble orientations in recent sediment flow deposits. Direction of sediment flow prior to deposition is shown. Water content of source flow decreases from left to right and top to bottom.

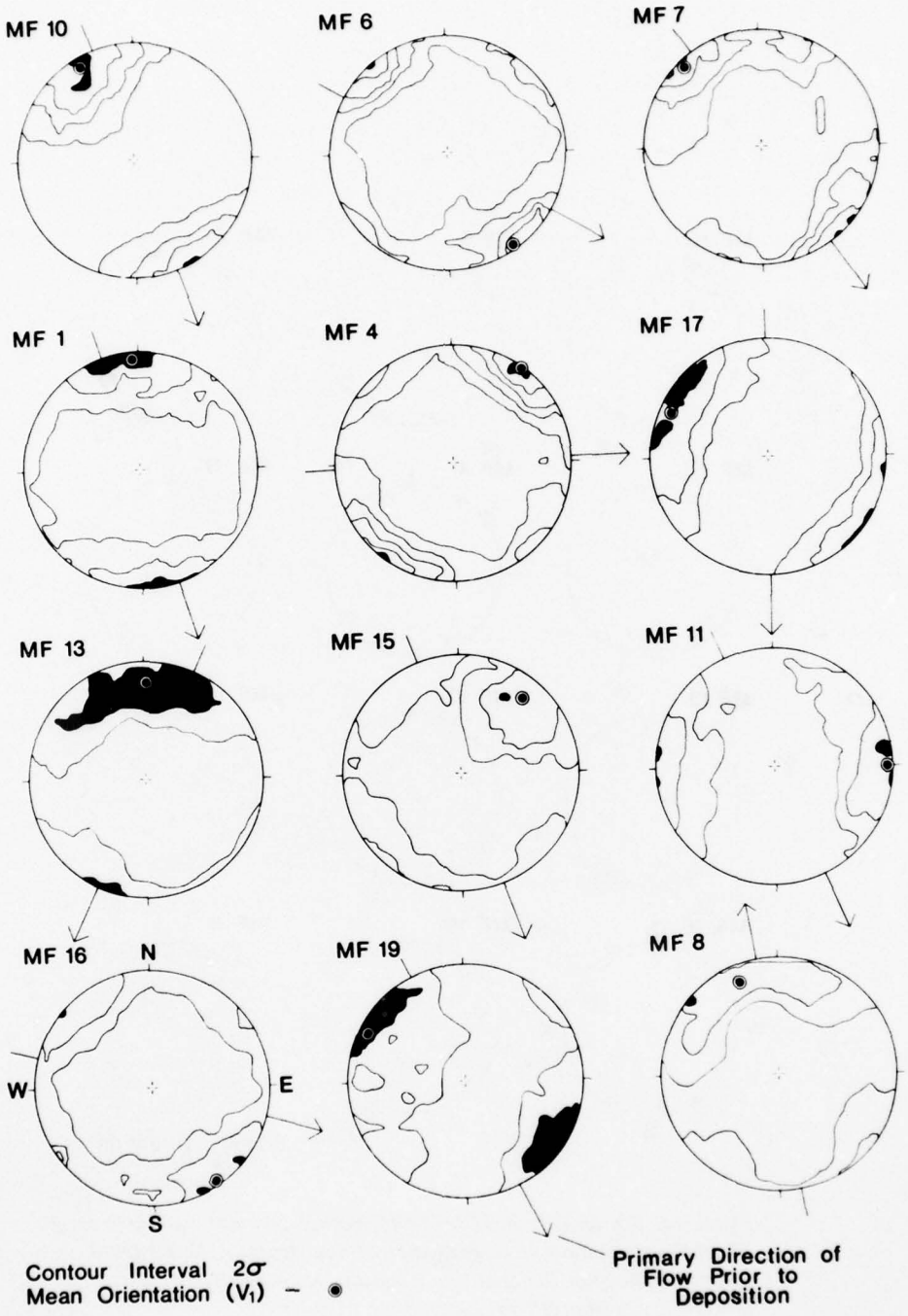
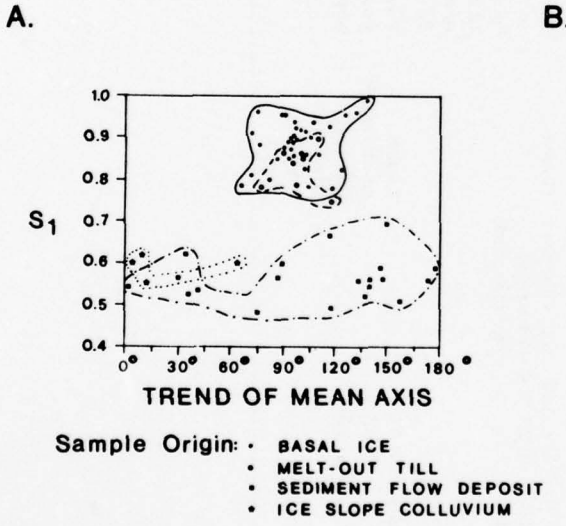


Figure 45. Schmidt equal-area nets of samples in Figure 43 contoured according to Kamb (1959) at a 2 σ interval. Orientation of mean axis and direction of sediment flow prior to deposition are shown.

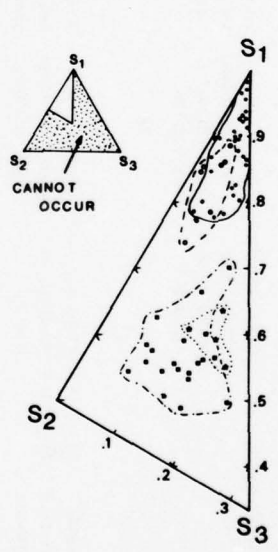
Table VIII. Results of the pebble fabric analyses of sediment flow deposits.

Sample	V_1 Azimuth (°C)	plunge	S_1	Primary direction of flow prior to deposition (°C)	Deviation of V_1* from primary flow direction (°C)	V_3 Azimuth (°C)	plunge	S_3
MF 1	357	7	0.590	162	165	172	83	0.122
MF 2	221	18	0.535	82	139	18	71	0.156
MF 3	73	9	0.487	100	27	260	81	0.164
MF 4	37	1	0.624	88	51	277	87	0.062
MF 5	133	5	0.563	135	2	30	69	0.166
MF 6	146	3	0.583	120	26	19	84	0.073
MF 7	318	6	0.557	145	173	205	76	0.122
MF 8	338	15	0.508	350	12	171	75	0.137
MF 9	318	11	0.547	128	170	86	72	0.070
MF 10	330	9	0.698	160	170	83	67	0.123
MF 11	90	2	0.600	156	66	183	57	0.145
MF 12	87	6	0.565	82	5	181	34	0.173
MF 13	2	18	0.542	205	157	138	65	0.113
MF 14	317	5	0.547	152	165	209	74	0.137
MF 15	41	18	0.540	160	119	198	69	0.153
MF 16	147	3	0.560	106	41	14	85	0.085
MF 17	296	11	0.667	180	116	74	75	0.102
MF 18	357	17	0.578	210	147	172	73	0.087
MF 19	298	9	0.498	154	144	34	49	0.222
MF 20	30	12	0.559	190	160	264	71	0.154

*Direction of V_1 taken upslope.



a. Comparison of S_1, the degree of scatter of individual axes about the mean, and the trend of the mean axis.



b. Comparison of S_1, S_2, and S_3.

Figure 46. Comparison of statistical data of pebble orientations in basal ice, melt-out till, sediment flow deposits and ice slope colluvium. Two distinct groupings occur - one of melt-out till and basal ice, and the other of sediment flows and ice slope colluvium.

Table IX. Characteristics of some deposits of resedimentation processes.

Process	Deposit	Texture: Type	Texture: 1) Mean (ϕ) 2) σ (ϕ)	Internal organization: General	Internal organization: Structure	Internal organization: Pebble fabric	Surface forms	Contacts-basal surface features	Pene-contemporaneous deformation	Geometry-maximum dimensions	Miscellaneous properties
Spall	Slope colluvium	Any; poor sorting		Clasts dispersed randomly in matrix to clast supported.	Massive to intraformational blocks in massive material.	Absent; vertical clasts.	Irregular	Conformable to former surface, non-erosional.	Absent.	Irregular cross sections; band parallel to former slope of variable length, 2 m thick.	Loose; chaotic intraformational block orientations.
Slump	Slump	Silt-sand-gravel; silty sand; sandy silt	1) 1.5 to 5 2) 1.5 to 4	Clasts dispersed randomly in matrix.	Massive to undisturbed blocks over slip plane.	Absent, except in some blocks.	Irregular.	Shear plane may occur; conformable contacts.	Possible in or adjacent to slump block.	Irregular; hundreds of m^2 in area, 2.5 m thick.	Loose to dense.
Ablation	Ice slope colluvium	Gravelly sand; sandy gravel; sand-silt-gravel.	1) -2 to 2 2) 2.5 to 4	Clasts dispersed in matrix to clast supported.	Massive.	Weak; parallel to trend of ice slope; low to high angle of dip. $S_1 < 0.70$.	Irregular.	Conformable to former surface; non-erosional.	Absent.	Discontinuous thin sheets to wedge of variable area; 3.5 m thick.	Loose to dense.
Meltwater Flow	Meltwater Sheet and rill deposits	Silt to silty sand	1) 1.2 to 6 2) 1.5 to 2.5	Matrix.	Parallel stratification; deltaic cross stratification; massive to graded.	Parallel to flow; downslope dip.	Planar; channel patterns.	Conformable to non-conformable; erosional to non-erosional.	Absent.	Thin sheets; wedges, lenses; 1000 m^2 in area; 0.5 m thick.	Dense; associated with sediment flow deposits commonly.

larger in sediment flow deposits than in basal ice and melt-out till. Comparison of the direction of the mean axis with the significance value S_1 produces two separate groupings, one for till and ice, and one for sediment flows (Fig. 46a). Similarly, comparison of the significance values for fabrics in ice, till, and sediment flows reveals two distinct groups (Fig. 46b).

An important property of clast orientations in sediment flow deposits, particularly those of lower water content (about 8 to 18%), is "unstable" near vertical to vertical orientation (Fig. 41 and 44). Steep orientations of this magnitude were generally not observed in melt-out tills.

OTHER RESEDIMENTATION PROCESSES

The primary process of resedimentation is sediment flow, but other important processes of resedimentation include meltwater flow, ablation of exposed ice slopes, and the spall and slump of slopes of sediment. The characteristics of deposits of these processes are presented in Table IX.

Meltwater flow

Meltwater is closely associated with most processes of sedimentation in the terminus region, but in particular with sediment flows. Meltwater flow is one of the few processes of the terminus that results in improved size sorting, both by formation of fine-grained, principally silt-size, deposits and of coarse-grained, sand-size and larger, lags. It is an important process for the selective removal of fine-grained material from sediments of the terminus, which it transports to larger outwash streams that drain the area.

Types of meltwater flow

Insufficient time prohibited detailed analysis of this process, but a few observations were made. Meltwater flow occurred in sheets (1-10 mm thick) and rills of variable size (up to 5-6 cm deep and a few centimeters wide). Most flow appeared laminar, but sharp breaks in slope and irregular surfaces of the bed of larger rills apparently introduced a transient turbulence. Surface flow rates were variable, but generally exceeded 1 cm/s. Suspended sediment content was also variable; the maximum amounts were in meltwater flow associated with sediment flows. The suspended sediment content of meltwater flows immediately prior to and after the passage of a channelized sediment flow (type III) was measured at between 15 and 30% by weight. Very minor amounts of large sand- and granule-size particles are transported as bedload.

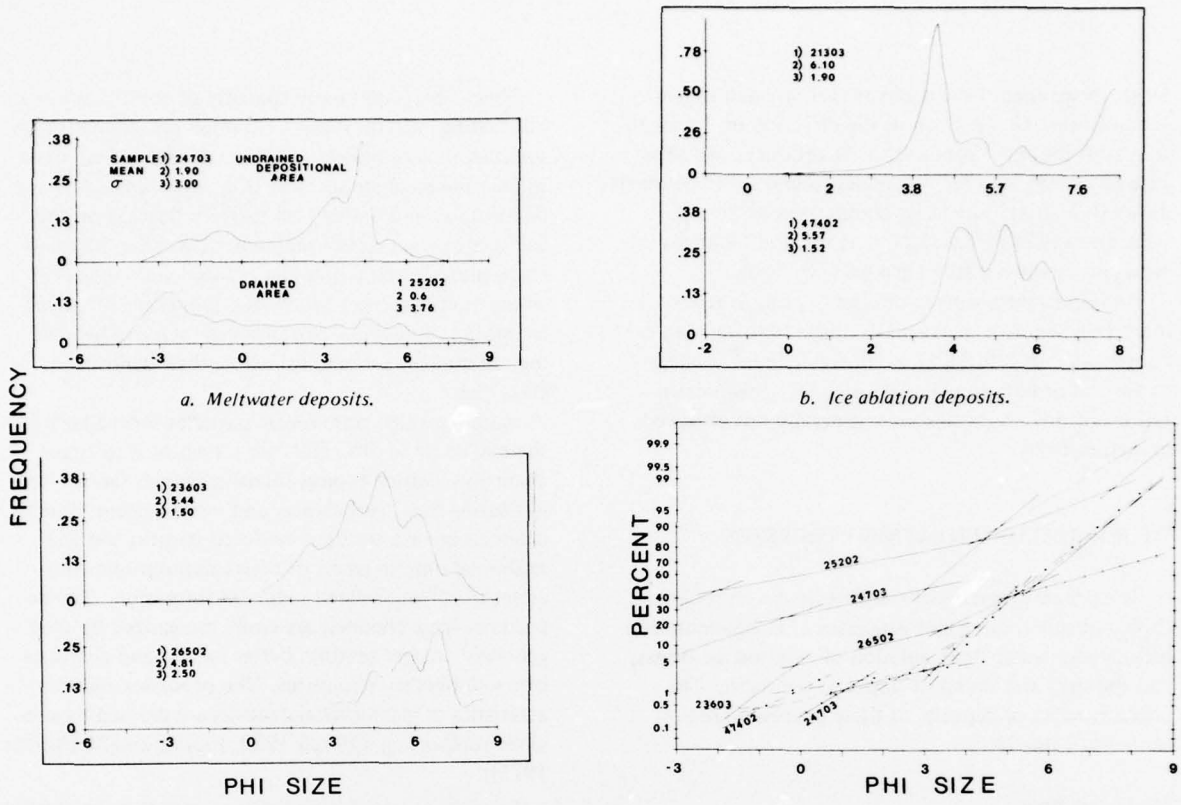
Sheet flow, commonly spatially discontinuous in a bifurcating pattern, is most common on sediment flow surfaces, mainly plug-type flows, and on and adjacent to ablating basal ice surfaces (Fig. 36). Single rills and distributary and braided rill patterns develop on the surfaces of some active sediment flows (Fig. 36), and rill patterns develop on older resedimented material where meltwater seeps form due to melting of buried ice blocks. Individual rills often deepen and become incised on flow surfaces following their deposition (Fig. 39).

Sand- through granule-size particles form a lag on the bed of these rills. Rills are transitional to larger channels in which typical fluvial processes (active sorting during flow, turbulence, and others) occur. Such channels are arbitrarily considered streams and were examined only in terms of their relationship to processes of till and related sediment formation. The deposits of large channels are easily recognized by their generally coarser texture, better sorting and characteristic sedimentary structures. The processes and characteristics of glaciofluvial deposits are defined by previous studies (e.g. Church 1972, Jopling and McDonald 1975).

Deposition of the material in transport by meltwater results after a sharp decrease in flow velocity following a decrease or loss of slope; much of the sediment is, however, transported into outwash streams that flow out of the terminus region. Rates of sedimentation are totally dependent on factors controlling melting rates and the availability of sediment in any given area. Rates measured with sedimentation stakes ranged from 0.1 to 10 cm/day for meltwater flowing from ablating active basal ice and backwasting ice-cored slopes.

Character of the deposits

Deposits from sheet and rill flow of meltwater are relatively well-sorted and fine-grained (Table IX). Most range from fine silt to silty sand with a sorting coefficient of 1 to 2 (Fig. 47). Internally, they are massive to normally graded. Massive layers are usually silts and clays deposited on recent sediment flow deposits. Parallel stratification (1 to 10 mm) occurs often in sediments deposited by multiple meltwater sheet and rill flows; typically, individual strata vary in grain size. Multiple thin sheet flows from ablating active basal ice are texturally similar to these deposits, but they produce a thinly laminated deposit possessing fissility (Fig. 48a). Larger particles and aggregates released by the ice occur sporadically in the vertical



a. Meltwater deposits.

b. Ice ablation deposits.

c. Lacustrine deposits.

d. Cumulative curves of samples.

Figure 47. Typical grain size distribution of deposits of meltwater flow origin, ice ablation and lacustrine activity (intermittent and annual ponds) shown by frequency curves.

section, sometimes deforming underlying laminae. A deltaic stratification forms where concentrated flows develop fan-shaped deposits at a sharp change in slope angle, mostly off coalesced, recently deposited sediment flows (Fig. 48b). These deposits are often interlayered with thin sediment flow deposits. Mean grain size decreases down the fan axis. Deposits range in thickness from less than 0.1 cm to 100 cm. The shapes of the deposits are laterally thinning sheets, wedges (for fans), and lenses or infillings of former topographic lows. Channel lags occur as thin lenses or stringers, usually with voids filled by sediment of the overlying deposit. Surface features on meltwater deposits are rare; most surfaces are relatively smooth and planar. In late spring and early fall ice crystal casts commonly develop in thin sheet flow deposits covering ice (Fig. 48c). Secondary development of channels on fans may result from reestablished meltwater flow. Distributary and braided rill patterns and larger single rills and gullies may be preserved on sediment flow and other depositional surfaces.

Ice ablation

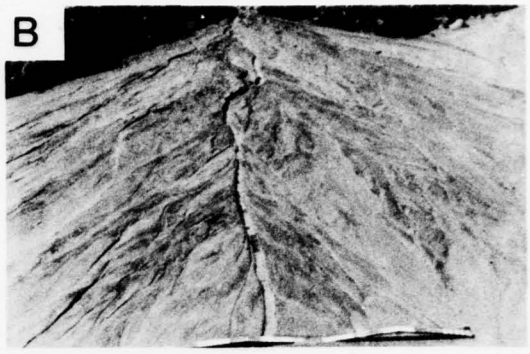
Sediment entrained in the glacier may be released at the surface by ablation of exposed ice of the basal zone and accumulate on or at the base of that slope. Although the deposit that results may be transitional to melt-out till under the proper conditions, the deposits are considered resedimented because the debris in the ice is disaggregated and redeposited, often with loss of some of the fine-grained fraction, and the acquisition of new properties.

Description of the process

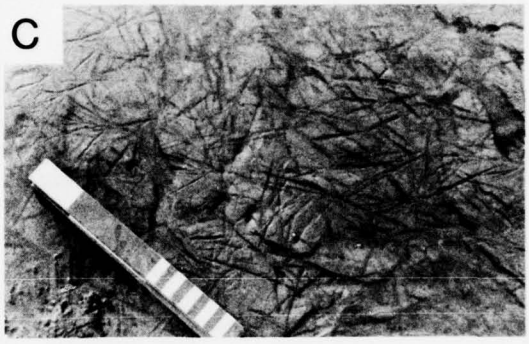
The slope angle of the ablating ice controls the nature of sediment release and deposition. On high-angle slopes, ablation releases individual particles and still-frozen clots of sediment which slide, roll, and fall from the exposed ice to the base of the slope (Fig. 49). Meltwater containing silt and clay flows off the slope in sheets and rills. Mixing saturates the sediments and decreases their strength, permitting some penetration of falling particles.



a. Thinly laminated, meltwater sheet flow deposit posessing a discontinuous fissility. Sediment texture is silty sand to sandy silt. Scale is in centimeters.



b. Meltwater flow fans. View upslope toward ablating stagnant basal ice source. Scale is 1 m long.

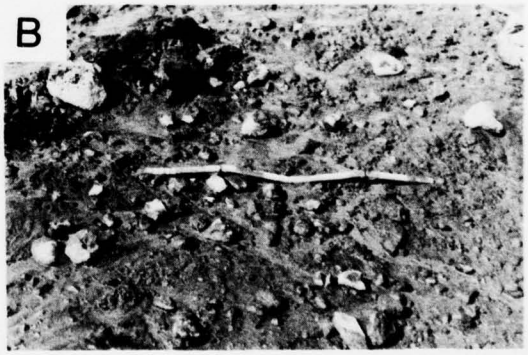


c. Ice crystal casts developed in silts of sheet flow origin deposited over basal ice. Scale is 25 cm long.

Figure 48. Meltwater flow deposits.



a. Surface view of sediment deposited by ablation from basal ice (top of photo) with a high-angled slope. Coarse surface is due to deflation by meltwater flow. Standing water is common on deposits on horizontal slopes over ice. Scale is 1 m long.



b. Surface of ablating basal ice with low-angled slope to right. Small rills and sheet flow of meltwater a few millimeters deep remove fine-grained constituents of basal ice debris. Scale is 1 m long.

Figure 49. Ice ablation sediments.



c. *Ridge deposit resulting from ablation of stable, steep-angled basal ice slope. Partially coarsened surface due to meltwater flow removal of fine-grained matrix. Scale in center of ridge is 2 m wide; ridge is about 4 m wide.*



d. *Texturally heterogeneous deposit formed by ablation of high-angled, basal ice slope. Variable clast orientation is shown. Scale is in centimeters.*

Figure 49 (cont'd). Ice ablation sediments.

The local topographic slope determines if sediments accumulate after release. Near-horizontal slopes and those which dip towards the ablating source are most conducive to deposition. Slopes dipping away from the source induce flow of meltwaters and the saturated sediments, commonly creating thick meltwater sheet flow deposits adjacent to the ice.

Deposition from high-angle slopes onto other sediments generally results in fluid loss by seepage into these sediments with little mixing of the debris. Sediments that accumulate on ice, however, remain saturated, and melting of the buried ice further increases its water content. Small pools of water form in the surface lows due to oversaturation—conditions that are conducive to the development of excess pore pressures, partial to full liquefaction, and coarse grain settlement. Mud volcanoes develop where sediments liquefy at depth and water containing silt and clay is dispersed at the surface from fluidization channels. Meltwater flow from the exposed ice may coarsen the surface of the deposit by removal of the matrix material.

On low-angle slopes (generally less than 20°), ablation of debris-laden ice releases a surface deposit that is rapidly coarsened by meltwater flow (Fig. 49). On low-angle slopes of about 1° to 10°, thin, fine-grained sediment flows may also remove the matrix of the surface material and leave a coarse gravel lag on the ice surface. On slopes with angles closer to 20°, pebbles and granules tend to become aligned, with their long axes trending parallel to the direction of slope. As the remaining coarse-grained sediment thickens, it inhibits the removal of fine-grained sediment by meltwater. This sediment cover reduces the rate of melting and may become stabilized. However, the differential topography of the ice surface and the variability in thickness of the sediment cover usually results in differential melting and failure of the sediment. Open, ablating ice slopes are maintained in this way. In some cases, inhibited melting and thus removal of the sediment cover results in the formation of deposits transitional to melt-out till.

The actual rates of ablation of open ice slopes are dependent on several factors including the debris content of the ice (Østrem 1959), the thickness and texture of the sediment cover formed by ablation (Østrem 1959, Loomis et al. 1970), and climatic factors, the most important of which is solar radiation (Mayo and Péwé 1963). The large and variable rates of ablation observed daily during preliminary attempts to measure these rates, the complexities of establishing a survey network necessary for the measurement of these rates (see, for example, Peterson 1970), and time limitations on this study did not permit evaluation of the controlling factors.

The rate and extent of sediment accumulation at the margins of high-angle ice slopes are variable. Slopes observed in 1974 formed deposits ranging from 4 to 25 m wide and in 1975 from 3 to 18 m wide, with thicknesses ranging from 0.25 to 2.5 m. This variation in extent and thickness results from the factors controlling ablation rate as well as spatial variation in the rate of ice flow, local topographic slope, debris content of the basal ice, dip of the debris stratification, and local slope of the bed of the glacier. Progressive melting and recession of the ice slope produce a sheet or wedge-shaped deposit in cross section; an ablating but stable ice slope produces a ridge (Fig. 49). In plan view, the deposit forms a discontinuous band that parallels, and marks the former position of, an exposed ice slope.

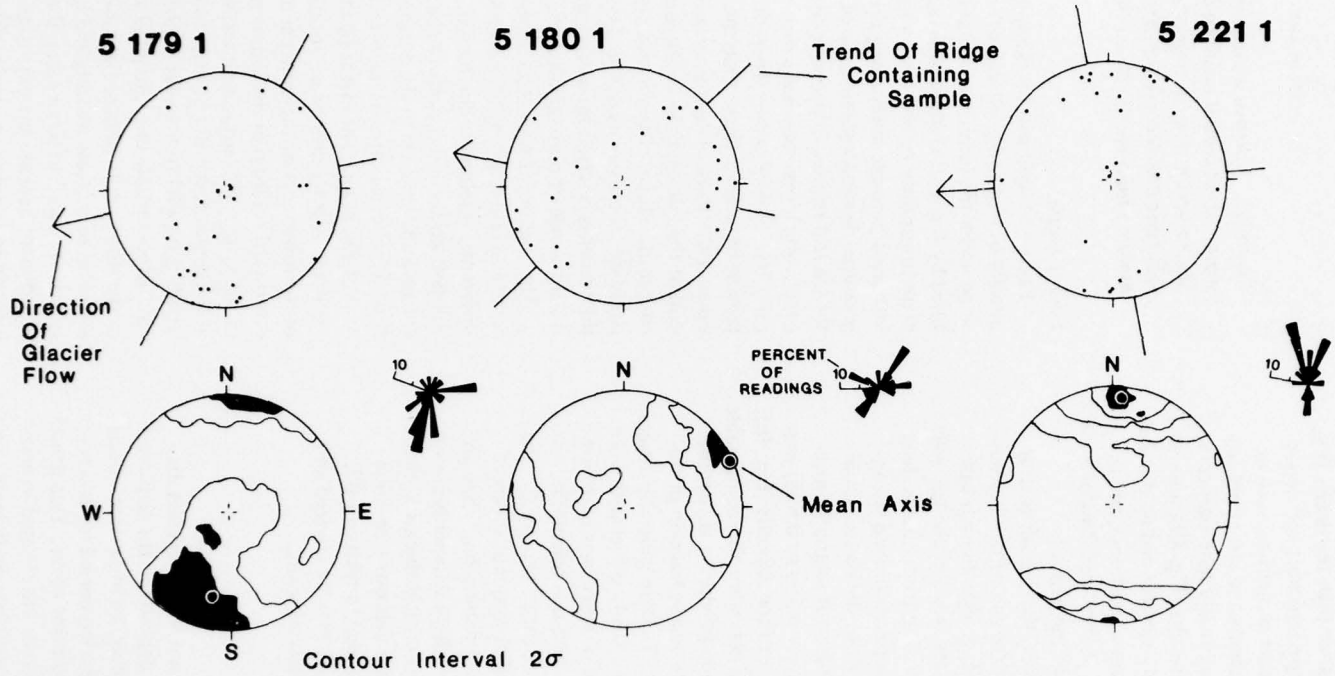


Figure 50. Scatter, contour and rose diagrams of pebble orientations in sediments deposited by ablation of high-angle, basal ice slopes. The trend of the ridge containing the deposits, the direction of glacial flow and the mean axis (V_1) are shown. Orientation is approximately parallel to the trend of ice slope.

Character of the deposits

Deposits derived from ablation of high-angle slopes inherit much of the bulk textural character of the ice debris, but are in general coarser than the debris (Fig. 48). Mixing during downslope transport and deposition results in a loss of all other properties, such as texturally segregated components and structural features of the basal zone. A texturally heterogeneous, poorly sorted deposit often results (Fig. 49), and lenses of well-sorted clayey to sandy silt (formed by ponded meltwater under poor drainage conditions), and of well-sorted sand (formed by channelized flow of meltwater), may occur throughout the deposit.

With the exception of fabric, the deposit is structureless. A weak long axis alignment of pebbles was measured in three localities (Fig. 50). In each case, the mean axis lay parallel to the trend of the ice ridge, and pebbles varied in dip direction from near vertical to horizontal. Because the slopes examined lay approximately tranverse to ice flow, the mean axis of the fabric did as well. The degree of scatter of measured axes about the mean (S_1 = 0.550 to 0.638) was comparable to that of sediment flow deposits (Fig. 46), and the contoured equal-area nets were also comparable.

Low-angle slopes in ablation produce a lag deposit because it consists of only the coarse fraction of the debris of the basal ice source. Texture generally ranges from a coarse pebbly sand to a sandy gravel with poor sorting (Fig. 48). An absence of fabric was observed in the deposits, although the long-axis orientations observed on exposed ice slopes might be preserved. The deposits are thin (5-30 cm), discontinuous sheets of variable spatial distribution and dimension. They are preserved on low-angle slopes where sediments are sufficiently stable to increase to a critical thickness that inhibits ice melt. As with some deposits from high-angled slopes, they are transitional to melt-out till. Gravel lags formed on ice slopes may be covered and preserved beneath sediment flow deposits.

Slope failure

Slope failure is less significant than processes discussed previously in terms of deposits of the terminus that are preserved. It is, however, an important means of initiating reworking by exposing buried ice and remolding the initially stable sediment cover. Two principal modes of failure that are often interrelated in areas of thin sediment cover are recognized. Sediments overlying low-angle ice slopes fail mainly by slumping, whereas sediments of high-angle slopes overlying high-angle ice slopes fail predominantly by spall and collapse.

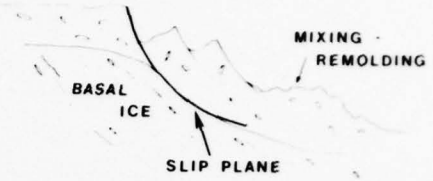


Figure 51. Schematic diagram of slump of sediment on buried basal ice of low-angle slope. Slump occurs due to rotational slip along ice/sediment interface; sediments may undergo remolding followed by flow after slope failure.

Failure modes

Failure of sediment by slumping is shown schematically in Figure 51. Blocks of sediment rotate downslope under the influence of gravity along planes defined by the ice/sediment interface. Slip along this plane apparently results from a loss of strength due to increased pore pressures along the melting surface. Pore pressures develop here because of the impermeability of the ice and relative impermeability of the sediment cover, which generally has a high proportion of silt-size particles. Failure occurs when the gravitational component of stress is larger than the total resistance to shear at the ice/sediment interface and along the extension of the failure plane in the sediment cover at the base of the slope. The situation is analogous to the landslide failures analyzed by Terzaghi (1950) to which the reader is referred for a more detailed discussion of the influence of pore pressure and the failure mechanism.

The spalling of high-angle slopes results from an effective over-steepening of the slope sediments due to differential melting of the buried ice. Sediments are thinnest on the lower parts of the slopes that undergo collapse and thickest in the adjacent surface cover (Fig. 52); hence, rates of melting are largest near the base of the slope. The effect of this melting is an inward and slightly downward rotation of the sediments of the lower part of the slope, and an outward and downward rotation of the sediments of the upper part of the slope. This rotation increases the tensile stress in the upper cover of sediment and extension fractures trending parallel to the edge of the slope develop (Fig. 53). Blocks rotate until they fail and fall to the base of the slope. Sufficient sediment is removed in certain instances to increase melting and induce failure of the sediment cover. In some cases, the decreased thickness of sediment beneath the extension fractures causes an increase in temperature and melting of the buried ice that in turn causes localized collapse. Continued melting and collapse may eventually reduce the ice-cored sediments to a pile of chaotic blocks.

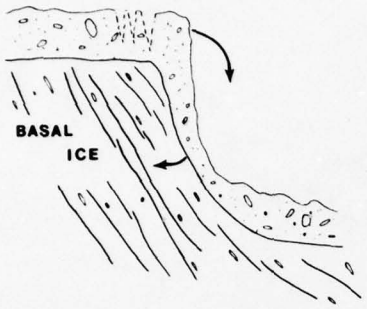


Figure 52. Schematic diagram of spall of sediment on buried basal ice of high-angle slope. Spall occurs due to differential melting of buried ice with the maximum rate occurring in the lower part of slope beneath the thinnest sediment cover. Differential melting causes outward and downward rotation of sediments at the top of slope and its eventual failure. Extension fractures develop in slope marginal surface sediments.



Figure 53. Extension fractures developed in surface cover adjacent to a slope undergoing spall. Rotation to left. Scale, lying across largest fracture at photo center, is 2 m long.

Character of the deposits

Because the failure of a slope by either spall or slump occurs irrespective of the textures of the sediment cover, the texture of the deposits cannot be specified. Most of the sediment that fails is deposited by resedimentation processes. If rotational blocks remain intact during slumping, both the plane of failure and the block may be recognized. For example, stratified materials define preserved blocks of sediment. The partially saturated to saturated state of most sediment transported by slumping prevents simple breakage and collapse of rotational blocks. Internal deformation during slip may be expected under these conditions, but none was observed in recent deposits. If sufficient water is available, sediments may fail internally, mix, and undergo complete remolding as described previously. Deposits become texturally heterogeneous, massive, and without distinctive features. Dewatering of excess pore fluids through expulsion tubes was observed in poorly drained areas of failure. Water escape structures may develop under these conditions.

Spall and collapse result in a chaotic deposit at the base of the slope. It may consist of intact blocks of upper slope sediment in variable orientations, some with structure, which are surrounded by unsorted and texturally diverse materials lacking structure. The surface of the sediment pile is initially irregular, but slope wash and other processes partially or fully disintegrate blocks exposed at the surface and deposit sediment in the voids between them. The base of the deposit is defined by the configuration of the slope it is covering.

Other processes and deposits

Other primary and post-depositional processes include slopewash, ponding, eolian transport, differential melting, groundwater flow, and ice flow. The former three processes produce deposits that are minor in occurrence, whereas the latter three affect sediments after deposition. Creep, the slow downslope deformation of surface sediments (transitional to type I flows) was not observed but may be effective in reorienting particles and structures in sediments over ice and permafrost (Boulton 1971).

Small pools (1 to 30 m wide, up to several meters deep) of ponded waters derived locally from the melting of buried ice (kettles) and from extrabasin sources of ablating basal zone ice and other surface runoff dot the low-sloping areas of the terminus. These ponds may be "permanent" from melt season to melt season or be intermittently filled only during periods of heavy melting and precipitation. Periods of deposition may therefore be sporadic or somewhat continuous, depending upon the source of water and sediment. Most small ponds develop on the sediment cover and are not fed by ablating ice, but are intermittently dry. The weekly rates of sedimentation measured in four small ponds

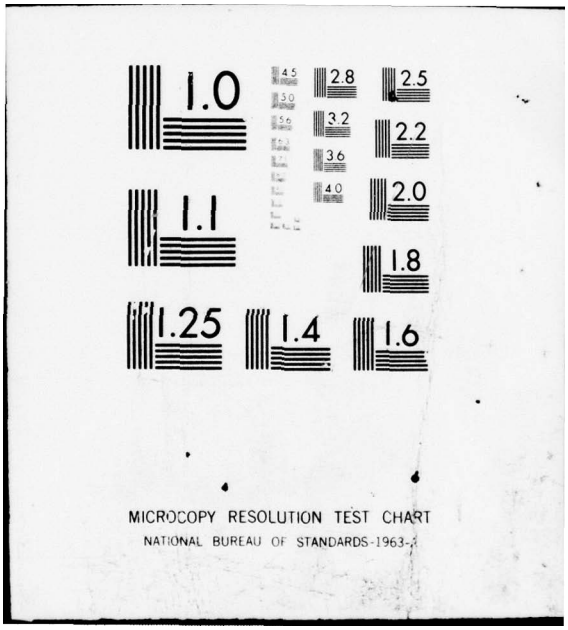
AD-A072 000 COLD REGIONS RESEARCH AND ENGINEERING LAB HANOVER NH F/G 8/12
SEMDIMENTOLOGICAL ANALYSIS OF THE WESTERN TERMINUS REGION OF TH--ETC(U)
MAY 79 D E LAWSON

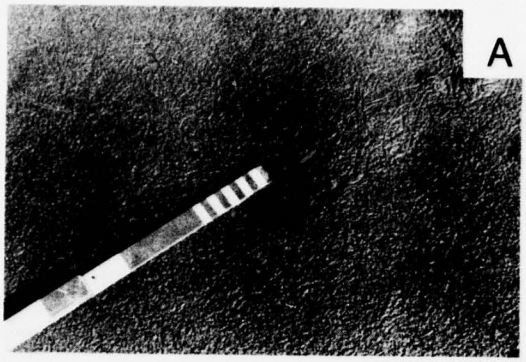
UNCLASSIFIED CRREL-79-9 NL

2 OF 2
AD
A072000

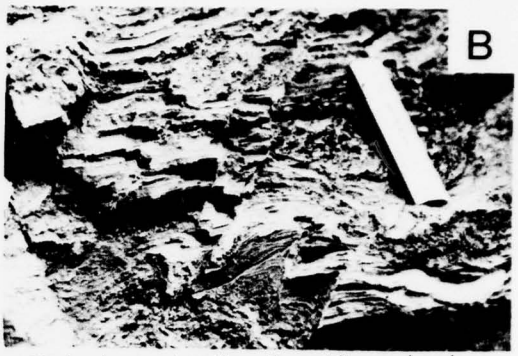


END
DATE
FILMED
8-79
DDC

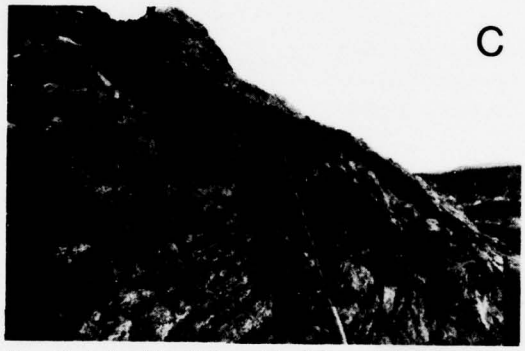

1.0
4.5
5.0
5.6
2.8
3.2
3.6
4.0
2.5
2.2
2.0
1.8
1.1
1.25
1.4
1.6
MICROCOPY RESOLUTION TEST CHART
NATIONAL BUREAU OF STANDARDS-1963-A



a. Crawling traces formed by water beetles in intermittently filled pond. Sediments are silty clays. Scale segment is 35 cm long.



b. Stratified meltwater sheet flow silts and fine sand, and stream-deposited sands and granules deformed by reverse faulting due, apparently, to differential melting of buried basal ice. Scale is 15 cm long.



c. Stratified silts of lacultrine origin deformed during override by recent advance of Matanuska Glacier. Scale is 90 cm long. Glacier flow from right to left.

Figure 54. Miscellaneous features.

(≤ 10 m across), one of which was fed by distant ablating ice, ranged in 1974 from < 0.1 to 8.1 cm, and in 1975, weekly rates varied from ≥ 0.1 to 4.8 cm. Most sediment is transported into the ponds in suspension, and the sediments of all but small pools show a textural fining towards the center of the basin. Sediments are typically well-sorted clayey silt to silt except for those of the immediate nearshore area, which are usually sandy (Fig. 48). Sediments in intermittently filled low areas of the surface cover are massive and very well sorted fine silt. Small lakes fed by ablating ice are laminated (typically less than 0.5 cm thick), with the texture of individual strata ranging from clay to sand. Normally graded, fine sand layers are present in several of the thin (2- to 30-cm-thick) deposits. Dessication cracks and raindrop imprints were observed on the surfaces of intermittently filled ponds. Several of the intermittent and permanent pools supported a water beetle population and the surfaces of their deposits were covered by crawling traces (Fig. 54a).

Slopewash is an important agent for locally reducing surface irregularities in sediments, transporting small amounts of sediment downslope, and coarsening the surface materials. Sedimentation stakes placed at the margin of steep slopes (30-60°) of relatively stable, dry sediment recorded rates of deposition ranging from 0.05 mm to 3 mm in 1974 and 1975. Recent deposits are thinly laminated to massive and conform to the local topography. Texturally, they range from sandy silt to pebbly silty sand.

Eolian processes are important where surface sediments are dry; they are thus restricted to the outer margin of the terminus. Observations on windy days (15-50 km/hr) indicate that sand- through clay-size particles are readily entrained and transported from the terminus region, either onto the glacier surface or downstream into the Matanuska River Valley. This process is an important mechanism of deflation and coarsening of stable (limited internal melting) sediments, and of deposition of thin, well-sorted sands on the lee side of



a. Near vertical ice-cored slope consisting of about 6 m of exposed basal ice and a 1.5- to 5-m-thick sediment cover. Saturated sediment pile lies on low-angled slope in foreground. Material covering basal ice has been released recently from sediment cover due to backwasting process. Photo shows decreased meltwater activity in early morning.



b. Partially uncovered, ice-cored slope (upper left) shown with recently deposited sediment flows (light grey lobes) and meltwater fans at base of slope on dry stream bed sediments. Slope is about 4 m tall. Active and abandoned rills and small stream channels occur across coalesced flow deposits. Slope to right of open basal ice is covered; sediment is slumping with gradual incorporation of slump blocks into sediment cover.

Figure 55. Ice-cored slopes.

ridges on windy days. On high-angle slopes, removal of the interstitial fine-grained particles eliminates support for gravel-size particles, which then fall and accumulate at the base of the slope as a partially sorted gravel lag.

Differential melting of buried ice, although insufficient to generate large-scale resedimentation, causes internal deformation of the deposits. The variable rates of melting associated with the deposition of melt-out till are transmitted into the overlying sediment cover and initiate differential settlement and folding or faulting of these sediments. Structured sediments readily show the effects of such melting (Fig. 54b). Extensive differential melting may cause collapse of the surface cover.

The flow of meltwater at the ice/sediment interface results in thermal erosion of the ice. Flow is often concentrated along former surface channels and other ice surface irregularities, and is probably derived mainly from melting of the buried ice. As discussed previously, temperatures may rise several degrees and, where melting is sufficient, cause collapse of the surface materials.

The local readvance of the glacier over the resedimented materials and tills may affect their properties. The most spectacular are the deformation of structured sediments; Figure 54c shows stratified lake sediments overturned by the glacier advance of the winter of 1966-1967.* The effect of override on sediments now found as interlayers between two blocks of basal ice is unknown. The layers examined were generally stratified (Fig. 20) and showed no apparent alteration by the overriding ice. Characteristics of the deposits indicate that they are of meltwater and sediment flow origin. In one instance, pebble fabrics measured in two layers, one of meltwater origin and a second of sediment flow origin, revealed relatively strong unimodal patterns with mean axes similar to those of pebbles in the overlying ice. These patterns may indicate reorientation due to shear during ice override. However, no other features or disturbance of existing internal structure were observed.

The presence of overridden materials between layers of basal zone ice will, upon melt-out, form a deposit that may appear to have originated from separate ice advances. Distinguishing this locally derived sequence from a sequence deposited by a regional glacial advance would mainly require defining the lateral extent and other stratigraphic relationships of the deposit.

Gravel lags result from a number of processes and occur throughout the terminus sediments. Small stream lags, fall lags released by eolian deflation, and sediment flow lags left by flows incompetent to transport the gravel are possible origins. Although it is unlikely their origin can be determined, their presence in a sedimentary sequence would be a characteristic suggestive of a former surface of ice or sediment. Their geometry varies from tabular to shoe-string shape.

* J. Kimball, personal communication, 1974.

RESEDIMENTATION PROCESS RELATIONSHIPS

The thickness of sediment covering the stagnant basal zone ice of the terminus insulates it rather effectively. Rates of melting are generally slow and the amount of sediment produced in a summer melt season is not large. Hence, under these conditions, little reworking should occur and the production of melt-out till should dominate the sediment system. However, much of the sediment of the terminus is reworked frequently in short time periods. In 1974, for example, sediments in a wide area of the northern two-thirds of the terminus were reworked in cycles of mobilization, transport, and deposition two to three times from June to mid-August (see next chapter). In 1975, a single cycle occurred over most of the same region.

Reworking results primarily from the combined effects of the processes of sedimentation of the terminus with the ablation of a limited thickness of the surface of the basal zone ice. This backwasting involves the lateral retreat of near-vertical, ice cored slopes, which stand generally between 1 to 3 m tall (exceptionally 8 m tall), throughout the sediment-covered region of the terminus (Fig. 55). The rates of lateral retreat and hence reworking are controlled by the rates of ablation of exposed debris-laden basal ice rather than by the much slower rates of melting of sediment-covered basal ice. Ice may be exposed by several processes including slope collapse due to differential ablation, slumping along the ice-sediment interface, in-situ saturation and flow, fluvial erosion at the base of a slope, or any other process or combination of the above processes that cause failure of the sediment cover and its transport from the immediate slope area.

Ablation of the ice releases water and sediment and causes collapse of the sediment cover. These products combine, generally in sediment and meltwater flows, and are removed from the immediate area of the slope (Fig. 55). Normally, sunny skies for relatively short periods of time (tenths of an hour) melt sufficient ice to cause backwasting, and extended periods of clear skies and warm temperatures result in rapid slope retreat. Because sediment often accumulates at the base of an ice-cored slope prior to flow, the ice buried beneath it melts at much slower rates than the backwasting slope. Hence, lateral recession of the ice-cored slope with only minor vertical recession of the base of that slope occurs. This process results in the "skimming" of the upper 0.5 to 5 m from the surface of the buried basal ice with the wave-like movement of the backwasting slope across the terminus.

Backwasting continues as long as ablation generates sufficient meltwater to transport the sediment released from the ice and the undermined surface cover from the ablating ice slope. Slopes become covered, principally during the fall, because of a decline in the air temperature and the intensity and duration of solar radiation, which in turn decreases meltwater production. Extended cold, cloudy periods during the summer melt season show the same effect; these conditions apparently account for the less extensive reworking observed in the terminus region in 1975. The decline in meltwater production decreases the mixing and remolding of the sediment cover and decreases the water content of sediments accumulated at the base of the slope. As water availability decreases, the accumulated sediments lose water that is not replaced, due to evaporation and downslope seepage, and the effective strength of the sediment pile increases to the point where failure and flow will not occur. Slope angles of the ice face are reduced by gradual covering of the lower part of the slope by remolded sediments and partially disaggregated sediments released by the ablation of the upper part of the ice slope. The slope is eventually buried in its own debris. Slumping of the sediment cover along the buried ice was observed in some cases, but insufficient water was available to mobilize slump material to flow.

The rates of lateral slope retreat were measured for several slopes in 1974 and 1975. Location of the slope was determined daily using tape and compass and weekly by plane table and alidade. A minimum volume of sediments reworked during the monitored period was determined by calculating the average thickness of the sediment cover in regions over the area below the final slope location. Table X lists the rates of slope retreat and volumes of sediment reworked for slopes monitored in 1974 and 1975. An example of lateral slope movement is given in Figure 56 for Stake V. The location of the slope is shown from 10 June, at about the time ice became exposed, until 26 July when the slope, parts of which were slumping, was covered by sediment. The original sediment thickness ranged from 0.4 to 2.2 m with an average of 1.0 m, while the thickness after 26 July ranged from 0.3 to 2.0 m. An average daily rate of retreat of 0.6 m/day was recorded, and the maximum daily rate was 2.5 m. In 47 days approximately 1000 m^3 of sediment was reworked. (This value is conservative as it does not consider the amount of debris released from the ice.) Rates of retreat and volumes of sediment reworked that were larger and smaller than these were recorded for the other monitored slopes (Table X). The maximum daily rate of retreat measured was 4.1 m at stake I, where over 1800 m^3 of sediment was reworked in the 35 days of monitoring. Rates (weekly, daily) were smaller in 1975 than 1974 and as stated above, may be the result of cooler temperatures and increased cloudiness in 1975.

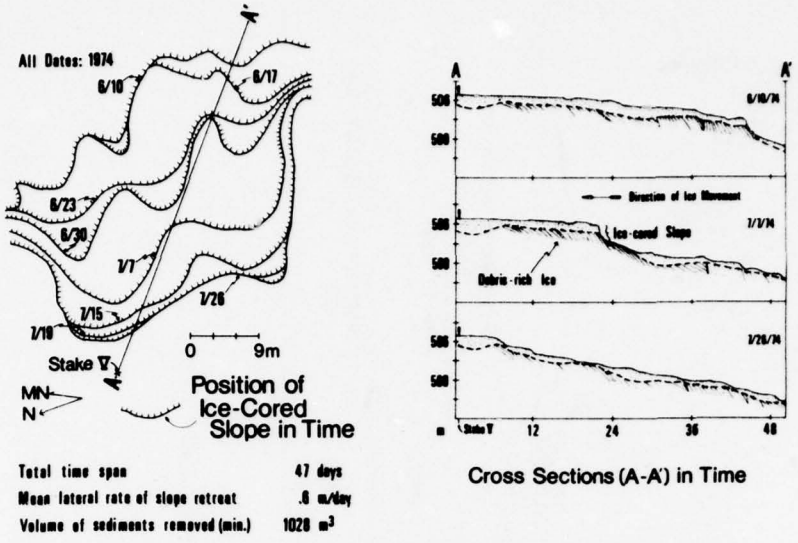


Figure 56. Results of monitored slope retreat at stake V in 1974. Lateral rate and volume of sediments removed during retreat are shown. Cross section A-A' shows change in slope morphology with time; map view at left shows position of ice-cored slope at one-week intervals.

Table X. Backwasting rates of ice-cored slopes.

	Slope	Time (days)	Mean daily lateral retreat (m)	Max. daily lateral retreat (m)	Total vol. sediment removed (m^3)
1974	I	35	0.8	4.1	1808
	II	35	0.5	2.8	1064
	III	47	0.7	3.8	2110
	VI	47	0.4	1.8	665
	V	47	0.6	2.5	1028
1975	VI	45	0.5	2.0	858
	VII	45	0.3	1.5	545
	VIII	45	0.3	1.4	724

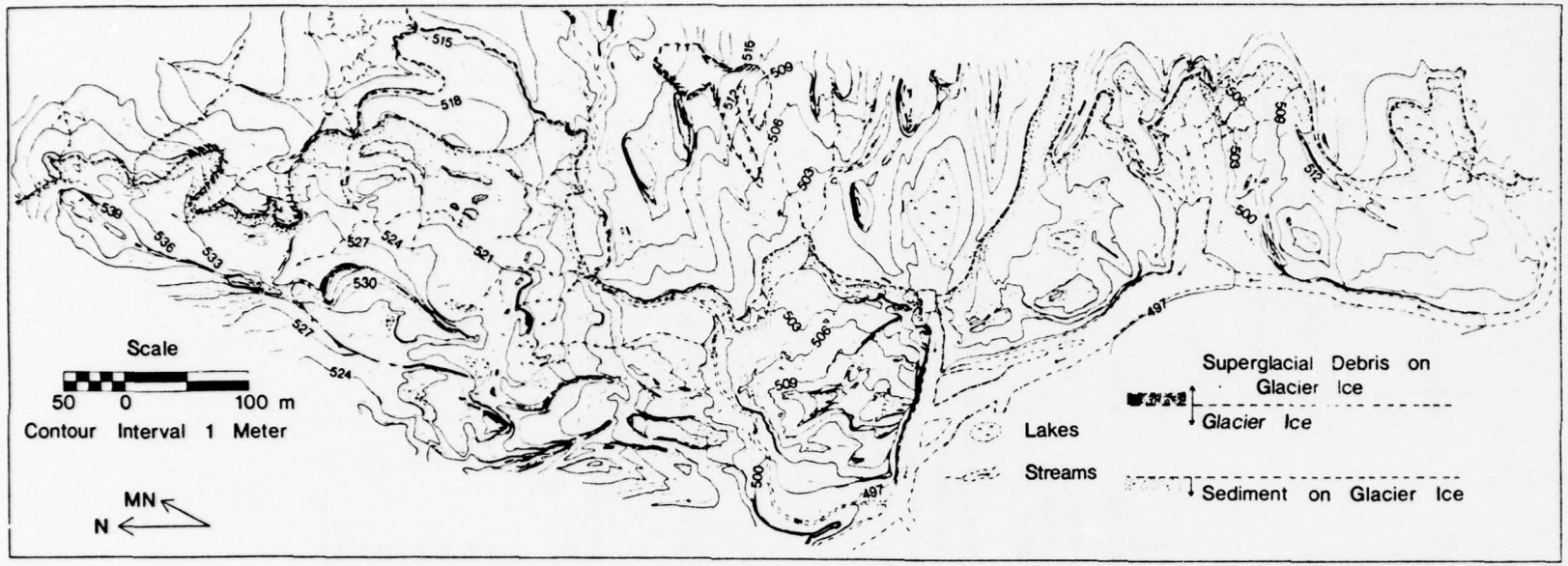


Figure 57. Topographic map of study area of terminus region, Matanuska Glacier, Alaska, 1974.

CHAPTER 6. PROCESS DISTRIBUTION, SEDIMENT DISPERSAL AND DEPOSITIONAL PATTERNS

The sedimentary sequence that develops from sedimentation at the margin of the Matanuska Glacier is determined by both the characteristics of individual deposits and the spatial relationships of the depositional processes in the terminus environment. For this reason, the physical characteristics of the surface-near-surface zone, the lateral and vertical distribution of processes and their depositional facies, and sediment dispersal in the terminus region were analyzed. Till and related sediments are considered in detail, whereas other sediment types are examined simply in terms of their interrelationships with those sediments.

PHYSICAL CHARACTERISTICS

Topography

The topography of the terminus in the area of study, including the adjacent active ice surface, was mapped fully in June 1974, using plane table and alidade (Fig. 57). For the discussion, the map area is considered in three sections (north, central, south) that are separated by the two east-west trending, fountain-fed outwash streams. In the northern area of the map, the surface slopes generally upglacier from a series of ridges which trend parallel to former locations of the ice margin and which are separated by valleys last occupied by streams (Fig. 58). This trend is broken where a former outwash stream flowed through the ridge system and the surface slopes towards the channel in this area. Small streams tend to flow towards and adjacent to the margins of the active ice. The largest amount of reworking of the sediment cover is associated with backwasting ice-cored slopes and is concentrated between the ridges and active ice. Sediment flow, slump, ablation of exposed basal ice, meltwater sheet and rill flow, and fluvial and lacustrine activity are processes often occurring in this region. The width of this zone ranges from about 50 to 200 m. The zone of reworking narrows to the north due to inhibited melting of the basal ice by the superglacial debris cover. The ridges are affected primarily by slope spall and collapse, differential melting rates of the buried ice, slopewash, and eolian processes. The westernmost, generally continuous ridge at the map edge marks the approximate location of the extent of colonizing vegetation on the terminus sediments. The immediate proglacial region adjacent to this area slopes

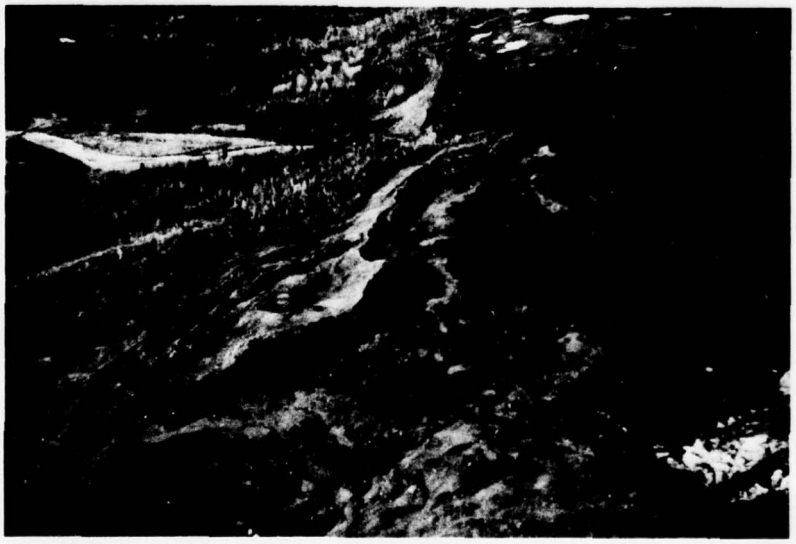


Figure 58. Aerial photograph showing upper two-thirds of north area of Figure 57. Vegetated proglacial region, ridge zone, zone of resedimentation and active glacier ice are shown from left to right. Surface slopes away from ridge zone.

in the downglacier direction toward a series of older moraines. Stagnant glacial ice underlies parts of the westernmost ridge.

The surface slopes mainly downglacier in the south area of the map. Reworking is confined to a narrow 10- to 50-m wide zone that was formed by recent recession of the active ice margin directly adjacent to the active ice. Slump, sediment flow, and meltwater sheet and rill flow are processes commonly active here. The remainder of the sediment is apparently stable and reworked a minimal amount by slopewash, fluvial activity, and eolian processes. Streams from the areas sloping downglacier are small, following the slope directly, and only locally rework the surface materials.

The surface of the central area, which is transitional in character to the north and south areas, is approximately horizontal but shows local variations in relief. Reworking is mainly the result of the backwasting of ice-cored slopes located in the marginal areas adjacent to active ice and outwash streams. A small ridge, probably related to those in the north, lies along the western outwash stream. At present, reworking is minimal in the central area.

Sediment thickness

The terminus region is fully ice-cored by both active and overriden, stagnant basal zone ice. The sediment covering this ice varies in thickness areally and with time. The thickness of the sediment cover in June 1974 decreased generally towards the margin of the active ice (Fig. 59). Exceptions include the region lying adjacent to the ice margin in the north, where the deposits were derived from sediment flows and ablation of high-angle ice slopes, and the thinly covered region to the west-northwest of this area from which these sediment flows originated. Areas reworked by backwasting ice-cored slopes and sediment flow are characterized by thicknesses ranging typically from 0 to 2 m, although flows may originate from areas of ice covered by up to 6 m of sediment. Surface materials in this area are moist to wet; areas with minor slope are covered by small pools of standing water. Stippled areas with thicknesses in excess of 2 m (most are greater than 3 m) in Figure 59 are characterized by limited reworking by surface processes. These processes include slopewash, wind, and melting of the buried ice. Most of the sediment, except that at the base of slopes, is dry and consolidated in summer. Topographically high areas are generally underlain by the thickest sediment cover, derived almost totally from fluvial and resedimentation processes.

The south area is characterized by large regions of sediments in excess of 2 m thick and the thinly covered (usually less than 1-m-thick) area of reworking which lies adjacent to the active ice margin. This distribution was controlled by the local topographic slope, which induced flow of sediment and water from the ice margin to form the wedge-shaped deposit now on the stagnant basal zone ice. The central area, with its near-horizontal topographic slope, is characterized by a sediment cover of relatively constant thickness that is surrounded, except in the northwest corner, by marginal, thinly covered areas. The sediment cover in the north area is generally thin between the ridge zone and the active ice, but exceeds 8 m in thickness in several of the ridges.

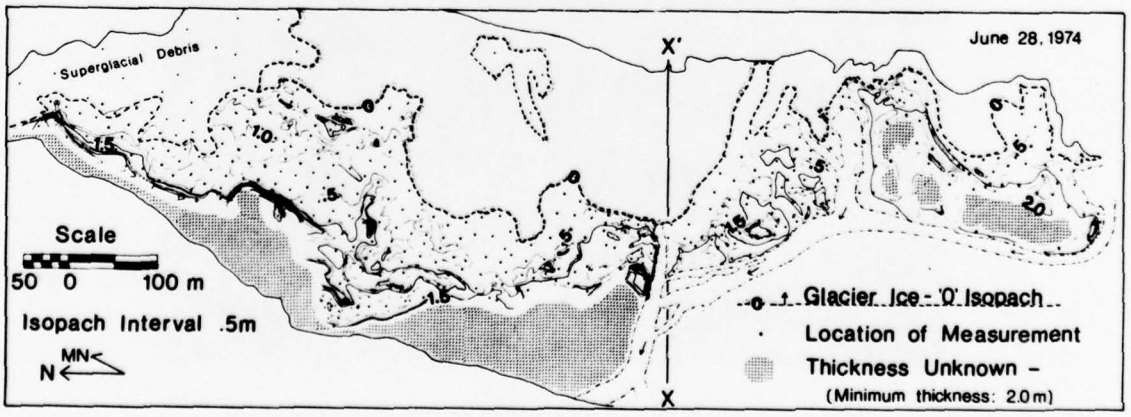


Figure 59. Isopach map of thickness of sediment covering the stagnant basal ice of terminus in area of topographic map (Fig. 57) on 28 June 1974. Thickness decreases generally toward active ice margin.

Ridges, although composed of fluvial and resedimented material, mark the former location of a steep, active ice margin. Ice-cored backwasting slopes occur throughout areas of reworking, but do not appear on the map because of its scale.

Sediment texture

The textural distribution of the surface materials is complex and does not show a definitive trend or pattern (Fig. 60). This distribution is as expected because the analyses of individual processes and their deposits indicated their textural similarity and potentially complex interrelationships. Field observations permit the conclusion that the textural distribution is related to the depositional and post-depositional processes of the terminus. The coarse-grained debris (sandy gravels) on the active and stagnant basal zone ice in the north are deposits of ablation of basal zone ice of high and low angle slope. The remaining coarse sandy gravel areas (primarily sandy to silty sandy pebbles) are most often former and active stream channel deposits or surface sediments coarsened by fluvial activity (south area). In the south area, the thinly covered zone of sandy silt is sediment released from high-angle slopes of active basal zone ice onto the low sloping, poorly drained marginal surface. Although resedimentation mechanisms occur here, the source of sediment is limited to the basal ice and therefore the sediment remains relatively homogeneous. Silt to sandy silt deposits of limited extent are of meltwater and lacustrine origin. The nondescript pattern of silt-sand-gravel (silty sandy pebbles to pebbly sandy silt) that pervades the middle of the map reflects the predominance of the resedimenting processes of slump and sediment flow. These sediments are derived from other sediments of multiple origins and diverse texture, and resedimented with little sorting in multiple overlapping and coalesced deposits. The samples upon which the sediment distribution is based in these areas are too few to define those individual events.

One aspect of the texture not considered in the mapped distribution is the coarsening of the surface due to wind and water deflation. There are large amounts of unsupported and partially-supported gravel-size particles scattered randomly across the surface. Deposits that are exposed for a short period of time display this coarsening. This accumulation is often preserved in vertical sequences of older deposits in the proglacial region as a "stone line" and indicates a former horizon exposed for at least a brief period of time to surface processes.

Variation in time

Changes in topography and sediment thickness were monitored by iterative mapping of a part of the terminus in 1974 and 1975. The area remapped is that located to the north of X-X' on Figure 59. Although samples of the sediment at the surface were taken, they could not be analyzed due to an insufficient amount of time. Field observations indicate a complex nondescript sediment distribution, similar to that shown in Figure 60, was present during each mapping.

The mapped variations in topography are shown in Figure 61. Most changes in the topography and sediment thickness that occur between 12 August and 3 September actually took place prior to 5 July, when the 1975 field season began. A single cycle of reworking took place in the northern half of the map area after 5 July. During the period of field work, the major change in the terminus was an increase in area of the zone of reworking. This increase resulted primarily from a decrease in the elevation and lateral recession of parts of the debris-free, active ice margin, and also from upslope backwasting (opposite direction from ice recession) of the ridge lying closest to this ice margin. The net loss in surface elevation varies from no detectable change to over 8 m where ice-cored ridges were reworked. Most change appears to be limited to less than 3 m. The outermost ridges varied little. Unfortunately, the scale of mapping and the time between those mappings are too large to show the numerous rapid alterations that are characteristic of this environment and that occur over periods of days. This rapid change is indicated by the backwasting rates discussed previously and the facies mapping to be discussed below.

The isopach maps of sediment thickness for 1974 and 1975 are shown in Figure 62. As indicated for the topographic maps, the rapid variations and multiple cyclicity of reworking are not illustrated by the maps of sediment thickness. The sediment thickness change in any given area indicates only the net sediment loss or accumulation over the time interval between mappings. Thus, the sediment in any given area may be newly released and deposited from the basal zone ice, may have undergone multiple resedimenting or may be unchanged.

The sediment thickness in a given area changed markedly in 1.5 months in 1974 and from the end of the 1974 field season to just prior to observations in July of 1975. The overall trend is an increase in the area of sediment-covered basal zone ice, with the thinnest sediment cover on and adjacent to sloping surfaces of active and stagnant basal zone ice. The thickness in areas actively being reworked is generally maintained at 1.5 m or less.

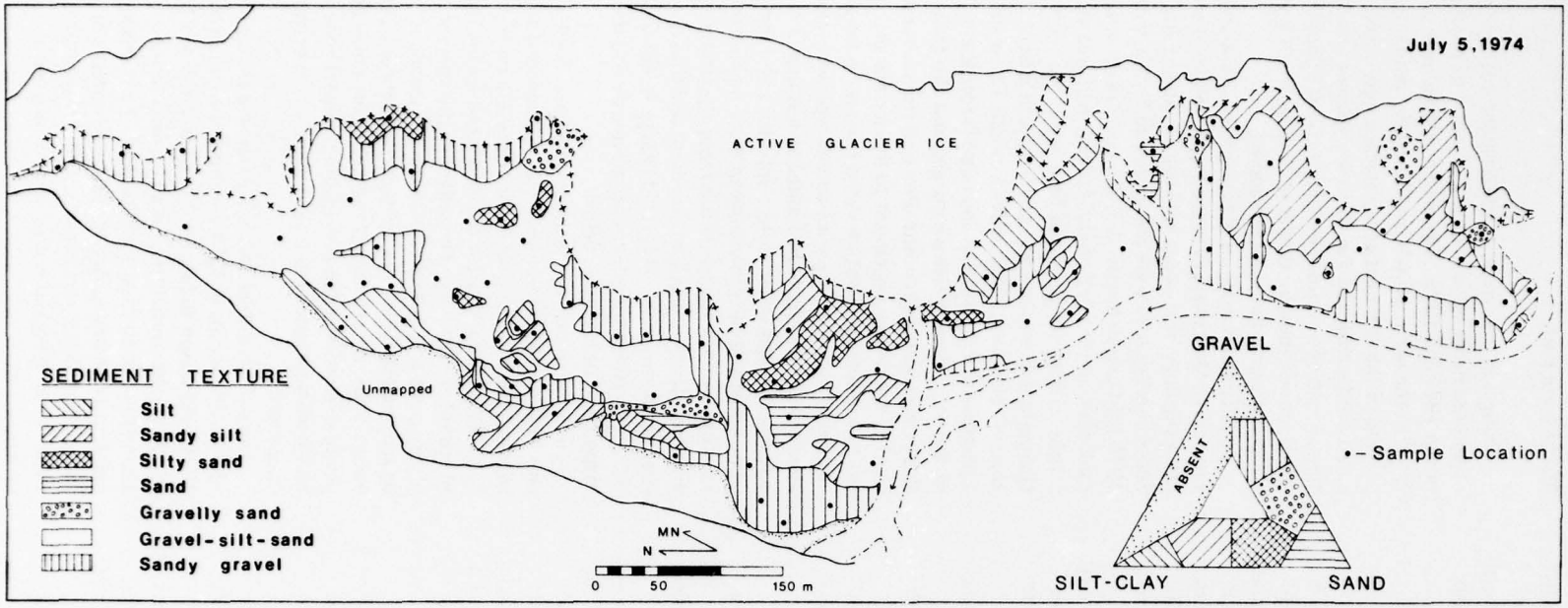


Figure 60. Texture of the surface sediments in the study area of the terminus on 5 July 1974. An absence of pattern characterizes the distribution.

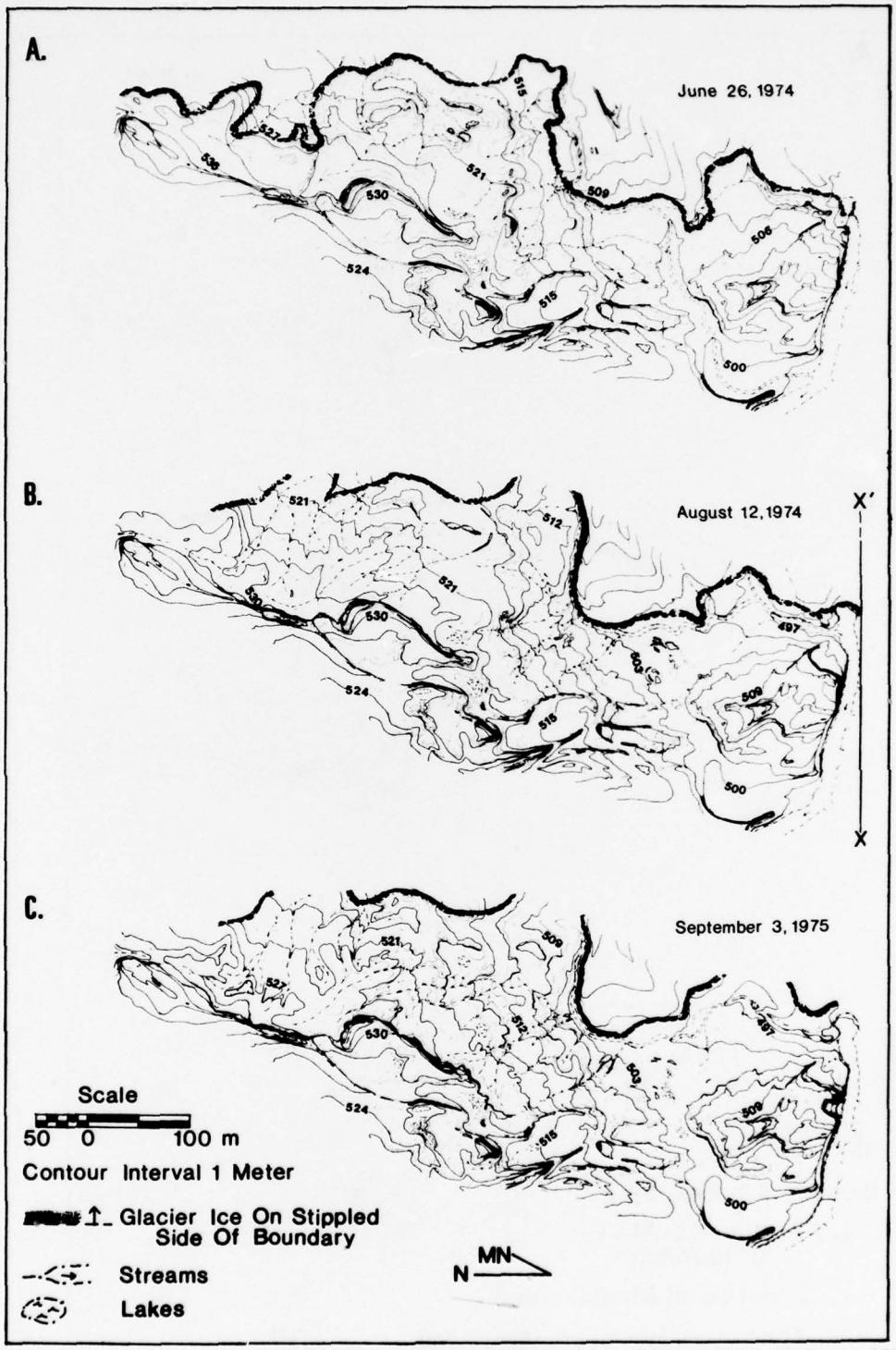


Figure 61. A, B and C show the topography of the north area of Figure 57 on 26 June 1974, 12 August 1974 and 3 September 1975, respectively. During this time period, most sediments of the mapped region underwent reworking at least 2 to 3 times, while the area of resedimentation expanded and the surface elevation decreased. Rates of change are more rapid than time between mappings.

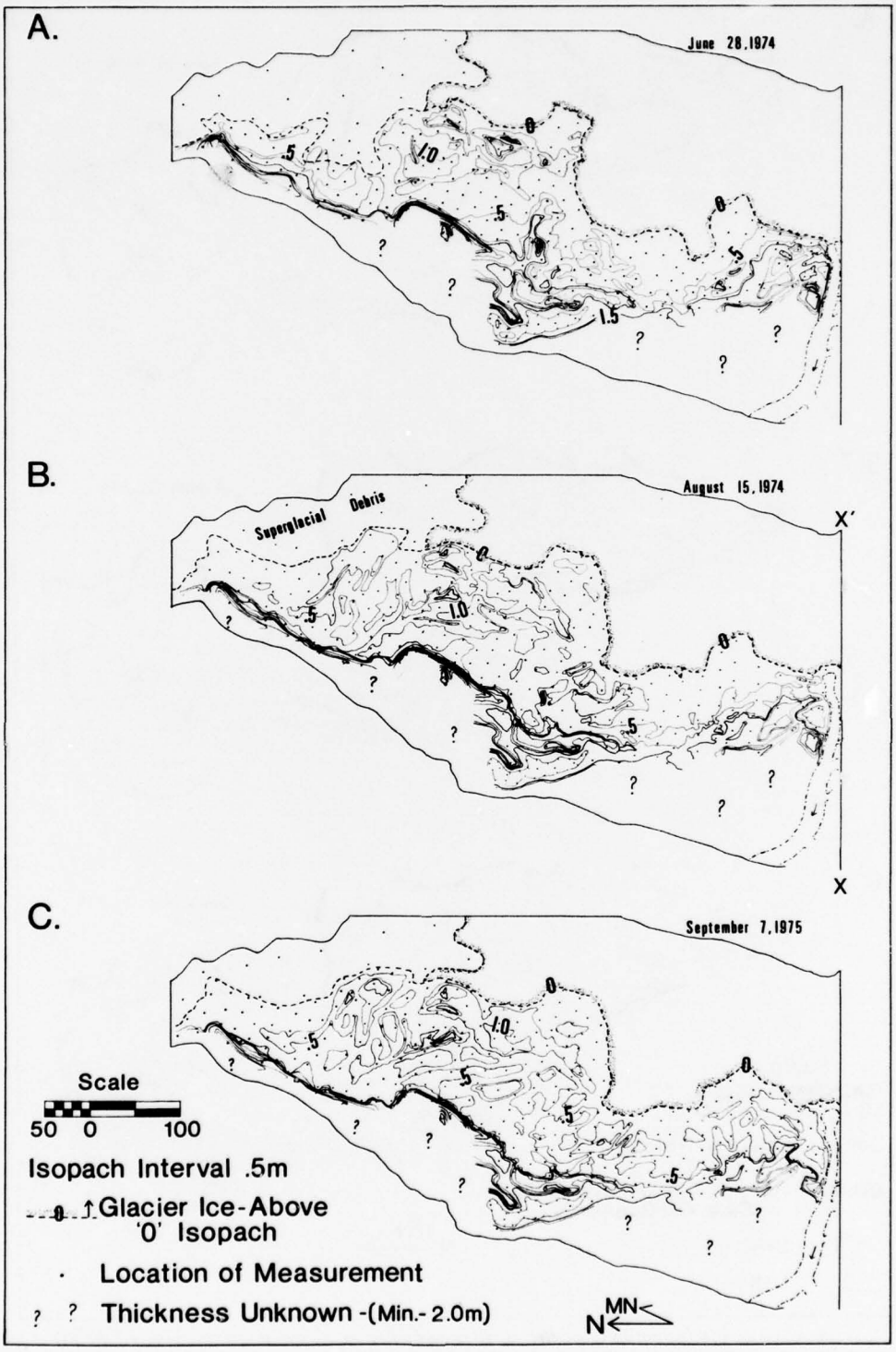


Figure 62. A, B and C are isopach maps of sediment thickness of north area of Figure 57 on 28 June 1974, 15 August 1974 and 7 September 1974, respectively. Maps show thicknesses at points in time; change in thickness is more rapid than time between mappings.

The measurements of thickness indicate a general downslope shift in sediment with expansion of the zone of resedimentation. The pattern associated with that shift is inconsistent, but often shows a downslope elongation that results from the contemporaneous and post-depositional development of sediment flow and meltwater channels. Areas with a low slope adjacent to the present active ice margin are of irregular shape and reflect active deposition.

During the same period of observation, the south area of the terminus underwent only minor change, whereas the central area underwent reworking by backwasting of marginal ice-cored slopes over about half its surface. The changes in the south area were restricted to the ice-marginal zone, which increased in width by 5 to 10 m due to ablation and recession of the active ice margin. Ice buried outside of this zone was not exposed. Sediment and meltwater flows were channeled along the ice margin to stream and surface outlets over the marginal sediments. The remainder of the sediment was unaffected by these surface processes.

SEDIMENT DISPERSAL

Sediment dispersal in the active parts of the surface cover is controlled by the local relief in the surfaces of the ice and sediment. Field observations of the active processes (most often meltwater and sediment flow) and of the directional properties inherited in the recently deposited surface sediments (discussed below) indicate that dispersal in the zone of resedimentation ranges between ± 90° of the regional direction of slope when it is well developed (as in the north area). Across the area of study, however, dispersal occurs through a range of 360°.

The variance in the direction of sediment dispersal by sediment flows is indicated by Figure 63. The direction of flow of active sediment flows observed over a warm and sunny two-day period in 1974, and the direction of flow indicated by some recent sediment flow deposits are shown in this figure. In the north area, flow is principally towards the active ice margin, parallel to the direction of surface slope. No preferred orientation is present in the central area but flow is confined to the areas of thinnest sediment cover at the margins. The pattern of the south area reflects the insulation of the ice by the thick surface cover and the ice-marginal "trough" formed by the recent recession of the ice margin. There is no direct relationship in the direction of sediment flow to the direction of glacial flow.

The patterns of sheet and rill flow of meltwater are similar to those of the sediment flows and are also related to the local topography. Figure 64 shows the direction of flow of meltwater rill and stream flow in active and abandoned channels. The ridges and upglacier slope in the north area control stream flow development and migration, whereas the downglacier slope of the south area is the primary control over meltwater dispersal.

Directional properties, except in fluvial sediments, are few in the deposits of the resedimented zone. For sediment flows, surface forms include the arcuate ridges, the lobate shape of the deposit, flow lineations (trend only), and braided and distributary rill patterns (see Figures 34, 36 and 39); internal indicators are limited to the weak to poorly developed fabric (with the strongest relationship in the more fluid flows), subflow and

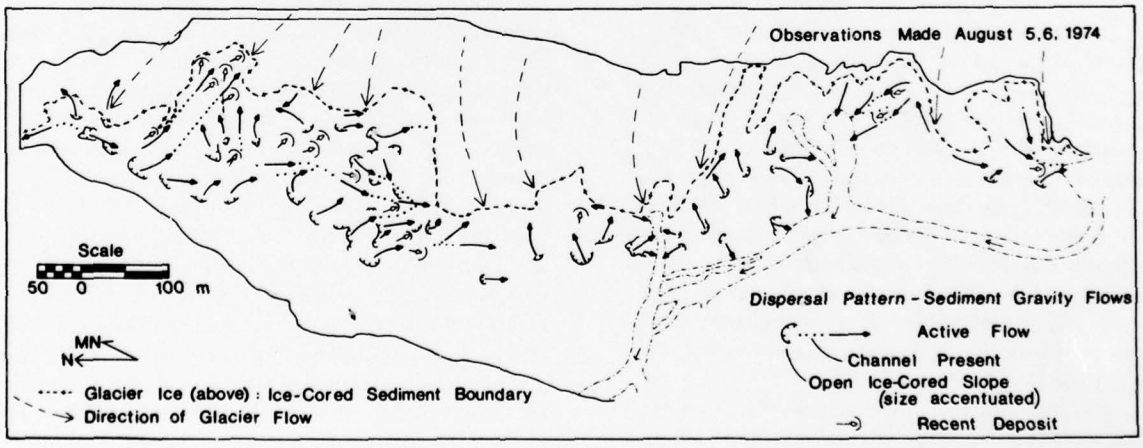


Figure 63. Sediment dispersal pattern observed for active sediment flows and some recent deposits of sediment flows on 5 and 6 August 1974. No preferred orientation of flow or relationship to the direction of glacier flow occurs. Direction of flow is slope controlled.

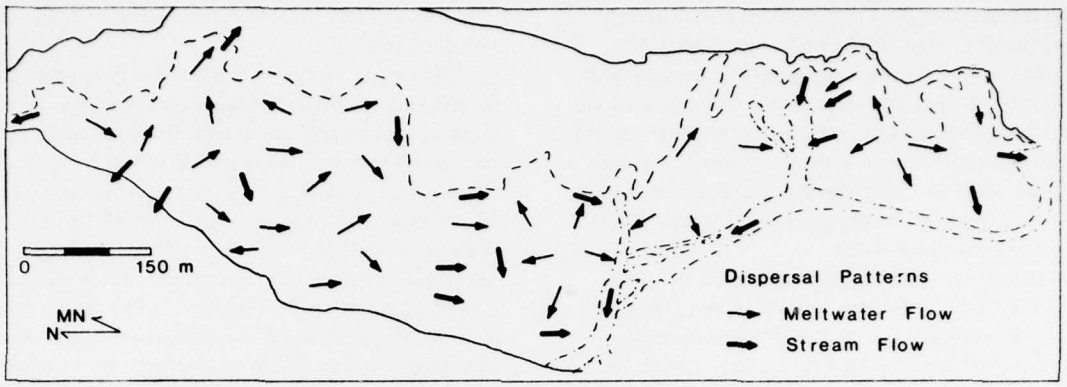


Figure 64. Sediment dispersal pattern observed for meltwater flows and streams from active and abandoned rills and channels in early August 1974. Direction of flow is related to topography but not to glacier flow.

marginal deformation structures, and the location of the head of the sediment flow. Meltwater flow indicators are limited to braided and distributary rill patterns and microdelta cross stratification developed in fan deposits. Fluvial properties in small streams were not examined in detail, but include such features as ripple cross lamination and fabric, and small scale ripples and transverse bars. For mapping purposes, a unimodal orientation of flow parallel to abandoned channels is assumed. A detailed examination of fluvial properties in glacial streams is presented in several of the articles in Jopling and McDonald (1975). The limited observations of the directional properties at the surface of sediment and meltwater flows and the orientation of small streams indicate a polymodal distribution that is determined by the local direction of slope, as clearly shown by Figures 63 and 64.

Fabric is the only directional indicator characteristic of tills. Melt-out till shows a strong unimodal orientation of pebbles parallel to the local direction of ice flow. It is inherited from the basal zone ice and is the only directional property of the terminus sediments that could be related directly to ice flow. The dip of *a-b* planes of disk- and blade-shaped pebbles and the plunge of the *a*-axis of prolates is not, however, necessarily related to ice flow. In tills formed by melt-out at the upper surface of buried ice, the dip or plunge reflects primarily the effect of melt-out on the original orientation in the ice, whereas in basally-formed melt-out tills it is determined mainly by the orientation of the melting surface and, near the base of the deposit, the relief of the glacier bed.

Figure 65 shows the local direction of ice flow determined from aerial photographs taken in 1949, 1969, and 1974, and for comparative purposes, the rose diagrams with mean axes indicated of the pebble orientations in melt-out till. The mean axes and the primary mode of the rose diagrams represent the local direction of glacial flow. Figure 66 shows the pebble orientations on rose diagrams measured in sediment flows in the terminus area (data in Table VII). Orientations for sediment flows are totally variable. The best orientations with respect to the direction of flow at deposition are in the deposits of sediment flows with the largest water contents (for example, MF-10). Individual readings may by chance parallel the direction of ice flow but they are not related to it. The unimodal patterns and consistent orientations of the melt-out tills serve to differentiate them from the inconsistent orientations and diverse patterns of the sediment flows.

SEDIMENTARY FACIES

Genetic facies and facies associations are defined for the sediments of the terminus (Table XI) on the basis of the previous analysis of the depositional processes. Facies identification requires the recognition of an assemblage of characteristics, because of the similarity in characteristics of deposits of different origin, and the variability in properties of deposits of the same origin (for example, texture). The full assemblage of characteristics used to map the surface distribution and interpret vertical sequences of the terminus is given in Tables V, VII and IX. Lodgement till characteristics are taken from the indicated references. Glaciofluvial deposits occur across the terminus but are a small part of the total depositional sequence. Their characteristics are described in Church (1972), Rust (1972), and Jopling and McDonald (1975).

The first problem which must be solved in delineating the facies and thus the origin of deposits is to determine whether the sediments are of the resedimented or till facies association. If it can be shown that the resedimented facies association is absent or limited in occurrence, many of the problems associated with distinguishing

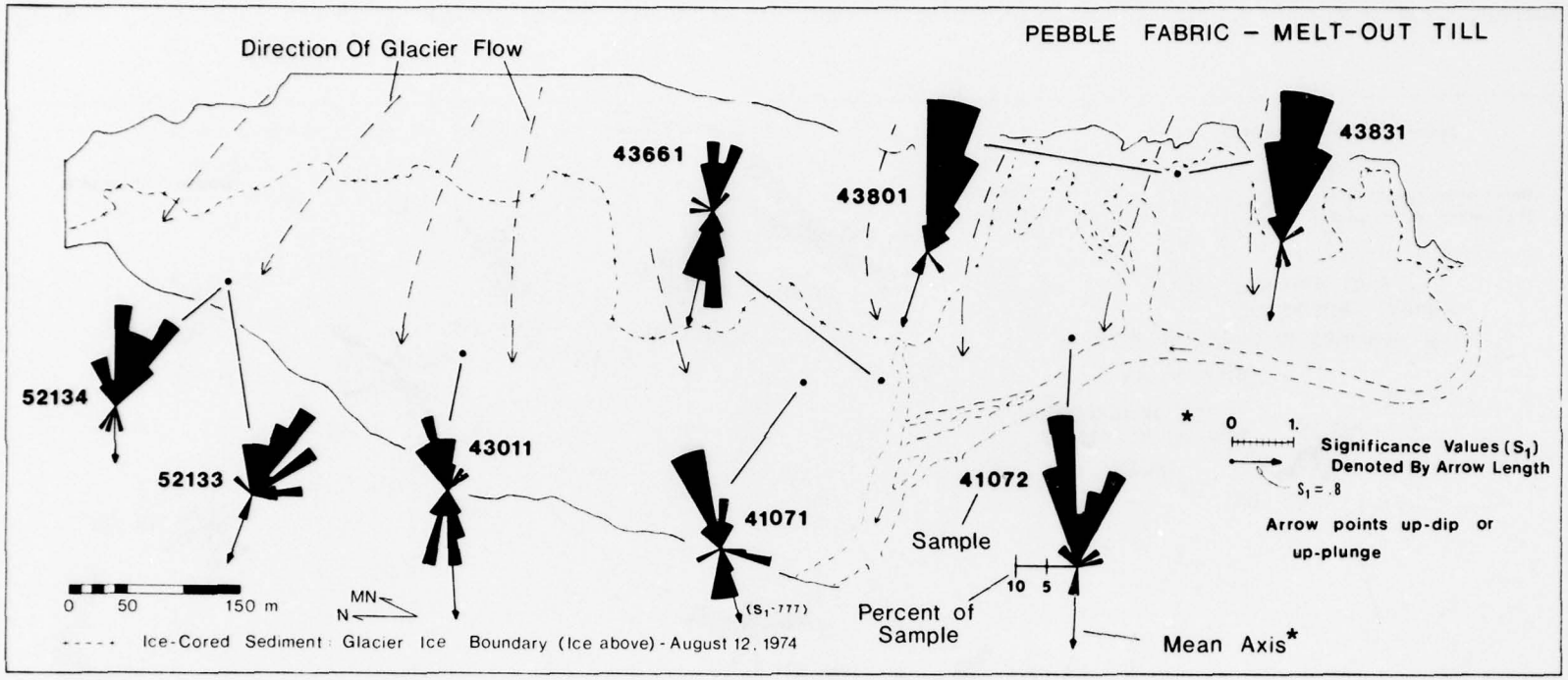


Figure 65. Pebble orientations in melt-out tills. Local direction of glacier flow, fabric mean axis and its significance value are shown. Pebble fabric in melt-out tills is consistent and reflects the local direction of glacier flow.

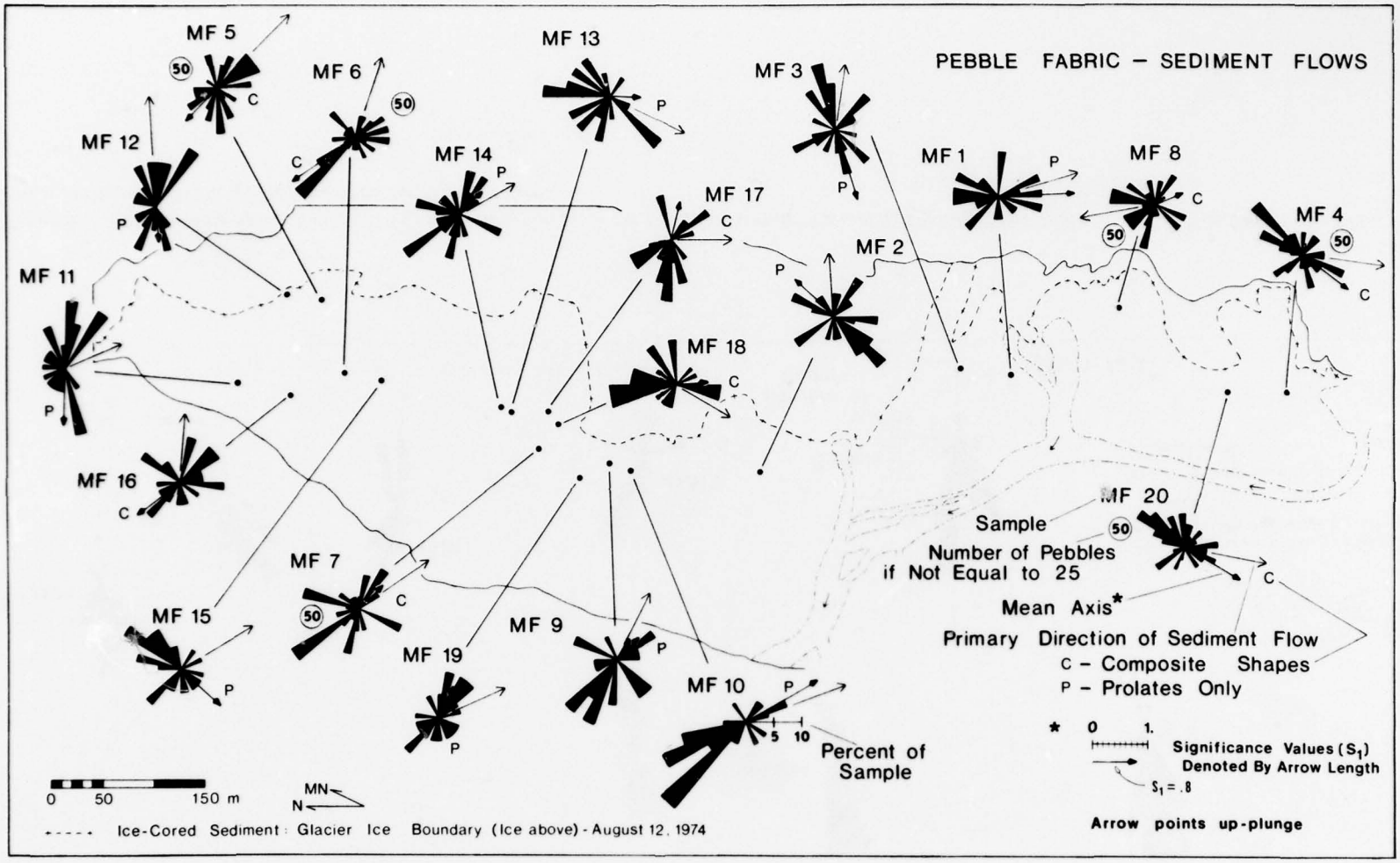


Figure 66. Pebble fabric in sediment flow deposits. Mean axis and its significance value, and direction of sediment flow prior to deposition are given. Strongest orientations are found in sediment flows of higher water content. Polymodal distribution of fabric and lack of relationship to glacier flow are clearly shown.

Table XI. Genetic facies classification of sediments.

Composite vertical sequence	*Facies association*		*Genetic sedimentary facies*	*Subfacies*
Subaerial	Resedimented	Unsorted	Sediment flow	Type I Type II Type III Type IV
			Slope failure	Slump Spall–Collapse
			Ice ablation	Colluvium (high-angle slope) Lag (low-angle slope)
		Sorted	Meltwater flow	Sheet Rill
			Fluvial	
			Lacustrine	Intermittent ponding Semipermanent lakes
Subsurface	Till	Unsorted	Melt-out till Lodgement till	Upper Lower
	Subglacial-resedimented	Unsorted	Sediment flow Ice ablation	
		Sorted	Fluvial Lacustrine	

particular facies are eliminated. The resedimented facies association is often characterized by: 1) rapid lateral and vertical variations in texture; 2) individual sedimentary units of varied geometry, orientation and dimensions, with adjacent deformed units often present; 3) individual fabric orientations that are weakly defined, bi- to multimodal, and vary over short distances in a vertical direction, forming as a set a laterally nondefinitive directional pattern; 4) laterally discontinuous (tens of meters) stratification over significant thicknesses; and 5) internal surface contacts of irregular shape that may be defined by a caliche coating, sharp change in density due to dessication, randomly dispersed subparallel alignment of single-layer-thick gravel particles, cut and fill structures or other unconformities, and lag concentrates. The general description of the resedimented facies association would be a heterolithic, discontinuous deposit of variable dimensions and internal complexity.

The identification of individual facies and subfacies must be based upon an assemblage of properties. Distinguishing between deposits formed by sediment flow, slope failure, and ice ablation, and those formed by direct release from glacial ice is most difficult and often requires the recognition of subtle differences. For example, the meltwater flow facies is distinguished by its texture (relatively well-sorted, silt to sandy silt grain size), well defined upper and lower layer contacts, and often parallel stratification. Similarly, the fluvial facies is identified by its sorted, sand- through gravel-size texture, internal structures including fabric, and geometry of its deposits.

The properties critical to defining the melt-out till facies are: 1) strongly developed pebble fabric (in a unimodal pattern with minor scatter and low angle of dip) with a relatively consistent regional mean axis, 2) tabular geometry with dimensions that vary from meters in thickness to kilometers in breadth, 3) lack of distinct, continuous internal contacts, and 4) generally massive appearance, within which discontinuous layers, lenses, and pods of texturally distinct material may occasionally occur. The preservation of sets of strata from the basal zone ice may confuse interpretation but these strata generally appear in the sediment as a diffuse lamination with poorly defined boundaries. Individual layers may show sedimentary structures that are terminated sharply and lie unconformably over lower sediments. In addition, the properties of the other sediments of the stratigraphic sequence should distinguish such layered zones from layers of other origin.

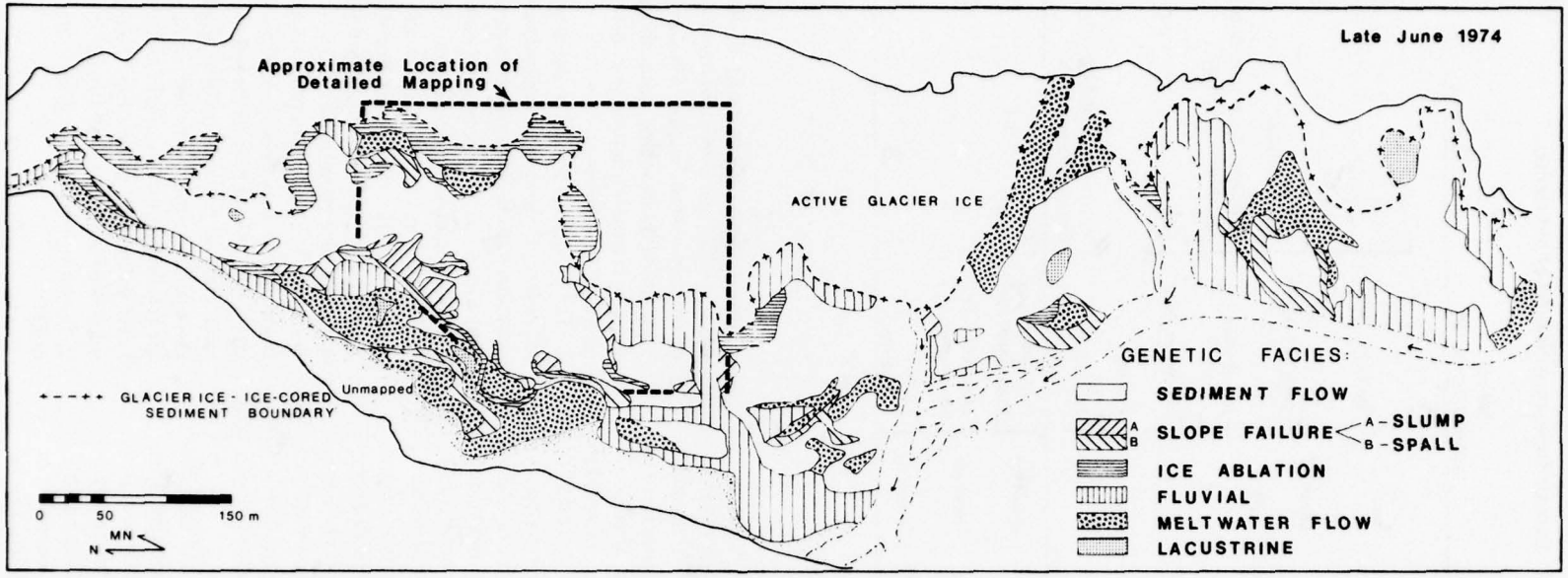


Figure 67. Map of surface distribution of genetic facies in late June 1974. A lack of pattern and dominance of the sediment flow facies are shown. Dashed line encloses approximate location of Figures 68 and 69.

The variability in the sediment flow facies is its principal distinction from the till facies. Individual sediment flows are in general characterized by: 1) weakly developed pebble fabric (multimodal, dispersed particle orientations) with vertical clasts and inconsistent areal and vertical mean axes patterns; 2) facies dimensions limited generally to a thickness of 2 m or less but several hundred meters in maximum extent, 3) upper and lower contacts generally distinct, but nonerosional, perhaps defining several contemporaneous flow events, 4) variable surface features, often associated with a meltwater facies cap, 5) a massive to graded appearance, possibly with intraformational blocks present, and a tractional gravel base, and 6) variable geometry and deposit orientation. The association with meltwater deposits is common. The basic properties required to distinguish individual flow types, in order of importance, are internal organization, upper and lower surface features, bulk texture, geometry, and pebble fabric.

The slope failure facies is mainly differentiated from the other facies on the basis of its irregular geometry and dimensions, chaotic internal organization including intraformational blocks and slip surfaces, and lack of pebble fabric. The ice ablation facies are distinguished by: 1) the weak banded surface pattern parallel to the deposit trend in the fabric, 2) rectangular to wedge-shaped cross section, 3) a lack of internal structure, 4) coarse texture, and 5) irregular surface of the deposits.

Surface distribution

The surface materials are dominated by the sediment flow facies. On a map of the full area of study, they account for over 50% of the surface (Fig. 67). Slump, meltwater flow, fluvial, and ice-slope facies account for most of the remainder of the surface. The distribution does not form a pattern nor can it be simply related to any property. The concentration of the meltwater facies in the outer ridge zone on surfaces which slope predominantly downglacier is due to secondary deposition by the latest advance of a part of the ice margin. Aerial photographs taken in 1969 indicate formation of these deposits at that time. The meltwater facies overlie older deposits mostly consisting of the sediment flow facies.

The facies distribution was mapped in more detail over a part of the terminus (Fig. 67) in order to establish, if possible, the distribution and relationships of each facies at the surface (Fig. 68). The detail of mapping is more closely equivalent to the distribution observed in vertical sequences and represents the process distribution at a point in time. A complex distribution of facies dominated by the sediment flow facies emerges. The subfacies mapping indicates that the idealized type II sediment flow is more prevalent than others. Meltwater flow deposits are more widespread than shown, because where they occur as a contemporaneous deposit with a sediment flow, they are not mapped separately. The basic character of the facies distribution shows rapid areal transitions without definitive relationships (except for meltwater-sediment flow facies as noted). However, the expected relationships between topography and facies emerge. Slope spall and collapse is restricted to the base of steep slopes, while the fluvial and lacustrine facies lie within the topographically lowest regions. Slump, sediment flow, and meltwater flow facies are confined mainly to the areas that slope upglacier. The ice ablation facies marks former and currently active ice margin locations and generally parallels the orientation of ridges.

The extreme rapidity of change in the active zone of resedimentation as the result of reworking associated with backwasting ice-cored slopes is indicated by comparison of Figure 68 with Figure 69, a map of the same area approximately one month later. This area of the terminus changes rapidly; other parts are similar or less active. Most of the surface is now being actively reworked, is covered by newly deposited sediments or has been covered by one or more depositional events. The maps also indicate what has previously been shown: sediment dispersal that is slope-controlled on a local and regional scale.

The difference in the type of facies found in a given area of the map indicates potential vertical sequence variations that develop from the depositional processes of the resedimentation zone. Some of the relationships shown by comparison of the two maps include the associations of the following facies: sediment flow over fluvial, meltwater flow, other sediment flow and ice ablation facies; meltwater flow over sediment flow and fluvial facies; and lacustrine over meltwater flow, sediment flow and slump facies. These relationships are discussed in the next section.

Vertical distribution

The facies associations in the order listed in Table XI compose the composite vertical sequence for the terminus. The development of the vertical sequence results from several processes which, in contrast to most sedimentary environments, involve contemporaneous surface and subsurface deposition. Subglacial sedimentation (lodgement, glaciofluvial, glaciolacustrine) may also occur prior to or during terminus sedimentation. Resedimentation associated with subglacial caverns may produce subglacial ice slope colluvium and sediment flow deposits. Thus, the full vertical sequence of a single ice advance and retreat cycle, which the composite sequence represents, may develop with essentially no time difference between the formation of the upper



Figure 68. Surface distribution of genetic facies over a part of north area of study region on 2 July 1974. Location shown on Figure 67. Symbols A through D indicate flow types I through IV which were identified where possible. A complex distribution without definitive relationships between facies is shown. Sediment flow facies, mainly type II, dominate the surface materials.

and lower units. Melt-out till itself is progressively younger from the central part of the deposit to the upper and lower surfaces. At the same time, variations in the sediment source (texture, fabric, composition, and other properties) may be preserved in the individual units and further confuse interpretation of their historical development.

The distribution of a genetic facies in the composite sequence may vary considerably because of the nature of the depositional processes and the conditions of the terminus. Individual facies may be absent or occur several times in a vertical sequence that may in turn differ laterally across the terminus. Since an entire vertical sequence of the glacier could not be observed either in the process of formation or as a deposit in the proglacial region, the characteristics observed in actively forming facies of the resedimented and till facies associations were assumed representative of the characteristics of a full depositional sequence.

The variability in the surface distribution of the genetic facies (Fig. 68, 69) is retained in the depositional sequence of the resedimented facies association; no repetitious or typical vertical sequence was observed in deposits of either the active or proglacial regions. However, certain relationships, principally between the predominating sediment flow facies and other facies, were observed to recur in deposits of both the terminus and proglacial regions. They appear to mainly reflect the topographic slope, sediment cover thickness, meltwater availability, and location of the source of the depositional process. The most common associations of the genetic facies in ice-cored regions include: 1) most

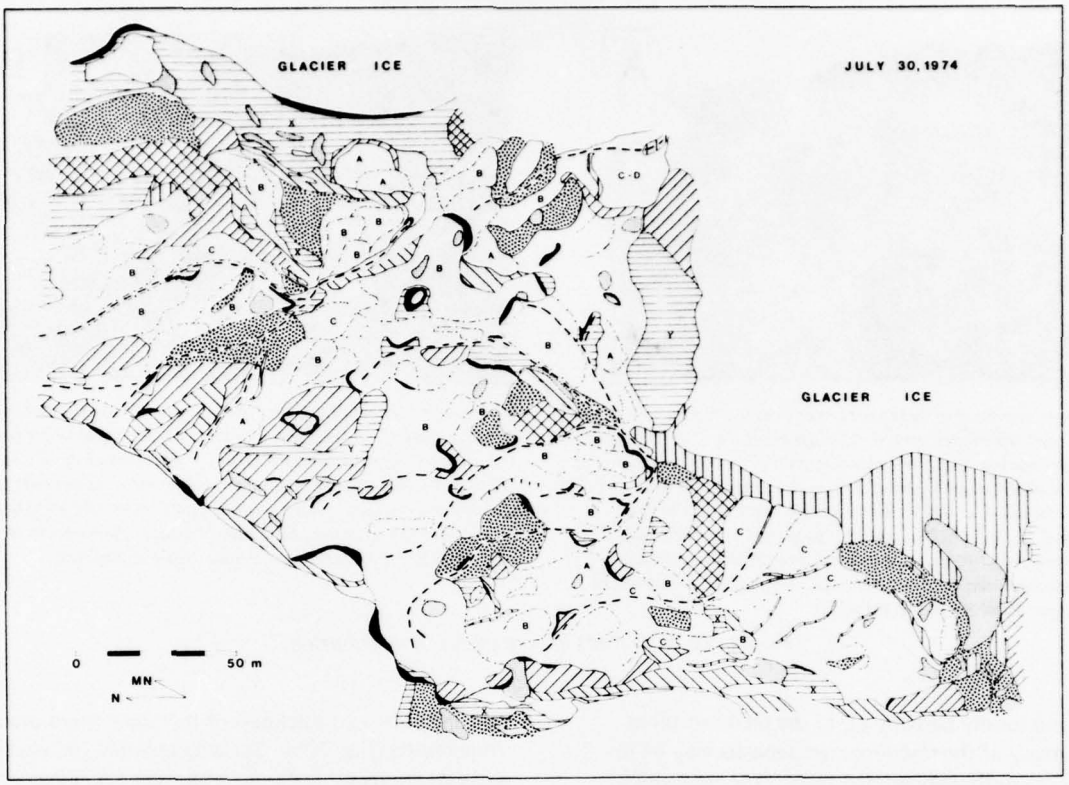
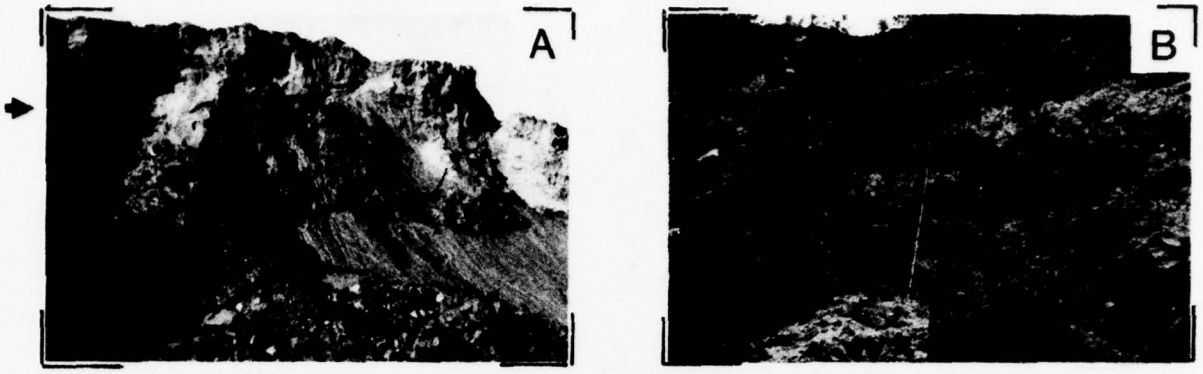


Figure 69. Surface distribution of genetic facies in area of Figure 68 approximately one month later. Comparison to Figure 68 shows rapidity of reworking of surface cover and interrelationships of facies which may occur in a vertical sequence developed from sedimentation here.

commonly sediment flow facies (types I, II) stacking at the base of the topographic slope, often with the meltwater flow facies separating them, 2) sediment flow facies (types II, III), lying on fluvial and ice ablation facies at the active ice margin, 3) meltwater sheet flow facies, interbedded with fluvial, sediment flow and slump facies, and 4) lacustrine facies on any other facies. Associations in regions sloping away from an active ice front also include: 1) meltwater sheet flow facies stacked adjacent to the active ice margin, 2) ice ablation facies lying on meltwater sheet flow facies, and 3) fluvial facies or fluvially-coarsened surface materials forming a sediment cap. Sediment flows (I-II) were observed to incorporate or deform thin and small surface deposits, usually of ponding, stream or meltwater origin. These relationships between genetic facies occur as sequential units with an apparently random distribution in the vertical sequence of the resedimented facies association.

The genetic facies of the till facies association, under normal conditions, also occur in the sequence listed in Table XI. The melt-out till facies must occur beneath a sediment cover in undisturbed sequences. It generally forms beneath a stable sediment cover of resedimented materials but may be transitional to a coarse lag released by ablation on a low-angled ice slope. The result of melt-out of an entire basal ice sequence is unknown, but it is assumed that its effects will be localized. The maximum melt-out till thickness is determined by the sediment content of the ice source; active reworking, for example, due to backwasting of ice-cored slopes, will reduce that thickness. The formation of lodgement till is probably restricted to the active glacier sole external to the terminus region. Hence, unless it is incorporated into the glacier or removed by subglacial streams, it occurs as the basal member of the till facies association. Conditions suitable for lodgement may not exist beneath parts of the glacier; thus, a discontinuous lateral distribution may develop (Boulton 1975).

The vertical distribution of facies developed in the terminus region is generally more complicated than the composite sequence. As mentioned above, members of the sequence may be removed or thinned by erosional processes. The continued reworking by resedimentation processes in the north area of the terminus, including regions with a thick sediment cover, suggests that



a. Multiple sequence of sediment cover over ice formed by ice advance over sediment-covered stagnant basal ice. Upper basal ice unit is exposed in upper center portion of photo. Thickness of sediment cover is about 3.5 m; the overridden sediments are about 4 m thick. Mean pebble orientation in the upper basal ice layer differs by 35° from that in lower basal ice. Sediments both above and below the upper ice unit are of the resedimented facies association. Scale lying on sediment below upper basal ice is 2 m long.

b. Deposit resulting from multiple periods of resedimentation. Arcuate contact above light gray material separates older resedimented facies from more recent resedimented materials deposited adjacent to a readvanced ice margin. Sediments on which scale rests are coated with calcium carbonate deposited by evaporation of fluids during dessication. Upper materials are loose; lower materials are dense. Scale is 2 m long.

Figure 70. Variations in vertical facies distribution.

much, and locally perhaps all, of the melt-out till as well as many of the resedimented deposits may be reworked or continually eroded away. The total thickness of melt-out till formed where conditions maintain open ice-cored slopes is thus reduced and bears no correlation to the thickness and debris content of the basal ice source. The extent to which this reduction will occur in the north area is unknown. In regions such as the south area where an apparently stable cover is established, a thicker melt-out till should develop. The lateral continuity of the entire vertical sequence may, however, be broken by thermal and mechanical stream erosion. Thus, even a single ice advance and retreat cycle may produce a vertical sequence that varies spatially in the type and dimensions of facies preserved.

The repetition of ice advance and retreat has led to increased thickness of the vertical sequence and stacking of the members of the composite profile. Figure 70a shows a multiple sequence of sediments over ice that was formed by ice advance over resedimented materials. Preservation of this sequence by burial and melt-out will develop a repetitious multitill sequence. This sequence would result from a readvance of the ice margin, but not as the result of a second glaciation. Many such advances over relatively large areas would develop thick sequences of stacked till and resedimented facies that may be misinterpreted in terms of historical development.

Resedimentation may be initiated adjacent to a readvanced ice margin. Multiple periods of sedimentation and increased thickness of the upper resedimented zone results (Fig. 70b). Surfaces exposed for a period of years are recognizable beneath such secondary deposition.

PATTERNS OF TERMINUS SEDIMENTATION

The surface and subsurface conditions of the terminus are shown schematically in Figures 71 and 72 for areas of regional upglacier and downglacier slope. The upglacier slope from an outer, currently stable ridge zone is characteristic of most of the western margin of the glacier. Local variations in slope, as in areas bisected by outwash streams, affect the direction of sediment dispersal, but the mode of sedimentation remains basically the same. The characteristics of areas of mostly horizontal slopes are primarily controlled by local variations in slope and sediment thickness. The depositional processes and facies relationships are similar to those elsewhere in the terminus, but they are totally divergent in terms of process location and sediment dispersal. The conditions observed for areas of near-horizontal slope appear to be analogous to those described by Boulton (1972a) for hummocky moraine development.

The principal differences in the surface and near-surface conditions in sloping areas are mainly the large zone of resedimentation on the upglacier slope and the predominance of areas of deposition and limited resedimentation on the downglacier slope. Also, the directions of primary sediment dispersal are opposite.

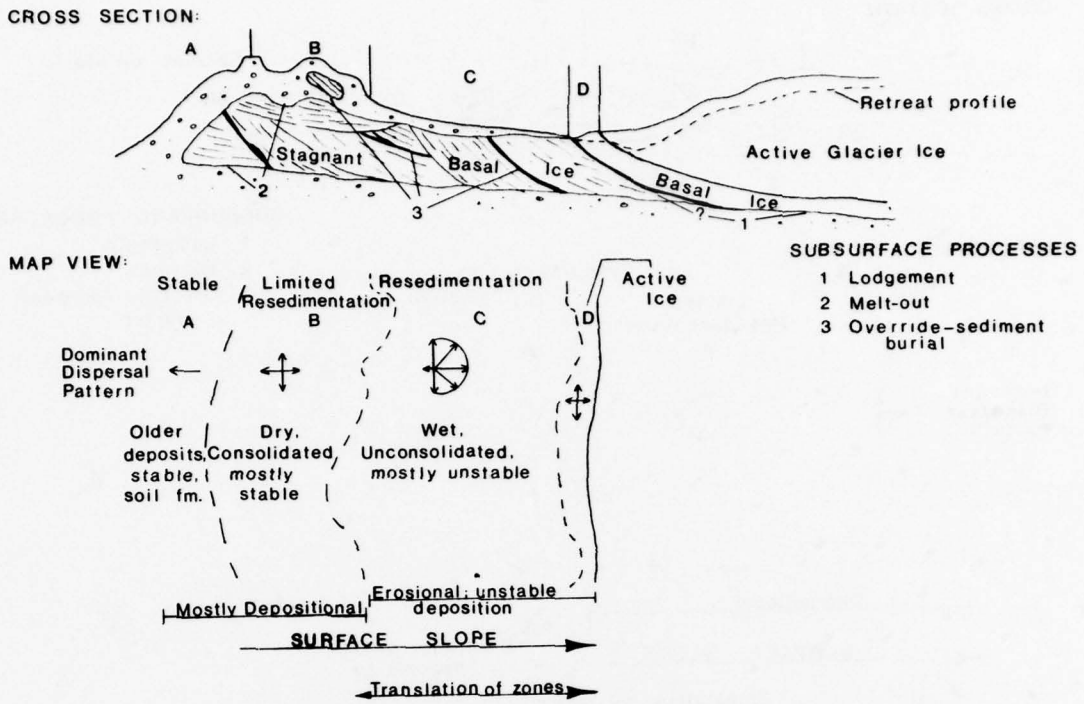


Figure 71. Idealized cross section and map view of process distribution at glacier margin with regional upglacier slope. The processes occurring within each zone are: A) Stable older deposits may overlie ice, which melts out over a long period of time; surface materials may be reworked by eolian and fluvial processes. B) Limited resedimentation may include failure of slopes, but is dominated by internal melting; wind and slopewash locally rework surface materials. C) Resedimentation including active slope spall and slump, sediment flow, meltwater flow, ice ablation associated with backwasting ice-cored slopes and fluvial and lacustrine processes. (Buried ice melt may occur, but the products are rapidly reworked by surface processes.) D) Control of debris and meltwater release by ablation.

Characteristics of processes and their deposits in the zones shown in Figures 71 and 72 are similar in each case. The changes observed in the two years of study suggest that the location and migration of the boundaries of these zones are determined by the location of the active glacial margin, ice surface topography, sediment thickness, and past conditions of ice flow and sedimentation. The expansion of the zone of resedimentation by backwasting of ice-cored slopes into thickly covered, apparently stable areas suggests that these stable conditions are not in equilibrium with the currently active resedimentation processes of the terminus. On a local scale, the boundary location and internal diversity of a given zone are determined by local topography and sediment thickness.

The idealized development of the sedimentary sequence of the Matanuska Glacier terminus is illustrated for various conditions in Figure 73. The general distribution of the facies associations in a vertical sequence may be similar for both directions of regional slope. As mentioned previously, the genetic facies sequence of the resedimented facies association is totally variable for either condition. A higher proportion of fluvial and meltwater flow facies may be present in the depositional sequence developed on a downglacier slope, whereas sediment and meltwater flow facies dominate on an upglacier slope. The thick sediment cover and its wide distribution in the downsloping areas, in contrast to the reworking of the surface cover and basal ice due to backwasting in the upsloping areas, suggest that the melt-out facies should be thicker for downglacier slopes. Also the extensive reworking observed in the zone of resedimentation on upglacier slopes suggests that uninhibited reworking may result in loss of all sediment except that of the resedimented facies association. Stacking of the melt-out facies on the resedimented facies appears common across the terminus, especially on upglacier slopes, and results in the formation of discontinuous till sheets (restricted to the marginal zone under present conditions) which in outcrop would appear to be the result of multiple glaciations.

The observations of this study indicate that the immediate controls over the sediment system are 1) sediment and meltwater availability, which determine the

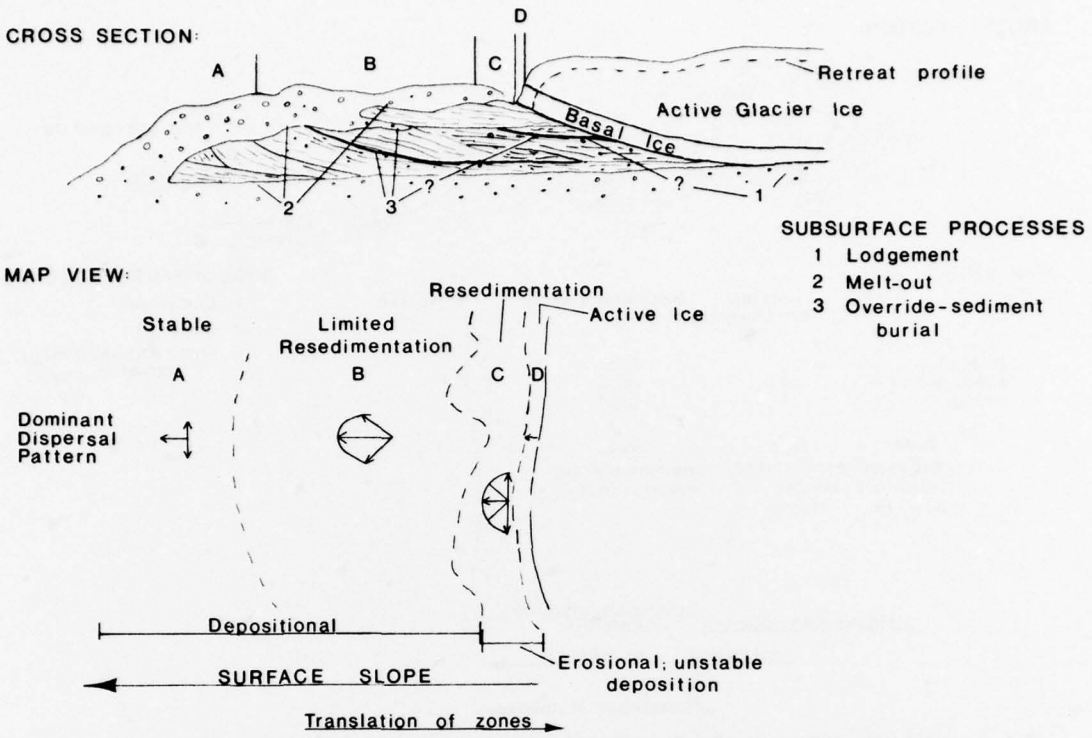


Figure 72. Idealized cross section and map view of process distribution at glacier margin with regional down-glacier slope. Process occurrences in zones given in Figure 71.

type and properties of the depositional processes as well as their frequency of occurrence, 2) surface slope, which controls sediment dispersal and influences process initiation and glacial flow, 3) location of the active ice margin and its flow condition, which define the area of sedimentation and local meltwater and sediment availability, and 4) extent and thickness of sediment cover and buried basal zone ice, which affect process initiation and type and also determine meltwater and sediment availability. The influence of these conditions on terminus sedimentation suggests that the overall controls on terminus system are: 1) glacier mass balance, which determines the location and condition of the ice margin, the extent of buried basal zone ice, the availability of sediment and water, and the development of the vertical sedimentary sequence, 2) glacier bed conditions, which influence surface topography and other physical conditions at the ice margin, 3) thermal conditions at the sole of the glacier, which determine the extent and quantity of sediment entrained by the glacier, and 4) climate of the terminus region, which primarily determines rates of melting of exposed and buried ice. The conditions at the Matanuska Glacier terminus include a complex mass balance (repetitive advance and retreat with stacking of stagnant basal ice), complex thermal conditions (mainly temperate, but with discontinuous areas of freezing at the sole enabling large amounts of sediment to be entrained), a variable topography, and a maritime-continental transition climate (Selkregg 1976), with an estimated annual precipitation of 35 cm, mean temperature of 0°C, mean annual solar radiation of 250 g-cal/cm^2, and a summer melt season of about 90 days.

The processes and characteristics of deposition and thus the sedimentary sequence may vary to an unknown extent for glaciers under different terminus conditions. For example, a generally colder, drier climate with an increased number of cloudy days should reduce the depth of summer melting, the length of time ice-cored slopes are open, and thus the rates of sediment and meltwater production. These conditions would be more conducive to low water content sediment flows, a more stable sediment cover, and probably formation of melt-out till. A warmer climate with many cloudless days may lead to increased rates and extent of surface reworking and loss of sediments other than those of the resedimented facies association.

A documented example of the effect of variation in terminus conditions is sedimentation by a true temperate glacier. Because temperate glaciers are at the melting point at their sole, they entrain little sediment [perhaps a 10- to 20-cm-thick basal zone (Boulton 1975)].

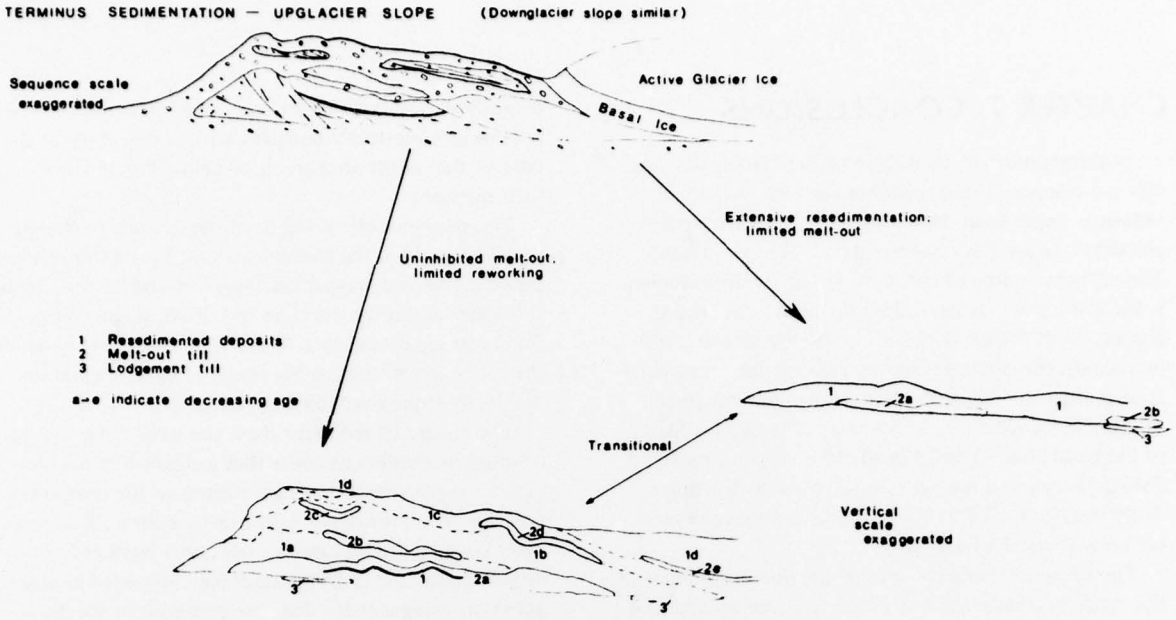


Figure 73. Idealized development of sedimentary sequence from Matanuska Glacier terminus sedimentation. Uninhibited melt-out results in a stacked sequence of resedimented and till facies units; more continuous deposits than shown may form. Extensive resedimentation may eliminate all deposits except those of the resedimented facies association. Facies associations which occur may be similar for regional upglacier or downglacier slopes; sediments derived from regional upglacier slope will probably show greatest diversity. Extent of reworking will determine this diversity. Conditions may exist which permit a vertical sequence to develop that contains multiple till or resedimented units, or lacks either of these, from a single period of glaciation.

Sediment availability at the margin is therefore low but meltwater is readily available. The melting conditions at the base of the glacier promote lodgement till formation (Boulton and Dent 1974). The vertical depositional sequence consists primarily of the lodgement and perhaps subglacial resedimented facies, whereas melt-out and resedimented facies are of minor importance. Future study is required to determine the importance and influence of the factors listed above on sedimentation by glaciers of different types.

CHAPTER 7. CONCLUSIONS

Sedimentation at the margin of the Matanuska Glacier is a complex interaction between ice, water and sediment under boundary conditions imposed by the physical characteristics of the terminus environment. The primary source of sediment in the terminus region is the lowermost facies of the thin basal zone of the glacier. With the exception of randomly scattered debris bands, the thick (estimated 300 m) upper englacial zone contains a negligible amount of sediment (mean of 0.002% by volume). The lower, stratified ice facies of the basal zone (3 to 15 m thick) contains a mean of 25% debris by volume per sample, whereas the upper, dispersed facies (0.2 to 8.0 m thick) in this same zone contains about 4% by volume.

The physical characteristics of the debris and ice and the mode of distribution of debris indicate a subglacial origin for most of the sediment entrained in the basal zone. The O^{18} values of ice of the basal and lower englacial zones indicate formation of the ice of the dispersed facies as well as the englacial zone by snow diagenesis in the accumulation area of the glacier. The stratified facies, however, contains abnormally large amounts of O^{18} indicating an origin different from snow diagenesis. The young radiocarbon ages of wood taken from the stratified facies require the production of its ice in the ablation area. The non-uniform angularity, coarse texture and uniform distribution of the debris, and the grain size of the ice indicate mostly subglacial entrainment of the dispersed facies debris. The rounded and subrounded pebbles, diverse texture and undisturbed sedimentary structures of the debris, and the thickness, debris stratification, debris content, paucity of air bubbles and small grain size of the ice of the stratified facies are evidence of a subglacial origin for the debris of this facies.

The debris and ice of the stratified facies originate primarily by the subglacial freeze-on of isotopically enriched meltwater, probably surface-derived, to the glacier sole, whereas the debris of the dispersed facies is mainly entrained by localized pressure-melting and freeze-on of individual particles followed by their vertical dispersion into the surface-derived glacial ice. The variable thickness, extent and discontinuity of individual strata, the non-uniform thickness of the entire stratified facies, the undisturbed sedimentary structures, and the age of wood in the stratified facies indicate that location, extent, and rate of ice formation and debris entrainment are variable. Parameters such as bed topography, ice flow rate, and ice thickness are probably responsible for these variations. The Matanuska Glacier is therefore thermally complex with zones of ice at the base of the glacier that are at or below the pressure-melting point.

The sediment entrained in the basal zone of the glacier is released in the terminus region by ablation of exposed active and stagnant ice surfaces and by melting of the upper and lower surfaces of buried, stagnant ice. The basal ice occurs as a 300-m-wide band that parallels the active ice margin, as the result of basal stagnation and its multiple overriding by active ice.

The release of sediment from the basal zone ice has resulted in a sediment cover that exceeds 8 m in some places. Under the present conditions of the terminus, however, the thickness of the mostly cohesionless sediment cover is inadequate to maintain a blanket-like covering over the stagnant basal ice. Slopes of exposed active and stagnant basal ice are common in the discontinuous sediment cover; hence, meltwater and saturated sediment are readily available. Rates of reworking are essentially controlled by the extent and location of these ice-cored slopes. Thus, the rate at which debris-laden basal zone ice undergoes ablation controls the extent and rate of reworking of the sediment cover and therefore the importance of specific depositional processes to sedimentation in the terminus region of the Matanuska Glacier. This situation would change if conditions were altered so that the sediment cover became stable. Under these conditions, instead of processes of resedimentation being most important, internal melting would be the primary mode of sediment formation. The primary conditions influencing the modes of sedimentation and stability of the sediment cover are apparently: 1) extent, thickness, and morphology of the sediment cover; 2) extent and debris content of the buried basal zone ice; 3) availability of meltwater; and 4) climate (solar radiation, precipitation, mean temperature) (Table XII).

Two general types of depositional processes are recognized; one type results in the formation of till, and the second in deposits that are resedimented. Till is defined as sediment deposited directly from glacial ice that has not undergone subsequent disaggregation and resedimentation. Thus, the deposits of sediment flows, previously called "flowtill," are not considered till. Although other processes may occur upglacier, till formation is limited to a single process in the terminus region: the in-situ melting of the upper and lower surfaces of buried basal zone ice to form a deposit referred to as melt-out till. Rates of till deposition at the upper surface, which ranged from 2.0 to 24.5 cm during the

Table XII. Summary of depositional processes, conditions of occurrence, and influencing factors.

Depositional process	*Environmental conditions of occurrence*	*Apparent factors influencing rates and other properties*
Melt-out	Stagnant basal zone ice with stable sediment cover greater than a few centimeters, but thickness less than depth of summer thaw.	Upper surface: Sediment cover texture, composition and thickness; local topography; climate (long and short term); thickness and extent of basal ice; debris content of basal ice. Lower surface: Geothermal gra[illegible]t; possibly groundwater.
Sediment flow	Low angle slopes; readily saturated, low strength sediments; readily available meltwater; impermeable ice bed; generally associated with backwasting ice-cored slopes.	Water available relative to sediment available; grain size of available sediment; slope angle of flow system; bed material.
Meltwater sheet and rill flow	Generally, exposed ablating basal zone ice (stagnant or active) source; also buried ice melt with seep at surface; sheet flow best developed on low-angle slopes on ice and sediment; rills on sediment of slope greater than 10°.	Factors affecting uncovered basal ice ablation, as below, and factors affecting buried ice melt, as above; meltwater availability (time, quantity), local angle of slope.
Slope failure:		
Slump Spall	Sediment on ice of low angle; buried ice melt. Sediment in high-angle slope over ice of high-angle slope; differential sediment cover thickness; buried ice melt.	Factors affecting buried ice melt, as above; shear strength and grain size distribution of sediment cover.
Ice ablation	Exposed slopes of stagnant and active basal zone ice.	Weather, mainly solar radiation, precipitation, air temperature; debris content and topography of ice.

1974 and 1975 field seasons, vary as the result of differences in the topography, thickness and physical properties of the sediment cover, the short- and long-term changes in weather, and the debris content of the basal zone ice. Sediment deposition at the base of a buried ice block, where rates are determined by geothermal heat flow, is at least an order of magnitude slower than for surface melt-out.

Because melting occurs under confining conditions that inhibit deformation and reworking, the properties of till formed by melt-out are inherited primarily from the basal ice source and secondarily from depositional and post-depositional processes. During melt-out, the sediment so released collapses due to readjustment of grain contacts and particle packing, and fine-grained sediment migrates downward into pore spaces between larger particles. The extent of mixing is a function of the debris content, dimensions, texture, and orientation of individual and composite ice strata. Mixing is normally sufficient to obliterate the debris stratification and properties of individual ice strata, although the bulk texture of the debris and variations in it are generally preserved. Individual strata of high debris content may be preserved if they possess well-defined boundaries and a distinct texture. The parallel-to-flow orientation of pebbles in the basal ice is also preserved. A minor increase in the degree of scatter of orientations about the mean axis and a general decrease in the dip of pebbles to near horizontal result from melt-out. Basally-formed tills are apparently more similar in character to the ice source than upper melt-out tills.

Sedimentation in the terminus region is dominated by processes of resedimentation; it is estimated that at present 95% of the deposits are resedimented. Sediment flow, the primary process of resedimentation, is characterized by multiple mechanisms of grain support and transport. The properties of individual flows indicate that they are members of a continuum controlled mainly by water content. Sediment flows range from those of low water content in which the gross sediment strength is the primary grain support mechanism to those of high water content which are apparently liquefied. Grain interactions, localized liquefaction and fluidization, traction, and other grain support and transport mechanisms may also be important.

Sediment flows are generally derived from the sediment and meltwater released by backwasting of ice-cored slopes. Piles of disaggregated and remolded sediments usually accumulate at the base of the ice-cored slope, although in some cases sufficient mixing with meltwater may occur so that flow occurs directly off the slope. A rotational landslide failure of the downslope end of the sediments initiates a second remolding and flow of the sediment. Dense, low-water-content flows are apparently initiated by failure along one and then a series of discrete planes at the base of these sediments.

The properties of both active flows and their deposits are transitional to one another, and thus certain trends are apparent in many of these properties. At low water contents, the body of the flow possesses a yield strength, and shear occurs only in a thin basal zone. Low water content sediment flows are characterized by lobate morphology without channelization, similarity of texture and other physical properties throughout the body of the flow, slow rate of flow, and a relatively large thickness. As the water content increases, the zone of shear also increases in thickness to form a rafted, nondeforming plug zone. At larger water contents, the entire flow is in shear and the density, maximum thickness, overall dimensions, shear strength, and mean grain size generally decrease, while the degree of channelization, erosion, and maximum flow rate increase. Other processes of grain support and transport, including traction and saltation of coarse bedload materials, grain interactions, local liquefaction and fluidization, and transient turbid mixing, also increase in importance with increased water content. At the largest water contents, these mechanisms are reduced in effectiveness as flows become fully liquefied.

Sediment flow deposition results from either a decrease in slope angle, thinning of the sediment flow, or loss of water. Flow deposits with lower water contents retain most of the properties of their source. Increased water content and associated meltwater flow reduce the potential for preservation. The deposits of sediment flows are complex, yet have certain distinguishing characteristics derived from the primary and secondary processes of grain support and transport. The deposits of sediment flows are generally distinguishable from one another by their internal organization, surface features, bulk texture, geometry, and pebble fabric.

Surface processes intimately associated with sediment flow include meltwater sheet and rill flow, slope spall, slump, ice ablation, and other minor processes. Slope failure by spalling occurs in the sediment cover overlying high-angle basal ice slopes as the result of differential melting of this ice. Melting is largest near the base of the slope, causing effective outward rotation of the sediment, extension fractures in the upper sediment cover, and failure of the upper slope sediments. Slumping occurs where sediments overlie low-angled ice slopes. It is initiated by melting, buildup of excess pore pressure, and rotational slip of the sediment along the ice/sediment interface. Both processes are important in breaking down the sediment cover and initiating reworking by sediment flow and other mechanisms. Because these processes occur, irrespective of texture and most other sediment properties, over buried ice slopes, the deposits may be similarly diffuse in character. Preservation of blocks of the original sediment cover, often with structural features, and the non-sorted chaotic nature of the deposit are characteristic.

Meltwater sheet and rill flow, in contrast to other processes associated with till formation, result in an effective sorting of sediments by the selective deposition of primarily silt-size sediments and the formation of coarse-grained lags. Deposition is limited to near-horizontal surfaces and low-lying areas at rates determined by factors controlling sediment and meltwater availability. Much of the meltwater (with its entrained fine-grained sediment) flows into streams which transport it from the terminus region. The sorting, grain size, and often stratification and deposit geometry are distinctive for meltwater flow deposits.

The ablation of exposed basal ice slopes, whether of stagnant or active ice, is a sediment-forming process and a source of sediment and water throughout the terminus, as well as a process of reworking the sediment cover. On active ice, high-angle slopes adjacent to near-horizontal slopes are conducive to deposition, whereas low-angle ice slopes induce meltwater and sediment flow removal of the fine-grained materials and the formation of a lag deposit. Both deposits may be transitional to melt-out till. The extent and thickness of the deposit are determined by the rate of ablation, debris content of the ice, local topography, and glacier mass balance. The massive to fissile deposits from high-angle slopes possess a weak fabric parallel to the trend of the ice slope and are texturally similar or coarser than the ice source. Lag deposits are probably indistinguishable from lags of other origin, except where distinctly transitional to melt-out till.

Processes are often related in a cyclical reworking of the sediment cover of the terminus that results from backwasting of ice-cored slopes combined with the processes of resedimentation. Rates of sedimentation are thus much larger than would be expected, because they are controlled by the ablation of open basal ice surfaces rather than by the melting of buried ice. Reworking may be initiated by slope failure due to differential ablation, slumping, in-situ saturation and flow, fluvial

erosion, and any other mechanism or combination of these that results in removal of the sediment cover. Ablation of the open ice-cored slope results in its lateral recession, undermining and collapse of the surface sediments, and release of sediment and meltwater. Meltwater and flow originate directly from the ablating ice slope, or from an accumulating sediment pile at the base of such slopes. Ice slopes become covered, generally in the fall, because of a decline in mean air temperature and in the intensity and duration of net solar radiation. These conditions reduce the quantity of meltwater available and sediment production, although minor, is sufficient to gradually cover and stabilize the slope. This total process of backwasting results in a rapid reworking of the sediment cover and at the same time the release of debris in the glacier. Monitored slope areas, where many of the surface materials were reworked several times during 1974 and 1975, retreated laterally at rates up to 4.1 m/day, reworking over 1800 m^3 of sediment at one site.

The resedimentation processes, with the exception of meltwater flow, deposit sediments that are often similar in character. These deposits are typical of traditional "tills." They are generally unsorted, lack structure, contain lenses and other bodies of sorted sediments, show a variable fabric, and are of differing geometry. Thus, the deposits of the primary processes, those which result in resedimented materials, may be easily misinterpreted as "till."

A major problem in glacial geology has been an inability to recognize and define sedimentologically Pleistocene and ancient glacigenic sequences and, further, to delineate from those sequences the conditions of deposition. The magnitude of this problem is indicated in part by the widespread arguments over the origin of Precambrian "tillites" (Schermerhorn 1974) and the disagreements over origins of Pleistocene "tills" (Drake 1971, Pessl 1971). A major part of this problem stems from a lack of knowledge of processes of sedimentation by glaciers and their effect on glacially transported materials.

By utilizing the conservative, genetic definition of till stated above, the origin of sediments that are considered "till" in the traditional sense, yet are clearly differentiable when examined sedimentologically, can be determined and related to the depositional processes. This definition excludes the deposits of sediment flows, previously referred to incorrectly as "flowtill," from consideration as a true till. Tills and related deposits can be differentiated by examining characteristics acquired by the sediment from its processes of transport and deposition.

The analysis of the processes of sedimentation and the characteristics of their deposits indicates that the product of a given process is generally distinguishable from others by detailed analysis of an *assemblage* of characteristics (Table XIII). For resedimented materials, these characteristics are derived primarily from the depositional processes and only secondarily from the properties of the source. For melt-out till, the characteristics are mainly inherited from the basal ice source. The general properties which appear to be most important for use in defining the genesis are internal structure including pebble fabric, deposit geometry and dimensions, and surface, contact and deformational features.

On a gross scale, it is clear that investigation of a single property is inadequate to distinguish unequivocally the origin of a deposit, as is true for any sedimentary environment. This inadequacy is especially true for distinguishing till from sediment flow deposits. Parameters, such as texture or pebble fabric that are commonly used in traditional studies of glacial sediments, are possibly the least important method, by themselves, for determining the origin of a deposit.

The sedimentary sequence generally resulting from terminus sedimentation is determined by the characteristics of the individual deposits and their spatial relationships in the depositional environment. Analysis of the physical properties of the terminus environment indicates that the immediate controls over the sediment system are sediment and meltwater availability, local and regional slope of the surface, location of the active glacier margin, and extent and thickness of the sediment cover and buried basal ice. The overall controls on the sediment system thus appear to be glacial mass balance, glacial bed conditions, the thermal regime of the glacier, and the climate of the terminus region. The conditions of the Matanuska Glacier include a variable local and regional topography, complex thermal conditions, complex glacier mass balance, and a maritime-continental transition climate. The physical properties of the terminus environment include a thin-to-thick sediment cover, a large zone of buried basal ice, a receding active ice margin, and readily available meltwater and sediment. Rapid short-term changes in these conditions are characteristic of this environment.

A composite depositional sequence is recognized for the terminus region on the basis of the distribution and characteristics of the depositional processes. The idealized composite sequence is defined in terms of genetic facies associations: an upper, resedimented facies association, a middle, till facies association, and a lower, subglacial resedimented facies association. The genetic facies which compose each association represent the depositional processes, and the identification of each facies requires the recognition of the assemblage of characteristics.

Table XIII. Characteristics of the deposits, terminus region, Matanuska Glacier, Alaska.

Process	*Deposit*	*Type*	*1) Mean (ϕ) 2) σ (ϕ)*	*Internal organization*			*Surface forms*	*Contacts– basal surface features*	*Pene-contemporaneous deformation*	*Geometry-maximum dimensions*	*Miscellaneous properties*
				General	*Structure*	*Pebble fabric*					
Buried ice melt	Melt-out till	Gravel-sand-silt; silty sand; sandy silt.	1) 1 to 6 2) 1.8 to 3.5	Clasts randomly dispersed in matrix.	Massive; may preserve individual or sets of ice strata.	Strong; unimodal parallel to local ice flow; low angle of dip; $S_1 > 0.75$.	Similar to ice surface; may be deformed.	Upper sharp, may be transitional; sub-ice probably sharp.	Possible; observable if structured sediments present.	Sheet to discontinuous sheet; km² to m² in area, m thick.	Internal contacts of strata are diffuse; loose.
Lodgement at glacier sole	**Lodgement*** till	Gravel-sand-silt; silty sand.		Clasts randomly dispersed to clustered in matrix.	Massive; shear foliation, other "tectonic" features.	Strong; unimodal(?) pattern; orientation influenced by ice flow and substrate; low angle of dip.	Similar to base of ice.	Image of substrate.	Possible subglacial.	Discontinuous pockets of sheets of variable thickness and extent.	Usually dense, compact.
Sediment flow	Sediment flow Type I	Gravel-sand-silt; sandy silt	1) -1 to 2 2) 3 to 4.5	Clasts dispersed in fine-grained matrix.	Massive.	Absent to very weak; vertical clasts; $S_1 \cong 0.49$ to 0.55.	Generally planar; also arcuate ridges, secondary rills and dessication cracks.	Non-erosional, conformable contacts; contacts indistinct to sharp; load structures.	Possible subflow and marginal deformation during and after deposition.	Lobe; maximum of 1000 m² in area, 2.5 m thick.	Dense, compact.
	Type II	Gravel-sand-silt; sandy silt, silty sand.	1) 2 to 3 2) 3 to 4	Plug zone; clasts dispersed in fine-grained matrix;	Massive; intraformational blocks.	Absent to very weak; vertical clasts.	Arcuate ridges; flow lineations, mud volcanoes; braided and distributary rills on surface.	Non-erosional, conformable contacts; contacts indistinct to sharp.	Generally absent; possible subflow deformation on liquified sediments.	Lobe; maximum 600 m² in area; 1.5 m thick; sheet of coalesced deposits.	Dense, compact.
				Shear zone; gravel zone at base, upper part may show decreased silt-clay and gravel content; overall, clasts dispersed in fine-grained matrix.	**Massive; deposit may appear layered where shear and plug zones distinct in texture.**	**Absent to weak; bimodal or multimodal; vertical clasts; $S_1 \cong 0.50$ to 0.65.**					

	Type III	Gravelly sand to sandy silt	1) -2.5 to 2.5 2) 2 to 3.5	Matrix to clast dominated; lack of fine-grained matrix possible; basal gravels.	Massive; intraformational blocks occasionally.	Moderate, multimodal to bimodal parallel and transverse to flow. $S_1 \cong 0.60$ to 0.70.	Irregular to planar; singular rill development; mud volcanoes.	Non-erosional, conformable contacts; contacts indistinct to sharp.	Generally absent; possible subflow deformation on liquified sediments.	Thin lobe; 200 m^2 in area; 0.5 m thick; fan wedge; 2000 m^2 in area; 3.5 m thick rarely; sheet of coalesced deposits.	Dense to loose.
	Type IV	Sand, silty sand, sandy silt	1) $\geq$ 3.5 2) $\leq$ 2.5	Matrix, except at base, where granules possible.	Massive to graded (distribution, coarse tail).	Absent.	Smooth, planar; mud volanoes possible.	Contacts conformable; indistinct.	Absent.	Thin sheet; 200 m^2 in area, 0.3 m thick; fills surface lows of irregular size and shape.	Loose.
Spall	Slope colluvium	Any; poor sorting.		Clasts dispersed randomly in matrix to clast supported.	Massive to intraformational blocks in massive material.	Absent; vertical clasts.	Irregular.	Conformable to former surface, non-erosional.	Absent.	Irregular cross sections; band parallel to former slope of variable length, 2 m thick.	Loose; chaotic intraformational block orientations.
Slump	Slump	Silt-sand-gravel; silty sand; sandy silt.	1) 1.5 to 5 2) 1.5 to 4	Clasts dispersed randomly in matrix.	Massive to undisturbed blocks over slip plane.	Absent, except in some blocks.	Irregular.	Shear plane may occur; conformable contacts.	Possibly in or adjacent to slump block.	Irregular; hundreds of m^2 in area, 2.5 m thick.	Loose to dense.
Ablation	Ice slope colluvium	Gravelly sand; sandy gravel; sand-silt-gravel,	1) -2 to 2 2) 2.5 to 4	Clasts dispersed in matrix to clast supported.	Massive.	Weak; parallel to trend of ice slope; low to high angle of dip. $S_1 < 0.70$.	Irregular.	Conformable to former surface; non-erosional.	Absent.	Discontinuous thin sheets to wedge of variable area; 3.5 m thick.	Loose to dense.
Meltwater flow	Meltwater sheet and rill deposits	Silt to silty sand	1) 1.2 to 6 2) 1.5 to 2.5	Matrix.	Parallel stratification; deltaic cross stratification; massive to graded.	Parallel to flow; downslope dip.	Planar; channel patterns.	Conformable to non-conformable; erosional to non-erosional.	Absent.	Thin sheets; wedges, lenses; 1000 m^2 in area; 0.5 m thick.	Dense; associated with sediment flow deposits commonly.

*From Boulton (1970b, 1971); Lavrushin (1970a, 1970b); Mickelson (1973); Boulton and Dent (1974).

The surface distribution and hence the lateral relationships of the facies in the resedimented facies association do not show a simple correlation with topography or other property. Sediment flow facies, particularly those of the plug type, dominate the distribution. The surface distribution of these facies is characterized by rapid transitions between different and similar facies without a definitive pattern of relationships. These nonrepetitive distributions are retained in the vertical sequence developed for the resedimented facies association. Certain relationships between individual facies, principally sediment flows and others, recur as sequential units with an apparently random distribution in the vertical sequence of the resedimented association.

The till facies association is of subsurface origin. The basic relationship of an upper melt-out facies and lower lodgement facies occurs if both are in the same sequence. One or both may be absent if conditions for their formation do not initially exist, or if they are reworked by surfaces processes.

The vertical sequence for the Matanuska Glacier is more complex than the composite sequence. This complexity results mainly from: 1) overriding of ice that is covered by the resedimented facies, and thus stacking of resedimented and till facies, 2) reworking of the surface of the basal zone ice and sediment cover by ablation, sediment flows, and streams so that the melt-out facies becomes variable in thickness and discontinuous in lateral extent, 3) increased thickness of the resedimented facies association by adjacent local advances of the ice margin, and 4) greater buildup of the meltwater flow and fluvial facies in areas sloping away from the ice margin than in areas sloping upglacier where meltwater and sediment flow facies are most important.

The composite sequence which develops under conditions different from those of the Matanuska Glacier terminus may vary in terms of the importance of a given genetic facies or facies association. The controls over the sediment system, stated earlier, will determine the extent of this variation.

The general conclusions of this study appear to be two:

1. Sedimentation by glaciers results from many processes that may produce deposits surficially similar to one another and to the "ideal till." However, the deposit of a given process can be identified only by using an assemblage of characteristics, including till types. Pleistocene deposits have not, in most cases, been examined sedimentologically and have not been based upon sedimentological analyses of active glaciers. Therefore, sequences previously interpreted as multi-till may in fact be the result of a single glacial advance, with or without ice override. The classic till-outwash-till sequence, as pointed out by Boulton (1972a), may be resedimented in origin. Similarly, a sequence of deposits previously interpreted as two or more tills may be the result of a single ice advance-retreat cycle.

2. The variability of the sedimentary sequence of the Matanuska Glacier terminus and the conditions that result in its deposition suggest that it may be very difficult to correlate directly individual units of vertical sequences. Only if it is demonstrated through a controlled investigation that a unit is in fact regionally extensive can such correlations be made. Whether a sequence based on the controls defined in this study ever develops is in fact questionable. This study indicates that a vertical sequence must be examined in detail and defined genetically before it can be correlated with other sequences that must be similarly defined. Further studies of active glaciers in other environments should provide data that can eventually be correlated with climatic and other terminus and subglacial conditions. Based on these analyses, composite vertical sequences may then be correlated with one another on a regional scale in terms of ice marginal conditions. It is probable that reliable data that define the age relationships of vertical sequences are required in many cases to make local and regional correlations. Future studies must sedimentologically examine glacial sediments in detail to define their origin and the conditions of the ice and terminus at the time of their deposition.

LITERATURE CITED

Ambach, W., H. Eisner and K. Pessl (1972) Isotopic oxygen composition of firn, old snow and precipitation in alpine regions. *Zeitschrift für Gletscherkunde und Glazialgeologie*, vol. 8, p. 125-135.

Ambach, W., H. Eisner and M. Url (1973) Seasonal variations in the tritium activity of run-off from an alpine glacier (Kellelwandfeiner, Oetztal Alps, Austria). In *Symposium on the hydrology of glaciers*, International Union Geodesy and Geophysics, International Association of Scientific Hydrology Publication no. 95, p. 199-204.

Andresen, A. and L. Bjerrum (1967) Slides in subaqueous slopes in loose sand and silt. In *Marine Geotechnique* (A.F. Richards, Ed.). Urbana: University of Illinois Press, p. 221-239.

Andrews, J.T. and D.I. Smith (1970) Statistical analysis of till fabric: Methodology, local and regional variability. *Geological Society of London Quarterly Journal*, vol. 125, p. 503-542.

Bagnold, R.A. (1954) Experiments on a gravity-free dispersion of large solid spheres in a Newtonian fluid under shear. *Royal Society (London) Proceedings*, Series A, vol. 225, p. 49-63.

Bishop, B.C. (1957) Shear moraines in the Thule area, northwest Greenland. U.S. Army Snow, Ice and Permafrost Research Establishment (USASIPRE) Research Report 17, 46 p.

Blackwelder, E. (1928) Mudflow as a geologic agent in semiarid mountains. *Geological Society of America Bulletin*, vol. 39, p. 465-484.

Boothroyd, J.C. and G.M. Ashley (1975) Processes, bar morphology and sedimentary structures on braided outwash fans, Northeastern Gulf of Alaska. In *Glaciofluvial and glaciolacustrine sedimentation* (A.V. Jopling and B.C. McDonald, Eds.). Society of Economic Paleontologists and Mineralogists Special Publication no. 23, p. 193-222.

Boulton, G.S. (1967) The development of a complex supraglacial moraine at the margin of Sorbreen, NY Friesland, Vestspitsbergen. *Journal of Glaciology*, vol. 6, p. 717-735.

Boulton, G.S. (1968) Flowtills and related deposits on some Vestspitsbergen Glaciers. *Journal of Glaciology*, vol. 7, p. 391-412.

Boulton, G.S. (1970a) On the origin and transport of englacial debris in Svalbard Glaciers. *Journal of Glaciology*, vol. 9, p. 213-229.

Boulton, G.S. (1970b) On the deposition of subglacial and melt-out tills at the margins of certain Svalbard Glaciers. *Journal of Glaciology*, vol. 9, p. 231-245.

Boulton, G.S. (1971) Till genesis and fabric in Svalbard, Spitsbergen. In *Till: A symposium* (R.P. Goldthwait, Ed.). Columbus: Ohio State University Press, p. 41-72.

Boulton, G.S. (1972a) Modern arctic glaciers as depositional models for former ice sheets. *Geological Society of London Quarterly Journal*, vol. 128, p. 361-393.

Boulton, G.S. (1972b) The role of thermal regime in glacial sedimentation. *Institute of British Geographers*, Special Bulletin no. 4, p. 1-19.

Boulton, G.S. (1974) Processes and patterns of glacial erosion. In *Glacial morphology* (D.R. Coates, Ed.). New York: State University of New York (Binghamton), p. 41-88.

Boulton, G.S. (1975) Processes and patterns of subglacial sedimentation: A theoretical approach. In *Ice ages: Ancient and modern* (A.F. Wright and F. Moseley, Eds.). *Geological Journal*, Special Issue no. 6, p. 7-42.

Boulton, G.S. and D.L. Dent (1974) The nature and rates of post-depositional changes in recently deposited till from southeast Iceland. *Geografiska Annaler*, vol. 56, Series A, p. 121-134.

Boulton, G.S., D.L. Dent and E.M. Morris (1974) Subglacial shearing and crushing, and the role of water pressures in tills from southeast Iceland. *Geografiska Annaler*, vol. 56, Series A, p. 135-145.

Boulton, G.S. and M.A. Paul (1976) The influence of genetic processes on some geotechnical properties of glacial tills. *Quarterly Journal of Engineering Geology*, vol. 9, p. 159-194.

Buller, A.T. and J. McManus (1973) The quartile-deviation/median diameter relationships of glacial deposits. *Sedimentary Geology*, vol. 10, p. 135-146.

Burger, H. (1976) Log-normal interpolation in grain size analysis. *Sedimentology*, vol. 23, p. 395-405.

Carter, R.M. (1975) A summary discussion of subaqueous mass transport with particular respect to grain-flows and fluxoturbidities. *Earth Science Review*, vol. 11, p. 145-177.

Chamberlain, T.C. (1894) Proposed genetic classification of Pleistocene glacial formations. *Journal of Geology*, vol. 2, p. 147-248.

Church, M. (1972) Baffin Island sandurs. *Canada Geological Survey Bulletin*, no. 216, 205 p.

Clayton, L. (1964) Karst topography on stagnant glaciers. *Journal of Glaciology*, vol. 5, p. 107-112.

Clifton, H.E. (1969) Beach lamination. Nature and origin. *Marine Geology*, vol. 7, p. 553-560.

Craig, H. (1957) Isotopic standards for carbon and oxygen and correction factors for mass-spectrometric analysis of carbon dioxide. *Geochimica et Cosmochimica Acta*, vol. 12, p. 133-149.

Craig, H. (1961) Standard for reporting concentrations of deuterium and oxygen-18 in natural waters. *Science*, vol. 133, p. 1833-1834.

Curry, R.R. (1966) Observation of alpine mudflows in the Tenmile Range, Central Colorado. *Geological Society of America Bulletin*, vol. 77, p. 771-776.

Dansgaard, W. (1964) Stable isotopes in precipitation. *Tellus*, vol. 16, p. 436-468.

Deutsch, S., W. Ambach and H. Eisner (1966) Oxygen isotope study of snow and firn on an alpine glacier. *Earth and Planetary Science Letters*, vol. 1, p. 197-201.

Drake, L.D. (1971) Evidence for ablation and basal till in east-central New Hampshire. In *Till: A symposium* (R.P. Goldthwait, Ed.). Columbus: Ohio State University Press, p. 73-91.

Dutro, J.T. and T.G. Payne (1957) Geologic map of Alaska. U.S. Geological Survey Base Map E.

Epstein, S. and T. Mayeda (1953) Variation in O^{18} content of waters from natural sources. *Geochimica et Cosmochimica Acta*, vol. 67, p. 88-102.

Epstein, S. and R.P. Sharp (1959) Oxygen isotope variations in the Malaspina and Saskatchewan Glaciers. *Journal of Geology*, vol. 67, p. 88-102.

Fahnestock, R.K. (1963) Morphology and hydrology of a glacial stream: White River, Mount Rainier, Washington. U.S. Geological Survey Professional Paper 422A, 70 p.

Flint, R.E. (1971) *Glacial and quaternary geology.* New York: John Wiley and Sons, 892 p.

Garwood, E.J. and J.W. Gregory (1898) Contributions to the glacial geology of Spitsbergen. *Geological Society of London Quarterly Journal*, vol. 106, p. 197-225.

Goldthwait, R.P. (1951) Development of end moraines in east-central Baffin Island. *Journal of Geology*, vol. 59, p. 567-577.

Goldthwait, R.P. (1971) Introduction to till today. In *Till: A symposium* (R.P. Goldthwait, Ed.). Columbus: Ohio State University Press, p. 3-26.

Gow, A.J., W. Sheehy and S. Epstein (1978) On the origin of stratified debris in ice cores from the bottom of the Antarctic ice sheet. Abstract from Proceedings, Symposium on Glacier Beds: The Ice-Rock Interface. *Journal of Glaciology*, In press.

Grant, U.S. and D.F. Higgins (1913) Coastal glaciers of the Prince William Sound and Kenai Peninsula, Alaska. U.S. Geological Survey Bulletin, 526 p.

Grantz, A. (1964) Stratigraphic reconnaissance of the Matanuska Formation in the Matanuska Valley, Alaska. U.S. Geological Survey Bulletin, 1181-I, 33 p.

Grove, J.M. (1960) A study of Veslgjuv-Breen. In *Norwegian cirque glaciers* (W.W. Lewis, Ed.). Royal Geographical Society Research, series 4, p. 69-82.

Gustavson, T.C. (1975) Sedimentation and physical limnology in proglacial Malaspina Lake, southeastern Alaska. In *Glaciofluvial and glaciolacustrine sedimentation* (A.V. Jopling and B.C. McDonald, Eds.). Society of Economic Paleontologists and Mineralogists, Special Publication no. 23, p. 249-263.

Gustavson, T.C., G.M. Ashley and J.C. Boothroyd (1975) Depositional sequences in glaciolacustrine deltas. In *Glaciofluvial and glaciolacustrine sedimentation* (A.V. Jopling and B.C. McDonald, Eds.). Society of Economical Paleontologists and Mineralogists, Special Publication no. 23, p. 264-280.

Hampton, M.A. (1970) Subaqueous debris flow and generation of turbidity currents. Ph.D. dissertation, Stanford University (unpublished).

Hampton, M.A. (1972) The role of subaqueous debris flow in generating turbidity currents. *Journal of Sedimentary Petrology*, vol. 42, p. 775-793.

Hampton, M.A. (1975) Competence of fine-grained debris flows. *Journal of Sedimentary Petrology*, vol. 45, p. 834-844.

Hartshorn, J.H. (1958) Flowtill in southeastern Massachusetts. *Geological Society of America Bulletin*, vol. 69, p. 477-482.

Hewitt, K. (1967) Ice-front deposition and the seasonal effect: A Himalayan example. *Inst. British Geog. Trans.*, vol. 42, p. 93-106.

Hjulström, F. (1952) The geomorphology of the alluvial outwash plains of Iceland and the mechanics of braided rivers. *Proceedings, 8th General Assembly of the International Geographical Union Congress*, Washington, p. 337-342.

Holdsworth, G. (1974) Meserve Glacier, Wright Valley, Antarctica. Part 1. Basal processes. Ohio State Institute of Polar Studies Report No. 37, 104 p.

Hooke, R.L. (1967) Processes in arid-region alluvial fans. *Journal of Geology*, vol. 75, p. 438-460.

Hooke, R.L. (1973) Flow near the margin of the Barnes Ice Cap, and the development of ice-cored moraines. *Geological Society of America Bulletin*, vol. 84, p. 3939-3948.

Howard, P.J. and R.J. Price (1969) The proglacial lakes of Breidamerkurjökul and Fjallsjökull, Iceland. *Geographical Journal*, vol. 135, p. 573-581.

Howarth, P.J. (1971) Investigations of two eskers at eastern Breidamerkurjökul and Fjallsjökull, Iceland. *Geographical Journal*, vol. 135, p. 573-581.

Jewtuchowicz, S. (1965) Description of eskers and kames in Gashomnöyra and on Bungebreen, south of Hornsund Vestspitsbergen. *Journal of Glaciology*, vol. 5, p. 719-725.

Jewtuchowicz, S. (1968) Accumulation in stagnant ice, with the Spitsbergen Glaciers as examples. *Geog. Polonica*, vol. 13, p. 49-56.

Johnson, A.M. (1965) A model for debris flow. Ph.D. dissertation, Pennsylvania State University (unpublished).

Johnson, A.M. (1970) *Physical processes in geology.* San Francisco: Freeman Cooper and Company, p. 423-572.

Johnson, A.M. and M.A. Hampton (1968) Subaerial and subaqueous flow of slurries. Progress report to the U.S. Geological Survey (unpublished). Branner Library, Stanford, California.

Johnson, A.M. (1969) Subaerial and subaqueous flow of slurries. Progress report to the U.S. Geological Survey (unpublished). Branner Library, Stanford University.

Johnson, A.M. and P.H. Rahn (1970) Mobilization of debris flows. *Zeitschrift für Geomorphologie*, Supplementband 9, p. 168-186.

Jopling, A.V. and B.C. McDonald (Eds.) (1975) Glaciofluvial and glaciolacustrine sedimentation. Society of Economic Paleontologists and Mineralogists, Special Publication no. 23, 320 p.

Jordan, C.F., G.E. Fryer and E.H. Hemmen (1971) Size analysis of silt and clay by hydrophotometer. *Journal of Sedimentary Petrology*, vol. 41, p. 489-496.

Kamb, N.B. (1959) Ice petrofabric observations from Blue Glacier, Washington, in relation to theory and experiment. *Journal of Geophysical Research*, vol. 64, p. 1891-1909.

Kamb, B. and LaChapelle (1964) Direct observations on the mechanism of glacier sliding over bedrock. *Journal of Glaciology*, vol. 5, p. 159-172.

Karlstrom, T.N.V. (1965) Upper Cook Inlet Area and Matanuska River Valley. INQUA, 7th Congress, *Guidebook for field conference F: Central and southcentral Alaska*, vol. 6, p. 114-146.

Krigström, A. (1962) Geomorphological studies of sandur plains and their braided rivers in Iceland. *Geografiska Annaler*, vol. 44, p. 328-346.

Lambe, T.W. and R.V. Whitman (1969) *Soil mechanics.* New York: John Wiley and Sons, 553 p.

Lamplugh, G.W. (1911) On the shelly moraine of the Sefström Glacier and other Spitsbergen phenomena illustrative of British glacial conditions. *Yorkshire Geological Society Proceedings*, vol. 17, no. 3, p. 216-241.

Lawson, D.E. (1976) Observations on flutings at Spencer Glacier, Alaska. *Arctic and Alpine Research*, vol. 8, p. 289-296.

Lavrushin, Y.A. (1970a) Reflection of the dynamics of glacier movement in the structure of a ground moraine. *Litologiya i Poleznye Iskopaemye*, vol. 1, p. 115-120.

Lavrushin, Y.A. (1970b) Recognition of facies and subfacies in ground moraine of continental glaciation. *Litologiya i Poleznye*, vol. 6, p. 38-49

Lewis, W.V. (1940) Dirt cones on the northern margins of Valnajökull, Iceland. *Journal of Geomorphology*, vol. 3, p. 16-26.

Lewis, W.V. (1949) An esker in process of formation: Böverbreen, Jotunheimen, 1947. *Journal of Glaciology*, vol. 1, p. 314-319.

Loomis, S.R., J. Dozier and K. Ewing (1970) Studies of morphology and stream action on ablating ice. Arctic Institute of North America Research Paper no. 57, 156 p.

Lowe, D.R. (1975) Water escape structures in coarse-grained sediments. *Sedimentology*, vol. 22, p. 157-204.

Lowe, D.R. (1976a) Grain flow and grain flow deposits. *Journal of Sedimentary Petrology*, vol. 46, p. 188-199.

Lowe, D.R. (1976b) Subaqueous liquified and fluidized sediment flows and their deposits. *Sedimentology*, vol. 23, p. 285-308.

Macpherson, D.A. and H.R. Krouse (1967) O^{18}/O^{16} ratios in snow and ice of the Hubbard and Kaskawulch Glaciers. In *Isotope techniques in the hydrologic cycle* (G.E. Stout, Ed.). *American Geophysical Union Monograph*, no. 11, p. 180-194.

Mark, D.M. (1973) Analysis of axial orientation data, including till fabrics. *Geological Society of America Bulletin*, vol. 84, p. 1369-1374.

Mathews, W.H. (1964) Water pressure under a glacier. *Journal of Glaciology*, vol. 5, p. 235-240.

Mayo, L. and T.L. Péwé (1963) Ablation and net total radiation, Gulkana Glacier, Alaska. In *Ice and snow* (W.D. Kingery, Ed.). Cambridge: MIT Press, p. 633-643.

McCall, J.G. (1960) The flow characteristics of a cirque glacier and their effect on glacial structure and cirque formation. In *Norwegian cirque glaciers* (W.V. Lewis, Ed.). Royal Geographical Society Research Series, vol. 4, p. 39-62.

McKenzie, G.D. (1969) Observations on a collapsing kame terrace in Glacier Bay National Monument, southeastern Alaska. *Journal of Glaciology*, vol. 8, p. 413-425.

Mickelson, D.M. (1973) Nature and rate of basal till deposition in a stagnating ice mass, Burroughs Glacier, Alaska. *Arctic and Alpine Research*, vol. 5, p. 17-27.

Middleton, G.V. and M.A. Hampton (1973) Sediment gravity flows: Mechanics of flow and deposition. Society of Economic Paleontologists and Mineralogists, Short Course Notes, Anaheim, Pacific Section, p. 1-38.

Middleton, G.V. and M.A. Hampton (1976) Subaqueous sediment transport and deposition by sediment gravity flows. In *Marine sediment transport and environmental management* (D.J. Stanley and D.J.P. Swift, Eds.). New York: John Wiley and Sons, p. 197-220.

Moravek, J.R. (1973) Some further observations on the behavior of an ice-dammed self-draining lake, Glacier Bay, Alaska, USA. *Journal of Glaciology*, vol. 12, p. 505-507.

Morgenstern, N. (1967) Submarine slumping and the initiation of turbidity currents. In *Marine geotechnique* (A.F. Richards, Ed.). Urbana: University of Illinois Press, p. 189-220.

Nye, J.F. (1970) Glacier sliding without cavitation in a linear viscous approximation. *Royal Society (London) Proceedings A*, vol. 315, p. 381-403.

Nye, J.F. (1976) Water flow in glaciers: Jokulhlaups, tunnels and veins. *Journal of Glaciology*, vol. 17, p. 181-207.

Nye, J.F. and F.C. Frank (1973) Hydrology of the intergranular veins in a temperate glacier. International Union of Geodesy and Geophysics, International Association of Scientific Hydrology, *Symposium on Hydrology of Glaciers* publ. no. 95, p. 157-161.

O'Neil, J.R. (1968) Hydrogen and oxygen isotopic fractionation between ice and water. *Journal of Physical Chemistry*, vol. 72, p. 3683-3684.

O'Neil, J.R., L.W. Adami and S. Epstein (1975) Revised value for the O^{18} fractionation between CO_2 and H_2O at 25°C. *U.S. Geological Survey Journal of Research*, vol. 3, p. 623-624.

Østrem, G. (1959) Ice melting under a thin layer of moraine, and the existence of ice cores in moraine ridges. *Geografiska Annaler*, vol. 41, p. 228-230.

Østrem, G. (1975) Sediment transport in glacial meltwater streams. In *Glaciofluvial and glaciolacustrine sedimentation* (A.V. Jopling and B.C. McDonald, Eds.). Society of Economic Paleontologists and Mineralogists, Special Publication no. 23, p. 101-122.

Ovenshine, A.T. (1970) Observations of iceberg rafting in Glacier Bay, Alaska, and the identification of ancient ice rafted deposits. *Geological Society of America Bulletin*, vol. 81, p. 891-894.

Pessl, F. (1971) Till fabrics and till stratigraphy in western Connecticut. In *Till: A symposium* (R.P. Goldthwait, Ed.). Columbus: Ohio State University Press, p. 92-105.

Peterson, D.N. (1970) Glaciological investigations on the Casement Glacier, southeast Alaska. Ohio State University, Institute of Polar Studies Report no. 36, 161 p.

Potter, P.E. and F.J. Pettijohn (1963) ***Paleocurrents and basin analysis.*** New York: Academic Press, 296 p.

Powers, M.C. (1953) A new roundness scale for sedimentary particles. *Journal of Sedimentary Petrology*, vol. 23, p. 117-119.

Price, R.J. (1966) Eskers near the Casement Glacier. *Geografiska Annaler*, vol. 48, p. 111-125.

Price, R.J. (1969) Moraines, sandar, kames and eskers near Breidamerkurjökull, Iceland. *Institute of British Geographers Transactions*, vol. 46, p. 17-43.

Ray, L.L. (1935) Some minor features of valley glaciers and valley glaciation. *Journal of Geology*, vol. 43, p. 297-322.

Reheis, M.J. (1975) Source, transportation and deposition of debris on Arapaho Glacier, Front Range, Colorado, U.S.A. *Journal of Glaciology*, vol. 14, p. 407-420.

Reid, H.F. (1896) The mechanics of glaciers. *Journal of Geology*, vol. 4, p. 912-928.

Reid, J.R. (1968) Origin and characteristics of superglacial drift, Martin River and Sioux Glaciers, Alaska. Geological Society of America Special Paper 101, Abstract, p. 173.

Reid, J.R. and E. Callender (1965) Origin of debris-covered icebergs and mode of flow of ice into "Miller Lake," Martin River Glacier, Alaska. *Journal of Glaciology*, vol. 5, p. 497-503.

Richter, K. (1936) Gefügestudien im Engebrae, Foudalsbrae, und ihren Vorlandsedimenten. *Zeitschrift für Gletscherkunde*, vol. 24, p. 22-30.

Robin, G. deQ. (1976) Reconciliation of temperature-depth profiles in polar ice sheets with past surface temperatures deduced from oxygen-isotope profiles. *Journal of Glaciology*, vol. 16, p. 9-22.

Rodine, J.D. (1974) Analysis of the mobilization of debris flows. Ph.D. dissertation, Stanford University (unpublished).

Rodine, J.D. and A.M. Johnson (1976) The ability of debris, heavily freighted with coarse clastic materials, to flow, on gentle slopes. *Sedimentology*, vol. 23, p. 213-234.

Russel, I.C. (1893) Malaspina Glacier. *Journal of Geology*, vol. 1, p. 219-245.

Rust, B.R. (1972) Structure and process in a braided river. *Sedimentology*, vol. 18, p. 221-245.

Schermerhorn, L.J.G. (1974) Late Precambrian mixtites: Glacial and/or nonglacial. *American Journal of Science*, vol. 274, p. 673-824.

Schofield, A. and P. Wroth (1968) ***Critical state soil mechanics.*** London: McGraw Hill Book Company, 310 p.

Scott, R.F. (1964) Heat exchange at the ground surface. CRREL Cold Regions Science and Engineering Monograph IIA1, 49 p. AD 449434.

Selkregg, L.L. (1976) Alaska regional profiles, south-central region. Univ. of Alaska, Arctic Environmental Information and Data Center, 255p.

Sharp, R.P. (1949) Studies of superglacial debris on valley glaciers. *American Journal of Science*, vol. 247, p. 289-315.

Sharp, R.P. and L.H. Nobles (1953) Mudflow of 1941 at Wrightwood, southern California. *Geological Society of America Bulletin*, vol. 64, p. 547-560.

Sharp, R.P., S. Epstein and I.W. Vidziunas (1960) Oxygen-isotope ratios in the Blue Glacier, Olympic Mountains, Washington, U.S.A. *Journal of Geophysical Research*, vol. 65, p. 4043-4059.

Shaw, J. (1977) Tills deposited in arid polar environments. *Canadian Journal of Earth Sciences*, vol. 14, p. 1239-1245.

Shreve, R.L. (1972) Movement of water in glaciers. *Journal of Glaciology*, vol. 11, p. 205-214.

Slatt, R.M. (1971) Texture of ice-cored deposits from ten Alaskan Valley glaciers. *Journal of Sedimentary Petrology*, vol. 41, p. 828-834.

Slatt, R.M. and C.M. Hoskin (1968) Water and sediment in the Norris Glacier outwash area, Upper Taku Inlet, southeastern Alaska. *Journal of Sedimentary Petrology*, vol. 38, p. 434-456.

Stone, K.H. (1963) Alaskan ice-dammed lakes. *Association of American Geographers Annals*, vol. 53, p. 332-349.

Swithinbank, C. (1950) The origin of dirt cones on glaciers. *Journal of Glaciology*, vol. 1, p. 461-465.

Tarr, R.S. (1908) Some phenomena of the glacier margins in the Yakutat Bay region, Alaska. *Zeitschrift für Gletscherkunde*, vol. 3, p. 81-110.

Tarr, R.S. and L. Martin (1914) ***Alaskan glacier studies.*** **Washington, D.C.: National Geographic Society, 498 p.**

Terzaghi, K. (1950) Mechanics of landslides. In *Application of geology to engineering practice* (S. Page, Ed.). Geological Society of America, Berkey Volume, p. 83-124.

Terzaghi, K. and Peck, R.B. (1967) ***Soil mechanics in engineering practice.*** New York: John Wiley and Sons, 729 p.

Theakstone, W.H. (1976) Glacial lake sedimentation, Austerdalsisen, Norway. *Sedimentology*, vol. 23, p. 671-688.

Trewartha, G.T. (1954) *An introduction to climate.* New York: McGraw-Hill Book Company, 402 p.

Vivian, R. and G. Bocquet (1973) Subglacial cavitation phenomena under Glacier D'Argentiere, Mont Blanc, France. *Journal of Glaciology*, vol. 12, p. 439-451.

Weertman, J. (1957) On the sliding of glaciers. *Journal of Glaciology*, vol. 3, p. 33-38.

Weertman, J. (1961) Mechanism for the formation of inner moraines found near the edge of cold ice caps and ice sheets. *Journal of Glaciology*, vol. 3, p. 965-978.

Weertman, J. (1964) The theory of glacier sliding. *Journal of Glaciology*, vol. 5, p. 287-303.

Weertman, J. (1972) General theory of water flow at the base of a glacier or ice sheet. *Review of Geophysics and Space Physics*, vol. 10, p. 287-333.

Williams, J.R. and O. Ferrians (1961) Late Wisconsin and recent history of the Matanuska Glacier, Alaska. *Arctic*, vol. 14, p. 82-90.

Youd, T.L. (1973) Liquefaction, flow and associated ground failure. U.S. Geological Survey Circular 688, 12 p.

A facsimile catalog card in Library of Congress MARC format is reproduced below.

Lawson, Daniel E.
Sedimentological analysis of the western terminus of the Matanuska Glacier, Alaska / by Daniel E. Lawson. Hanover, N.H.: U.S. Cold Regions Research and Engineering Laboratory; Springfield, Va.: available from National Technical Information Service, 1979.
x, 122 p., illus., 27 cm. (CRREL Report 79-9.)
Prepared by U.S. Army Cold Regions Research and Engineering Laboratory.
Bibliography: p. 109.
1. Glaciers. 2. Glacial deposits. 3. Glacial morphology. 4. Sedimentology. 5. Sediment transport. I. United States. Army. Corps of Engineers. II. Cold Regions Research and Engineering Laboratory, Hanover, N.H. III. Series: CRREL Report 79-9.